LUNG EPITHELIAL PROGENITOR CELL-MEDIATED RELEASE OF TGF-β REGULATES INDUCTION AND PERSISTENCE OF LUNG CD8$^+$ T_{RM} CELLS FOLLOWING MUCOSAL BCG VACCINATION

Judith Anne Blake

A thesis submitted in total fulfilment of the requirements of the degree of Doctor of Philosophy

December 2024

Australian Institute of Tropical Health and Medicine

James Cook University

Acknowledgements

Firstly, I would like to extend my sincere gratitude to James Cook University, its College of Public Health, Medical and Veterinary Sciences, the Australian Institute of Tropical Health and Medicine and my principal supervisor Associate Professor Andreas Kupz for the opportunity to undertake this study. It was an absolute privilege to be trusted with this project, funded by Associate Professor Kupz' National Health and Medical Research Council Investigator grant and the James Cook University Prestige Scholarship.

I extend my warmest thanks to my advisory panel of Associate Professor Kupz, Professor Denise Doolan and Dr Paul Giacomin for their valuable time, insightful suggestions, and unwavering confidence in this unique project.

I am very grateful to Dr Felicity Davis of the University of Queensland, Professor Edward Morrisey of the University of Pennsylvania, Professor Dean Sheppard of the University of California San Francisco, and Professor Scott Mueller of the University of Melbourne for generously sharing their mouse lines. I would also like to sincerely thank Dr Leanne Clark for the management of our mice genotyping through the University of Queensland Genetic Research Services.

I would like to particularly acknowledge the following colleagues of the Australian Institute of Tropical Health and Medicine, namely, Phill Walsh for his constant assistance in the lab, Serrin Rowarth for the breeding and care of our mice, Professor Jamie Seymour for use of his lab as well as Lynne Saunders and Brook Possa for their administrative support.

I would like to express my sincere gratitude to Dr Jen Whan, Dr Roland Ruscher, Julia Seifert and Dr Mark Stafford for technical support and training.

A special thanks goes out to my peers and colleagues of the Australian Institute of Tropical Health and Medicine for collegial (and not so collegial!) discussions, unwavering friendship, and fellowship.

I could not have accomplished this work without the loving support of John Daunt and my family.

Most importantly, I humbly acknowledge the Unmoved Mover, without whom there would be no human reason and therefore no valid science.

Statement of the Contribution of Others

Dr. Paul Giacomin, Professor Denise Doolan and A/Prof. Andreas Kupz contributed to the conception, design, experimental analyses and edited the manuscript.

Julia Seifert performed intratracheal vaccinations and Dr. Roland Ruscher performed intraperitoneal tamoxifen injections.

Abstract

A principal reason for the high global morbidity and mortality of tuberculosis (TB) is the lack of efficacy of the only licensed TB vaccine, Bacillus Calmette-Guérin (BCG), as parenteral BCG does not induce local pulmonary immune memory. Animal studies have shown that mucosal (inhaled) BCG vaccination provides superior protection against TB due to generation of lung resident memory T cells (T_{RM}). Here, we demonstrated that following mucosal vaccination with the genetically modified virulent BCG strain, BCG::RD1, distal airway epithelial progenitors were mobilized to assist with restoration of alveolar epithelium. By way of their activation of latent TGF-β from alveolar interstitium, lung $CD8^+$ T_{RM} differentiation was induced. Mucosal vaccinations using nonvirulent strains of BCG in which airway epithelial progenitors were not mobilized, as well as genetic inhibition of migration-mediated activation of TGF-β, resulted in significantly lower numbers of $CD8^+$ T_{RM}. In addition, we discovered $CD8^+$ cells with ex-lung and stem-like T_{RM} phenotypes that persisted in the lung-draining mediastinal lymph nodes for up to four months following mucosal BCG vaccination. These results intimately link airway epithelial progenitor-mediated repair of injured lung tissue with the induction of resident T cell memory in the lung and delineate why the persistence of T_{RM} in the lung is transient and short-lived. These findings may explain why mucosal vaccination with virulent BCG strains is more protective against TB and may thus have notable implications for future TB vaccine development.

Declaration

I certify that this work contains no material which has been accepted for the award of any other degree or diploma in my name, in any university or other tertiary institution and, to the best of my knowledge and belief, contains no material previously published or written by another person, except where due reference has been made in the text.

Table of Contents

List of Abbreviations

TB	Tuberculosis
Mtb	*Mycobacterium tuberculosis*
BCG	Bacillus Calmette-Guérin
T_{RM}	resident memory T cells
AEC1	Type 1 alveolar epithelial cell
AEC2	Type 2 alveolar epithelial cell
Wnt	Wingless-related integration site
AEP	AEC progenitor
LNEP	lineage negative epithelial progenitors
DASC	distal airway stem cells
T cells	T lymphocytes
TCR	T cell receptors
MHC	major histocompatibility complex
HIV	human immunodeficiency virus
SLECs	short lived effector cells
MPEC	memory precursor effector cells
KLRG-1	killer cell lectin-like receptor G1
IL-7Rα	IL-7 receptor subunit-α
CXCR3	CXC-chemokine receptor 3
CD62L	L selectin
Tscm	stem-like memory T cells
T_{CM}	central memory T cells
CCR7	CC chemokine receptor 7
T_{EM}	effector memory T cells
KLF2	Kruppel-like transcription factor 2
S1PR1	sphingosine 1–phosphate receptor 1
S1P	sphingosine 1-phosphate
CCR7	chemokine receptor 7
CD69	C-type lectin cell surface molecule
CD103	αE subunit of the αE/β7 integrin
Eomes	Eomesodermin
TF	transcription factor
LAP	latent protein
LTBP	latent TGF-β binding protein
RNAseq	RNA sequencing
FRT	female reproductive tract
IFN-λ	interferon gamma
IL-2	interleukin-2
TNFα	tumour necrosis factor alpha
IFN	interferon
SLO	secondary lymphoid organ
PD-1	programmed cell death protein 1
Tcf1	T-cell factor 1
LCMV	lymphocytic choriomeningitis virus

Scgb1a1	secretoglobin 1A1
RAMD	repair-associated memory depot
mLN	mediastinal lymph node
IT	intratracheal
IN	intranasal
SC	subcutaneous
BASC	bronchioalveolar stem cells
SPC	surfactant protein c
PR8	murine-adapted H1N1 influenza A
p63	tumour protein 63
Dpi	days past infection
BSC	basal stem cell
Krt5	keratin 5
IPF	idiopathic pulmonary fibrosis
Sox2	SRY-box 2
HIF1α	Hypoxia inducible factor 1α
EpCAM	pan-epithelial cell marker
CD49f	α6 integrin
CD104	β4 integrin
scRNA-seq	single-cell RNA sequencing
LPS	Lipopolysaccharide
Krt8	keratin 8
DATP	damage associated transitional progenitors
Il1r1	interleukin 1 receptor type 1
PATS	pre-alveolar type-1 transitional cell state
KIRA	kinase-inhibiting RNase attenuator
RIDD	regulated IRE1α-dependent decay
ER	endoplasmic reticulum
ECM	extracellular matrix
ZBF	zinc-based fixative
PFA	paraformaldehyde
CFU	colony forming units
PBS	phosphate buffered saline
BCS	body condition score
TBS	Tris-buffered saline
TBS-Tw	TBS-Tween ABC
ABC	avidin biotin complex
BCG SSI	Danish strain of BCG
pSPC	pro-surfactant protein C
T1α	type 1 alpha protein
Dpv	days past vaccination
RD1	region of difference 1
H&E	haematoxylin and eosin
TP	transitional progenitor
STAT	signal transducer and activator of transcription
NF-κB	nuclear factor-kappa beta
IRF	interferon regulatory factor

ESAT-6	early secreted antigenic target 6
CFP-10	culture filtrate protein 10
HGF	hepatocyte growth factor
Fgf	fibroblast growth factors
IHC	immunohistochemistry

List of Tables

List of Figures

Background

The Covid-19 pandemic made people more aware of the ineffectiveness of a vaccine injection to protect against lung infection, a problem that was well acknowledged amongst tuberculosis (TB) immunologists for years (Kaufmann, 2013). TB is primarily a respiratory infection caused by *Mycobacterium tuberculosis* (*Mtb*); boasting 10.6 million new infections in 2022 and 1.3 million deaths, TB is one of the top ten fatal diseases globally (World Health Organisation, 2023). These statistics highlight the inadequacy of the only licensed TB vaccine - BCG (Gengenbacher et al., 2017; Kaufmann, 2013; Kaufmann et al., 2014). BCG is an attenuated strain of *Mycobacterium bovis* which is given parenterally to postnatal infants in TB endemic regions and confers immunity against acute septic forms of TB in children (Mangtani et al., 2014), however, immunity is lost in adolescence (Mangtani et al., 2017). Failure of BCG to provide life-long immune protection against *Mtb* is thought to be due to insufficient generation of antigen-specific $CD8^+$ memory T cells in the lungs (Behr et al., 1999). This is a key area of vaccine improvement where recombinant modifications of BCG aim to generate a more persistent $CD8^+$ T cell memory. For example, mice and guinea pigs vaccinated with BCG strains in which the region of difference 1 genes that encode *Mtb* virulence genes ESAT-6 and CFP-10 have been recombined into *M. bovis* (Pym et al., 2002) showed improved protection against *Mtb* challenge (Aguilo et al., 2017; Hsu et al., 2003).

A major goal of vaccination is to induce circulatory and tissue-resident (T_{RM}) antigen-experienced memory T cells that respond rapidly to secondary infection. It has been demonstrated that a mucosal (or inhaled) BCG vaccination, as opposed to parenteral BCG, generated superior protection against TB in animal vaccinations and this protection was linked to generation of lung T_{RM} (parenteral BCG did not lead to T_{RM} in the lungs) (Aguilo et al., 2017; Perdomo et al., 2016). Mucosal delivery of BCG has been further shown to induce significant numbers of airway T_{RM} (Muruganandah et al., 2020) and conferred superior immunity against aerosol *Mtb* infection in diabetic mice (Sathkumara et al., 2020). Thus, inclusion of immunogenic antigens of *Mtb* into BCG (Aguilo et al., 2017) combined with a mucosal delivery strongly contributes to vaccine-induced protection against *Mtb*.

Stem/progenitor cells perceive damage, and designate resident and recruited immune cell roles. Evidence of interactions between immune and progenitor cells is seen in the array of immune receptors and cytokine signalling systems of progenitor cells (Agudo et al., 2018; Alvarado & Lathia, 2016; Atladottir et al., 2010) and dysregulation of immune-progenitor cell crosstalk results in chronic disease (Belkaid & Hand, 2014; Ordovas-Montanes et al., 2018; Rieder et al., 2007). In mouse vaccinations of influenza infection, there is an invariable association of $CD8^+$ T_{RM} and lung epithelial progenitor cells in areas of severe tissue destruction (Chua et al., 2020; Fang et al., 2020; Jyothula et al., 2022; Kumar et al., 2011; Takamura, 2017; Vaughan et al., 2015; Zacharias et al., 2018; Zhao et al., 2020). In that context it has been suggested that "cells constituting such auxiliary developed regenerative tissues could be a source of unique factors necessary for differentiation and maintenance of T_{RM} cells, such as TGF-β" (Takamura et al., 2016).

Lung injury activates adult epithelial progenitors to regenerate the alveolar epithelium which consists of Type 1 and Type 2 alveolar epithelial cells (AEC1 and AEC2, respectively). AEC1 are responsible for gas exchange while AEC2 secrete surfactant to prevent alveolar collapse. Using a Cre-reporter for Wingless-related integration site (Wnt) signalling, a rare AEC progenitor (AEP) that constitutes `20% of all AEC2 was described (Nabhan et al., 2018). Although considered stem cells, AEP express AEC2 markers and function as AEC2 (Zacharias et al., 2018). Lineage-labelled AEP expanded six-fold relative to unlabelled AEC2 during a 1-year chase, while injury was also shown to activate quiescent AEC2 (Messier & Leblond, 1960) to proliferate (Nabhan et al., 2018). Zacharias *et al*. (Zacharias et al., 2018) reported the distinct functional AEP gene expression profile enriched in lung developmental genes and epigenome. Thus, a small subset of AEC2 termed AEP possess bipotency while conventional AEC2 *can* be recruited to repair alveolar damage.

Following severe injury and depletion of normally abundant local alveolar progenitor cells, wound-healing responses originate from stem cells in the airways (Ray et al., 2016). Of relevance to our studies are lineage negative epithelial progenitors (LNEP) and distal airway stem cells (DASC). LNEP in the distal bronchioles are quiescent in uninjured lungs, however, alveolar injury can elicit their proliferation, such

that daughter cells migrate into alveolar tissue and differentiate into AEC1 or AEC2 (Kathiriya et al., 2020; Strunz et al., 2020). LNEP are targeted by murine PR8 influenza virus and lose their proliferative capacity (Quantius et al., 2016); therefore, rare, quiescent DASC proliferate, and daughters migrate to occupy alveolar areas depleted of epithelium where they form $Krt5^+$ "pods" with $CD8^+$ T_{RM} (Takamura, 2018; Vaughan et al., 2015).

How T_{RM} induction and maintenance is regulated following mucosal exposure to mycobacteria, particularly parental and recombinant strains of BCG, and if it is linked to airway progenitor-mediated restitution of injured lung tissue, remained unknown. Thus, we studied $CD8^+$ lung T_{RM} and lung epithelial progenitors to elucidate how they cooperate for restoration of lung function following inhaled BCG vaccination. We describe a novel mechanistic association between airway epithelial progenitor paracrine cues and induction of $CD8^+$ lung T_{RM}.

CHAPTER 1. LITERATURE REVIEW

Those who wish to succeed must ask the right preliminary questions.

ARISTOTLE, *METAPHYSICS*

1.1 $CD8^+$ Tissue Resident Memory T Cells

1.1.1 T Cell Mediated Immunity

T lymphocytes (T cells) are the central component of cell-mediated immunity which provides defence against extra- and intracellular microbes. $CD4^+$ helper T cells secrete cytokines that recruit other leukocytes to ingest and destroy extracellular microbes and stimulate expansion of $CD8^+$ T cells. $CD8^+$ cytotoxic T cells directly kill cells infected with intracellular microbes such as *Mtb*. T cell receptors (TCR) recognise antigen and when antigen binds a naïve TCR in the context of major histocompatibility complex (MHC) molecules on the surface of antigen presenting cells, complex cellular cascades mediate downstream T cell specification and responses. Although T cells harbor a large repertoire of different TCRs with diverse reactivity, there are only a small number of TCR-specific cells within the total number of T cells a human can host. Therefore, effective guard of the body against pathogen invasion involves T cell circulation, not only during active infection but also for maintenance of protective immune memory after resolution of an infection.

A major goal of vaccination is to safely induce immune memory with a population of antigen-experienced (or memory) T cells that are poised to respond rapidly to a secondary challenge by the microbe. T cell memory not only has circulatory components throughout blood, lymphatic, and peripheral tissue but also a significant proportion of non-circulatory tissue-resident memory cells (T_{RM}) in diverse sites throughout the body. In visceral organs T_{RM} serve as an immune reservoir that sustains durable tissue-autonomous immunity (Wijeyesinghe et al., 2021). This has important implications for

cancer (Molodtsov et al., 2021), human immunodeficiency virus (HIV) (Buggert et al., 2018) and TB vaccine strategies (Perdomo et al., 2016). Hence, mechanistic understanding of T_{RM} responsiveness and longevity are a contemporary focus of immunology research. Considering the facts that TB and HIV are largely comorbid infections (Bruchfeld et al., 2015) where HIV destroys $CD4^+$ T cells thus greatly impairing their responses to *Mtb* infection, as well as clinical trial failures of vaccine candidates designed to generate *Mtb*-specific $CD4^+$ T cell immunity (Ndiaye et al., 2015; M. D. Tameris et al., 2013), this project and its review of the literature focused on $CD8^+$ T_{RM} fate distinction, specification and persistence, particularly in the lungs.

First characterised in 2001 (Masopust et al., 2001; Reinhardt et al., 2001), archetypal $CD8^+$ T_{RM} are a population of T cells that inherit a phenotype which not only grants the ability to permanently reside in non-lymphoid tissue but also specifies their unique function as immune sentinel cells with rapid and effective responses to previously encountered intracellular pathogens (Jiang et al., 2012; Mackay et al., 2012; Shin & Iwasaki, 2012). $CD8^+$ T_{RM} are anatomically poised within barrier tissues at key sites of pathogen entry and infection (Ariotti et al., 2012; Gebhardt et al., 2011) where they secrete pro-inflammatory cytokines and chemokines that recruit natural killer cells, B cells and circulatory memory $CD8^+$ T cells to the site of pathogen re-entry (Ariotti et al., 2014; Schenkel, Fraser, Beura, et al., 2014; Schenkel et al., 2013). The ontogeny of $CD8^+$ T_{RM} from naïve T cell has been elegantly unravelled over two decades with several models of diversification hypothesised throughout this time (Kaech & Cui, 2012; Xu et al., 2023; Yuzefpolskiy et al., 2015) .

1.1.2 Fate Distinction of $CD8^+$ T_{RM}

Following T cell priming by antigen activation, naïve T cells proceed through sequential phases of clonal expansion, contraction, and formation of memory populations, when transcriptional divergence occurs in the first division (Kakaradov et al., 2017). When antigen-specific $CD8^+$ T cells clonally expand, they differentiate into short lived effector cells (SLECs) or memory precursor effector cells (MPECs) (Huster et al., 2004; Joshi et al., 2007; Kaech et al., 2003; Kalia et al., 2010; Sarkar et al., 2008) as they

enter the circulation and lymphatics to migrate to sites of infection. Distinct *in vivo* heterogeneity of killer cell lectin-like receptor G1 (KLRG-1), IL-7 receptor subunit-α (IL-7Rα), CD27, CXC-chemokine receptor 3 (CXCR3) and L selectin (CD62L) expression is strongly associated with diverse SLEC and MPEC fates (Kaech & Cui, 2012; Yuzefpolskiy et al., 2015). Between 2005 and 2015 it was discovered that primed naïve T cells also provide a small subset of stem-like memory T cells (Tscm) with the capacity to self-renew and furnish all future antigen-specific effector and memory T cell subsets (Fuertes Marraco et al., 2015; Oliveira et al., 2015; Zhang et al., 2005).

In the setting of intracellular viral or bacterial infection, a Type 1 immune response is induced which in turn promotes specification of $CD8^+$ T cells into cytotoxic T cells capable of killing infected cells with perforins and granzymes. It has been shown that prolonged antigenic stimulation drives terminal effector differentiation of SLECs through repeated rounds of killing in non-lymphoid tissue. Conversely, MPECs preferentially localise to lymphoid tissues where lower levels of antigen (and more rapid antigen clearing) are thought to direct their specification toward the memory phenotype (Yuzefpolskiy et al., 2015).

After pathogen clearance, effector $CD8^+$ T cell contraction occurs with the majority of SLEC undergoing apoptosis while MPECs survive and mature into distinct memory subsets classified by function, localisation and identified by specific cell surface markers and gene expression profiles. Those that routinely 'patrol' blood and lymphoid tissues are central memory T cells (T_{CM}). $CD8^+$ T_{CM} express CC chemokine receptor 7 (CCR7) and CD62L which provide access to secondary lymphoid organs where they retain capacity to survey for cognate antigens. $CD8^+$ T_{CM} possess a high proliferative potential upon reactivation in lymph nodes and provide a major source of secondary effector cells to expediate pathogen clearance (Sallusto et al., 2004) (**Fig. 1**).

MPEC that fail to receive tissue-instructive signals for residency differentiate into effector memory T cells (T_{EM}) (Iijima & Iwasaki, 2015; Takamura, 2017). $CD8^+$ T_{EM} transit between blood, lymphatics and non-lymphoid barrier tissues such as skin, lung, intestines and female reproductive tract (Masopust &

Picker, 2012) express Kruppel-like transcription factor 2 (KLF2) and tissue exit receptor sphingosine 1–phosphate receptor 1 (S1PR1) to facilitate their migration and exit through tissues back into blood and lymphatics by binding signalling molecule sphingosine 1-phosphate (S1P) (Rosen, 2005). Upon secondary infection, $CD8^+$ T_{EM} exhibit immediate local effector functions while $CD8^+$ T_{CM} undergo extensive clonal expansion in the interim (Sallusto et al., 2004) (**Fig. 1**).

Core T_{RM} genes have been shown to be expressed by a subset of early post-activated T_{EM} (Kok, 2022) thus the fate decision of T_{RM} precursors may occur prior to the effector stage, however, further research is required to validate this. Early Inflammatory signals definitively guide the fate of $CD8^+$ T_{RM}. It is known that lymph node $CD8\alpha^+$ DCs provide signals, including IL-12, IL-15, and co-stimulation via CD24, that contribute to early fate distinction of T_{RM} (Iborra et al., 2016). Inflammatory cytokines also downregulate expression of *KLF2* and upregulate expression of cell surface CD69 and CD49a adhesion molecules (Bankovich et al., 2010; Mackay, Wynne-Jones, et al., 2015). In these early $CD8^+$ T_{RM} precursor cells, gene-expression analysis demonstrated that 90-96% of characteristic genes associated with tissue residency were upregulated and upon entry to non-lymphoid tissue during the effector stage of infection, precursor $CD8^+$ T_{RM} already have a unique chromatin landscape that foreshadows their unique and distinct transcriptional fate (Milner et al., 2017) (**Fig.1**).

1.1.3 $CD8^+$ T_{RM} Specification

Antigen-specific T_{RM} are present in epithelial barrier tissues (skin, lung, intestine, and reproductive tract), non-epithelial tissues (brain, liver, kidneys, pancreas, heart, and dorsal root ganglia) and lymphoid tissues (lymph node, spleen, thymus and bone marrow) (Mueller & Mackay, 2016; Takamura, 2018) where instructive signals for their specification and maintenance differ significantly across various tissues (Christo et al., 2021; Iijima & Iwasaki, 2015).

Absence of chemokine receptor 7 (CCR7) and expression of the C-type lectin cell surface molecule CD69 were first identified as key contributors to tissue resident phenotype of T_{RM} (Sallusto et al., 1999;

Teijaro et al., 2011) as CD69 mediates internalisation and degradation of S1PR1 (Bankovich et al., 2010; Mackay, Braun, et al., 2015) which is attracted to S1P ligand released by blood and lymph endothelial cells. S1P/S1PR1 binding directs memory T cells from tissues back into circulation (Rosen, 2005). Although forced expression of S1PR1 inhibits establishment of tissue residency in memory CD8+ T cells (Skon et al., 2013) and results in the return of precursor T_{RM} cells to circulation (Evrard et al., 2022), parabiosis[1] and CD69 mutant studies have shown that T_{RM} populations that lack CD69 can form (Beura, Wijeyesinghe, et al., 2018; Steinert et al., 2015). As CD69 is expressed early in T_{RM} development, before tissue egress receptors are completely downregulated (Mackay et al 2015, Skon et al, 2013), it is said possible for $CD69^+$ $CD8^+$ T cells to return to circulation. So, not only is the functional requirement for CD69 in generation of T_{RM} tissue specific and highly variable (Walsh et al., 2019), but also, CD69 alone is not a reliable marker for T_{RM} residency (Mackay, Braun, et al., 2015).

Another important cell surface molecule found expressed on most $CD8^+$ T_{RM} is CD103 (Mackay et al., 2013)- the αE subunit of the αE/β7 integrin which binds epithelial E-cadherin at mucosal barrier sites (Pauls et al., 2001). When circulatory T cells are depleted from non-lymphoid tissues, most remaining T cells express CD103 (Mackay, Braun, et al., 2015). These tissue-harboured $CD103^+$ $CD8^+$ memory T cells are resistant to parabiotic equilibration (Wijeyesinghe et al., 2021) and survive in transplanted mouse and human tissues (Gebhardt et al., 2009; Snyder et al., 2019). Blockade of CD103 binding to E-cadherin results in a significant decrease of T_{RM} (Y. T. Lee et al., 2011; Mackay et al., 2013; Sheridan et al., 2014; Zaid et al., 2017) and E cadherin ligand adherence is thought to play a role in the initial

[1] Parabiosis is the conjoining of vasculature between two mice used to test for T_{RM} residence as compared to circulatory T cells that equilibrate between the two parabionts.

accumulation of T_{RM} in non-lymphoid tissues (Reilly et al., 2020). Like CD69, CD103 expression is not mandatory for all T_{RM} residency programs (Casey et al., 2012; Topham et al., 2019), however, $CD103^+$ $CD8^+$ tissue T cells are identified as the archetypal T_{RM} (Carbone, 2023).

Comparative gene expression amongst a variety of tissue $CD103^+$ $CD8^+$ T_{RM} populations demonstrated that Eomesodermin (Eomes) was significantly downregulated in T_{RM} as opposed to circulatory memory T cells (Mackay et al., 2013). Further examination of the roles of both T-box transcription factors (TF) Eomes and T-bet showed that down-regulation of both TFs was required for T_{RM} differentiation while forced expression of both TFs inhibited formation of T_{RM} in the skin (Mackay, Braun, et al., 2015). While Eomes expression is terminated in mature T_{RM}, residual T-bet expression is required for surface expression of the IL-15R β-chain. As IL-15 signalling is also requisite for T_{RM} differentiation, Eomes and T-bet expression is tightly regulated in T_{RM} (Mackay, Braun, et al., 2015).

Another TF specific to T_{RM} is Hobit; homologous to TF Blimp-1, both regulate the tissue residency program of numerous populations of tissue T_{RM} (Mackay et al., 2016; Wakim et al., 2012). Hobit and Blimp-1 co-coordinate termination of the tissue exit pathways of CCR7 and S1PR1 (Mackay et al., 2016) by direct competitive binding to *KLF2* (drives expression of S1PR1) and *Tcf7* loci (upregulates CD62L and CCR7) as well as binding downstream target loci of S1PR1 and CCR7 (Mackay et al., 2016; Skon et al., 2013). It has long been known that TF Runx3 has a crucial role in the cytotoxic activity of mature $CD8^+$ T cells (Cruz-Guilloty et al., 2009; Shan et al., 2017) and it is now known that Runx3 is a master regulator of T_{RM} differentiation and homeostasis. Retroviral microRNA-adapted short hairpin RNA to suppress *Runx3* expression and a tamoxifen-inducible deletion of *Runx3,* demonstrated a 50-150-fold decrease in $CD69^+$ $CD103^+$ T_{RM} in two independent infection mouse vaccinations in both barrier (enteric) and non-barrier (salivary gland and kidney) tissues (Milner et al., 2017). Consistent with other reports of Runx3 regulation of CD103 (Grueter et al., 2005; Reis et al., 2013) ectopic expression of Runx3 was shown to accelerate T_{RM} differentiation, enhance CD103 expression and significantly increase T_{RM} numbers. In cells that over-expressed Runx3, core T_{RM} tissue residency genes were up-

regulated whereas in *Runx3*-deficient cells, these were downregulated (Milner et al., 2017).

The tissue milieu of infection provides factors associated with metabolite availability and cytokines required for T_{RM} differentiation; of these, TGF-β is obligatory. TGF-β is a family of regulatory cytokines consisting of three members- TGF-β1, TGF-β2 and TGF-β3 where TGF-β1 is the predominant cytokine related to immune function (Li et al., 2006). TGF-β is produced as a precursor protein which is further processed in the Golgi as a latent protein (LAP) which may be secreted or associated with a latent TGF-β binding protein (LTBP) incorporated into the extracellular matrix (Robertson et al., 2015). TGF-β cannot bind its receptor when in latent form but requires liberation from the LAP and LTBP to become active (Robertson et al., 2015; Shi et al., 2011). Active TGF-β binds to TGF-β type I and type II serine/threonine receptor complexes to initiate Smad or Smad-independent signalling pathways and further complex with TFs in order to regulate target gene expression (Li & Flavell, 2008).

$CD8^+$ T_{RM} with mutant TGF-β receptors unable to bind TGF-β do not upregulate CD103 and do not establish residency in non-lymphoid tissue (Casey et al., 2012; Y. T. Lee et al., 2011; Mackay et al., 2013; Sheridan et al., 2014; Zhang & Bevan, 2013). Furthermore, continuous signalling by TGF-β is necessary for long-term maintenance of $CD8^+$ T_{RM} in non-lymphoid tissue (Ma et al., 2017; Mohammed et al., 2016). $CD8^+$ T cells stimulated *in vitro* with TGF-β and profiled using RNA sequencing (RNAseq) demonstrated that a large part of the $CD8^+$ T_{RM} transcriptome (including CD103 and CD49a) is attributed to TGF-β signalling (Nath et al., 2019). TGF-β receptor signalling causes initiation of the core transcriptional network including Klf2, Hobit, and Runx3 in precursor $CD8^+$ T_{RM} (Casey et al., 2012; Mackay et al., 2013; Sheridan et al., 2014; Skon et al., 2013; Zhang & Bevan, 2013) leading to the total maturation of $CD103^+$ $CD8^+$ T_{RM} (Christo et al., 2021; Hirai et al., 2021) (**Fig. 1**).

1.1.4 $CD8^+$ T_{RM} Function and Persistence

$CD8^+$ T_{RM} are spatially and temporally poised in tissues as first-responders to reinfection with a more rapid, powerful, and sensitive ability compared to innate immune cells to induce and recruit bystander

immune cells to the reinfection. When $CD8^+$ T_{RM} of the female reproductive tract (FRT) encountered their cognate antigen, their rapid and robust secretion of interferon gamma (IFN-λ) led to a timely accumulation of resting memory $CD8^+$ T cells from spleen and blood (Schenkel et al., 2013). In this FRT vaccination, a fraction of bystander $CD8^+$ T_{EM} and T_{CM} cells recruited to the site of reinfection by $CD8^+$ T_{RM} upregulated CD69 but not CD103 and persisted at the site of recruitment for longer than 75 days. This indicated that circulatory memory T cells retain developmental potential to differentiate into $CD8^+$ T_{RM} following periodic reinfection (Beura, Mitchell, et al., 2018) and that their phenotypic diversion is linked to the sentinel functions of reactivated $CD8^+$ T_{RM}. Other than their 'sense and alarm' role in this vaccination, $CD8^+$ T_{RM} were also demonstrated to *actively* survey the FRT. Using two-photon microscopy of live female mice, it was visualized that local reactivation of $CD8^+$ T_{RM} with cognate antigen arrested 25% of highly motile cells as they underwent proliferation before regaining motility following cytokinesis (Beura, Mitchell, et al., 2018).

More than reactivation of the acquired immune response to previously recognised antigens/pathogens, $CD8^+$ T_{RM} are potent inducers of the innate immune response with a role in DC maturation and granzyme B upregulation in natural killer cells through secretion of cytokine interleukin-2 (IL-2) and tumour necrosis factor alpha (TNFα) within 12 hours of local reactivation (Schenkel, Fraser, Beura, et al., 2014). Importantly, $CD8^+$ T_{RM} of the gut are also known to trigger an 'organ-wide antiviral state' through functional upregulation of antiviral interferon (IFN)- responsive genes in local epithelial cells attributed to their production of type I, II and III IFNs which rendered the epithelial cells resistant to murine norovirus within 40 hours of gastrointestinal infection (Swamy et al., 2015). Thus $CD8^+$ T_{RM} function as sensory cells for previously encountered intracellular pathogens and they communicate re-entry of pathogens to innate and acquired immune cells as well as non-immune cells.

1.1.5 Ex-$CD8^+$ T_{RM}

It was originally thought that $CD8^+$ T_{RM} were terminally differentiated, permanent residents of the non-

lymphoid tissue in which they develop, however, a growing body of literature has shown that they not only retain developmental plasticity but also have the capacity to recirculate in blood, rehome to lymph nodes and other non-lymphoid tissues (including the tissue of their origin) as well as give rise to both $CD8^+$ T_{CM} and T_{EM}.

Recall that $CD8^+$ T_{RM} have a unique transcriptional profile which is postulated to be acquired initially in the lymph node and then further in response to inductive cues upon migration into non-lymphoid tissues. As T_{RM} were not *originally* thought to patrol secondary lymphoid organs (SLO) (Mackay et al., 2012) their bona fide residence (demonstrated by parabiosis) in SLO of mice (Schenkel, Fraser, & Masopust, 2014) disclosed gaps in the knowledge of T_{RM}. Several studies using *in situ* antigen stimulation via peptide challenge have demonstrated that secondary antigen exposure of T_{RM} at barrier non-lymphoid sites can cause progeny T_{RM} to gain access to draining lymph nodes during the activation stage of the secondary immune response leading to abundant numbers of antigen-specific $CD8^+$ T_{RM} in draining lymph nodes (Beura, Wijeyesinghe, et al., 2018; Fonseca et al., 2020; Stolley et al., 2020). Fonseca et al. further demonstrated that after local reactivation of $CD8^+$ T_{RM} in skin, 'displaced residents' were observed in draining lymph nodes with progeny $CD8^+$ T_{CM} and T_{EM} found in distant lymph nodes. In this study it was revealed that T_{RM} share a phenotypic signature close to recently activated effector T cells while at the epigenetic level they share similarities to resting memory T cells (such as T_{CM}) and their developmental potential is comparable to $CD8^+$ T cells that have not undergone terminal differentiation. Importantly, while durable maintenance of $CD8^+$ T_{RM} has been demonstrated in mice within most non-lymphoid tissues, dislodged circulatory ex-T_{RM} are thought able to contribute back to long term maintenance of memory in tissues with high attrition of T_{RM} such as liver, kidney and lung (Wijeyesinghe et al., 2021).

1.1.6 Chronic Antigen Leads to Stem-like $CD8^+$ T cells that Differentiate into T_{RM}

Persistence of antigen and exposure to chronic antigen stimulation in unresolved infections such as HIV, hepatitis C virus, Epstein Barr virus and TB causes $CD8^+$ T_{CM} and T_{EM} cell exhaustion resulting in a

transcriptional and epigenetic differentiation into cells with poor proliferation and effector function linked to dysregulated cytokine production, metabolism and overexpression of inhibitory receptors, such as programmed cell death protein 1 (PD-1) (Barber et al., 2006). PD-1 regulates $CD8^+$ T cell exhaustion as interaction with cognate ligands PD-L1 and PD-L2 inhibits activation of T cells and cytokine production while blockade of its inhibitory pathway augments T cell function during chronic infections and cancer (Sharma & Allison, 2015).

Despite chronic antigen stimulation, however, subsets of $CD8^+$ T cells become resident in SLO that retain a proliferative capability and can restrain chronic viral infection (Paley et al., 2012). *TCF7* encodes transcription factor T-cell factor 1 (Tcf1) that has an essential role in maintenance of protective immunity following acute infection; therefore, it was thought that its role may extend during chronic infection. Using a Tcf1 reporter mouse strain and *Tcf7*-null mice, a subpopulation of $Tcf1^+$ $CD8^+$ T cells necessary for re-expansion of antigen-specific $CD8^+$ T cells during chronic lymphocytic choriomeningitis virus (LCMV) infection was identified. $Tcf1^+$ $CD8^+$ T cells resemble T_{CM} in terms of proliferation potential, but their progeny has an exhausted PD-1^+ T_{EM} phenotype (Utzschneider et al., 2016). Wu *et al.* demonstrated that when $CD8^+$ T cells are chronically stimulated with antigen they differentiate into a $TCF1_{high}$ $CD8^+$ T cell that express lower levels of exhaustion markers, such as Tim3, and act as progenitor cells resident within SLO whose progeny terminally differentiate into $TCF1_{low}$ $Tim3_{high}$ $CD8^+$ T cells that will eventually exhaust after re-circulation. $TCF1_{high}$ $CD8^+$ T cells were also shown to persist longer as SLO residents than their $TCF1_{low}$ $CD8^+$ T cell progeny (Wu et al., 2016).

This novel 'less exhausted' virus-specific $CD8^+$ T cell subset is located solely in lymphoid tissue, characterized by a gene signature related to $CD8^+$ T memory precursors and hematopoietic stem cells, express CXCR5 and are able to proliferate following PD-1 blockade, self-renew and provide a burst of T cells with effector potential thus functioning as memory stem cells during chronic viral infection (Im et al., 2016). As CXCR5 directs T cells to secondary B-cell follicles in the lymph nodes and spleen, virus-specific $CXCR5^+CD8^+$ T cells transferred into B cell-deficient mice were poorly maintained indicating

that the less exhausted stem-like memory $CD8^+$ T cells are housed in B-cell follicles. This was supported by the finding that HIV-specific $CXCR5^+CD8^+$ T cells were found in the B-cell follicles of lymph nodes in persons with chronic HIV infection (He et al., 2016). Further characterization went on to describe these stem-like memory PD-$1^+Tcf1^+CXCR5^+$ T cells as cells that fail to recirculate following parabiosis, have high levels of CD69 expression (with low expression of *S1pr1)* and are resident T_{RM} in SLO (Im et al., 2020). Interestingly, $Tcf1^+PD1^+$ stem-like $CD8^+$ T cells have a distinct transcriptome and epigenome from both effector and memory $CD8^+$ T cells of acute infection (Beltra et al., 2020; Jadhav et al., 2019), with the locus for granzyme B silenced (Jadhav et al., 2019) indicative of their adaptation to chronic antigen stimulation. This adaptation has been aptly described as 'an altered differentiation program that provides some restrain on pathogen replication yet limits immunopathology. This adaptation is imprinted in stem-like cells and propagated to their progeny' (Ozga et al., 2022)

Knowledge of the molecular and cellular causes of T cell exhaustion as opposed to the antagonism of exhaustion have paved the way for therapies that seek to 'invigorate' stem-like $CD8^+$ T_{RM} cells in persons with cancer. Tumour-specific $CXCR5^+Tim3^-$ with a partially exhausted phenotype have been seen infiltrating tumours (Brummelman et al., 2018), while in ovarian cancer, $TCF1_{high}$ T_{RM} stem-like $CD8^+$ T cells (and not their re-circulatory $TCF1_{low}$ progeny) predict enhanced survival (Anadon et al., 2022). A mouse melanoma vaccination demonstrated that tumour-draining lymph nodes harbour antigen- experienced stem-like $Tcf1^+CD8^+$ T cells that differentiate into $CD69^+$ $CD103^+$ T_{RM} in a TGF-β - dependent manner with the percentage of T_{RM} directly related to the size and late stage of the tumour. It was further deciphered that $CD4^+$ T cell help, TGF-β and persistent antigen collectively contributed to differentiation of antigen- experienced stem-like $Tcf1^+CD8^+$ T cells into mature $T_{RM.}$ Adoptive-transfer of *TGF-βR2*$^{-/-}$ $CD8^+$ T cells, followed by subcutaneous tumour cell inoculation and subsequent anti-melanoma vaccine administration led to a significantly lower number of stem-like $Tcf1^+CD8^+$ T cells with enhanced differentiation of $CD8^+$ T_{EM}. These findings suggest that T_{RM} differentiation in tumour-draining lymph nodes is late tumour-stage dependent (linked to chronic antigen stimulation), and that early vaccine augments anti-tumour immunity before stem-like $Tcf1^+CD8^+$ T cell tissue

residency is fully established in tumour-draining lymph nodes (Z. Li et al., 2022)(**Fig. 1**).

In chronic *Mtb* infection, prolonged overexposure to antigens also causes T cells to lose effector functions and exhibit an exhausted phenotype (Pan et al., 2023) including expression of PD-1 (Jayaraman et al., 2016) while anti-TB therapy promotes reduced expression of PD-1 and its ligands (Bandaru et al., 2014; Hassan et al., 2015). Compared with mice that received transient *Mtb* antigen stimulation (boosted twice), mice that received persistent antigen stimulation (boosted > 10 times) showed a reduction of memory $CD8^+$ T cells, over-expression of PD-1 and impaired protective immunity against bacterial challenge induced by T cell dysfunction (Liu et al., 2022). Although there are ample research findings that discuss exhaustion of $CD8^+$ T cells in both chronic and latent *Mtb* infection, a Boolean search in Pubmed of the literature using combinations of the terms "Tcf1" OR "CXCR5" OR "stem-like $CD8^+$ T cell" AND *"Mtb"* OR *"BCG"* OR *"t*uberculosis" did not bring up any research studies investigating the development of Tcf1+CXCR5+ stem-like $CD8^+$ T cells or their T_{RM} differentiated progeny in chronic or latent TB infection.

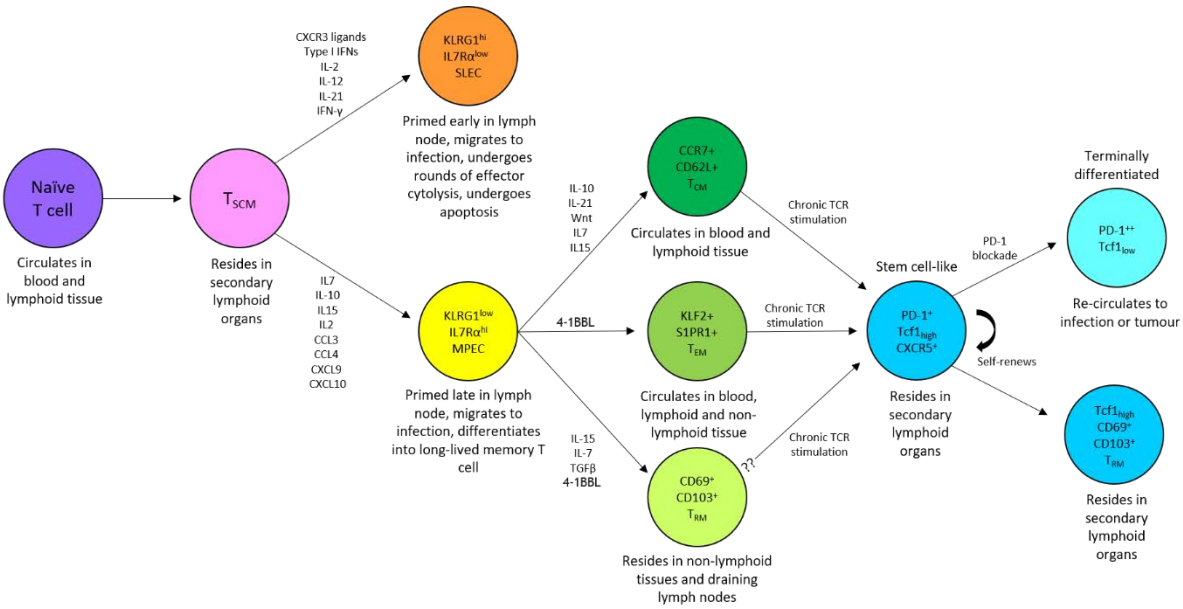

Figure 1. **Specification and development of $CD8^+$ T_{RM} and stimuli that drives differentiation.**

1.2 Development and Persistence of Lung $CD8^+$ T_{RM}

Not many years ago, there was lofty optimism that 'vaccine induced $CD8^+$ T_{RM} against *Mtb* could be established against the backdrop of existing T_{RM} to protect a large organ such as the lung' (Ogongo 2019). Alas, lung $CD8^+$ T_{RM} are now known to have a distinctive development and *lack* of endurance as compared to other tissues which is best understood in context with the harsh environment of the conducting airways, the highly vascularised, thin-walled distal parenchyma and the expansive surface area necessary for gas exchange. This pulmonary architecture has been theorised to be non-conducive to a permanent anatomical niche for $CD8^+$ T_{RM} from which to function, such as that known for skin, for example. Undeniably, lung $CD8^+$ T_{RM} have unique organ-specific mechanisms for maturation, persistence, and egress by which 'the complexity of this system and interdependence between the various components and changes that affect parameters such as the timing of T-box TF modulation and the coordination with TGF-β availability would have a profound effect on T_{RM} cell maturation' (Mackay 2015).

1.2.1 The Structure and Histology of the Normal Lung

Please note that it is out of the scope of this review to discuss all pulmonary cell types but is focused on those that are relevant for sake of understanding the present project goals.

The intrapulmonary airways are those entering the lungs that transition from the bronchus to bronchiole. The first bronchioles are purely conductive; the last distal bronchioles (or acinus) have alveoli opening directly off them and thus are respiratory bronchioles that participate in gas exchange. Histologically, proximal epithelium of primary airways is pseudostratified where all cells rest on the basement membrane, but many do not reach the lumen. Here, epithelial cells are columnar and ciliated and interposed with mucous cells, neuroendocrine cells, basal cells, brush cells, nerve terminals and migratory lymphocytes and mast cells.

Distal bronchioles are composed of cuboidal epithelium consisting of ciliated, club, brush, mucous, neuroendocrine, and basal cells. Ciliated cells have microvilli and cilia that pulse synchronously and co-ordinate with secretory cells for effective mucociliary clearance of particulate matter (Yoshisue et al., 2004). Club cells are most abundant in terminal bronchioles where they extend above ciliated cells into the airway lumen to secrete secretoglobin 1A1 (Scgb1a1) also known as CC10 which inhibits inflammatory cytokines and thus modulates bronchiolar inflammation (Hay et al., 1995; Nie et al., 2013). Brush cells occur infrequently throughout the airways; they have closely packed microvilli possibly related to fluid absorption (Reid et al., 2005). Mucous cells function through cycles of secretory activity to excrete mucus into the airways (Lillehoj et al., 2013). Neuroendocrine cells occur singly or in groups known as neuroepithelial bodies; they control lung development in embryogenesis and have a regulatory role of pulmonary regeneration (Noguchi et al., 2020). Basal cells are located primarily in large proximal airways and diminish in number distally within bronchioles, in both human and mouse. Their principal function is adhesion of the columnar and cuboidal epithelial cells to the basement membrane (Ruysseveldt et al., 2021) (**Fig. 2**).

Distal to bronchioles, terminal bronchioles lead to respiratory bronchioles that have alveoli opening directly off them via alveolar ducts; here is the merging point of cuboidal airway epithelium with squamous alveolar epithelium. Alveoli are polyhedral-like boxes with one open side which enables stretch on inspiration without occlusion of alveolar capillaries; alveoli are structurally comprised of two types of epithelial cells. Type 1 alveolar epithelial cells (AEC1) are very fine cells that cover the largest portion of alveolar surface to facilitate rapid gas exchange and prevent fluid loss (**Fig. 2**). Type 2 alveolar epithelial cells (AEC2) are twice as numerous yet cover a small percentage of the alveolar surface in adult mammals. Typically situated in corners of alveoli, the AEC2 free surface has apical blunt microvilli and openings through which pulmonary surfactant is secreted to prevent alveolar collapse due to the polar surface tension of water inside the alveolar space (Whitsett & Weaver, 2015) (**Fig. 2**).

1.2.2 Specification of Lung $CD8^+$ T_{RM}

There are indications of mechanisms involved in preferential generation of memory T cells in the acute phase of lung influenza infection. For example, $CD103^+$ DCs migrate from lung to mediastinal lymph node and prime during the early stage of infection (Kim & Braciale, 2009) to activate potent effectors (GeurtsvanKessel et al., 2008) while CD11b respiratory DCs migrate and prime later in the infection (Kim & Braciale, 2009) when it is thought that their weaker stimulatory potential preferentially generates a memory $CD8^+$ T cell population that persists in secondary lymphoid organs (Kim et al., 2014), in line with that reported by Yuzefpolskiy (Yuzefpolskiy et al., 2015).

Using an influenza virus mouse vaccination, the kinetics of $CD8^+$ T_{RM} specification during the expansion phase of the T cell response showed that CD69 is upregulated in the mediastinal lymph node by recently activated T cells and precedes their migration into the lungs (Eriksson et al., 2022). When $CD69^-$ $CD8^+$ T_{RM} cells are transferred to recipient naïve mice prior to influenza infection, T cells that lack CD69 expression fail to reach the lung mucosa efficiently after infection (Y. T. Lee et al., 2011; Walsh et al., 2019). At 8 days post-influenza infection in mice, in the expansion phase of T cell responses, a dominant subset of migratory (Reilly et al., 2020) $CD8^+$ $CD103^-$ $CD49a^+$ T cells coincides with the height of infection (Eriksson et al., 2022; Haddadi et al., 2017). CD49a binds interstitial collagen I (Bank et al., 1994) where it has been shown to facilitate cell motility both *in vitro* and *in vivo* (Reilly et al., 2020). These cells acquire CD49a expression before they home to the lung and become further enriched for CD49a expression in the contraction and memory phases (Haddadi et al., 2017). CD49a blockade leads to an increase of vaccine-activated T cells in the contraction phase of post-infection, in line with its key negative regulatory role of T cell numbers and responses in the lung at that time. CD49a blockade in the memory phase of post-infection has no effect on frequency or numbers of $CD8^+$ T_{RM} and is thus dispensable for $CD8^+$ T_{RM} maintenance (Haddadi et al., 2017).

In contrast to CD49a, following mucosal infection with either influenza or an adenoviral-vectored TB vaccine in mice, a small proportion of $CD8^+$ T cells express CD103 during the effector and expansion

phase of T cell responses. CD103 expression, however, increases significantly over the contraction and into the memory phases and from the memory phase onward, the dominant T_{RM} is $CD8^+CD103^+CD49a^+$ (Eriksson et al., 2022; Haddadi et al., 2017). CD103 expression is acquired in the lung (Lee 2011; Wakim, 2015) and $CD8^+CD103^+CD49a^+$ T_{RM} lodge and survey interstitium and epithelium after clearance of influenza virus owing to the binding capacities of CD103 to epithelial E-cadherin and CD49a to basal lamina collagen IV. Whether the origin of $CD8^+CD103^+CD49a^+$ T_{RM} are $CD8^+CD103^-CD49a^+$ cells that reach the epithelium (and therefore upregulate CD103) or the two cell types are distinct, remains unknown.

A third subset of $CD8^+CD103^+CD69^+CD49a^-$ airway epithelial effector $CD8^+$ T_{RM} (Topham et al., 2019) do not expand significantly after influenza infection of mice (Eriksson et al., 2022) and are specified transcriptionally and epigenetically by environmental cues (eg hypoxia and glucose starvation) for sole lodgement within airway epithelium where they are fated for apoptosis (Hayward et al., 2020). Thus, three distinct subsets of lung $CD8^+$ T_{RM} have been characterised where the primary cell surface proteins that specify their residency program throughout the expansion, contraction and memory phases of infection are CD69, CD49a and CD103 (Topham et al., 2019). CD103 and CD49a proteins have also been characterised on *Mtb*-specific $CD8^+$ T_{RM} (Perdomo et al., 2016).

Development of $CD8^+$ T_{RM} subsets in the lung are heavily dependent on cues from the local microenvironment received from local cognate antigen recognition, cellular interactions, and the cytokine milieu (Zheng & Wakim 2022). Mice infected intranasally with either an influenza virus or flu strain engineered to express the antigen OVA and subsequently inoculated with OVA-specific activated OT-I $CD8^+$ T cells demonstrated that only mice that received the influenza-OVA contained OT-I $CD8^+CD103^+$ T_{RM} (Wakim et al., 2015). This proved that once in the lungs, local cognate antigen recognition is necessary to drive differentiation of $CD8^+$ effector T cells to pulmonary $CD8^+$ T_{RM}.

Takamura *et al*. (Takamura et al., 2016) demonstrated that antigen-independent inflammation recruited $CD8^+$ T cells to the lungs, however, they completely disappeared upon resolution of

inflammation. In contrast, combination of local inflammation and cognate antigen robustly promoted T_{RM} development. They purported that antigenic and inflammatory signals, redundant early in infection, bias $CD8^+$ T cell differentiation toward terminal effector cells, while weak signalling later promotes memory differentiation. This is in line with the theory that activated T cells may be pre-committed as SLEC or MPEC before recruitment to the lung, while terminal differentiation to effector or memory cells, respectively, is secured following local reactivation (Joshi et al., 2007; Mackay et al., 2013; Yuzefpolskiy et al., 2015).

CXCR3 chemokine receptor has a key role in recruitment of effector $CD8^+$ T cells to the interstitium and airway (Abboud et al., 2016) as does IL-15 produced by $CD11b^+$ macrophages in the lung interstitium (Verbist et al., 2011; Yoshizawa et al., 2018). Local inflammatory cytokines type I IFN, IL-33 and TNF-α downregulate expression of *KLF2* and upregulate expression of key cell surface molecule CD69 (Skon et al., 2013) and activate CD49a to promote $CD8^+$ retention in lung interstitium (Ray et al., 2004; Takamura et al., 2016). The transcriptional control of T cell residency in mouse lung is under direct regulation of TGF-β where local exposure to the cytokine is necessary for CD103 expression (L. N. Lee et al., 2011; Wakim et al., 2015), causes downregulation of T-bet and Eomes (Mackay, Wynne-Jones, et al., 2015) and promotes localisation along the walls of small airways (Wu et al., 2014). Mice seeded with naïve OT-I T cells deficient in expression of TGF-β receptor showed that following infection with flu-OVA, OT-I T cells failed to upregulate CD103 (Wakim et al., 2015). Virus-specific $CD8^+$ T cells harbouring a dominant-negative form of TGF-β receptor II (under the control of a T cell specific promotor) demonstrated that following transfer into naïve mice, a significantly smaller percentage of cells that reached the lungs of recipient mice expressed CD103 (L. N. Lee et al., 2011). Phenotypic analysis of these cells indicated a preferential loss of CD69 which illustrated that recently activated T cells respond to TGF-β derived signals by upregulation of CD103 to prevent egress of $CD69^+CD8^+$ T cells from the lungs in early infection (L. N. Lee et al., 2011).

Laidlaw *et al*. (Laidlaw et al., 2014) demonstrated a critical role for $CD4^+$ T cells of mice in the acute

phase of influenza infection as ablation of CD4 help resulted in $CD8^+$ T_{RM} that were not only displaced from airway epithelia but also had an impaired ability to upregulate granzyme B following challenge. CD4 T cell-secreted IFNγ was theorised to prime the lung parenchyma for optimal influx of $CD8^+$ T_{RM} precursors and subsequent exposure to local TGF-β. Their work demonstrated that TGF-β promotes T-bet downregulation which releases the *CD103* locus from transcriptional repression. Loss of $CD4^+$ T cells resulted in impairment of T_{RM} to upregulate CD103, CXCR3 and CD69. Interestingly, CD4 help was only required during the early phase of T_{RM} development, with elimination of $CD4^+$ T cells having little impact after T_{RM} specification. Lastly, using virus-specific mouse $CD8^+$ T cells that lack TGF-β receptors, it has been shown in influenza challenge experiments that the size of the $KLRG1^+$ T effector population increased while $CD103^+$ T_{RM} were completely absent (Hu et al., 2018).

1.2.3 Persistence of Lung $CD8^+$ T_{RM}

Following resolution of viral and mycobacterial respiratory infections in mice, large numbers of antigen specific $CD8^+$ T_{RM} persist in both the airways and parenchyma (Hogan et al., 2002; Perdomo et al., 2016) and both populations are capable of mediating limitation of secondary infection (Hogan et al., 2001; McMaster et al., 2015; Perdomo et al., 2016; Roberts & Woodland, 2004; Wu et al., 2014). Initially, it was proposed that lung $CD8^+$ T_{RM} are maintained by continual recruitment from circulatory memory T cells, rather than survival- or cytokine-driven homeostatic proliferation within the lung itself (Ely et al., 2006). A vaccination arose in which it was described that reactivation of circulatory memory T cells by residual antigen in the mediastinal lymph nodes was required for continual precursor T_{RM} recruitment and residence in lung (Zammit et al., 2006). Using intravenous staining (to mark circulatory T cells) coupled with parabiosis following intranasal administration of influenza in mice, this concept was challenged (Takamura et al., 2016). Results described distinct populations of pulmonary $CD8^+$ T_{RM} and their *de novo* niches that form following influenza infection in mice. Referred to as repair-associated memory depots (RAMDs), these regenerative parenchymal niches are segregated from lymphatic-rich regions, conventional inducible bronchus-associated lymphoid tissue and lack $CD8^+$ T_{EM}. Enriched for

$CD8^+$ T_{RM}, RAMDs are described as 'peribronchiolar foci of lymphocytic infiltrates surrounded by aggregates of cytokeratin-expressing basal (progenitor) cells within thickened adjacent alveolar walls' (Takamura et al, 2016).

Their work further demonstrated that 2-7 weeks following influenza infection in mice, memory $CD8^+$ T cells in distal lung consist of a major population (~80%) in parenchymal RAMDs and abutting airways that are highly activated and have a resident memory phenotype. They described the minor population (~20%) as T_{EM} that have not been reactivated by antigen, retain S1PR1 expression and are able to transit through the interstitium either into the circulation in response to S1P or into the airways in response to CXCR3. Using a timed parabiosis approach they demonstrated that T_{EM} recruited to the lung later than the peak of T cell effector response (around day 10 post influenza virus infection) fail to occupy the RAMD niche or become T_{RM} (Takamura et al., 2016).

In mice, further characterisation of $CD8^+$ T_{RM} of parenchymal RAMDs and those that migrate to become tethered in airway epithelium unveiled that they are phenotypically and functionally distinct. $CD8^+$ T_{RM} of RAMDs are known to be stable several months after recovery from viral infection and although relatively quiescent, undergo homeostatic self-renewal within the RAMD. RAMD $CD8^+$ T_{RM} have significant production of granzyme B, IFNγ and TNFα when stimulated *in vitro* compared with airway tethered $CD8^+$ T_{RM} (Takamura et al., 2019). RAMD T_{RM} have increased expression of CXCR6 (a chemokine receptor that regulates T cell migration) compared to airway T_{RM} or T_{EM}. CXCL16, chemokine ligand for CXCR6, is widely expressed in alveolar epithelium where it is theorised to guide RAMD T_{RM} to airways. Indeed, blockade or genetic deletion of CXCL16 led to decreased numbers of virus-specific airway $CD8^+$ $T_{RM.}$ (Wein et al., 2019). Collectively, research supports a vaccination where airway T_{RM} are recruited from a pool of self-renewing RAMD-associated T_{RM} rather than the circulation (Takamura et al., 2019) and residual antigen-driven reactivation in the mediastinal lymph node independently drives continual recruitment of T_{EM} to the lung several months after infection (Slutter et al., 2017; Zammit et al., 2006). In mice, once localised in the airway epithelium, airway T_{RM} lose proliferative capacity

(Takamura et al., 2016), downregulate integrin LFA-1, lose cytolytic function (Ely et al., 2006; Hogan et al., 2001) but retain ability to produce IFNγ (McMaster et al., 2015; Perdomo et al., 2016).

1.2.4 Attrition of Lung CD8$^+$ T_{RM}

Another characteristic of pulmonary CD8$^+$ T_{RM} is that they wane over a short time (Hogan et al., 2001; Jozwik et al., 2015; Slutter et al., 2017; Wu et al., 2014) and cell-mediated protective immunity is lost in the lungs of mice 4-6 months post-infection (Perdomo et al., 2016; Takamura, 2017; Wu et al., 2014). This is unique in that in several other tissue types, T_{RM} persist for many years (Takamura, 2018). First-line airway CD8$^+$ T_{RM} are subjected to the harsh airway environment and mechanics of the mucociliary elevator, and this has been shown to contribute to their short-life span (Ely et al., 2006; Hayward et al., 2020; Perdomo et al., 2016; Slutter et al., 2017). It is intuitive that over the lifespan of a human whose lungs encounter a myriad of respiratory pathogens, numerous depots of accumulative parenchymal CD8$^+$ T_{RM} could be deleterious for the delicate architecture of the lung and the surface area required for efficient gas exchange. It has also been suggested that waning of local immune memory in lung is an organ-intrinsic protective mechanism which safeguards against the potential of CD8$^+$ T_{RM} in successive infections to mediate considerable tissue damage (Carbone, 2023; Stolley et al., 2020) as was seen in persons with successive SARS-CoV-2 infections (Hu et al., 2021; Merad & Martin, 2020).

It has been shown that the waning of lung T_{RM} following influenza infection may also be attributed to their migration via the lymphatics to the draining mediastinal lymph node (mLN) where they retain residency markers and resist parabiotic equilibration. mLN T_{RM} were shown to persist for 4 months after clearance of infection, retained cytolytic function, and were not senescent but able to proliferate following *in vitro* restimulation or secondary infection (Stolley et al., 2020). Explanations of this peculiar phenomenon of lung T_{RM} to egress to the draining mLN are that the intensity of tissue damage due to influenza infection may physically 'dislodge' T_{RM} into draining lymphatics; alternatively, a lack of tonic TGF-β signalling results in an immature CD103$^-$ phenotype that favours egress to the mLN

(Carbone, 2023). Again, it could also be a lung-specific mechanism to protect the delicate and functionally vital architecture of the lungs from ongoing cytolysis and yet provide a robust regional (rather than local) immune memory arsenal. In any case, many questions remain. What mechanisms are linked to T_{RM} egression from lung? What is the specific function of mLN T_{RM}? If reactivated, do mLN T_{RM} migrate back to the lung to function as lung T_{RM} again? Do mLN T_{RM} lose residency overtime to re-join the circulation? Could antigen-specific mLN T_{RM} be harnessed for improved anti-TB immunisation?

1.2.5 Lung $CD8^+$ T_{RM} Response to Mycobacteria

There are relatively few studies that have investigated the development, responses, and maintenance of *Mtb*- or BCG-specific $CD8^+$ T_{RM} in the lungs, which may be primarily linked to the supposition that $CD4^+$ T cells confer superior protection against *Mtb* (Flynn et al., 1993; Ndiaye et al., 2015; O'Garra et al., 2013; Sakai et al., 2014; M. Tameris et al., 2013). As stated previously, impairment of $CD4^+$ T cell responses and overall $CD4^+$ cell losses associated with HIV, however, greatly diminish the practicality of $CD4^+$ and $CD4^+$ T_{RM} targeted TB vaccine candidates. Therefore, this review of the $CD8^+$ T_{RM} responses to mycobacteria is limited to scarce studies.

Early studies blocked peripheral T-cell recruitment during mycobacterial challenge infection after vaccination as a way of demonstrating the importance of T_{RM}, although $CD8^+$ T_{RM} were not characterised per se (Connor et al., 2010). Perdomo *et al.* (Perdomo et al., 2016) found that intratracheal (IT) and intranasal (IN) BCG vaccination enhanced generation of $CD8^+$ T_{RM} and when adoptively transferred from the airway of vaccinated mice into naïve mice showed improved protection against *Mtb* challenge compared to subcutaneous (SC) delivery of BCG and subsequent adoptive transfer into naïve mice. These findings have been recently supported by a study of IN vaccination with BCG which induced $CD8^+$ T_{RM} throughout the upper and lower respiratory tract and IN vaccinated animals had superior protection against *Mtb* challenge compared to control animals (Wu et al., 2021).

Hu *et al.* showed that 2 weeks following IN vaccination with a Sendai virus- vectored TB vaccine, $CD8^+$ T_{RM} IFN-γ responses were strong in the mLN yet weak in the lung and spleen compared to lung $CD8^+$ T_{RM} IFN-γ responses from the SC BCG vaccinated group. At 8 weeks however, numbers of lung $CD8^+$ T_{RM} had diminished in the SC BCG group while those from the Sendai-vectored vaccine had increased; $CD8^+$ T_{RM} IFN-γ responses were also reversed compared to 2 weeks after vaccination. Only the lung $CD8^+$ T_{RM} of the Sendai-vectored vaccine group had rapid and strong antigen-specific responses against *Mtb* challenge. Further, a SC BCG prime and IN Sendai- vector boost vaccination approach significantly enhanced protection against *Mtb* challenge compared to SC BCG vaccination alone. This protection was lost when $CD8^+$ T_{RM} were depleted, which was not the case in the SC BCG vaccinated group (Hu et al., 2017).

Copland et al. (Copland et al., 2018) enhanced $CD69^+$ $CD103^+$ T_{RM} by boosting BCG vaccinated mice with intranasal *Bacillus subtilis* spores coated with TB antigens. This approach improved protection against *Mtb* challenge over BCG vaccination alone. Boosting BCG vaccinated mice via IN or IT nanoparticles coated with *Mtb* antigens was also found to induce TB-specific $CD8^+$ T_{RM} compared to SC BCG or uncoated nanoparticle vaccination (Hart et al., 2018). Haddadi *et al.* (Haddadi et al., 2019) showed that mucosal vaccination of SC BCG-primed mice using a nanoparticle coated with three *Mtb* antigens significantly enhanced protection against *Mtb* challenge; the enhanced protection was equated with improved $CD8^+$ proliferation and $CD8^+$ T_{RM} seeding of the lungs. The boost strategy was also shown to be most effective when carried out during the memory phase (as opposed to effector phase) of T cell response to parenteral BCG prime vaccination.

An initial study to characterise *Mtb*-specific $CD8^+$ T_{RM} from humans undergoing surgical excision of lung as treatment for ongoing or previous TB demonstrated that individuals with active TB had significantly higher numbers of $CD8^+$ T_{RM} than control groups. Although ~50% of these cells expressed both CD69 and CD103, the authors suggest that there were $CD8^+$ T_{RM} that lacked CD69 expression (such as seen in mouse vaccinations). Individuals with comorbid HIV infection had lower $CD4^+$ T_{RM} with decreased

functionality while $CD8^+$ T_{RM} numbers and functionality were comparable to matched controls (Ogongo et al., 2021).

Summary

$CD8^+$ T_{RM} reside to protect non-lymphoid tissue due to their role as immune sentinel cells with rapid and effective responses to previously encountered pathogens. Their ontogeny from naïve cells is highly diverse across a spectrum of tissue lineages and is linked to varieties of physiological milieu as well as complex transcriptional programs. Lung $CD8^+$ T_{RM} are an excellent example of diversity where the pulmonary architecture has undoubtedly underscored their unique developmental program and persistence. Currently, a model exists in mice where airway T_{RM} are recruited from a pool of self-renewing parenchymal T_{RM} while residual antigen-driven reactivation in the mediastinal lymph node independently drives continual recruitment of circulatory $CD8^+$ T_{EM} through the lung for several months after infection. A unique characteristic of lung $CD8^+$ T_{RM} is that they wane over a short time and cell-mediated protective immunity of the lungs is lost by 6 months after infection. Studies of $CD8^+$ T_{RM} following mycobacterial vaccination support the rationale of the use of mucosal delivered vaccine as this strategy consistently demonstrated superior generation of lung $CD8^+$ T_{RM} and subsequent superior protection against *Mtb* challenge as opposed to parenteral BCG vaccination.

1.3 Lung Epithelial Stem and Progenitor Cells

In the mouse models of influenza and in many cases of human SARS-CoV-2 infection, there is a spatial and temporal association of RAMD $CD8^+$ T_{RM} and lung epithelial progenitor cells in areas of severe tissue destruction (Chua et al., 2020; Fang et al., 2020; Jyothula et al., 2022; Kumar et al., 2011; Takamura, 2017; Vaughan et al., 2015; Zacharias et al., 2018; Zhao et al., 2020). As stem cells and immune cells depend on each other for tissue repair, the interdependence between these two cell types is a major focus of these studies. A review of the literature did not produce any research studies that have investigated or reported the roles of lung epithelial stem/progenitor cells following *Mtb* or BCG infection, therefore the literature discussed herein focuses on the stem/progenitor mechanisms associated with restitution of lung in mouse models such as naphthalene, hyperoxic or bleomycin injury as well as influenza and SARS-CoV-2 infections.

1.3.1 Alveolar Epithelial Progenitors

Animal studies have shown that the homeostatic turnover time of AEC2 is 4-5 weeks (Bowden, 1983) and when bulk labelled, their marked percentage over one year does not decrease, suggesting that new AEC2 originate from pre-existing ones (Barkauskas et al., 2013). By 1977, data had established AEC2 as a progenitor cell for lost AEC1 in response to injury (Mason & Williams, 1977). [3H]-thymidine incorporated ultrastructural analysis in nitrous dioxide-challenged animals[2] demonstrated that 1 hour after radiographic pulse, 88% of labelled cells were AEC2 with <1% AEC1 (Evans et al., 1973). It was

[2] Nitrous oxide solely depletes AEC1.

concluded that this unusually short period for labelling was a strong dispute against cell kinetics of a minor, yet unknown, stem cell population other than AEC2 (Uhal, 1997).

In animal models with accelerated alveolar epithelial cell turnover, AEC2 were capable of self-renewal and trans-differentiation into AEC1 (Adamson & Bowden, 1974; Evans et al., 1975; Kapanci et al., 1969). Lineage tracing of AEC2 in transgenic reporter mice confirmed that the AEC2 tag was evident in AEC1 during normal aging and following bleomycin injury[3] (Desai et al., 2014; Rock et al., 2011). Clonal analysis of AEC2 using Confetti Cre-dependent reporter mice determined that a single, long-lived, self-renewing AEC2 generates multiple AEC1 and/or AEC2 forming 'foci' of progeny across contiguous alveoli. It was demonstrated that while AEC2 are stem cells they also function as mature pneumocytes capable of surfactant secretion. Using hyperoxic injury[4], exposure of reporter mice to 88% oxygen tripled the number of renewed lineage- traced AEC1 (Desai et al., 2014).

It has been a debate whether all AEC2 or a subpopulation act as progenitors (Uhal, 1997); using a Cre-reporter for Wnt signalling, a rare AEC2 progenitor (AEP) that constitutes `20% of all AEC2 was found (Nabhan et al., 2018) (Fig. 2). Again, AEP express AEC2 markers and function as AEC2. Unlike quiescent AEC2 (Messier & Leblond, 1960), AEP undergo division where lineage-traced daughters remain local; lineage-labelled AEP also expanded six-fold relative to unlabelled AEC2 during a 1-year chase. Labelled AEP gave rise to AEC1 daughters that were also closely associated with founder AEP, supporting

[3] Bleomycin administration results in widespread bronchiolar and alveolar damage.

[4] Hyperoxia is toxic to AEC1 but not AEC2.

previous descriptions of “foci” of proliferation (Desai et al., 2014). Nabhan *et al*. (Nabhan et al., 2018) showed that in normal lung, AEP have active Wnt signalling and are adjacent to a single, Wnt-expressing fibroblast in a niche that provides juxtacrine Wnt for their maintenance. Inhibition of Wnt secretion depleted AEP by 68% and supports previous reports of interaction between AEC2 and fibroblasts following lung injury (Kasper & Haroske, 1996; O'Reilly et al., 2008). Daughter cells leaving the Wnt niche transdifferentiate into AEC1 as Wnts are local signals with a range of only one or two cells (Farin et al., 2016). Injury was shown to induce autocrine AEC2 Wnts that activated quiescent AEC2 to become proliferative. Thus, a small subset of AEC2 termed AEP possess bipotency while other AEC2 *can* be efficiently recruited to repair alveolar damage.

Zacharias *et al*. (Zacharias et al., 2018) concurred that a Wnt-responsive AEP lineage within the AEC2 population acts as a stable facultative progenitor in distal lung that expands rapidly after acute lung injury. They described the AEP distinct functional gene expression profile enriched in lung developmental genes and an epigenome that contains 40% differential genomic open chromatin near master genes of progenitor cell behaviour and cell cycle regulation all upregulated two weeks after influenza infection. Again, Wnt inhibition promoted AEC1 differentiation while activation promoted AEC2 differentiation in mouse and human organoids. Collectively, research efforts delineated a rare Wnt responsive subset of AEP that are phenotypically poised as progenitor cells while at the same time function as mature AEC2, undoubtedly preserving the efficiency of gas exchange across the alveolar epithelium.

1.3.2 Bronchioalveolar Stem Cells

At the junction of the respiratory bronchiolar and alveolar epithelium, a population of bronchioalveolar stem cells (BASC) that express club cell (Scgb1a1) and AEC2 surfactant protein c (SPC) markers (**Fig. 2**) have been reported (Giangreco et al., 2009; Kim et al., 2005) where lineage tracing demonstrated their role as progenitors for repair of bronchiolar epithelium but not alveolar epithelium in mouse

vaccinations of naphthalene[5] and hyperoxic injury (Rawlins et al., 2009).

Following bleomycin injury, *Scgb1a1-CreER:ROSATomato* mice demonstrated a significant increase in lineage-labelled AEC2 and AEC1 cells in fibrotic regions (Rock et al., 2011). Results of two further studies using *Scgb1a1* transgenic reporter mice also showed lineage-labelled cells in the alveolar region adjacent to the alveolar duct after bleomycin and influenza injury (Zheng et al., 2012, 2013). Notably, use of these three reporter animal vaccinations could not conclusively determine the origin of lineage-labelled alveolar cells as it was subsequently demonstrated by Vaughan *et al.* that using a chase period of 7-10 days following tamoxifen administration led to an erroneous result of *Scgb1a1*-labelled cells due to residual tamoxifen which continued to activate Cre driven promotors following lung injury (Vaughan et al., 2015).

Using a dual recombinase (Liu et al., 2019) and intein-mediated assembly of split-effectors (Salwig et al., 2019) lineage-tracing systems to track BASC *in vivo*, results showed that BASC respond distinctly to various lung injuries with the ability to differentiate into multiple lineages including club and ciliated cells after naphthalene-induced bronchiolar injury or AEC2 and AEC1 cells after bleomycin-induced alveolar injury (**Fig. 3**). In these BASC-related studies, all lineage- traced cells resided adjacent to the bronchioalveolar junction while daughter cells in alveoli were minimal, implying that club cells or BASC are not a primary source of replacement alveolar cells following lung injury.

[5] Napthalene administration selectively destroys club cells.

1.3.3 Distal Airway Stem Cells

Exposure of mice to murine-adapted H1N1 influenza A (PR8) induces significant loss of club, ciliated and AEC2 cells early after infection. During infection, there is a concomitant rise of stem cell marker tumour protein 63 (p63) expressing cells in bronchioles as they undergo expansion and migration to affected lung parenchyma (Kumar et al., 2011; Vaughan et al., 2015; Zuo et al., 2015). Coined distal airway stem cells (DASC) (**Fig. 2**), in normal mice, $p63^+$ DASC were scarce in bronchioles (Kumar et al., 2011; Ray et al., 2016; Xi et al., 2017). However, by 7 days past infection (dpi) following PR8 exposure, they were evident. By 11 dpi, $p63^+$ DASC and club cells were intermingled in bronchiolar epithelium and by 21 days bronchiolar epithelium was restored. In damaged distal alveolar lung parenchyma at 11 dpi, $p63^+$ DASC were co-stained with basal stem cell (BSC) marker keratin 5 (Krt5) and found to cluster in large concentric pods around terminal bronchioles where they proliferated robustly (of note, these are the $Krt5^+$ pod cells incorporated into the RAMD described by immunologists). Zuo *et al*. (Zuo et al., 2015) proposed that these clusters of DASC were in early stages of *de novo* alveoli formation. In a mouse model in which DASC were conditionally ablated, assembly of alveolar $Krt5^+$ pods in interstitial inflamed alveolar tissue were prevented; rather, distal lung showed persistent leukocyte infiltration, inflammatory and pro-fibrotic gene expression, as well as a decrease of gene expression linked to vasculature development.

Vaughan *et al*. (Vaughan et al., 2015) directly observed the migration of $p63^+$ $Krt5^+$ cells throughout injured small airway after PR8 infection of mice and identified co-expression of integrin a6ß4. To define cell-of-origin, they lineage traced using CC10− or SPC-CreERT2 driver reporter mice for club and AEC2 cells, respectively, and showed that at 11 dpi after PR8 infection, $p63^+$ $Krt5^+$ cells were completely untraced. Given that BSC of nasal and epithelia of the upper airways also express p63 (Rock et al., 2009), reporter tracheal transplants into syngeneic animals also revealed that proximal BSC were not the source of alveolar $Krt5^+$ pods. To locate quiescent lineage negative DASC, they used ß4 expression in *CC10-CreERT2* mice to segregate progenitors from club cells in uninjured lungs. The *CC10-* $ß4^+$

(progenitor containing) population distinctively expressed p63 and $p63^+$ cells were also identified *in situ* scattered very rarely throughout distal airways. RNA-seq analysis identified enrichment for CD14 in $p63^+$ CC10- ß4^+ cells. In combination with CD200, which further selects against ciliated cells, $\beta4^+$ $CD200^+$ $CD14^+$ cells were isolated and transplanted into *Krt5-CreERT2* animals prior to bleomycin or PR8 infection. Interestingly, relatively normal histology was seen in Krt5-CreERT2 traced tissue after bleomycin injury. After PR8 injury, however, only a few traced AEC2 were seen but large regions of Krt5-Cre traced epithelial cysts were evident in all mice up to 200 dpi. These persistent cysts resemble the micro-honeycombing of idiopathic pulmonary fibrosis (IPF); thus, abnormal $Krt5^+$ pods that arise following influenza infection were said to represent a failed regenerative process.

Using several reporter lines, Ray *et al*. (Ray et al., 2016) clarified that $Krt5^+$ pods originated from proliferative SRY-box 2 ($Sox2^+$) $Krt5^-$ $Scgb1a1^-$ progenitor cells from distal airways, not proximal $Krt5^+$ BSC, BASC or club cells. In 2017, Xi *et al*. (Xi et al., 2017) quantified $p63^+$ cells throughout uninjured airways as <0.01% of all lung epithelial cells. They theorised that scarcity of these $p63^+$ lineage negative epithelial progenitors and their infrequent contribution to AEC2 regeneration suggested an additional $p63^-$ $Sox2^+$ epithelial progenitor. Using studies of hypoxia following PR8 infection in mice, they showed that $Krt5^+$ areas formed after infection in hypoxic regions; when they deleted the key mediator of cell response to hypoxia (HIF1α), $HIF1\alpha^{-/-}$ mice showed significant decrease in alveolar $Krt5^+$ cell expansion, had a higher fraction of AEC2 and a quicker recovery. It seemed evident that HIF1α deletion substantially improved lung function by a mechanism that directed lineage negative epithelial progenitors toward AEC2 expansion and bypassed $Krt5^+$ basal-like metaplasia. It was shown that injury-induced hypoxia, via HIF1α, promoted lineage negative epithelial progenitor differentiation towards a motile $Krt5^+$ $p63^+$ basal-like cell. It was concluded that these $Sox2^+$ $p63^+$ progenitors are the major responders to HIF1α signals following PR8 influenza infection and produce a metaplastic BSC response, whereas Wnt suppresses this pathway to favour $Sox2^+$ $p63^-$ progenitor differentiation to AEC2. (Xi et al., 2017) (**Fig. 3**). They concluded that because activated $Krt5^+$ cells *in vivo* were derived entirely from rare $Sox2^+$ $p63^+$ cells that $Sox2^+$ $p63^-$ LNEP were rendered dysfunctional by PR8 infection (Ray et al.,

2016).

1.3.4 Lineage Negative Epithelial Progenitors

A complex epithelial progenitor population in distal lung to isolate and characterise has been this $Sox2^{+}$ $p63^{-}$ LNEP. These cells are multipotent stem cells that reside in terminal bronchioles and lack mature epithelial cell markers (**Fig. 2**). First reported by McQualter *et al*. (McQualter et al., 2010) using a novel clonogenic assay, a population of epithelial colonies was able to generate airway, alveolar, or intermediates of lung epithelial cell lineages when co-cultured with lung mesenchymal cells. Clonogenic cells were fractionated from mouse lung with pan-epithelial cell marker (EpCAM) and α6 integrin (CD49f); subsequently, colonies were restricted to the $EpCAM^{hi}$ $CD49f^{pos}$ cell fraction. All cells of the $EpCAM^{hi}$ fraction were $CD104^{pos}$ (β4 integrin) and immunostaining showed that this integrin localised to basal membrane of epithelial cells in bronchi and terminal bronchioles but not with AEC2.

Chapman *et al*. (Chapman et al., 2011) also reported a regenerative subpopulation (`8-10%) of mouse epithelial cells present in bronchoalveolar regions that expressed α6β4 and lacked AEC2 or club cell markers. *Ex vivo*, these cells expanded as progenitors and differentiated toward mature AEC2 and club cell types. *In vivo* embryonic lung organoids demonstrated that purified $β4^{+}$ cells organised into club cell airway-like and SPC^{+} saccular structures. Using a bleomycin mouse model and an SPC-driven inducible Cre animal to fate-map AEC1 and AEC2, they found that AEC2 in repaired areas were not derived from pre-existing AEC2. They suggested that, in the context of severe alveolar loss, pre-existing SPC^{-} epithelial progenitors contribute to repair.

Isolation of mouse airway epithelial cells using EpCAM, integrin β4 and negative expression of ciliated cell marker CD200 (Kathiriya et al., 2020), determined that 40% of isolated cells did not stain for any mature lineage markers and single-cell RNA sequencing (scRNA-seq) revealed high expression of antigen-presenting genes and MHC class I marker H2-K1. Transcriptomes were clustered using a gene signature assigned to embryonic epithelial stem cells which identified an enriched population with

negligible mature lineage markers, high expression of MHC and cell cycle genes. These cells were also distinguished by activation of host-defence-related signalling pathways and genes associated with viral infection and an interferon signature. When β4/H2-K1 cells were established in 2D culture and 3D organoids, they represented all colony-forming cells and were maintained for at least three passages. Immunostaining of whole colonies or cytospins from cultured cells revealed that these cells were able to differentiate toward AEC2 or Krt5$^+$ basal-like cells (**Fig. 3**).

Study of mice injured with bleomycin revealed that there is an initial expansion of H2-K1 progenitors with migratory capacity and a phenotype leaning toward alveolar fate prior to their restoration of AEC2 and AEC1 lineages *in vivo*. β4/H2-K1 progenitor cells isolated from unlabelled *SPC-CreERT2:mTmG* mice were *in vitro* SPC$^+$ labelled (using 4-hydroxytamoxifen), then transplanted into bleomycin-injured mice. 85% of restored regions were tdTomato$^+$ thus arisen from undifferentiated H2-K1 progenitors. Of relevant note is that in widespread bleomycin injury, Krt5$^+$ pods did not form. That Krt5$^+$ pods form with PR8 infection is thought due to virally targeted tropism to and loss of H2-K1 progenitors (Quantius et al., 2016). Consequently, after H1N1 (or PR8) infection, the lung is thought consigned to use airway p63$^+$ basal-like cell mobilisation for alveolar regeneration (Kathiriya et al., 2020). This opinion is supported by the fact that exposure to less virulent influenza strains does not trigger formation of Krt5$^+$ pods or proximal basal stem cell-associated alveolar epithelial cell replacement (McQualter, 2019).

1.3.5 Krt8 Transitional Progenitors

A novel distinct transitional progenitor cell population has been recently described by several groups that is relevant to this project. These cells represent the intermediate cell state in which cuboidal AEC2 and airway progenitor cells with a secretory phenotype convert physically, structurally, and mechanically into squamous AEC1 that function for gas-exchange.

In humans, IPF is a progressive fibrotic disease that is linked to ineffective regeneration of injured alveolar epithelium and excessive TGF-β signalling (Blackwell et al., 2014). As IPF epithelium is

hyperplastic with a transitional gene profile (Xu et al., 2016), it was theorised that regenerative defects of IPF may be linked to inadequate AEC2 to AEC1 transition. Lipopolysaccharide (LPS), a bacterial endotoxin, induces acute lung injury in mice when administered intratracheally and resembles acute respiratory distress syndrome in humans; LPS induced injury leads to lung fibrosis. Using lineage labelled AEC2 and an LPS mouse vaccination, scRNAseq uncovered an early (characterised by moderate expression of AEC1 markers and downregulation of AEC2 markers) and late (characterised by high expression of AEC1 markers and downregulation of AEC2 markers) transitional state of AEC2 to AEC1 differentiation. TGF-β signalling was necessary for early differentiation whereas inactivation was required later to promote terminal differentiation into AEC1 (Jiang et al., 2020). *In vitro*, when TGF-β was activated in the early state, keratin 8 (Krt8) was also upregulated. Inhibition of TGF-β signalling decreased Krt8 expression and short hairpin RNA mediated Krt8 knockdown attenuated AEC1 differentiation. Immunostaining of IPF mouse and human lungs confirmed clusters of hyperplastic cells that expressed high levels of Krt8 in fibrotic regions only. It was theorised that the Krt8 early state of transition was perpetuated in IPF linked to persistent TGF-β activation (Jiang et al., 2020).

Time-series scRNA in a bleomycin lung injury vaccination with trajectory modelling and lineage-labelling revealed that both airway and alveolar progenitors converge on a $Krt8^+$ transitional cell state during alveolar restitution which they termed $Krt8^+$ alveolar differentiation intermediate (ADI). Using *Sftpc-CreERT2* (AEC2) and *Sox2-CreERT2* (airway epithelial cell) reporter mice, they showed that around 40% of the new AEC1 cells after bleomycin injury were derived from the airways with an increased contribution in severely injured areas. Immunostainings of tissues from human acute respiratory distress syndrome linked to influenza and pneumococcal infection also demonstrated intense alveolar Krt8 expression in fibrotic areas (Strunz et al., 2020).

To further define states of AEC2 that respond to bleomycin injury, lineage labelled *SPC-CreERT2* cells were isolated on day 14 (acute injury) and day 28 (injury resolution) where scRNAseq uncovered three distinct cell populations consisting of primed AEC2, cycling AEC2 and $Krt8^+$ damage associated

transitional progenitors (DATP) after day 14. It was further demonstrated that macrophage-secreted IL-1β primed a subset of interleukin 1 receptor type 1 (*Il1r1)*$^{+}$ AEC2 to convert into DATP and that chronic inflammation mediated by IL-1β prevented AEC1 maturation leading to an aberrant accumulation of Krt8^{+} DATP. The authors went on to query whether there was a relationship between *Il1r1*$^{+}$ AEC2 and AEP (Choi et al., 2020).

The pre-alveolar type-1 transitional cell state (PATS) was also described *in vitro* in cultured organoids and *in vivo* following lung injury, where PATS were found to undergo extensive stretching and were therefore prone to DNA damage; scRNAseq analysis indicated DNA damage and senescence-associated genes were highly enriched. PATS were defined by tumour protein 53, Claudin 4 and *Krt8* expression. This study also reported the expression of PATS-like markers specifically in fibrotic regions of human IPF lungs but not in healthy control lungs (Kobayashi et al., 2020).

The group that developed kinase-inhibiting RNase attenuators (KIRAs) showed that KIRAs protected mice from pulmonary fibrosis induced by bleomycin (Thamsen et al., 2019) and reasoned that maladaptive cell fate switches related to regulated IRE1α-dependent decay (RIDD) were active in DATPs (Auyeung et al., 2022). RIDD is a process by which the endoplasmic reticulum (ER) stress sensor IRE1α, under continuous or high levels of ER stress, leads to degradation of mRNAs and microRNA localized in the ER membrane causing maladaptive cell fate outcomes such as senescence. Administration of kinase inhibitor of IRE1α decreased DATP number, DATP expression of *Itgβ6* (a critical activator of TGF-β in lungs) and TGF-β induced gene expression while accelerating the differentiation of DATPs into AEC1 (Auyeung et al., 2022).

For the sake of clarity, in this study DATPs, ADI and PATS are called Krt8^{+} progenitors; these transitional progenitors have now been shown to have a role not only in the healthy restitution of lung following injury, but also a role in pathogenesis of IPF as discussed, COVID-19 (Melms et al., 2021) and most likely bronchopulmonary dysplasia in pre-mature infants (Treutlein et al., 2014).

Summary

To summarise, homeostasis of alveolar epithelium responsible for gas exchange is accomplished through stable, slow turnover of selected mature progenitor cells. Exposure of the alveolar epithelium to injury results in activation of stem/progenitor cells in a regionally- and context-distinct manner. In alveolar tissue, a subset of ~20% functionally mature AEC2 cells termed AEP is uniquely poised phenotypically for rapid provision of new AEC2 and AEC1 following mild injury. Moderate-severe alveolar injury further recruits the normally non-proliferative AEC2 into multiplication. Where injury overwhelms the capacity of local alveolar epithelial cells to replenish lost alveolar epithelial cells, airway epithelial progenitor cells can differentiate into AEC2s and AEC1s. Both alveolar and airway epithelial progenitor cells converge into a $Krt8^{+}$ transitional cell state mediated by the injury milieu before terminal differentiation into AEC1. With widespread severe bronchiolar and alveolar damage and LNEP loss due to severe influenza infection, DASCs are mobilised for distal AEC2 and AEC1 replacement, albeit alveolar restitution is suboptimal. Importantly, prior to these studies, it remained unknown how and which pulmonary epithelial progenitors respond to *Mtb* or BCG infection.

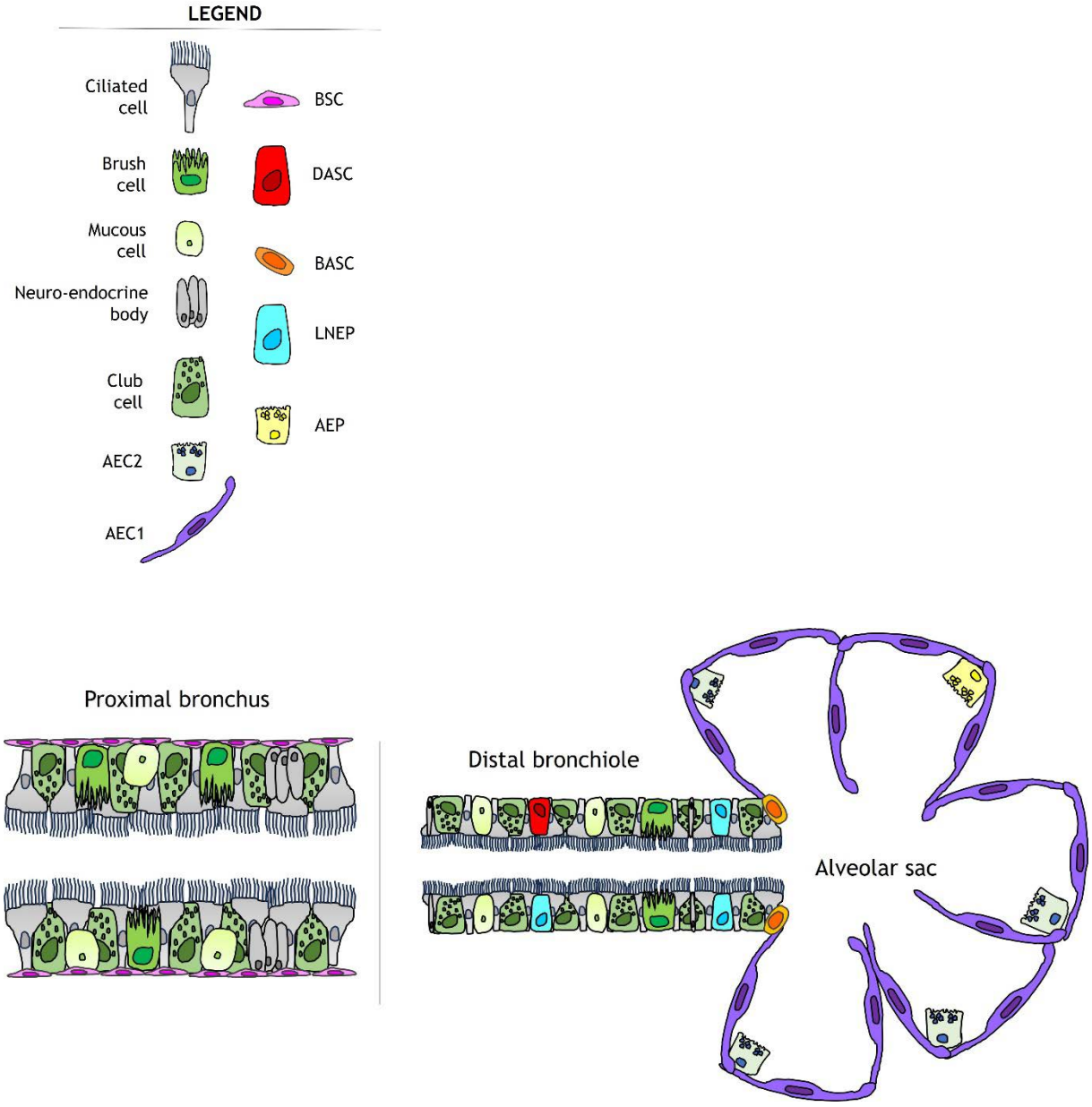

Figure 2. **Epithelial stem and progenitor cells of the lungs.**

Drawing depicts how stem and progenitor cells reside amongst their mature lineage-restricted counterparts.

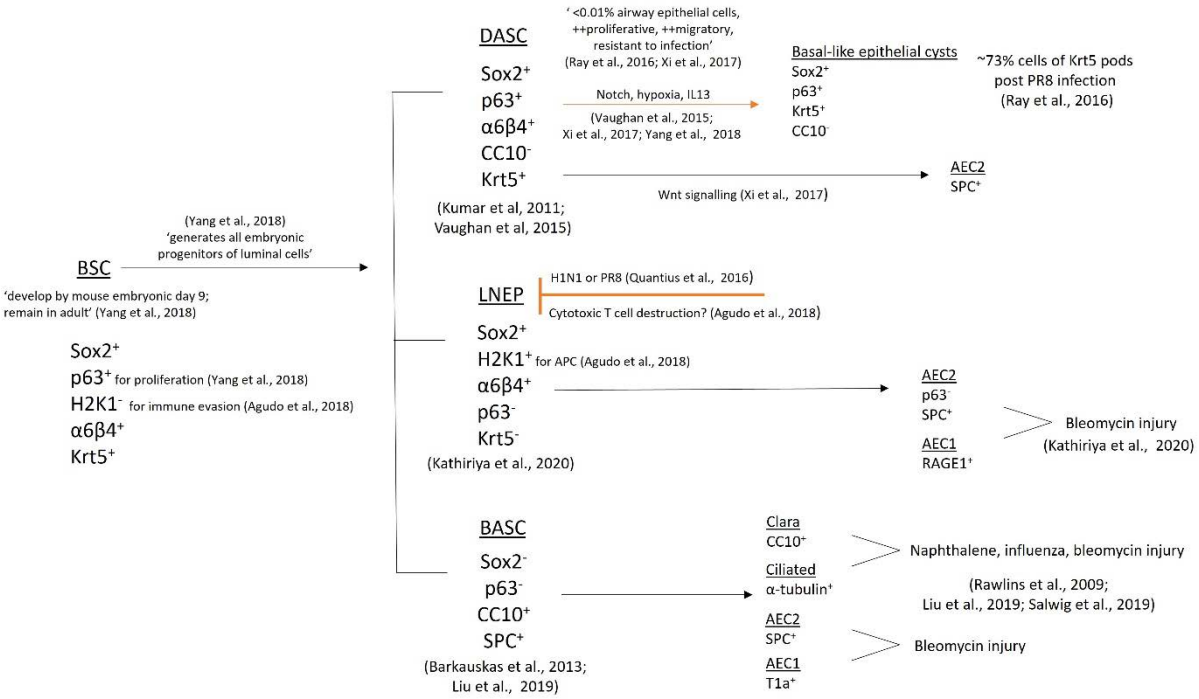

Figure 3. **Airway epithelial stem and progenitor cell contributions to alveolar lung regeneration.**

1.4 Interactions Between Lung Epithelial Progenitor Cells and CD8$^+$ T_{RM}

There is an increasing understanding of the capacity of stem/progenitor cells to perceive damage, correspond with, and designate resident and recruited immune cell roles. Evidence of crosstalk between immune and stem cell types is seen in the array of immune receptors and cytokine signalling systems found in stem cells (Agudo et al., 2018; Alvarado & Lathia, 2016; Atladottir et al., 2010). It is also known that immune cell signals are required for activation of quiescent stem cells in many tissues (Biton et al., 2018; Hirata et al., 2019; Lindemans et al., 2015; Naik et al., 2017; von Moltke et al., 2016) and that dysregulation of immune-stem/progenitor cell crosstalk results in aberrant healing and chronic disease (Belkaid & Hand, 2014; Ordovas-Montanes et al., 2018; Rieder et al., 2007). Three essential components of lung injury and restitution related to tuberculosis, namely, mycobacteria, lung epithelial stem/progenitors and CD8$^+$$T_{RM}$ have never been studied in conjunction. Therefore, this section of the review focused on studies across several vaccinations of lung infection and injury to provide compelling evidence that development and persistence of CD8$^+$ T_{RM} may be dependent upon lung epithelial progenitor cells during and following lung injury.

1.4.2 Specification of CD8$^+$ T_{RM} Coincides to Spatial Merging with Epithelial Progenitors

Following the acute phase of inflammation associated with PR8 murine influenza infection, viral clearance is accomplished due to elevation of immune infiltrates such as neutrophils and macrophages (Kumar et al., 2011). Cytolysis of infected cells leads to a peak of tissue damage (Kumar et al., 2011; Takamura et al., 2016) and there is a widespread destruction of club cells, ciliated cells and AEC2 (Kumar et al., 2011; Vaughan et al., 2015; Zacharias et al., 2018). CD8$^+$ T cells are seen in the interstitium and bronchioles where they are “distributed into the lung before the peak of T cell responses” (Takamura et al., 2016). At the same time, epithelial p63$^+$ Krt5$^+$ progenitor cells undergo robust proliferation both in bronchioles and, significantly, in the alveolar interstitium as tight clusters of cells where interstitial Krt5$^+$ pods are formed at the peak of tissue damage (Kumar et al., 2011; Takamura et al., 2016). This has been called “the critical turning point” for creation of the milieu

essential for differentiation of $CD8^+$ T_{RM} in this vaccination (Takamura et al., 2016). Temporally coincident with the 'window of memory' in which T_{RM} are differentiated (Kaech & Cui, 2012; Takamura et al., 2016), there is an increase of interstitial $Krt5^+$ pods now with lumens reminiscent of alveoli (Kumar et al., 2011). Importantly, $Krt5^+$ pods are only found in peribronchiolar zones of complete tissue damage and the peribronchiolar T_{RM} niche forms solely in the vicinity of $Krt5^+$ progenitor cells. The molecular mechanisms associated with $CD8^+$ T_{RM} and $Krt5^+$ cell migration and proliferation *exclusively* to zones of complete destruction remain unknown.

1.4.3 Do Lung Epithelial Progenitors Interact with $CD8^+$ T cells?

There is evidence that $Krt5^+$ cells may have a role in the development of T_{RM} in the RAMD. During development, Notch signalling is known to suppress alveolar differentiation in the lung (Guseh et al., 2009) and qRT-PCR of $Krt5^+$ cells following PR8 infection in mice revealed expression of nuclear Notch1ICD, Hes1, Hey1 and Jagged2 (Vaughan et al., 2015). Single-cell transcriptional profiling of human AEC2 from fibrotic lungs revealed a hypoxic subpopulation with activated Notch, suppressed SPC and trans-differentiation toward a $Krt5^+$ basal-like state (Vaughan et al., 2015). Therefore, Vaughan et al. (Vaughan et al., 2015) cultured bronchoalveolar lavage fluid in the presence of γ-secretase (Notch) inhibitors and observed strong induction of SPC expression and went further, in subsequent studies, to show that local lung hypoxia, via HIF1α, drives Notch signalling and $Krt5^+$ basal-like cell expansion (Xi et al., 2017). Interestingly, Notch signals in *Drosophila* stem cells occur at varying levels that in turn determine daughter cell fate (Ohlstein & Spradling, 2007). This finding has been recapitulated in BSC in that they regulate the maintenance of their own progeny through production of Jag2 which activates Notch2 in daughter cells to prevent differentiation into ciliated cells (Pardo-Saganta et al., 2015).

Samples of healthy lung tissue and peripheral blood from patients undergoing lung resection showed the most significantly enriched gene sets in an analysis of T_{RM} compared to T_{EM} were targets of *HIF-1α*, *NOTCH1* and *RBPJ* (encodes Notch DNA binding factor); furthermore, expression of *NOTCH1* was high

in human lung T_{RM} that also had surface expression of NOTCH2 (Hombrink et al., 2016). To study the function of Notch in mouse T_{RM}, lungs from *Notch1fl/flNotch2fl/flCd4-Cre*$^{+}$ mice (inactivated Notch1 and Notch 2) had considerably fewer T_{RM} than did those from their control littermates while surface expression of CD103 by the few remainder T_{RM} was also lower (Hombrink et al., 2016). Intranasal infection of wild-type mice by influenza followed by γ-secretase inhibitor from 35-40 dpi to block Notch signalling resulted in a significant decrease of T_{RM} and demonstrated that Notch signalling was required for persistence of T_{RM} (Hombrink et al., 2016). Inhibition of Notch not only significantly decreased T_{RM} expression of *Itgae* (gene that encodes CD103), but also genes that encode transporters for amino acids, metabolites, trace elements and nutrients. Therefore, Notch signalling in T_{RM} also has an essential role in the regulation of metabolic programs imperative for cell survival in a hypoxic environment (Borges da Silva et al., 2018; Hombrink et al., 2016; Liu et al., 2018). No studies have directly investigated whether forward Notch signals employed by Krt5^{+} pod progenitors to alter distribution of their progeny influence CD8^{+} T_{RM} with which they share cell-cell contact in the RAMD (**Fig. 4**).

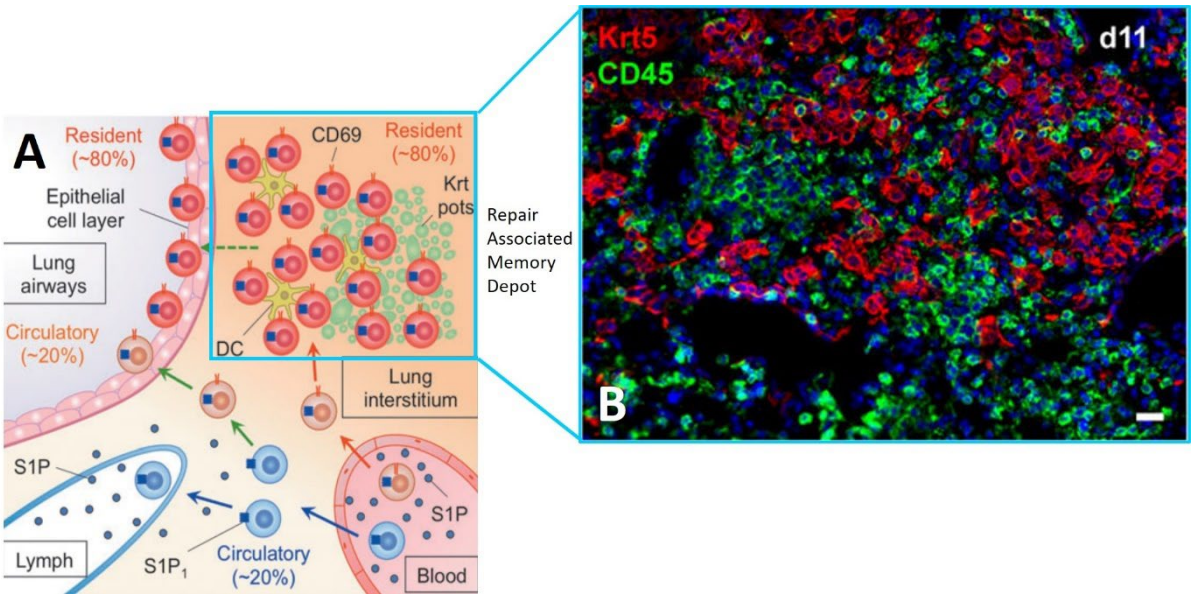

Figure 4. **Krt5⁺ pod and CD8⁺ T_{RM}.**

A) An illustration of the Repair Associated Memory Depot (RAMD) that forms in areas of complete destruction of lung tissue in mice following PR8 influenza infection. From (Takamura, 2017). **B)** Image of a Krt5⁺ pod with co-related CD8⁺ T_{RM} day 11 following mouse PR8 influenza infection. Scalebar 20µm. From (Vaughan et al., 2015).

1.4.4 αVβ6 regulation of TGF-β: a Role in Development of Lung CD8⁺ T_{RM}?

In the PR8 mouse model of influenza, lung CD8⁺ T_{RM} are segregated into specific niches associated with progenitor cells in the foci of tissue regeneration (Takamura et al., 2016) and these Krt5⁺ cells are known to migrate from the airway epithelium into the peribronchiolar interstitium (Vaughan et al., 2015). Takamura et al have suggested that "it is conceivable that cells constituting such auxiliary developed regenerative tissues could be a source of unique factors necessary for differentiation and maintenance of T_{RM} cells, such as TGF-β" (Takamura et al., 2016).

The integrin αVβ6 is expressed solely by epithelial cells and has been shown to bind and activate latent TGF-β in the lungs (Munger et al., 1999). TGF-β1 LAP is a ligand for αVβ6 and when latent TGF-β1 complexes bind to αVβ6, the β6 cytoplasmic domain is made able to fasten to its actin cytoskeleton.

This cytoskeletal-associated β6 integrin with LAP-bound αV combines with the mechanical tension of cell migration where extracellular matrix (ECM) provides traction to induce a conformational change in the LAP and releases free TGF-β (Giacomini et al., 2012; Munger et al., 1999; Shi et al., 2011). Importantly, active TGF-β generated by αVβ6 is only utilised by cells in direct contact with αVβ6 expressing cells (Annes et al., 2004; Henderson & Sheppard, 2013; Munger et al., 1999) (**Fig. 5**).

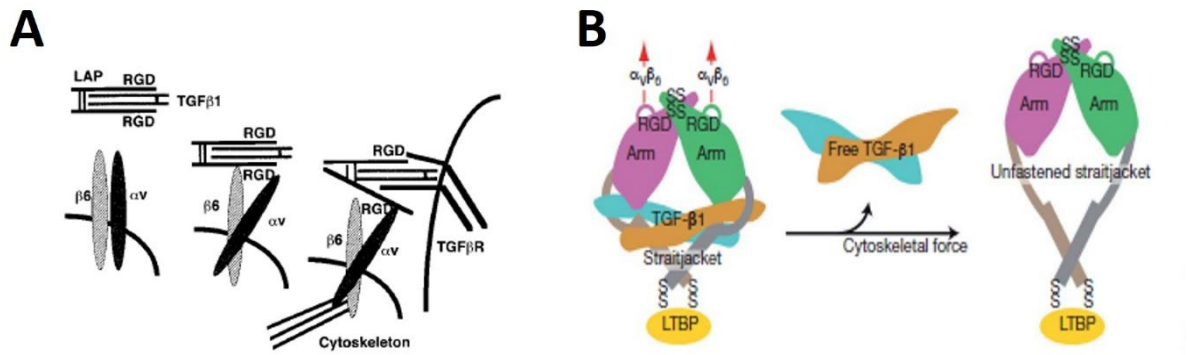

Figure 5. **αVβ6 binds and activates latent TGF-β.**

A & B) Diagram depicts the tethering of αVβ6 to LAP RGD and cytoskeleton to generate mechanical force required to activate latent TGF-β. **A)** From Munger *et al.* 1999. **B)** From Shi *et al.* 2011.

In mouse lungs, steady-state abundant levels of TGF-β are present (Sheppard, 2006) and these levels have been shown not to change after treatment with bleomycin (Munger et al., 1999; Pittet et al., 2001); conversely, diffuse low levels of αVβ6 are apparent in normal airway and alveolar epithelial cells (Breuss et al., 1995), while αVβ6 expression in these cells is significantly increased throughout lungs of injured mice (Huang et al., 1998; Munger et al., 1999). A vaccination has been suggested in which tissue injury induces αVβ6 expressing migratory cells that locally activate TGF-β already present in the lungs. TGF-β, once activated, enhances ECM deposition, and downregulates the inflammatory response of

injury (Munger et al., 1999) or, if aberrantly over-expressed, leads to fibrosis (Henderson & Sheppard, 2013).

Migratory Krt5$^+$ cells, airway and alveolar Krt8$^+$ transitional epithelial progenitors all express αVβ6 (Auyeung et al., 2022; Strunz et al., 2020; Takamura, 2017; Topham et al., 2019). These Krt5$^+$ pod cells and Krt8$^+$ transitional progenitor cells are unable to differentiate into AEC1 but accumulate in human fibrotic lungs (Auyeung et al., 2022; Kobayashi et al., 2020; Strunz et al., 2020; Takamura, 2017; Vaughan et al., 2015). Kinase inhibitor of IRE1α KIRA8 decreased expression of αVβ6 and decreased TGF-β- induced gene expression resulting in resolution of the Krt8$^+$ transitional state, amelioration of fibrosis and promotion of lung regeneration (Auyeung et al., 2022). Following IT bleomycin (known to induce both pulmonary oedema and fibrosis), mice in which the β6 subunit of αVβ6 is knocked out develop persistent inflammation of the lungs but are protected from oedema (Pittet et al., 2001) and subsequent fibrosis (Munger et al., 1999). Additionally, β6 inhibition by anti-αVβ6 antibodies prevented radiation-induced fibrosis (Puthawala et al., 2008), while β6 null mice were protected from ventilator-induced lung oedema (Jenkins et al., 2006). A microarray analysis of differentially upregulated genes in wild-type and β6 null mice following IT bleomycin showed substantially reduced levels of TGF-β inducible genes in the β6 knockout mice (Kaminski et al., 2000). These studies demonstrate that epithelial αVβ6 is a key regulator of TGF-β activation during lung injury.

It remains unknown whether migratory Krt5$^+$ pod cells or Krt8$^+$ transitional progenitors that express αVβ6 activate TGF-β (necessary for CD49a and CD103) to locally establish the CD8$^+$ T_{RM} niche in the precise areas of focal alveolar reconstruction where CD8$^+$ T_{RM} sentinels are most required. In the epidermis, TGF-β activation is mediated by αVβ6 and in *ItgB6*$^{-/-}$ mice following 1-Fluor-2, 4-dinitrobenzene (DNFB) treatment, CD8$^+$ T cell effectors were recruited into the epidermis, but no CD8$^+$ T_{RM} formed later. Also, blocking of αVβ6 with monoclonal antibodies in this vaccination could partially deplete CD8$^+$ T_{RM} in wild-type mice, suggesting that αVβ6-activated TGF-β is required for development and persistence of epidermal CD8$^+$ T_{RM} (Hirai et al., 2021). Therefore, a principle aim of this project was

to investigate the role of migratory αVβ6 lung epithelial progenitors in the development and persistence of pulmonary $CD8^+$ T_{RM} through activation of latent TGF-β in mycobacterial infected lungs.

Summary

Early in pulmonary infection, epithelial injury causes secretion of growth factors, chemokines, interleukins, and prostaglandins that coordinate complex processes involving epithelial restitution. As discovery of various stem cell populations in the distal lung are on-going, studies that specify mechanisms associated with their activation by immune mediators during acute inflammation are lacking. Similarly, it is unknown how AEPs, LNEP, BASC or DASC contribute to the acute inflammatory and adaptive immune responses. In zones of minimal, moderate, or severe distal tissue damage due to infection, facultative mature progenitors such as AEP, AEC2 and club cells are capable of local epithelial restitution where distinctive signalling pathways induce chemokines, cytokines and antimicrobial peptide secretion that not only modulates immune cell function but also provides paracrine signals into the local milieu that support tissue immune protection and restitution.

Pathogen clearance usually ensues due to innate immune responses but can eventuate in areas of complete cytolysis of club cells, LNEP, AEP and AEC2 linked to the adaptive effector stage of immune response. Where this loss of local distal stem cell pools occurs, proximal stem cells are activated, migrate to hypoxic areas where they proliferate and organise into pod- or cyst-like structures which 'restore' the epithelial barrier. Coincidently with formation of progenitor $Krt5^+$ pods, $CD8^+$ T_{RM} are differentiated in the vicinity possibly because TGF-β and IL-15 are available to upregulate expression of cell surface adhesion molecules CD103 and CD49a.

Notch signalling is the constitutive mechanism by which stem cells specify fate of daughter cells; evidenced in the hypoxic distal environment of the RAMD, $Krt5^+$ pod cells use Notch signalling to specify daughter cell fates (hence bronchiolisation of alveolar epithelium). The integrin αVβ6 is expressed by migratory $Krt5^+$ progenitor cells, airway and alveolar $Krt8^+$ transitional epithelial

progenitors; it remains unknown whether these migratory epithelial progenitors activate TGF-β (necessary for CD49a and CD103) to locally establish the $CD8^+$ T_{RM} niche in the precise areas of focal alveolar reconstruction where $CD8^+$ T_{RM} sentinels are most required. Importantly, mycobacteria, lung epithelial stem/progenitors and $CD8^+$ T_{RM} have never been studied in conjunction and therefore, together, were the basis of this project.

RESEARCH DESIGN

Hypothesis

It was hypothesised that lung epithelial progenitor cells have a key role in the development of local and regional pulmonary tissue immune memory following mycobacterial mucosal vaccination; namely, that they provide paracrine development and survival cues for lung $CD8^+$ T_{RM}.

Project aims

To address the hypothesis above, there were three specific aims:

AIM 1) Characterise lung epithelial progenitor cell responses to mucosal vaccination with BCG strains of distinct dose and virulence.

AIM 2) Characterise the development and persistence of lung and mLN $CD8^+$ T_{RM} following mucosal vaccination with BCG strains of distinct dose and virulence.

AIM 3) Investigate spatial, temporal, and mechanistic relationships between lung epithelial progenitor cells and lung $CD8^+$ T_{RM} following mucosal vaccination with BCG strains of distinct dose and virulence.

CHAPTER 2. LUNG EPITHELIAL CELL RESPONSES TO MUCOSAL BCG VACCINATION

To find out what is natural, we must study specimens which retain their nature and not those which have been corrupted.

ARISTOTLE, *POLITICS*

2.1 Introduction

Our first experimental aim was to characterise lung epithelial progenitor cell responses to mucosal BCG vaccination. We initially conceived that these responses would be heterogeneous based on numbers of alveolar epithelial cells lost linked to virulence and dose of the vaccine; therefore, we devised our experimental approach to include various doses and strains of *Mycobacterium bovis* BCG. The virulent BCG vaccine was comprised of *M.bovis* BCG recombined with the genes that encode *M.tuberculosis* virulence factors ESAT-6 and CFP-10 (Pym et al., 2002; Pym et al., 2003). These experiments were necessary to understand and describe the timeline of alveolar epithelial cell losses, innate and acquired immune cell responses as well as define which specific progenitor cells responded to tissue damage linked to the various vaccine doses and virulence factors.

2.2 Methods

2.2.1 Animals

C57BL/6 mice sourced from the ARC (Western Australia), *Krt5*^{CreERT2} mice (kindly provided by Dr Felicity Davis, University of Queensland), *Gt(ROSA)26Sor*$^{tm4(ACTB-tdTomato,-EGFP)Luo}$/J (also known as *mTmG*) mice (kindly provided by Prof Scott Mueller, University of Melbourne) were genotyped by Genetic Research Services (University of Queensland), bred and maintained in the animal facilities at James Cook University, Australia. Female mice were 6–8 weeks old at the time of vaccination and maintained in a biosafety level 2 facility under specific pathogen free conditions.

2.2.2 Bacteria

BCG SSI (ATCC no. 35733) and BCG::RD1 (kindly provided by Dr Roland Brosch, Institut Pasteur) were grown in Middlebrook 7H9 broth (BD Biosciences) supplemented with 0.2% glycerol, 0.05% Tween 80, and 10% ADC enrichment (BD Biosciences). Briefly, 250 µl- 500 µl stock BCG (1 x 10^8/ml) were incubated into 10 ml 7H9 medium; BCG::RD1 required addition of 50 µg/ml Hygromycin (Thermo Fisher). Bacterial cultures and no bacteria controls were cultured at 37° C shaking at 100 rpm for ~4-7 days until optical density (OD_{600}) reached 0.6-0.8 by spectrophotometry.

Bacteria were passaged by addition of 10 ml BCG culture into sterile flask with 150 ml 7H9 (and 50 µg/ml Hygromycin for BCG::RD1); 10 ml of negative control culture was incubated into a sterile 50 ml Falcon tube with 10 ml 7H9 (and 50 µg/ml Hygromycin for BCG::RD1). All were cultured at 37° C shaking at 100 rpm for ~2-4 days to until OD_{600} reached 0.8-1.0.

BCG cultures were subsequently aliquoted into 3 sterile 50 ml Falcon tubes, centrifuged at 4000 rpm for 15 minutes at 25° C prior to discard of supernatant and addition of 10 ml sterile PBS for washing. Bacteria were resuspended by gentle tapping and pipetting to break up clumps, centrifuged at 4000 rpm for 15 minutes prior to discard of supernatant. Following washing, bacteria were resuspended in

10 ml sterile PBS/15% glycerol, pooled in a sterile flask and brought up to a volume to reach desired OD ~1.0. Bacteria were distributed into 1ml labelled cryotubes and frozen at -80° C.

To enumerate vaccine stocks, random 1 ml frozen BCG stock aliquots were chosen to perform serial dilutions using sterile 1 × PBS with 0.15% glycerol in a 48 well plate (Sigma-Aldrich). 100 µl of the serial dilutions were plated on Middlebrook 7H11 agar plates supplemented with Middlebrook OADC (Sigma-Aldrich) and 50 ug/ml Hygromycin (Thermo Fisher Scientific) for BCG::RD1. Negative control plates consisted of LB broth with 100 µl 'neat' BCG. Agar plates were wrapped in 10% TriGene (Ceva) disinfected aluminium foil and incubated at 37° C for 3-4 weeks.

2.2.3 Mucosal Vaccination

Mice were immunised by IT instillation of 1×10^5 or 5×10^5 colony forming units (CFU) of BCG diluted in sterile phosphate buffered saline (PBS)as described previously (Perdomo et al., 2016). For vaccination, mice were anesthetised via inhalation of isoflurane administered with a calibrated vaporizer. Subsequently, the tongue was pulled out sideways using a blunt forceps, inoculum was administered into the oral cavity and the nostrils were covered to direct the inoculum into the trachea.

Animals were monitored on a weekly basis, with determination of weight and scoring of body condition (BCS) using the mouse BCS scale. Animals which lost >30% of weight or developed a BCS score of 1 (indicative of clinically relevant weight loss or dehydration) were sacrificed humanely prior to death. At the doses utilised in this study, none of animals met institutional animal care and use committee approved endpoints and they were analysed at the planned time-points.

2.2.4. Tissue Harvest

After euthanasia by CO_2 inhalation, animals were exsanguinated by the caudal vena cava to prevent flow of blood into bases of lungs. The thorax was carefully opened with a midline incision past the sternum, diaphragm cut away and lateral chest walls removed to expose lungs. A tracheostomy was

performed by surgical exposure of the ventral side of the trachea and small incision below the larynx before insertion of an 18-gauge stub needle tip and securing with an artery forceps. The luer end of the needle was connected to a reservoir containing fixative (described below). Lungs were inflated via the trachea by gentle infusion of fixative at a constant fluid pressure of 25 cm for 3 min. After the needle was removed and trachea tied off with a ligature, inflated lungs and heart were dissected out *en bloc.*

2.2.5 Development of an Original Fixation Method for Mouse Lung Tissue

Current literature demonstrates that formaldehyde-based fixatives denature proteins and hamper immunohistochemical visualisation of many antigens, particularly, immunological cell surface markers (Beckstead, 1994; Hicks et al., 2006; Mori et al., 2015). Moreover, downstream molecular analyses of BCG vaccinated lungs were thought to benefit from a more optimal fixation method as it is also known that formaldehyde-based fixatives have detrimental effects on DNA and RNA quality (Lykidis et al., 2007; Wester et al., 2003). Thus, development and optimisation of novel lung inflation, fixation and processing was undertaken using a 0.5% Zinc acetate, Zinc chloride in 0.5% Tris-calcium acetate buffer (Beckstead, 1994) zinc-based fixative (ZBF; BD Biosciences) as immunohistochemistry (IHC) is superior in ZBF-fixated tissue compared with formaldehyde-fixated for majority of tested antibodies, including CD3 and CD8 (Beckstead, 1994; Hicks et al., 2006; Mori et al., 2015). ZBF has also been shown to be significantly better than formaldehyde fixatives for DNA, RNA, and protein preservation. ZBF preserves flow cytometry scatter, fluorescence parameters, simultaneous analysis of DNA, intracellular and surface epitopes. ZBF is a reliable, cost-effective, and non-toxic fixative.

Thus, after tissue harvest as described above, excised tissues were placed in 30 ml ZBF at 25° C for 67 hrs. All inferior vena cava, thymus, oesophagus, and heart were removed prior to separation of the left and right lung lobes at the right main bronchus inferior to the bifurcation of the carina. Left and right lung lobes were further immersion fixed in ZBF at 25° C for 6 hrs followed by a one-hour wash in tap

water on an automated rocker at 49 rpm (ELMI) prior to a 24-hour incubation at 25° C in 50% ethanol (necessary to eliminate viable mycobacteria, see 2.2.5)

Not without short-comings, ZBF is known to poorly penetrate tissues (Beckstead, 1994) and is known not to be mycobacteriocidal ("Evaluation of Tissue Fixation Methods to Inactivate Mycobacterium bovis Under Routine Laboratory Conditions," 2017). Tissue penetration shortcomings of ZBF were overcome by using a ZBF lung inflation (to fix the tissue from within) and was combined with post-fixation of individual lung lobes in ZBF. Results demonstrated that whole ZBF inflated lungs excised *en block* with heart and postfixed in ZBF for 72 hours at 25° C exhibited optimal cell and tissue morphology (**Fig. 6**) on par with a 2% paraformaldehyde (PFA) inflated lung fixed overnight in 2% PFA (data not shown).

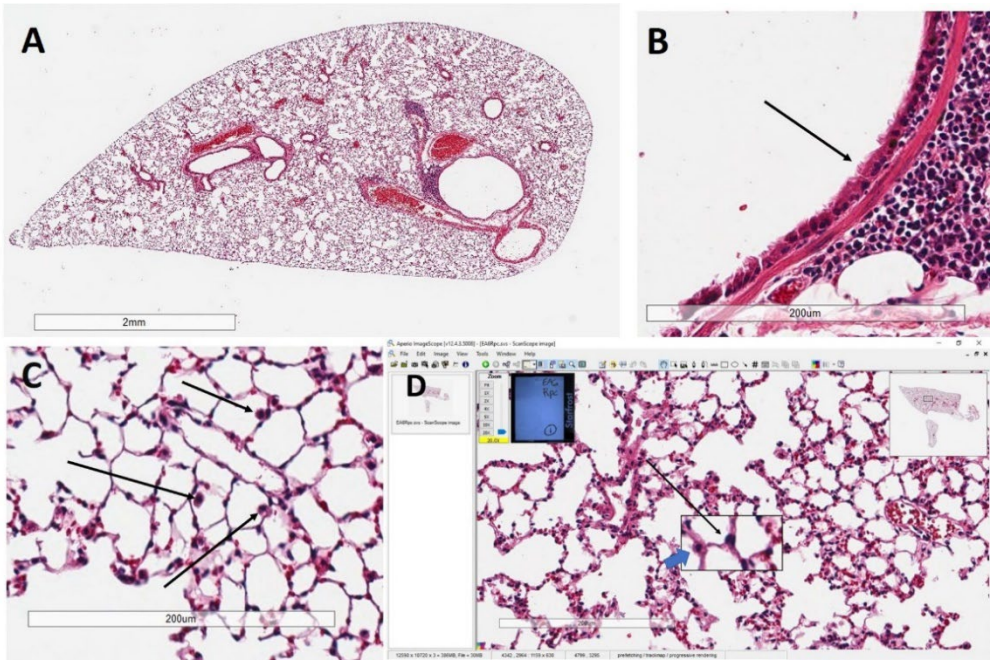

Figure 6. **Lung tissue preservation and morphology following zinc-based fixation.**

A) Cross section through proximal left lung lobe. **B)** ZBF preserves the fine structures of the ciliated epithelial cells of main bronchus shown in section A (arrow). **C)** The fine architecture of the alveolar walls is intact; alveolar macrophages are preserved in their intra-alveolar location (arrows). **D)** Alveolar

epithelial cells are distinguished by light microscopy; blue block arrow shows AEC2 in corner of alveoli while arrow shows two adjacent AEC1 that make up an alveoli wall. Representative images taken from 6 animals from two pooled independent experiments. **A)** Magnification, 1×; Scale bar 2 µm. **B-D)** Magnification, 20×; Scale bar 200 µm.

2.2.6 Determination of BCG Viability Following Zinc Fixation of Lung Tissue

It is known that zinc fixative does not inactivate *M. bovis* (Thacker, 2017); therefore, lung tissues required post-fixation with a mycobacteriocidal to render tissues safe for transition to biosafety level 2/1 laboratories for histopathologic examination. An analysis of clinical microbiology reviews demonstrated that mechanisms of action of alcohols are efficacious as mycobacteriocidals ("Evaluation of Tissue Fixation Methods to Inactivate Mycobacterium bovis Under Routine Laboratory Conditions," 2017; McDonnell & Russell, 1999; Russell et al., 1986), although the time and concentration for lung tissue immersion was to be determined in the context of ZBF fixation in the mucosal vaccination of mouse lung.

Across 2 independent experiments (n=4), animals were IT vaccinated with 5×10^5 CFU BCG SSI. 48 hours after IT BCG vaccination and ZBF fixation as described above, lungs were immersed in 50% ethanol (described in the literature as optimal concentration for ethanol penetration through tissue) for 0, 24 and 48 hours. Whole lungs were then homogenized in sampling bags (Nasco Whirl-Pak™) containing 1ml of PBS supplemented with 0.05% Tween 80. Dilutions of tissue homogenates were plated onto Middlebrook 7H11 agar supplemented with 10% OADC Enrichment (BD Biosciences). CFU were determined after 3–4 weeks incubation at 37° C based on dilution factor and organ size. These experiments demonstrated that following 72-hour fixation in ZBF with a 24-hour post-fix in 50% ethanol at 25° C, BCG were not viable (**Fig. 7**).

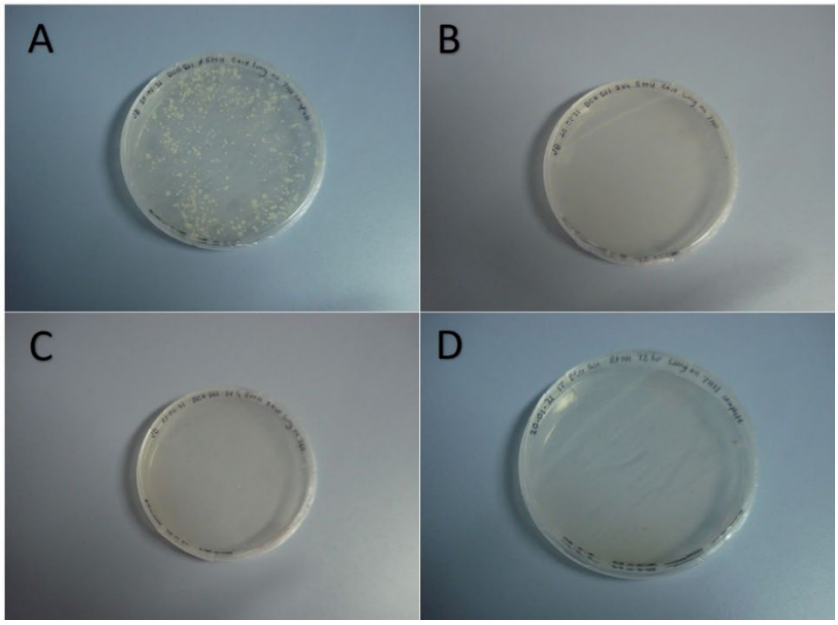

Figure 7. **BCG are not viable following fixation protocol.**

A) Lung lysates plated without 50% ethanol postfix ($^{+}$ control) show numerous CFU. **B, C)** Lung lysates plated after 24-hour immersion in 50% ethanol show no viable bacilli **D)** Lung lysates plated after 48-hour immersion in 50% ethanol show no viable bacilli.

After fixation and ethanol immersion, experimental tissues were dehydrated overnight with an automated tissue processor (Leica Biosystems) and promptly embedded in paraffin blocks. Routine 4 µm sections were cut, floated out on water at 39° C and sections collected on Polysine adhesion slides (ProSciTech). Slides were dried at 25° C overnight prior to deparaffinisation in three changes of xylene (5 minutes each), followed by three changes of absolute ethanol (3 minutes each), one immersion in 75% ethanol (2 minutes) and one in tap water (1 minute). Routine H & E staining was performed using an automated processor (Leica Biosystems) to analyse cell and tissue morphology using light microscopy.

2.2.7 Lineage Tracing

A single dose of 0.125mg/g body weight tamoxifen (Sigma-Aldrich) was dissolved in 50µl corn oil (Sigma-Aldrich) and administered to *Krt5^{CreERT2}/mTmG* mice intraperitoneally at day 14 after IT

vaccination with BCG::RD1. Tamoxifen-independent recombination in *Krt5^{CreERT2}/mTmG* mice was 0% with no systemic effects in floxed littermate controls.

2.2.8 Immunohistochemistry

Tissue sections were immunostained after washing slides twice with Tris-buffered saline (TBS) for 5 minutes each; blocking was then performed with 10% normal serum derived from species specific to the secondary antibodies at 25° C for 2 hours. Primary antibodies were incubated overnight at 4° C at optimised dilutions (Table 2).

Tissues were washed twice for 5 minutes with TBS and twice for 3 minutes with TBS before incubation with peroxidase inhibitor (Thermo Fisher) for 30 minutes at 25° C. For ABC IHC, endogenous avidin binding activity was quenched with avidin blocking buffer (Abcam) for 15 minutes at 25° C, tissue was washed once for 3 minutes with TBS and once for 3 minutes before incubation with biotin blocking buffer (Abcam) for 15 minutes at 25° C. Tissue was washed twice for 5 minutes with TBS, dipped in *% TBS-Tween (TBS-Tw) before incubation with secondary antibodies for 1 hour at 25° C at the optimised dilutions (**Appendix 1**).

For the avidin biotin complex (ABC) method, tissue was then washed twice for 5 minutes with TBS before incubation with 45 µl of Vectastain ABC kit reagents (Vector Laboratories) in 10 ml TBS for 30 minutes at 25° C. Tissue was washed 6 times for 5 minutes with TBS before incubation with DAB chromogen (Abcam) for 3-5 minutes. At 25° C, tissues were washed 3 times for 2 minutes in distilled water, counterstained with 25% haematoxylin (Sigma-Aldrich) for 10 seconds before final 5-minute rinse in distilled water. Tissues were cleared through changes of 50%, 70% and 90% ethanol (3 minutes each) followed by two changes of absolute ethanol (3 minutes each), three changes of xylene (3 minutes each) prior to cover-slipping with Surgipath mounting media (Leica) and #1 coverslips (Leica).

2.2.9 Microscopy

Images were acquired using an Aperio CS2 Digital Slide Scanner (Leica Biosystems) and analysed using Aperio ImageScope v12.4.3.5008 software (Leica Biosystems).

2.3 Results

2.3.1 BCG Virulence and Dose Affects Loss of Alveolar Epithelial Cells

To study the response of lung epithelial cells to mucosal vaccination with BCG strains across a spectrum of dose and virulence over time, we used IT vaccination of C57BL/6 mice (n=6/time point) with the Danish strain of BCG (BCG SSI) at a dose of 100,000 CFU, BCG SSI at 500,000 CFU, BCG::RD1 at 100,000 CFU or PBS (**Fig. 8A**). BCG::RD1 is the strain in which the region of difference 1 (RD1) genes that encode *Mtb* virulence genes ESAT-6 and CFP-10 have been recombined into *M. bovis* (Pym et al., 2002) Mycobacteria can enter and replicate in AEC2 following inhalation, so AEC2 are frontline cells of invasion (Chuquimia et al., 2012); moreover, loss of cell-to-cell contacts due to infection-related cytolysis of AEC2 also affects AEC1 that are particularly sensitive to damage (Whitsett & Weaver, 2015). To determine the relative number of AEC lost (the impetus for immune and subsequent epithelial progenitor cell responses) across our vaccinations, lung sections were immunostained using type 1 alpha protein (T1α), an apical membrane protein expressed exclusively by AEC1 cells in the lung (Gonzalez 1998) and a polyclonal antibody directed against pro-surfactant protein C (pSPC), expressed exclusively by AEC2 in the lung (Beers & Mulugeta, 2005; Kalina et al., 1992; Mulugeta & Beers, 2006). All lungs were analysed by a defined semi-quantitative scoring system using interpretation constancy (Crissman et al., 2004; Klopfleisch, 2013) where cell loss was graded as normal (Grade 0), minimal (Grade 1), moderate (Grade 2) or severe (Grade 3) (**Fig. 8B**). Haematoxylin and eosin (H&E) staining were employed to observe and report histopathology guided by the US Department of Health and Human Services National Toxicology Program (Lung) website (Cesta et al., 2024).

Following BCG SSI low dose vaccination, overall minimal AEC1 losses were observed. Losses peaked at 14 days past vaccination (dpv), reduced at 21 dpv and peaked again at 42 dpv with a subsequent reduction at 49 dpv before clearing across the lung by 120 dpv (**Fig. 8C**). Similarly, AEC2 loss was minimal across the BCG SSI low dose timeline with a peak at 28-35 dpv before clearing by 120 dpv (**Fig.**

8D). The AEC pathology of this vaccination consisted of small focal areas of lesions (**Fig. 9A**), as well as alveolar wall hyperplasia where the alveoli structure stayed intact.

After the BCG SSI high dose vaccination, minimal to moderate AEC1 loss was observed. Cell loss peaked at 21 dpv, was reduced at 70 dpv, and was largely cleared across the lung by 120 dpv (**Fig. 8C**). Moderate AEC2 losses in the SSI high dose vaccination appeared to have waves of peak and reduction from 21 dpv through to 70 dpv before clearing at 120 dpv (**Fig. 8D**). The AEC pathology of this vaccination consisted of numerous global focal areas of lesions. (**Fig. 9B**).

After the BCG::RD1 vaccination, a marked AEC1 loss occurred that peaked at 21 dpv, was reduced to moderate at 49 dpv, and continued with minimal losses across the lung until 120 dpv (**Fig. 8C**). Marked widespread loss of AEC2 was observed from 21 to 35 dpv across the alveolar epithelium and remained moderate from 49 dpv to 70 dpv with minimal continual losses until 120 dpv (**Fig. 8D**). The AEC pathology of this vaccination consisted of large global areas of complete destruction of both AEC1 and AEC2, and AEC necrosis evidenced by $T1\alpha^{+}$ and $pSPC^{+}$ cell debris in bronchiolar lumen (**Fig. 9C**).

Taken together, these results illustrated a direct relationship between dose and virulence of the BCG vaccine and AEC losses. The results raised the likelihood that immune responses to mucosal BCG would also vary significantly with dose and virulence.

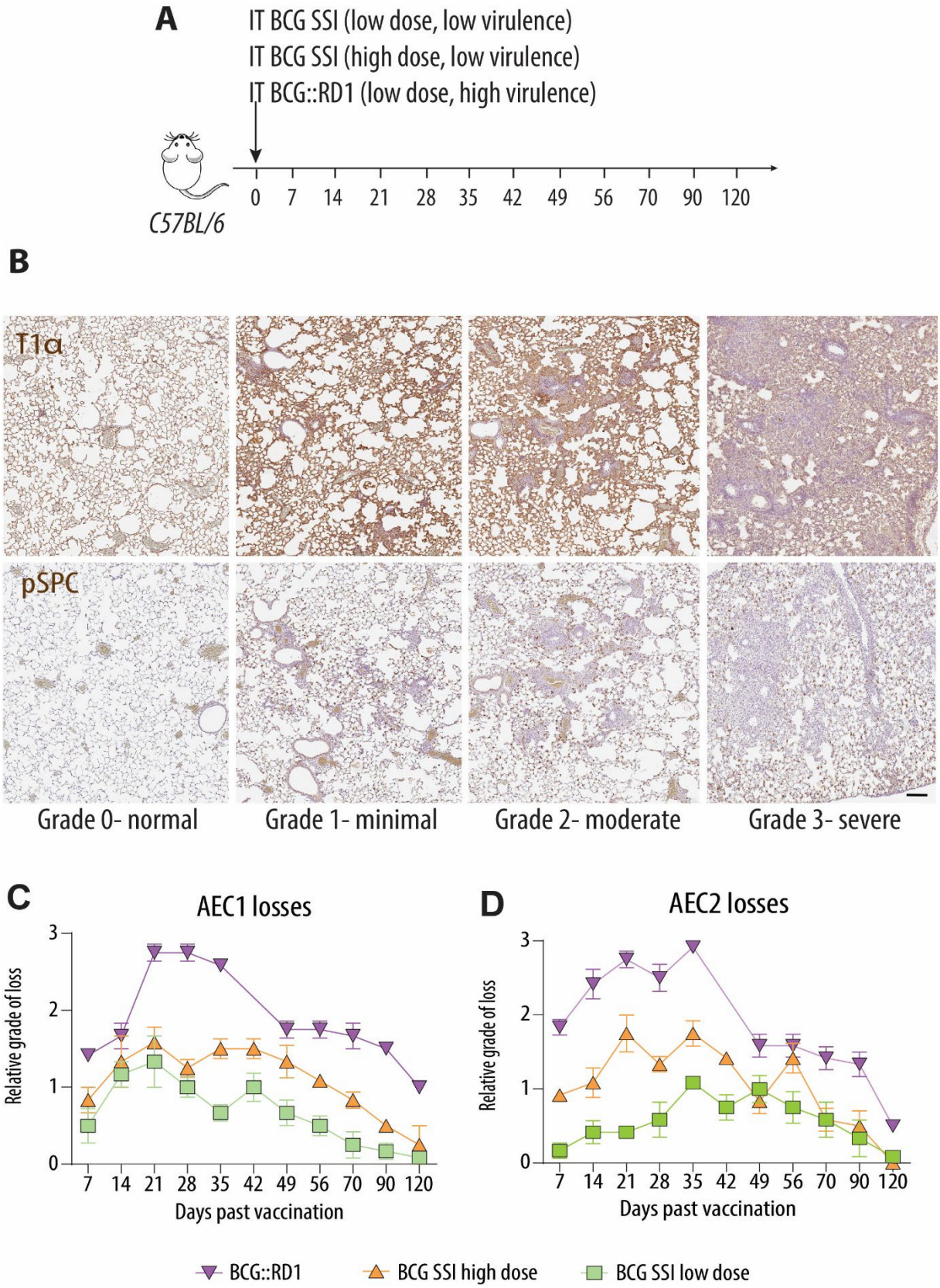
A
IT BCG SSI (low dose, low virulence)
IT BCG SSI (high dose, low virulence)
IT BCG::RD1 (low dose, high virulence)
C57BL/6
0 7 14 21 28 35 42 49 56 70 90 120
B
T1α
pSPC
Grade 0- normal
Grade 1- minimal
Grade 2- moderate
Grade 3- severe
C
AEC1 losses
Relative grade of loss
Days past vaccination
D
AEC2 losses
Relative grade of loss
Days past vaccination
BCG::RD1
BCG SSI high dose
BCG SSI low dose

Figure 8. **AEC losses are directly related to IT BCG dose and virulence.**

A) Experimental design to define AEC losses and immune responses. **B)** Examples of relative tissue grading of AEC1 and AEC2 losses using immunohistochemical (IHC) staining for T1α and pSPC, respectively. Semi-quantitative enumeration of **C)** AEC1 and **D)** AEC2 losses over time. Results are presented from representative images and pooled data means ± SEM from 6 mice per time group from two pooled independent experiments. **B)** Magnification, 5.2×; Scale bar, 400 µm.

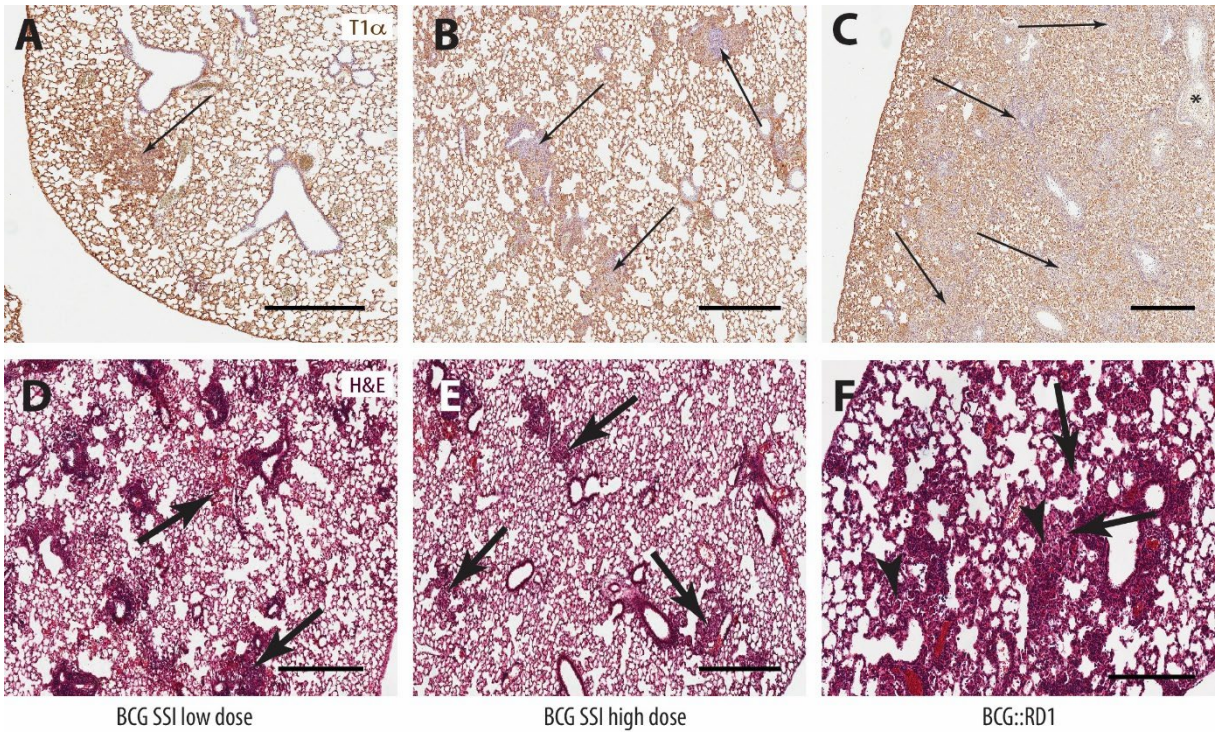

Figure 9. **Alveolar pathology due to mucosal BCG vaccination.**

A-C) Lesions with loss of T1α AEC1 marker staining (blue areas indicated by arrows) due to vaccine pathology. **C)** Necrotic AEC debris within bronchiole lumen (indicated by asterisk) due to BCG::RD1 vaccination. **D)** H&E staining shows focal areas of hemorrhage (arrows) due to the SSI low dose vaccination, **E)** interstitial giant cells (arrows) due to the SSI high dose vaccination **F)** alveolar giant cells (arrowheads) and foamy cells (arrows) due to the BCG::RD1 vaccination. Results are presented from

representative images from 3 mice per group and pooled data means ± SEM from two independent experiments (n=6). **A-C)** Magnification, 6x; Scale bar 400 µm. **D)** Magnification, 5×; Scale bar 500 µm. **E)** Magnification, 4.8×; Scale bar 500 µm. **F)** Magnification, 10×; Scale bar 300 µm.

2.3.2 BCG Dose, Virulence and Delivery Impacts Lung Inflammation and T Cell Influx

We next sought to broadly define immune responses to AEC loss to determine the time of peak tissue destruction associated with inflammation and cytotoxic T cell responses. Inflammation was an important aspect of the vaccinations to analyse as lack of resolution of inflammation leads to delay or disruption of tissue regeneration/restitution by epithelial progenitor cells. Here, inflammation was defined by leukocyte infiltration and vascular changes that resulted in haemorrhage or oedema and disruption of the normal architecture due to inflammatory infiltrates. T cell infiltration was graded distinctly from inflammation (due to lack of other tissue changes associated with inflammation) and generally corresponded to the peak of tissue damage. To determine the relative grade of inflammation and the number of T cell infiltrates across the timeline of each of the vaccinations, lung sections from each animal across the timeline were stained with H&E and analysed by a defined semi-quantitative scoring system using interpretation constancy (Crissman et al., 2004; Klopfleisch, 2013) where inflammation was graded as normal (Grade 0), minimal (Grade 1), moderate (Grade 2) or significant (Grade 3) (**Fig. 10A**). A monoclonal antibody directed against CD3 epsilon (CD3e), expressed by $CD4^+$ and $CD8^+$ T cells was used to identify and characterise T cell infiltration using the same relative grading scale (**Fig. 10A**).

After the BCG SSI low dose vaccination, inflammation rose slowly to peak at moderate levels by 28 dpv and was largely resolved by 35 dpv (**Fig. 10B**). T cells infiltrated relatively early compared to the other two vaccinations, reaching moderate numbers by 21 dpv and declining steadily thereafter (**Fig. 10C**). The inflammatory response associated with this vaccination consisted of minimal, small haemorrhagic lesions due to vascular changes (**Fig. 9D**) and minimal focal peribronchiolar and perivascular inflammation. T cell infiltration was noted in the interstitium; however, as we did not perform

intravascular staining prior to tissue harvest, it is unknown whether these T cells were in the circulation or parenchyma of the tissue.

When BCG SSI was administered at a high dose, inflammation did not peak until 35 dpv (**Fig. 10B**). Instead of a steady decline of inflammation, there were 3 waves of inflammation with a last peak at 70 dpv before resolution. T cell infiltration peaked later at 35 dpv and was graded relatively lower than the SSI low dose vaccination (**Fig. 10C**). The inflammatory response consisted of numerous (global) focal areas of haemorrhage due to capillary changes and moderate peribronchiolar (primarily T cells) and perivascular immune cell infiltrates, as well as moderate numbers and clusters of proximal peribronchiolar interstitial giant cell macrophages (**Fig. 9E**).

After the BCG::RD1 vaccination, global inflammation escalated to severe levels by 21 dpv and remained severe until 42 dpv (**Fig. 10B**). T cell infiltration also peaked by 21 dpv and T cells continued to infiltrate in high numbers until 56 dpv (**Fig. 10C**). The inflammatory response related to this vaccination consisted of early haemorrhage secondary to inflammation, marked peribronchiolar and perivascular infiltrates, and marked numbers of interstitial giant cells and foamy macrophages (**Fig. 9F**).

We observed that in distal areas of the lung at the level of the terminal bronchioles and alveolus, the BCG SSI high dose vaccination did not show infiltrating CD8 T cells (**Fig. 11B**). This was in marked contrast to that seen in the low dose BCG SSI and BCG::RD1 vaccinations (**Fig. 11A, C**). We reasoned that the concentrated numbers of bacilli in the vaccine may have made the vaccine more viscous and therefore bacilli may not have been delivered into the most distal parts of the lungs. Therefore, sections were cut into the more proximal levels of the BCG SSI high dose lungs where infiltration of T cells was noted, particularly in peribronchiolar regions (**Fig. 11D**).

Overall, we were able to determine the timeline associated with the expansion and contraction phases of the immune response in each of our vaccinations which gave insight into the corresponding times of tissue restitution and progenitor cell responses for each of the vaccinations. With these

experiments, we demonstrated that dose, virulence, and delivery of mucosal BCG vaccination had direct effects on inflammation and acquired immune responses.

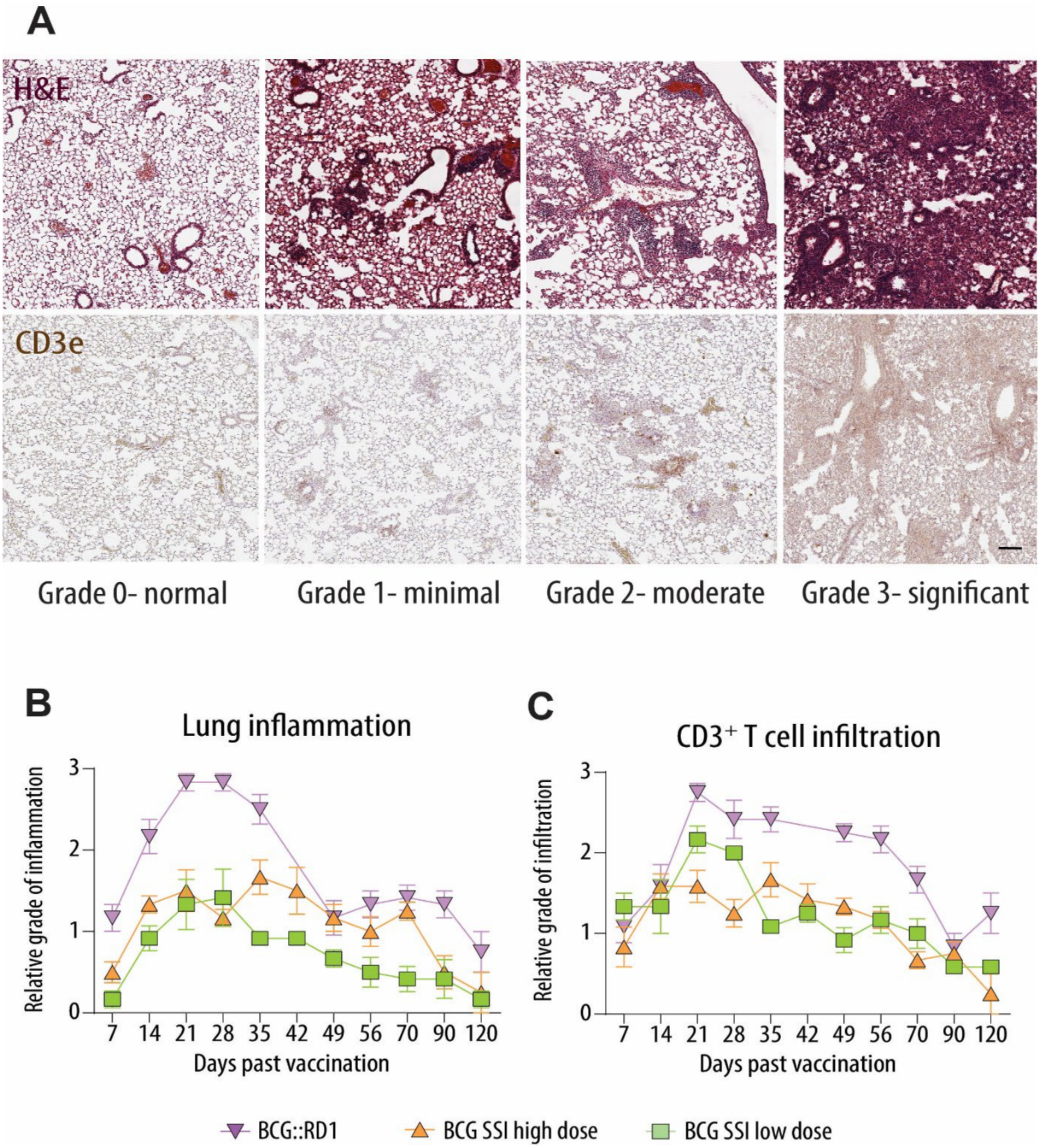

Figure 10. **Lung inflammation and acquired immune responses are directly related to IT BCG dose and virulence.**

A) Examples of relative alveolar tissue grading for inflammation and infiltration of T cells using H&E and CD3e, respectively. Semi-quantitative data of **B)** inflammation and **C)** T cell infiltration across the vaccinations and timeline. Results are presented from representative images and pooled data means ± SEM from 6 mice per time group from two pooled independent experiments. **A)** Magnification, 4.2×; Scale bar 500 µm.

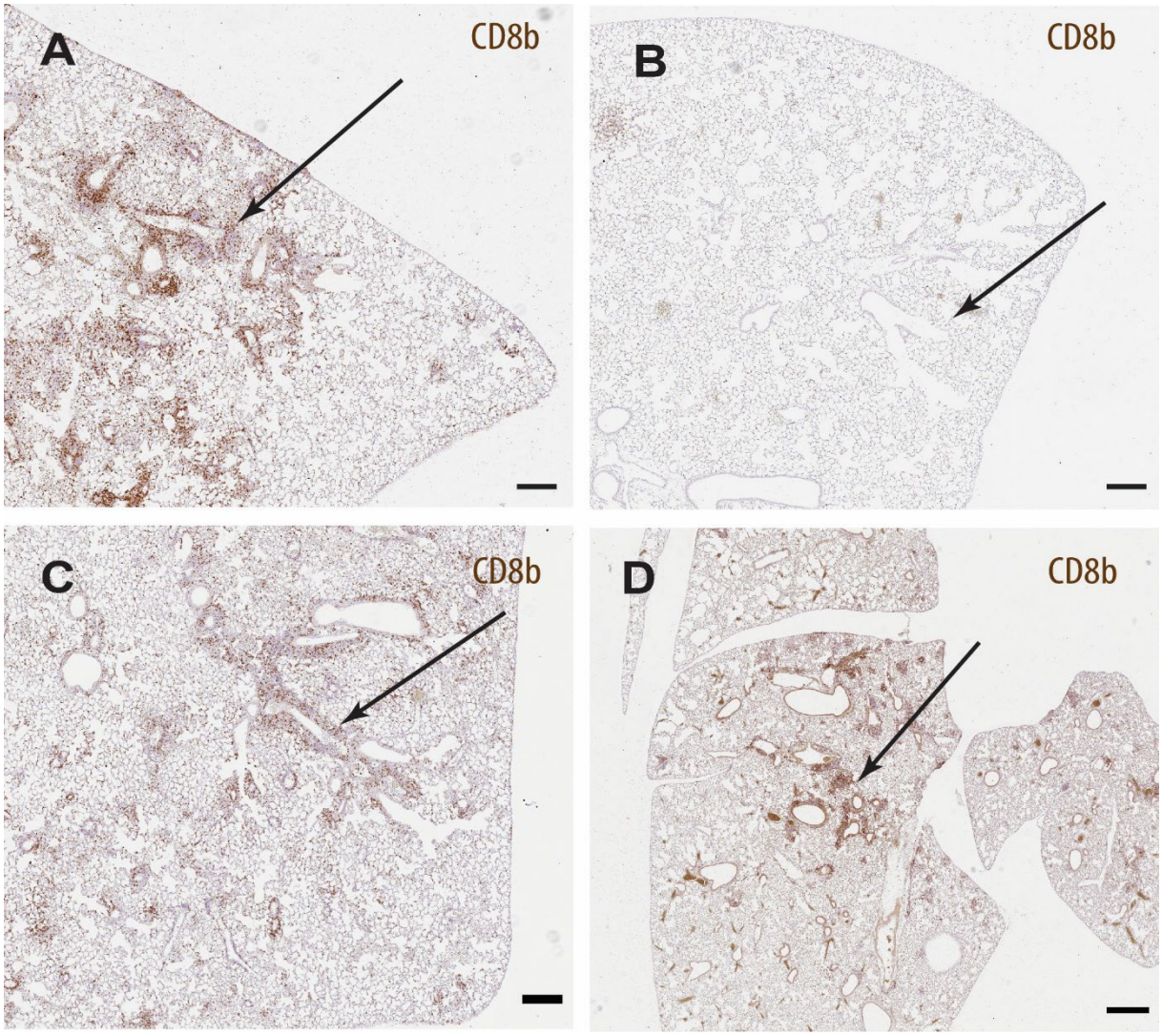

Figure 11. **T cell influx is directly related to delivery of IT BCG.**

Representative images of distal alveolar epithelium and terminal bronchioles (arrows) show significantly more infiltration by $CD8^+$ T cells in the **A)** BCG::RD1 and **C)** BCG SSI low dose vaccinated lungs as compared to **B)** BCG SSI high dose. **D)** Proximal sections of lungs vaccinated with BCG SSI high dose show $CD8^+$ T cell infiltration. Results are presented from representative images and pooled data means ± SEM from 6 mice per time group from two pooled independent experiments. **A-C)** Magnification, 2.5×; Scale bar 900 µm. **D)** Magnification, 1.5×; Scale bar, 2 mm.

2.3.3 Only $Sox2^+$ Distal Airway and Alveolar Epithelial Progenitors Respond to AEC Losses Associated with Mucosal BCG Vaccination

We next undertook an original characterisation of lung epithelial progenitor cell responses to mucosal BCG vaccinations. Lung sections were probed using antibodies against Krt5 for DASC, Sox2 for distal airway epithelial progenitors and pSPC for alveolar progenitors across the timeline. Results demonstrated that although Krt5 was expressed in basal cells of the large conducting airways, we did not observe $Krt5^+$ cells in alveolar tissue at any time after vaccination (**Fig. 12A**). We confirmed these findings using *Krt5^{CreERT2}/mTmG* reporter mice to indelibly tag DASC progeny with green fluorescent protein (Muzumdar et al., 2007)(**Fig. 12B**). Again, we observed green fluorescent protein in the large airway basal cells but never in alveoli (**Fig. 12C**).

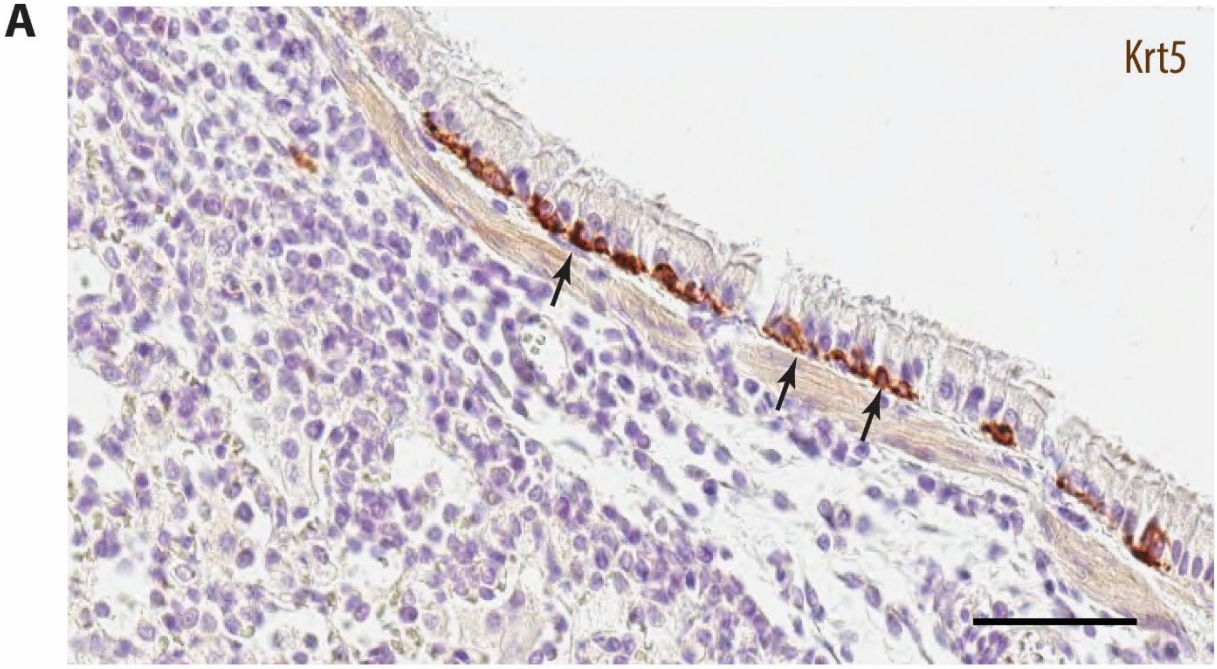
A
Krt5

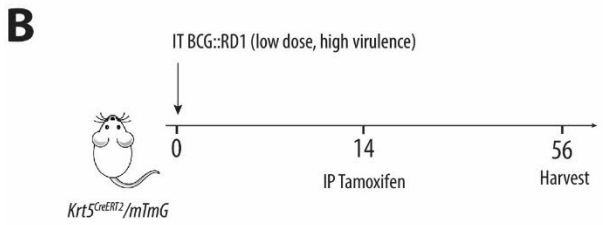
B
IT BCG::RD1 (low dose, high virulence)
0
14
IP Tamoxifen
56
Harvest
Krt5CreERT2/mTmG

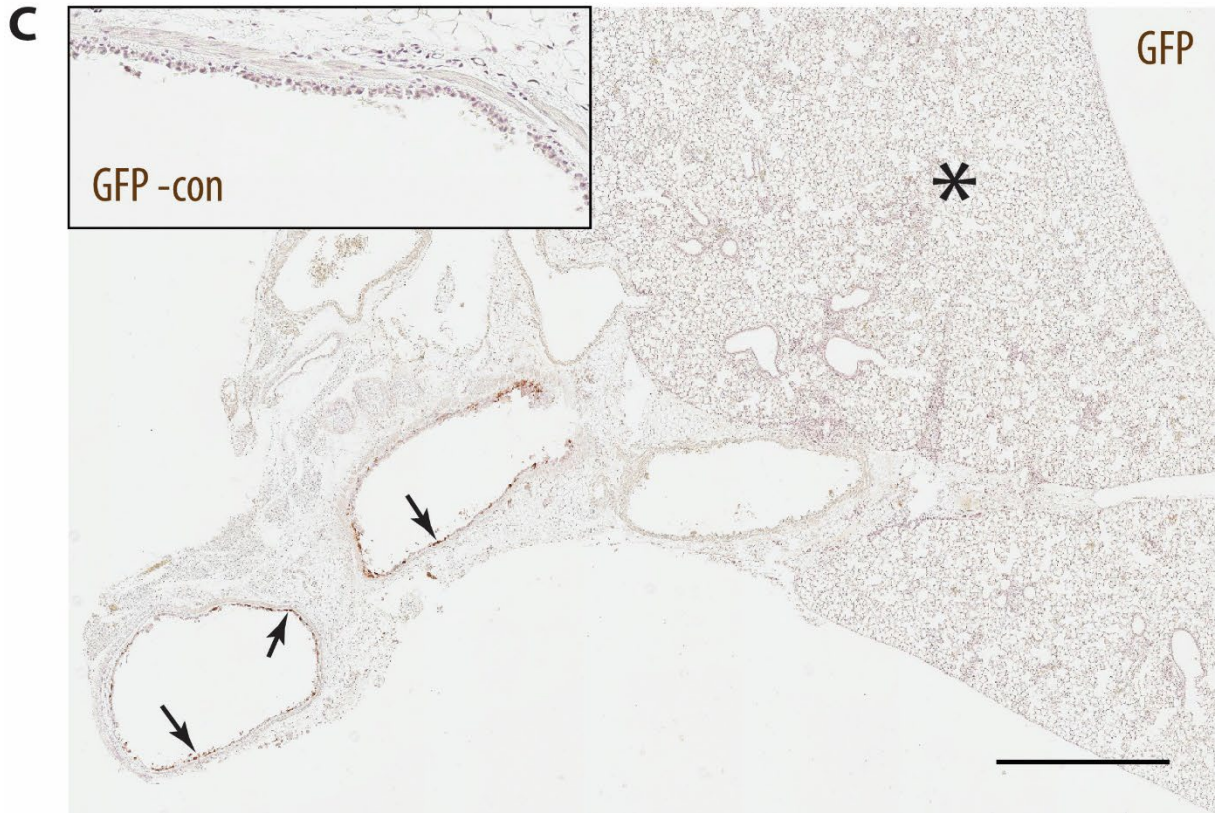
C
GFP -con
GFP

Figure 12. **DASC do not respond to injury following IT BCG vaccination.**

A) Representative image showing Krt5 staining evident in the large conducting airways (arrows) of *C57BL/6* mice was not seen in alveolar regions at any timepoint following any IT BCG vaccination. **B)** Experimental design for lineage tracing of $Krt5^+$ DASC that restituted the alveolar epithelium after mucosal BCG vaccination. **C)** Lineage tracing confirmed that basal cells of the proximal airways expressed green fluorescent protein (arrows) but that $Krt5^+$ DASC were not incorporated in the alveolar epithelium (asterisk) at 56 days past virulent BCG::RD1 IT vaccination. Results are presented from representative images and data means ± SEM from 3 mice per group from two pooled independent experiments (n=6/timepoint). **A)** Magnification, 20×; Scale bar 50 µm. **B)** Magnification, 1.5×; Scale bar 2 mm.

In contrast, by 7 dpv after the BCG::RD1 vaccination, rounded cells with nuclear $Sox2^+$ expression were seen in and adjacent to the terminal bronchiole (where cuboidal airway epithelium discontinues); in the contiguous alveolar epithelium, squamous cells with cytoplasmic $Sox2^+$ expression were noted (Fig. 13).

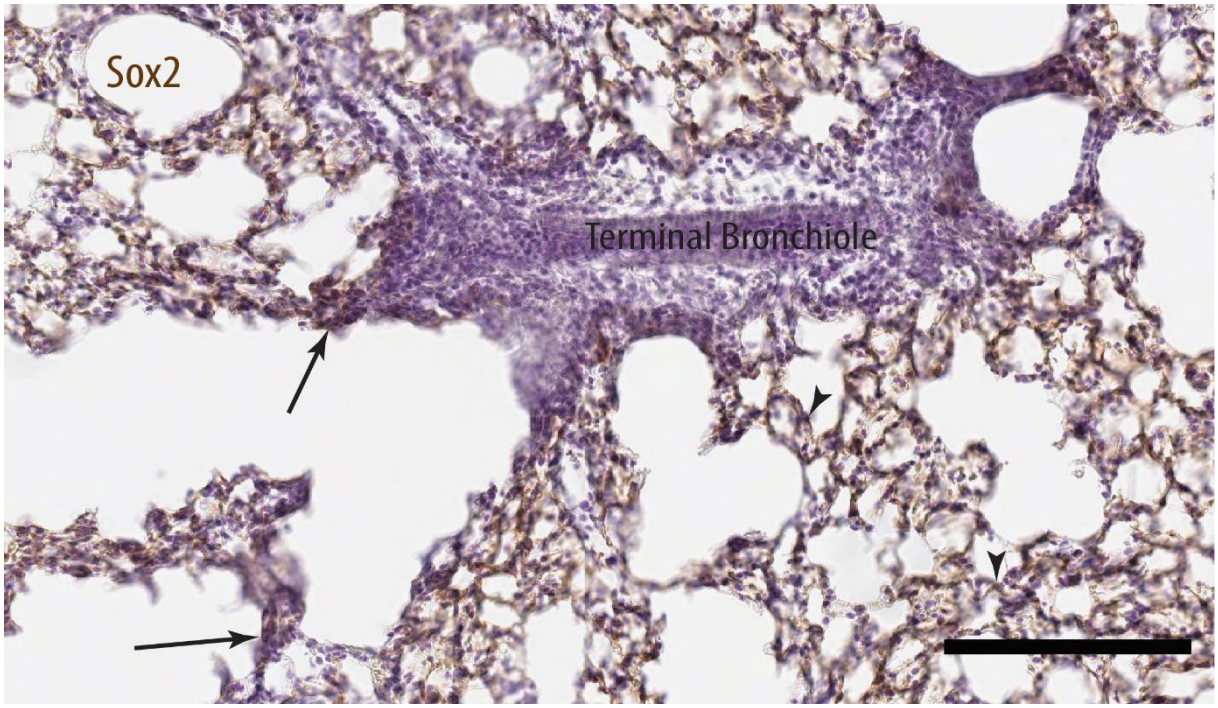

Figure 13. **Sox2$^+$ distal airway epithelial progenitors respond to mucosal BCG vaccination.**

Representative image at 7 days after BCG::RD1 vaccination, where Sox2 expression is seen in cells in (arrows) and adjacent to distal terminal bronchioles (arrowheads). Results are presented from representative images and data means ± SEM from 3 mice per group from two pooled independent experiments (n=6/timepoint). Magnification, 10×; Scale bar 200 μm.

Therefore, across our vaccination' timeline, relative enumeration of Sox2$^+$ distal airway and pSPC$^+$ alveolar epithelial progenitors were undertaken using the respective markers and analysed by a defined semi-quantitative scoring system using interpretation constancy (Crissman et al., 2004; Klopfleisch, 2013) where tissues were graded for normal (Grade 0), mild (Grade 1), moderate (Grade 2) or significant (Grade 3) numbers of the two epithelial progenitor cell types (**Fig. 14A**). Results demonstrated that following the BCG::RD1 vaccination, significant numbers of Sox2$^+$ airway progenitors were observed early but subsequently waned after day 21; conversely, numerous pSPC$^+$ alveolar progenitors were observed only after day 21 (**Fig. 14B, C**). In areas of severe destruction, pSPC$^+$ progenitors were not seen, although they were seen on the periphery of these lesions (**Fig. 28B**). After the SSI high dose vaccination, Sox2$^+$ airway progenitors were seen to peak in numbers later at 49 dpv (**Fig. 14C**) probably related to the later peak of cell losses, inflammation, and T cell responses; these cells were confined largely to proximal peribronchiolar regions. After the SSI low dose vaccination, pSPC$^+$ alveolar epithelial progenitors appeared largely as doublets recapitulating the pattern of 'foci' of progeny across neighbouring alveoli described by Desai (Desai et al., 2014), while Sox2$^+$ airway progenitor numbers were very minimal (**Fig. 14C**). Of note, Sox2$^+$ cells were seen throughout all areas of alveolar damage-from mild to severe in each of the three vaccinations, bar the BCG SSI low dose vaccination which did not cause any severe alveolar damage (**Fig. 14D**).

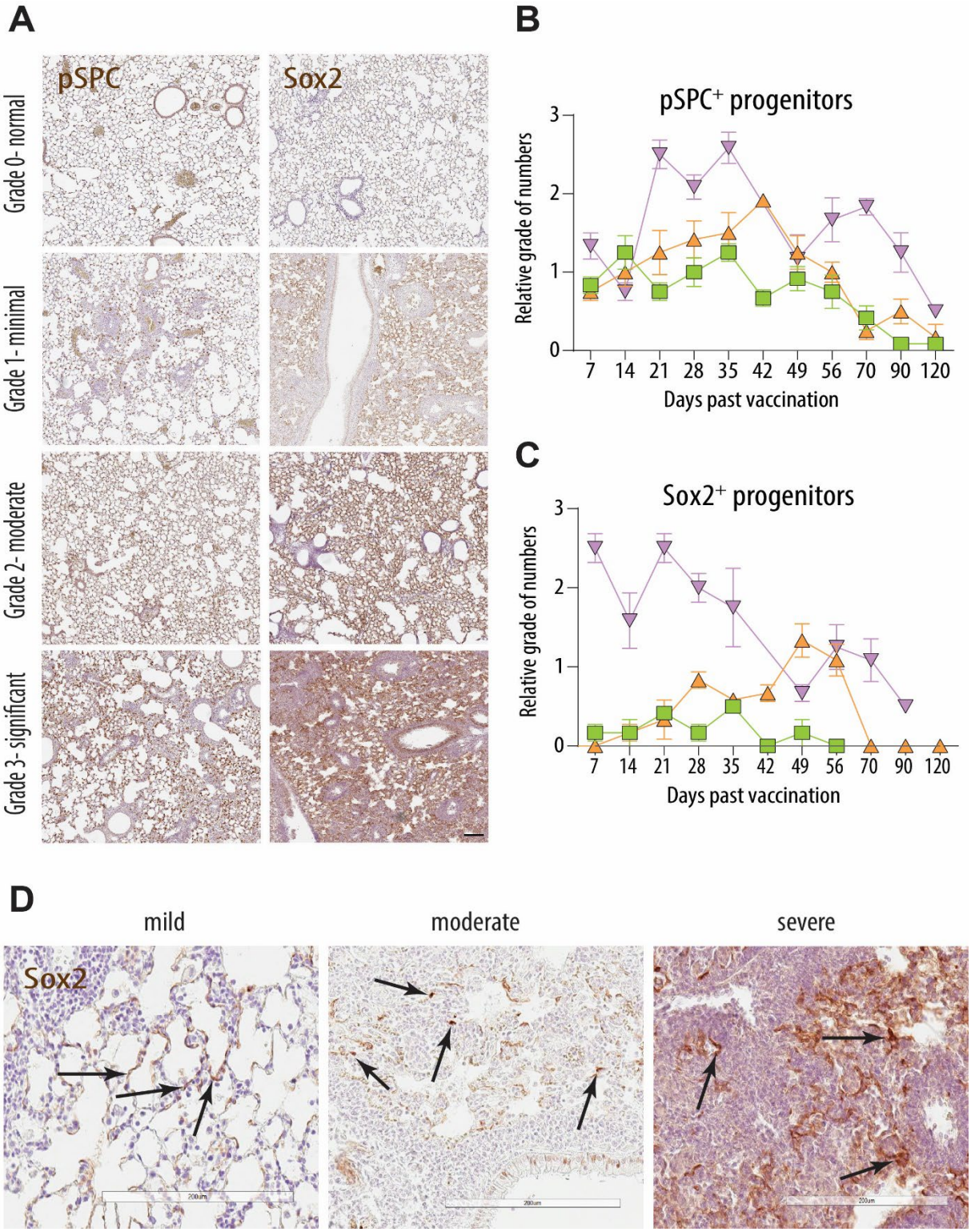
A
pSPC
Sox2
Grade 0- normal
Grade 1- minimal
Grade 2- moderate
Grade 3- significant
B
pSPC+ progenitors
Relative grade of numbers
0
1
2
3
7 14 21 28 35 42 49 56 70 90 120
Days past vaccination
C
Sox2+ progenitors
Relative grade of numbers
0
1
2
3
7 14 21 28 35 42 49 56 70 90 120
Days past vaccination
D
mild
moderate
severe
Sox2

Figure 14. **Activation of distal airway and alveolar progenitors is dependent upon dose and virulence of IT BCG vaccination.**

A) Examples of relative alveolar tissue grading for proliferation of alveolar and distal airway epithelial progenitors using pSPC and Sox2 IHC staining, respectively. **B, C)** Semi-quantitative data are presented from representative images and pooled data means ± SEM from 3 mice per time group from two independent experiments (n=6/timepoint). **D)** $Sox2^+$ airway progenitors (arrows) are seen throughout all areas of alveolar damage following each of the vaccinations. Results are presented from representative images and data means ± SEM from 6 mice per group from two pooled independent experiments. **A)** Magnification, 10×; Scale bar 200 μm. **D)** Magnification, 20×; Scale bar 200 μm.

2.3.4 Characterisation of $Krt8^+$ Transitional Progenitor Responses to Mucosal BCG Vaccination

More recently, a $Krt8^+$ transitional progenitor (TP) cell state that precedes differentiation of both $Sox2^+$ airway and $pSPC^+$ progenitors into AEC1 was described (Choi et al., 2020; Kobayashi et al., 2020; Strunz et al., 2020). We investigated $Krt8^+$ TP using our vaccinations as we reasoned that these lung epithelial progenitors interact with lung $CD8^+$ T_{RM}. In many serial sections, we observed an inverse staining pattern in which alveolar areas void of Sox2 staining had Krt8 staining and vice versa (**Fig. 15A**); this supported the notion that $Sox2^+$ airway cells were transitioning into $Krt8^+$ progenitors. By 14 dpv, the BCG SSI low dose had punctate areas of $Krt8^+$ TP, while the BCG::RD1 vaccination had broad diffusion of $Krt8^+$ TP throughout lungs (**Fig. 15B**). At 21 dpv after BCG SSI low dose, $Krt8^+$ cells acquired a squamous morphology and were likely transitioning into AEC1 (**Fig. 15B**); conversely, after BCG::RD1 vaccination, $Krt8^+$ cells remained round (**Fig. 15B**) and did not become squamous until after 28 dpv (data not shown). Quantification of $Krt8^+$ TP for both vaccinations showed a peak of $Krt8^+$ TP at 21 dpv where BCG::RD1 vaccinated lungs had an average alveolar area of ~20% occupied by $Krt8^+$ cells, while those of the SSI low dose had an area of ~5% (**Fig. 15C**). Recall that the BCG SSI high dose vaccination had little effects on distal alveolar epithelium, therefore was not included in these analyses.

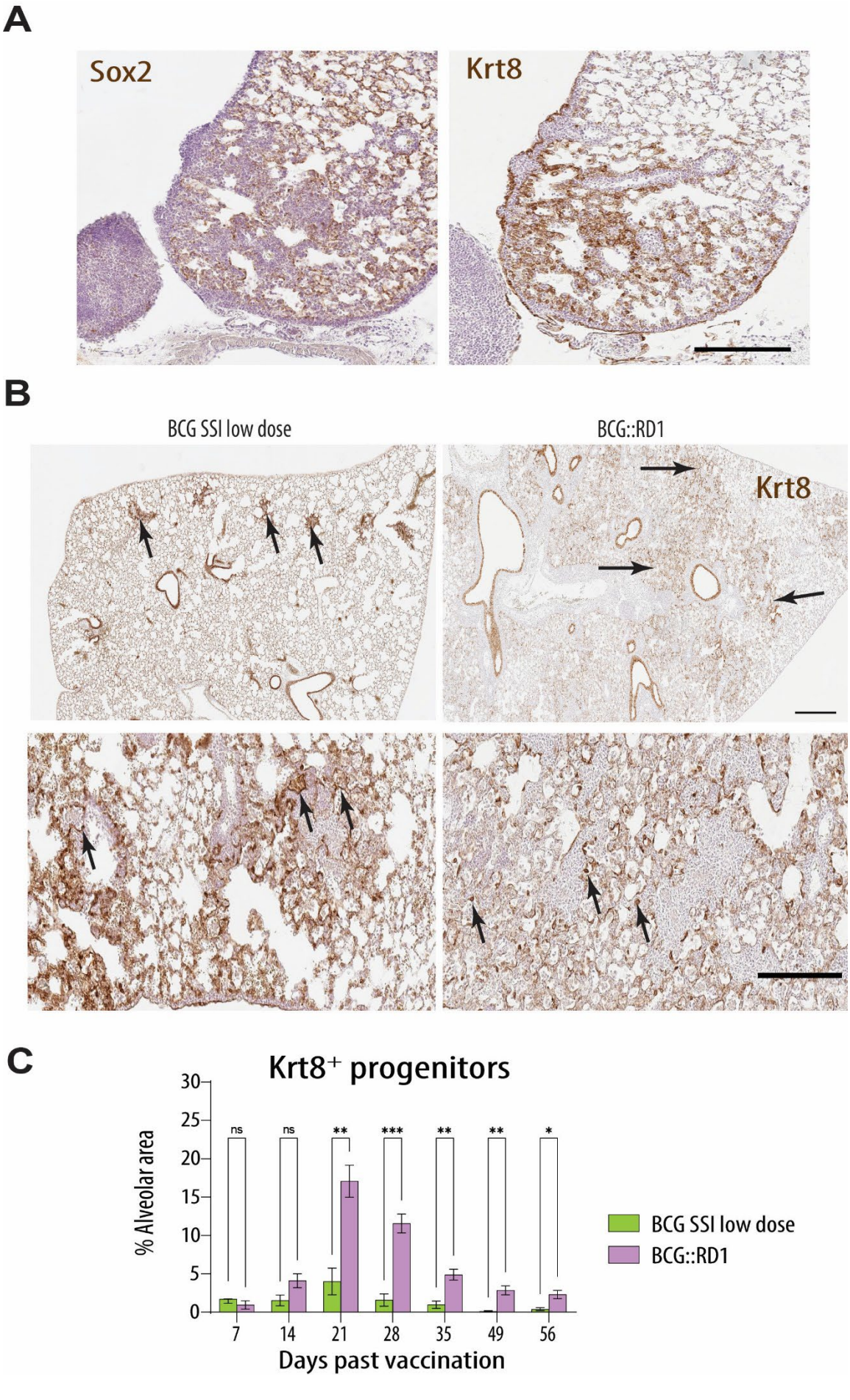
A
Sox2
Krt8
B
BCG SSI low dose
BCG::RD1
Krt8
C
Krt8+ progenitors
% Alveolar area
30
25
20
15
10
5
0
ns
ns
**
***
**
**
*
7
14
21
28
35
49
56
Days past vaccination
BCG SSI low dose
BCG::RD1

Figure 15. **Distal airway and alveolar epithelial progenitors transition through the Krt8$^+$ cell state following mucosal BCG vaccination.**

Krt8 staining revealed that **A)** the TP state was seen within tissue areas of Sox2 expression, in an 'inverse' relationship. **B)** Lungs 14 days after vaccination with BCG SSI showed punctate areas of Krt8$^+$ TP (arrows), while those from BCG::RD1 lungs showed diffuse Krt8$^+$ TP throughout (arrows). **C)** 21 days after BCG SSI vaccination, Krt8$^+$ cells had a squamous morphology (arrows) while in BCG::RD1 vaccinated lungs, Krt8$^+$ TP retained round morphology (arrows). **D)** Quantification of Krt8$^+$ TP numbers. Results are presented from representative images and data means ± SEM from 6 mice per group from two pooled independent experiments. **A, C)** Magnification, 10×; Scale bar 200 μm. **B)** Magnification, 4.2×; Scale bar 500 μm.

In summary, we demonstrated that solely Sox2$^+$ distal airway and alveolar epithelial progenitors responded to AEC losses associated with mucosal BCG vaccination. Where alveolar tissue damage was mild or moderate, alveolar epithelial progenitors were seen, whereas, where alveolar tissue damage was severe, Sox2$^+$ distal airway progenitors were seen while pSPC alveolar progenitors were not. Both progenitor cell types transitioned through the Krt8$^+$ TP state into AEC1, as evidenced by tissue restitution around 120dpv.

2.4 Discussion

We note first that although individual scoring systems for particular IHC markers was thought the best possible way to answer our initial scientific questions, due to nonstandardised approach, subjectivity and variability of visual inspection, the method of manual scoring IHC slides was less than precise. However, IHC is a well-established tool, which is used to help identify specific pathological processes and widely used in experimental research. Here, we combined descriptive analyses and semiquantitative scoring systems to evaluate different parameters; both represent a universal approach to include histopathologic information in biomedical research (Fedchenko & Reifenrath, 2014).

Our study demonstrated that dose and virulence of mucosal BCG vaccination had a direct influence on alveolar epithelial cell losses. Although AEC1 are particularly sensitive to damage due to their long, thin delicate cytoplasmic extensions, (Whitsett & Weaver, 2015), lost AEC1 are rapidly and efficiently regenerated by AEP (and AEC2 under certain conditions). Conversely, severe damage to or loss of AEC2 results in considerable vulnerability of the alveolus (Fehrenbach, 2001). More than just progenitor cell of the alveolar epithelium, AEC2 are also immunoregulatory (Fehrenbach, 2001) and have long been described as 'the defender of the alveolus' (Mason & Williams, 1977). AEC2 constitute 15% of all lung cells (Castranova et al., 1988) and due to their location, the chance that they encounter pathogen is notable. Moreover, compared to bronchiolar epithelial cells, AEC2 are more susceptible to BCG infection *in vitro* (Bermudez & Goodman, 1996; McDonough & Kress, 1995). Mycobacteria can enter and replicate in AEC2 and in early lung infection, AEC2 are frontline cells of invasion (Chuquimia et al., 2012).

AEC2 are non-phagocytotic, however, *in vitro* studies have demonstrated that receptors such as integrins, carbohydrate receptors and ECM components (Dias et al., 2012; Kinhikar et al., 2010; Kuo et al., 2012; Kuo et al., 2013; Lerner et al., 2015) facilitate BCG adherence and internalisation (Zimmermann et al., 2016) by macropinocytosis (Bermudez & Goodman, 1996; Garcia-Perez et al.,

2003) and endocytosis following binding. It has been shown that AEC2 internalise mycobacteria at a high rate *in vitro* co-culture (Ganbat et al., 2016) and it has been demonstrated that once internalised, AEC2 are able to *control* BCG bacterial growth and go on to play a prominent role in shaping the ensuing immune response.

Inflammatory cytokines secreted by AEC2 not only modulate immune cell function but also provide paracrine signals into the local milieu to activate inflammatory transcription factors such as signal transducer and activator of transcription (STAT), nuclear factor-kappa beta (NF-κB) and interferon regulatory factors (IRFs) in adjacent epithelial cells (Lin et al., 1998; Mendez-Samperio, Miranda, & Vazquez, 2006; Mendez-Samperio et al., 2008b; Sharma et al., 2007). AEC2 also produce biomolecules involved in enhancement of phagocytosis and microbial killing, including complement proteins and antibiotics such as defensins (Lin et al., 1998; Mendez-Samperio et al., 2007; Mendez-Samperio, Miranda, & Trejo, 2006; Mendez-Samperio, Miranda, & Vazquez, 2006; Mendez-Samperio et al., 2008b; Sharma et al., 2007).

A549 cells (immortalised AEC2) stimulated by BCG cause the inhibition of the Wnt/B-catenin pathway which leads to the secretion of IL-6 and TNFα pro-inflammatory cytokines (Li et al., 2014; Ma et al., 2014). Following *in vitro* BCG infection, of A549 cells activate various signalling pathways to induce chemokines CXCL8, CXCL10, CCL5, CCL2, cytokine IL-10, and antimicrobial peptides b-defensin- 2, cathelicidin LL-37 and hepcidin (Iliopoulos et al., 2009; Johnnidis et al., 2008; Mendez-Samperio et al., 2008a; Sheedy et al., 2010; Tili et al., 2007). Importantly, AEC2 that express homing receptor chemokines during inflammation provide access to precursor T_{RM} for their entry into inflamed tissue (Kohlmeier et al., 2008; Mackay et al., 2013). Thus, from this perspective, the lesser magnitude of AEC2 losses and inflammation seen in our BCG SSI vaccinations combined with a transitory yet robust adaptive immune response, allude to the ability of AEC2 to initiate and control the magnitude of both the innate and adaptive immune responses of the host.

The recombinant BCG::RD1 strain used in our vaccinations possessed the ESX-1 secretion system encoded by the RD1 gene group; in this strain, early secreted antigenic target 6 (ESAT-6) and culture filtrate protein 10 (CFP-10) are secreted by the ESX-1 system (Wong, 2017). Therefore, in contrast to the repercussions of non-virulent BCG invasion of AEC2 as described above, BCG::RD1 that replicate in AEC2 use ESAT-6 to anchor onto the basolateral laminin-expressing surface of AEC2, damage basement membrane, cause membrane lysis and cell necrosis to directly disseminate through the alveolar wall into the pulmonary interstitium (Krishnan et al., 2010). Our results confirmed that these virulence factors of the mucosal BCG::RD1 vaccine had a direct influence on both the severity and extended time of AEC cell losses, inflammation and acquired immune responses.

Restoration of cell number and tissue function are the roles of stem cell progeny; these progenitors begin migration the first day of injury and will continue to proliferate and differentiate onsite of injury for weeks following primary infection (Puchelle et al., 2006; Stripp & Reynolds, 2008; Zahm et al., 1991; Zahm et al., 1997; Zahm et al., 1992). Restitution of the epithelial barrier occurs as epithelial progenitor cells spread and migrate to cover denuded areas; if the basement membrane underlying the injured epithelium is intact, epithelial progenitor cells migrate along the matrix using filopodial and lamellipodial extensions (Puchelle et al., 2006; Tam et al., 2011) until they meet adjacent epithelial cells and form new tight junctions. Restitution is supported by growth factors secreted by mesenchymal and epithelial cells, such as hepatocyte growth factor (HGF), keratinocyte growth factor, epidermal growth factor, TGF-β and fibroblast growth factors (Fgf) (Puchelle et al., 2006; Vaughan & Chapman, 2013).

The dynamics of progenitor cell responses to lung infection, across spatially heterogeneous zones of injury, are influenced by factors such as pathogen burden, stage of infection, numbers of cells infected, differences in host susceptibility, virulence of pathogen strain and host lung health. At the start of our research, most of what was known about epithelial progenitor cell responses in the lung was gleaned through influenza and bleomycin models. In both these models, airway progenitors that migrate into

the alveolar regions to assist with tissue restitution are of a basal cell-like Krt5^{+} phenotype (Kumar et al., 2011; Vaughan & Chapman, 2013; Xi et al., 2017; Zuo et al., 2015). It has been theorised that exhaustion or depletion of alveolar epithelial progenitors in areas of complete alveolar destruction activates Krt5^{+} airway progenitors to respond for restitution following influenza infection (Vaughan et al., 2015). Thus, we investigated whether Krt5^{+} airway progenitors had a role in alveolar restitution in our mucosal BCG::RD1 vaccination; remarkably, despite significant alveolar destruction, IHC histology showed that proximal Krt5^{+} airway epithelial progenitors did not proliferate and migrate into alveolar regions as they have been reported to in other lung infection models with similar magnitude of alveolar loss (Kumar et al., 2011; Vaughan et al., 2015; Zacharias et al., 2018).

The Sox2 TF is constitutively expressed and required for the maintenance of bronchiole airway epithelial cells (Tompkins et al., 2009). Moreover, Sox2^{+} lineage positive progenitors (these express mature epithelial lineage markers such as Clara cell marker SCGB1A1) and Sox2^{+} lineage negative progenitors (these do not express any epithelial lineage markers) are known to be a major source of replacement cells in zones of airway and alveolar cell loss associated with influenza infection (Ray et al., 2016). In the bleomycin vaccination of alveolar injury, in severely damaged areas, 40% of newly formed AEC1 are derived from airway stem cells as determined by *Sox2*^{CreERT2} lineage tracing (Strunz et al., 2020).

In the distal terminal bronchioles, by virtue of strong peribronchiolar Sox2 expression, distal airway progenitors appeared to migrate into the alveolar regions robustly after the BCG::RD1 vaccination. We also observed squamous cells in the alveolar epithelium with cytoplasmic Sox2^{+} expression, suggestive of acetylation-mediated nuclear export of Sox2. Acetylation-mediated nuclear export leads to reduction in Sox2 TF levels by ubiquitination and proteasomal degradation, thus abrogating the TF's ability to drive transcription of target genes. This a commonly used regulatory mechanism for many Sox family members (Baltus et al., 2009) and importantly, the Sox2 TF is known to regulate cell proliferation and differentiation of airway progenitors (Tompkins et al., 2009). We reasoned that cells

with cytoplasmic Sox2 expression within the alveolar regions may be airway progenitor cells undergoing transition into Krt8 TP.

We further characterised the contribution of $Sox2^+$ progenitors to restitution of areas of mild, moderate and severe alveolar epithelial cell losses, as it has been reported in influenza vaccinations that the airway progenitor's role in alveolar tissue restitution may be restricted to areas of severe epithelial cell loss (Vaughan et al., 2015; Zacharias et al., 2018). After the BCG::RD1 vaccination, which included areas across the spectrum of mild-severe epithelial losses, we showed that $Sox2^+$ progenitors were not restricted to areas of severe/complete cell losses but were seen throughout the entire regenerative alveolar epithelium. These findings were in direct contrast to those seen for $pSPC^+$ alveolar epithelial progenitors; in areas of severe/complete destruction, we did not see proliferative foci of these cells. However, $pSPC^+$ progenitors were abundant after all our vaccinations throughout areas of mild and moderate alveolar damage suggesting a model in which $pSPC^+$ progenitors are the major lineage contributing to restitution of lungs with mild or moderate injury, while airway progenitors assist with restitution throughout lungs that have been severely damaged by mucosal BCG::RD1 vaccination.

We also investigated the transitional $Krt8^+$ progenitor's contribution to tissue restitution across areas of mild, moderate, and severe/complete alveolar epithelial cell losses as it was unknown whether airway and alveolar progenitors transition through this cell state associated with mycobacterial lung injury. Here, we demonstrated that this transitional progenitor cell did function after mucosal BCG vaccinations. We observed $Krt8^+$ TP in all areas of regenerative tissue, and because restitution did (primarily) occur within four months of mucosal BCG vaccination across the vaccinations, we concluded that the airway and alveolar progenitors did successfully transition through $Krt8^+$ TP into AEC1.

CHAPTER 3. DEVELOPMENT AND PERSISTENCE OF LUNG CD8$^+$ T_{RM} FOLLOWING MUCOSAL BCG VACCINATION

There is a sense in which no doctor ever heals…what the treatment does is to stimulate natural functions or to remove what hinders them.

C.S. LEWIS, *Miracles*

3.1 Introduction

Although T_{RM} are a contemporary focus in immunology, there are gaps in the knowledge of lung CD8$^+$ T_{RM} following mucosal BCG vaccination. For example, is there a diverse CD8$^+$ T_{RM} bionetwork linked to mucosal BCG vaccination? There is nothing in the literature that describes RAMD formation such as is described in depth in the PR8 mouse model of influenza. Other important unresolved concepts include the kinetics of lung CD8$^+$ T_{RM} development, characterisation of CD8$^+$ T_{RM} subsets and demonstration of CD8$^+$ ex-lung T_{RM} found in the lung-draining mediastinal lymph nodes after mucosal BCG vaccination. Moreover, although it was originally thought that CD8$^+$ T_{RM} were terminally differentiated, permanent residents of the lungs in which they developed, a growing body of literature has shown that CD8$^+$ T_{RM} retain developmental plasticity, as well as their unique properties of attrition and egression from the lungs. Thus, our next aim was to characterise the development and persistence of lung CD8$^+$ T_{RM} using our three mucosal BCG vaccinations across a protracted timeline to better understand the possibilities to harness them for novel TB vaccination strategies.

3.2 Methods

3.2.1 Animals

C57BL/6 mice sourced from the ARC (Western Australia) were bred and maintained in the animal facilities at James Cook University, Australia. Female mice were 6–8 weeks old at the time of vaccination and maintained in a biosafety level 2 facility under specific pathogen free conditions.

3.2.2 Bacteria

Bacterial culture and enumeration were as described in section 2.2.2.

3.2.3 Mucosal Vaccination

IT mucosal vaccinations were performed as described in section 2.2.3.

3.2.4 Lung and Mediastinal Lymph Node Dissociation

Lung and spleen dissociation kits (Miltenyi Biotec) were used to dissociate lung and mLN into single-cell suspensions, respectively, according to manufacturer's instructions. Briefly, PEB (FACS) buffer contained PBS (pH 7.2), 0.5% bovine serum albumin (BSA) and 2 mM EDTA and were kept at 2−8 ° C. Lung and mLN enzyme mixes were prepared by adding 2.4 mL of 1× Buffer S, 100 µL or 50 µL, respectively, of Enzyme D, and 15 µL of Enzyme A into gentleMACS C Tubes (Miltenyi Biotec). After euthanasia by CO_2 inhalation, animals were exsanguinated by the caudal vena cava. The thorax was opened with a midline incision past the sternum, diaphragm cut away and lateral chest walls removed to expose lungs. Lungs were perfused via the right ventricle with 10 ml PBS. Lungs were dissected out into single lobes (without extrapulmonary airways) and rinsed in a petri dish containing PBS to remove remaining blood. Each lung lobe was inflated with enzyme mix by injecting enzyme slowly using 25 G needle connected to 3 mL syringe. Lobes of one mouse were transferred into a gentleMACS C Tube

containing lung enzyme mix. The right superior mLN was dissected out and transferred into a gentleMACS C Tube containing spleen enzyme mix.

gentleMACS C Tubes were attached onto sleeves of the gentleMACS Dissociator (Miltenyi Biotec) and run without heating function using the gentleMACS Program m_lung_01 or m_spleen_02. Samples were then incubated for 30 minutes at 37 °C with gentle agitation. The gentleMACS Program m_lung_02 or m_spleen_03 were run to further dissociate the tissues. A short centrifugation step for 1 minute at 300g at 25° C was performed to collect sample material at the tube bottom. Samples were resuspended and applied to 70µm MACS SmartStrainer (Miltenyi Biotec) placed on a 15 ml Falcon tube. MACS SmartStrainers were washed with 2.5 ml FACS buffer and cell suspension centrifuged at 300 × g for 10 minutes at 25° C. Supernatant was aspirated before addition of 3 ml RBC lysis buffer (Thermo Fisher Scientific), resuspension and incubation for 2 minutes. FACS buffer was added up to 10 ml to stop reaction prior to centrifugation at 1500 rpm for 5 minutes at 25° C. Supernatant was discarded and cells resuspended with FACS buffer to 500 µl.

3.2.5 Flow Cytometry and Data Analyses

150 µl of lung and mLN sample cells were pipetted into wells of a 96 round bottom well plate and spun at 1500 rpm at 4° C for 5 min. Supernatant was flicked off and cells were resuspended in 50 µl Live/Dead cell stain 1:1000 (APC-Cy7 channel) (BD Biosciences) prior to incubation at 25° C for 10 min in the dark. Samples were washed with 100 FACS buffer, spun at 1500 rpm for 5 min. at 4° C. Supernatant was discarded and samples resuspended in 50 µl antibody master mix consisting of FACS buffer, CD49a/BV421 (1:200) (BD Biosciences), CD8a/FITC (1:200) (BD Biosciences), CD69/PE (1:100) (BD Biosciences), CD103/AF647 (1:200) (BD Biosciences), and CD16/32 (1:500) (BD Biosciences). Samples were incubated for 30 min on ice in the dark, washed twice with 100 µl FACS buffer, spun at 1500 rpm at 4° C for 5 min and supernatant discarded. 150 µl Sphero Blank Calibration Particles (BD Biosciences) at 1:75 was added to resuspend samples. Samples were filtered before cytometry

analyses were performed on a LSR Fortessa cytometer using FACSDiva software (BD Biosciences). The data were analysed by FlowJo software (Treestar).

3.3 Results

3.3.1 Lung $CD8^+$ T_{RM} Induction Depends on BCG Virulence and Dose

To define induction and persistence of $CD8^+$ T_{RM} subsets following vaccination with the three different BCG dose/virulence combinations, mice were given IT BCG vaccination as previously described in section 2.3.1. Whole lungs of experimental animals were harvested and processed into single-cell suspensions before $CD8^+$ T_{RM} quantification using flow cytometry (**Fig. 16A**).

The $CD103^+CD69^+CD49a^+$ T_{RM} subset that patrol airway epithelium and adjacent interstitium (Topham et al., 2019) is described as the archetypal $CD8^+$ T_{RM} as it is less malleable and restrained in its differentiation capacities due to a 'mature' T_{RM} phenotype linked to TGF-β-mediated upregulation of CD103 (Carbone, 2023; Christo et al., 2021; Zhang & Bevan, 2013). These $CD8^+$ T_{RM} are not stationary, but migrate slowly along the airway epithelial/ interstitial interface due to CD103 binding to E-cadherin and CD49a binding to collagen IV of the epithelial basement membrane (Reilly et al., 2020; Topham et al., 2019). Outside-in signalling due to direct contact with E-cadherin maintains expression of CD103 (Wu 2022 iELs). The interstitial subset of $CD103^-CD69^+CD49a^+$ T_{RM} are described as early, highly migratory effector T_{RM} (Reilly et al., 2020) that function as robust perforin producers within the interstitium to combat early interstitial pneumonia (Fukushi et al., 2011; Reilly et al., 2020; Topham et al., 2019). By virtue of CD103 binding to E-cadherin at airway epithelial cell junctions (Topham et al., 2019), short-lived (~28 days) $CD103^+CD69^+CD49a^-$ epithelial effector T_{RM} take up static residence solely in the airway epithelium (Eriksson et al., 2022; Reilly et al., 2020; Takamura et al., 2019; Topham et al., 2019; Wein et al., 2019). They have an apoptotic phenotype up-regulated by the harsh airway environment (Hayward et al., 2020) and are said to be replaced by proliferative $CD103^+CD69^+CD49a^+$ T_{RM} (Takamura et al., 2019; Wein et al., 2019).

BCG::RD1 vaccination led to a robust expansion of $CD103^+CD69^+CD49a^+$ T_{RM} from 14 to 35 dpv, with a peak at day 28; numbers contracted at day 42 yet remained significant until 120 days (**Fig. 16B**). After

BCG SSI high dose vaccination, the magnitude of $CD8^+$ T cells in the lung were about half the numbers of the BCG::RD1 vaccination (**Fig. 16C**). Of those, 25% were $CD103^+CD69^+CD49a^+$ T_{RM} at day 21 past-vaccination but waned consistently each week down to negligible numbers by day 120 (**Fig. 16C**). After the BCG SSI low dose vaccination, the magnitude of $CD8^+$ T cells in the lung were about one third the numbers of the BCG::RD1 vaccination (**Fig. 16 D**). Of those, 10% were $CD103^+CD69^+CD49a^+$ T_{RM} at day 21 past- vaccination and waned consistently each week down to negligible numbers by day 120 (**Fig. 16D**).

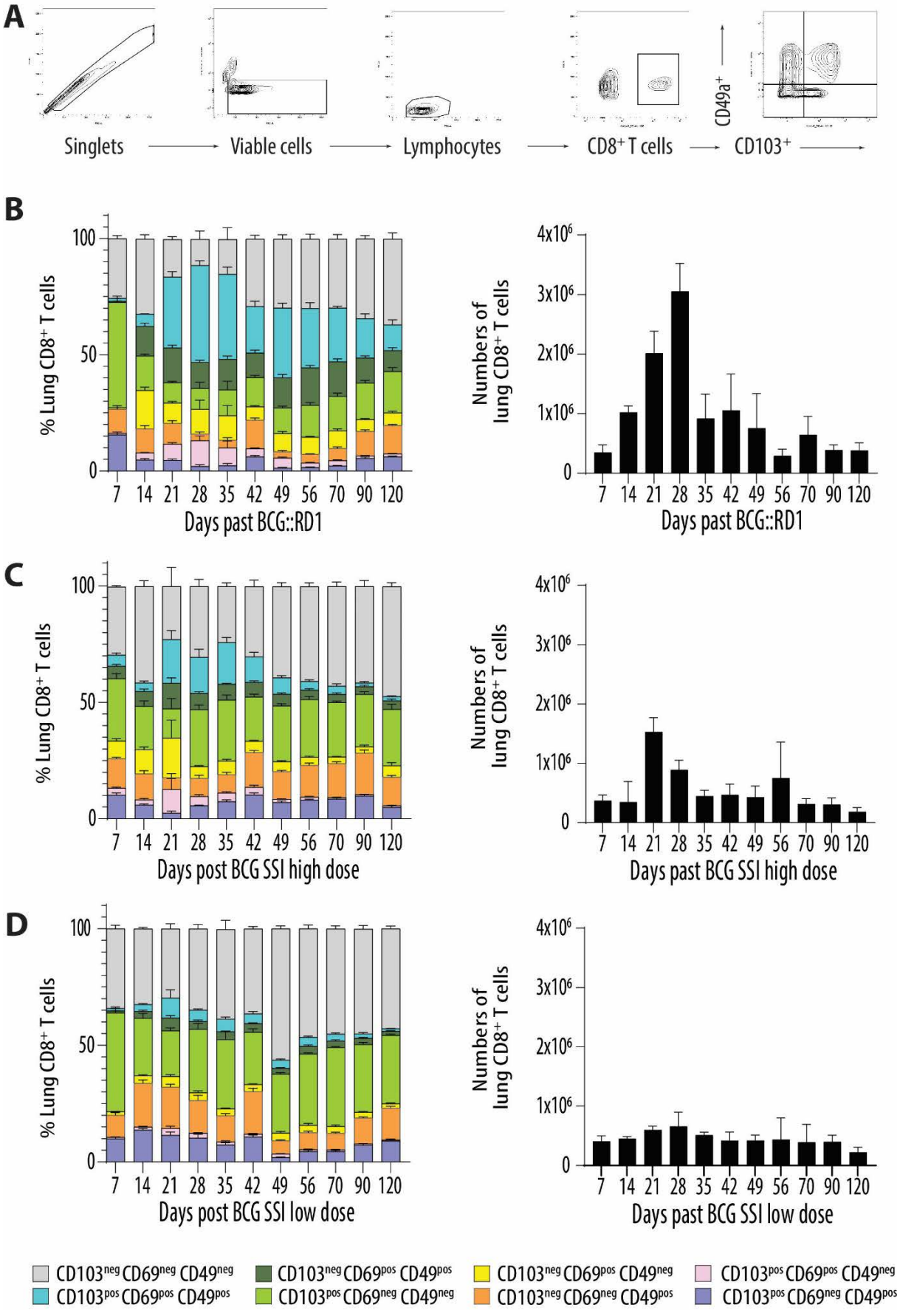
A
Singlets
Viable cells
Lymphocytes
CD8+ T cells
CD103+
CD49a+
B
% Lung CD8+ T cells
Days past BCG::RD1
Numbers of lung CD8+ T cells
Days past BCG::RD1
C
% Lung CD8+ T cells
Days post BCG SSI high dose
Numbers of lung CD8+ T cells
Days past BCG SSI high dose
D
% Lung CD8+ T cells
Days post BCG SSI low dose
Numbers of lung CD8+ T cells
Days past BCG SSI low dose
CD103neg CD69neg CD49neg
CD103pos CD69pos CD49pos
CD103neg CD69pos CD49pos
CD103pos CD69neg CD49neg
CD103neg CD69pos CD49neg
CD103neg CD69neg CD49pos
CD103pos CD69pos CD49neg
CD103pos CD69neg CD49pos

Figure 16. **CD8α$^+$ T cell numbers and percentages of lung CD103, CD69 and CD49a T_{RM} subsets following mucosal BCG vaccination.**

A) Flow cytometry gating strategy for CD8$^+$ T_{RM} quantification. Flow cytometry analysis of the percentages of CD8α$^+$ T_{RM} subsets and numbers of CD8α$^+$ T cells in the lungs of mice vaccinated with **B)** BCG::RD1 **C)** BCG SSI high or **D)** low dose. Pooled data from two independent experiments where n=4-10.

Following BCG::RD1 vaccination from day 14-120, CD103$^+$CD69$^+$CD49a$^+$ T_{RM} were the highest proportion (45% of CD8$^+$ T cells in the lung at their peak) and increased ~40% from 14-28 dpv (**Fig. 16B; 17A**). CD103$^-$CD69$^+$CD49a$^+$ T_{RM} early effectors (Eriksson et al., 2022; Topham et al., 2019) were also abundant (**Fig. 17B**). The short-lived CD103$^+$CD69$^+$CD49a$^-$ epithelial effectors (**Fig. 17C**) that patrol the airway epithelium only (Hayward et al., 2020; Topham et al., 2019) were significant at days 21-35 before waning at day 70 while CD103$^-$CD69$^+$CD49a$^-$ precursor T_{RM} (Eriksson et al., 2022) were continually replenishing the lung from day 14 to 120 (**Fig. 17D**).

At day 21 in the SSI high dose vaccination, numbers of CD103$^+$CD69$^+$CD49a$^-$ epithelial effector T_{RM} were higher than those seen in the BCG::RD1 vaccination (**Fig. 17C**). Although higher numbers of CD103$^-$CD69$^+$CD49a$^-$ precursor T_{RM} were seen particularly in the early weeks of this vaccination (in fact higher than BCG::RD1 at day 21) numbers of all subsets of T_{RM} peaked at day 21 and waned rapidly thereafter across the timeline (**Fig. 17**).

CD103$^-$CD69$^+$CD49a$^+$ T_{RM} interstitial effectors were observed at later days after the BCG SSI low dose vaccination (**Fig. 17B**). Although lower in numbers than the BCG::RD1 and BCG SSI high dose vaccinations, CD103$^-$CD69$^+$CD49a$^-$ precursor T_{RM} were kept at steady state levels throughout the time course of the BCG SSI low dose vaccination (**Fig. 17**). Taken together, we demonstrated that lung CD8$^+$ T_{RM} induction was virulence- and dose-related in all vaccination regimens and that CD8$^+$ T_{RM} waned in the lungs by 120 days after mucosal BCG vaccination.

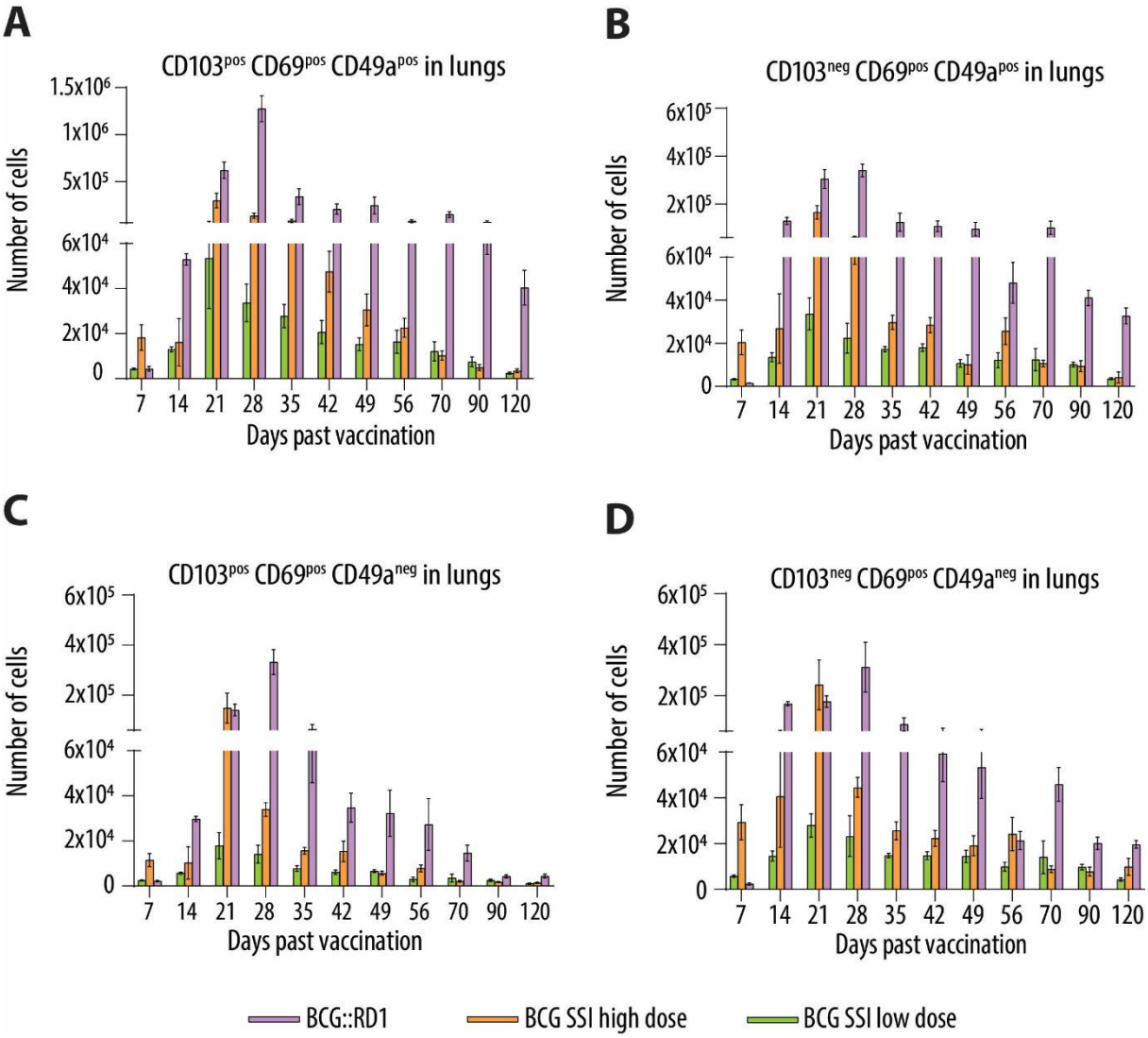

Figure 17. **Lung CD8⁺ T_{RM} counts.**

Quantification of CD8⁺ T_{RM} that **A)** patrol the airway/interstitial border of the airways **B)** patrol the lung interstitium **C)** solely patrol the airways **D)** are of the CD8⁺ T_{RM} precursor phenotype

3.3.2 Lung-draining Mediastinal Lymph Node Harbour CD8$^+$ T_{RM} Following Mucosal BCG Vaccination

It has been consistently demonstrated that lung CD8$^+$ T_{RM} wane over a short time (Hogan et al., 2001; Perdomo et al., 2016; Slutter et al., 2017; Wu et al., 2014), despite continual circulation of antigen-specific T cells in blood (Takamura, 2017). As lung CD8$^+$ T_{RM} are known to egress to the lung-draining mLN, (where they are said to provide regional immune memory for the lungs), (Stolley et al., 2020) we next investigated whether this was the case following mucosal BCG vaccination. Mice were given IT vaccination as previously described, the right superior mLN was extracted from all experimental animals across 7-120 dpv and processed into single-cell suspensions before quantification of CD8$^+$ T_{RM} using flow cytometry.

We discovered all phenotypes of ex-lung CD8$^+$ T_{RM} in the mLN. CD103$^+$CD69$^+$CD49a$^+$ T_{RM} that patrol the airway/interstitial border of the airways and CD103$^+$CD69$^+$CD49a$^-$ T_{RM} that solely patrol the airways were conceivably swept into lymphatics due to tissue damage that physically dislodged them (Carbone, 2023) (**Fig. 18**). We observed CD103$^+$CD69$^+$CD49a$^+$ T_{RM} subsets early, associated with the time of severe damage following BCG::RD1 vaccination (**Fig. 19A**) and later after BCG SSI high dose vaccination, likely associated with its characteristic late immune response (**Fig. 19A**).

CD103$^-$CD69$^+$CD49a$^+$ T_{RM} that patrol the lung interstitium (**Fig. 18**) and lack CD103 maturation are said to preferentially egress to the mLN (Carbone, 2023); also, when restimulated, CD103$^+$CD69$^+$CD49a$^+$ T_{RM} proliferate in the mLN and lose CD103 expression (Stolley & Masopust, 2017). Here, we showed for the first time that following mucosal BCG vaccination, mLN harbor cells with the CD103$^-$CD69$^+$CD49a$^+$ T_{RM} phenotype which, importantly, may have the capacity to repopulate the lungs as T_{RM} following secondary infection (Brewitz et al., 2017; Christo et al., 2021; Paik & Farber, 2021) (**Fig. 19B**).

We also noted CD103$^-$CD69$^+$CD49a$^-$ T_{RM} of the precursor phenotype (Eriksson et al., 2022) at the *latest* stages of the timeline in the mLN (**Fig. 19D**) when numbers of lung CD8$^+$ T_{RM} had steadily declined, and tissue was largely restituted. We reasoned that these may be exhausted effector T cells that home to

B cell follicles of draining lymph nodes due to chronic antigen stimulation where they become stem-like $CD8^+$ T_{RM} (Beltra et al., 2020; G. Li et al., 2022; Ozga et al., 2022). With chronic *Mtb* infection, prolonged overexposure to antigens has been reported to cause T cells to lose effector functions and exhibit an exhausted phenotype (Pan et al., 2023) including expression of PD-1 (Jayaraman et al., 2016); also anti-TB therapy has been shown to promote reduced expression of PD-1 and its ligands (Bandaru et al., 2014; Hassan et al., 2015).

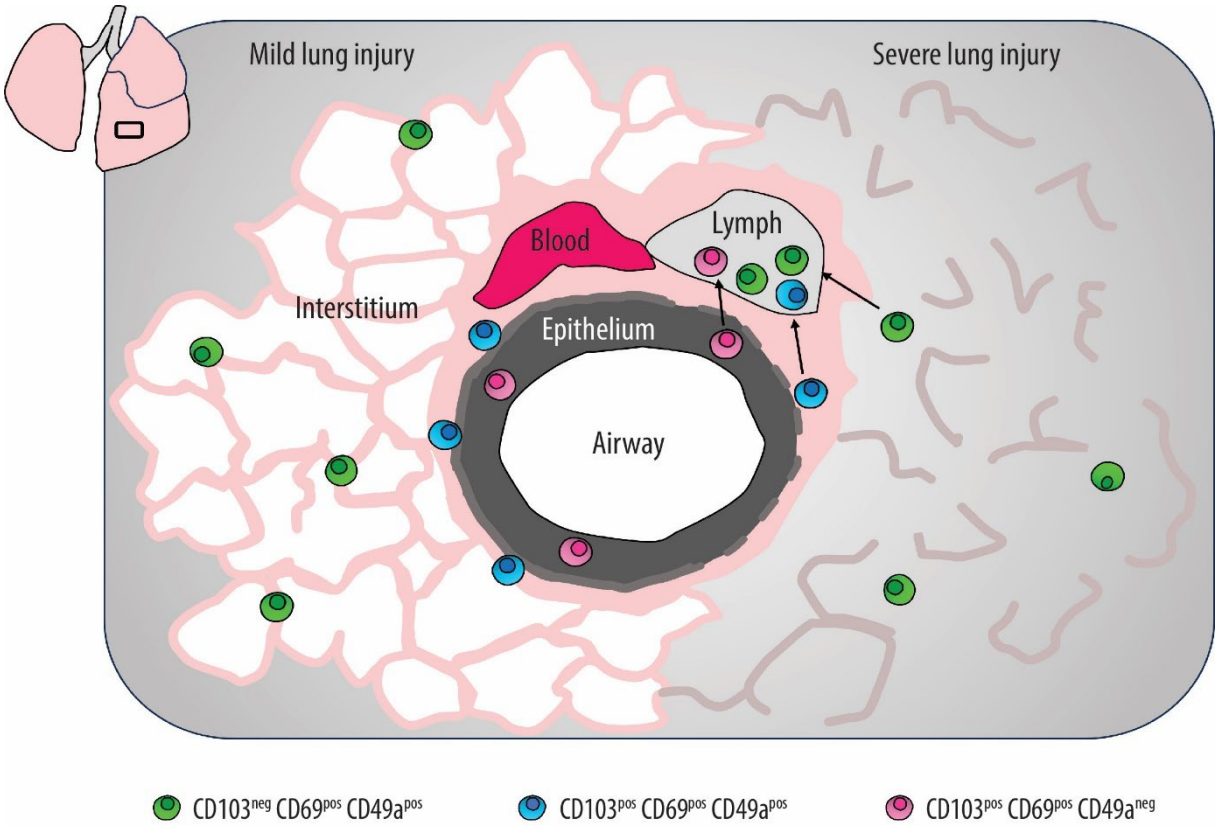

Figure 18. **Diagram of distribution of $CD8^+$ T_{RM} subsets in mildly injured lungs and their dissociation into lymphatics in severely injured lungs.**

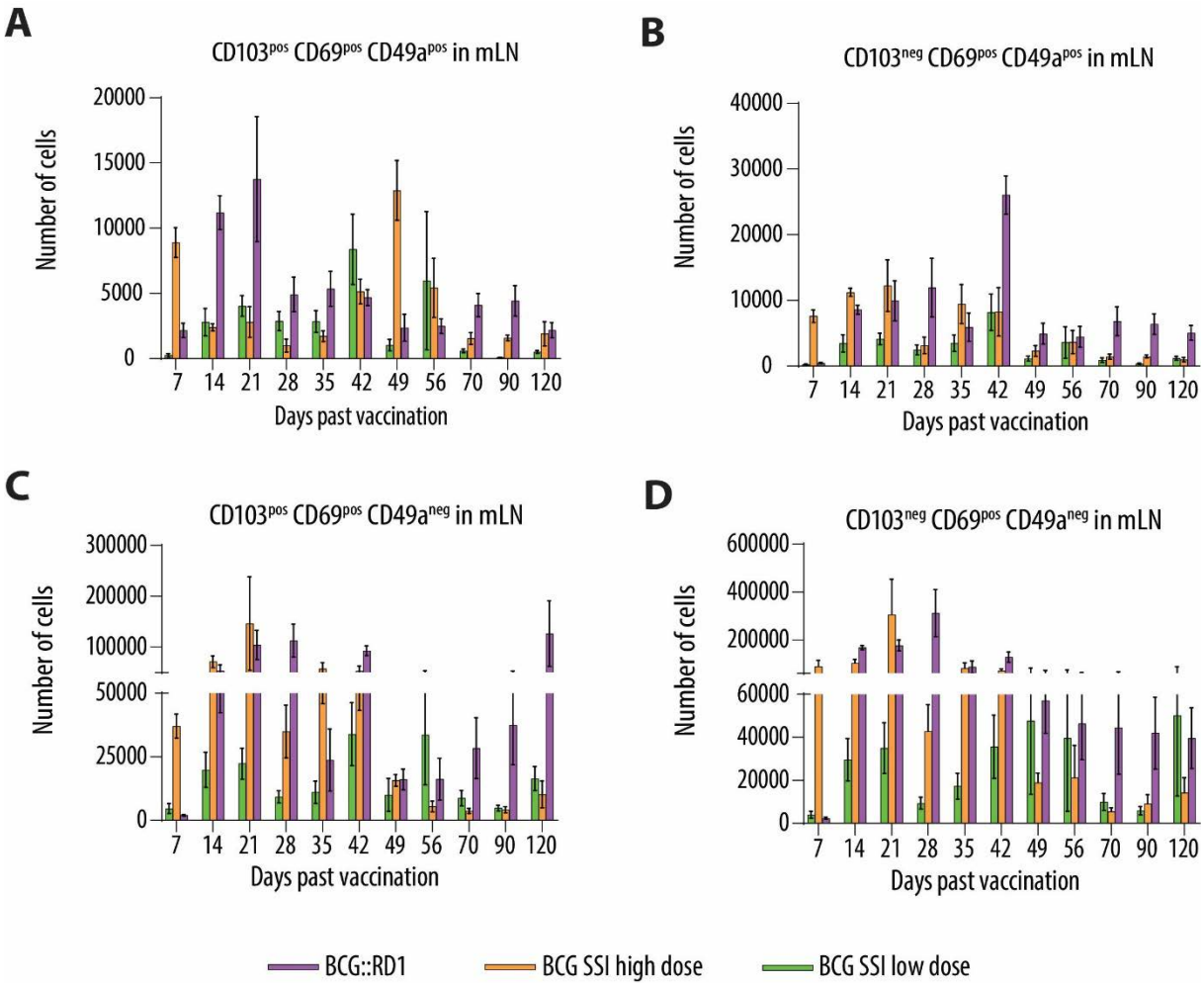

Figure 19. **Ex-lung CD8⁺ T_{RM} counts in mLN after mucosal BCG vaccinations.**

A-D) Flow cytometry quantification of CD8⁺ T_{RM} phenotypes in mLN of mice vaccinated with BCG::RD1, BCG SSI high or low dose.

3.3.3 Chronic *M. bovis* Antigen Leads to Cells with CD8⁺ Stem-like T_{RM} phenotypes in the mLN

As previous studies have shown the persistence of viable BCG in IT vaccinated lungs of mice up for to 6 months (Muruganandah et al., 2020), we next aimed to determine whether $CD8^+CD103^-CD69^+CD49a^-$ T_{RM} in the mLN were exhausted effector T cells with a stem-like T_{RM} phenotype. Mice were given IT vaccination with either SSI low dose or BCG::RD1 and mLN of experimental lungs harvested across 70, 90, and 120 dpv. mLN tissues were processed into single-cell suspensions and exhausted CD8⁺ T cell subsets (Beltra et al., 2020; He et al., 2016; Im et al., 2016) quantified using flow cytometry.

After both IT vaccinations, we observed cells in the mLN with a $CD69^{+}CXCR5^{+}PD\text{-}1^{+}$ T_{RM} phenotype that have been reported to be quiescent stem-like progenitors (Beltra et al., 2020) (**Fig. 20A**) as well as cells with a $CD69^{-}CXCR5^{+}PD\text{-}1^{+}$ phenotype that are reported to be actively cycling (**Fig. 20B**). These highly proliferative cells gave rise to reinvigorated mildly cytotoxic $CD69^{-}CXCR5^{-}PD\text{-}1^{+}$ effector T cells (**Fig. 20C**) and $CD69^{+}CXCR5^{-}PD\text{-}1^{+}$ effector T cells (**Fig. 20D**)(Beltra et al., 2020). Both subsets of progeny are reported to regain access to circulation, and the latter ultimately may become resident of non-lymphoid infected tissues (Beltra et al., 2020; Im et al., 2016). Although functional characterisation of these T cell subtypes could not be carried out as a part of our study, data across the 7-week timeline indicated that following IT vaccination with BCG SSI low dose an average 40% of all stem-like T_{RM} were proliferative and these cycling stem-like T_{RM} produced an average amount of ~13,000 reinvigorated circulatory memory T cells of which ~5,000 were mildly cytotoxic and ~8,000 had the capacity to regain residency within the infected lungs. 70-120 days after BCG::RD1 IT vaccination we observed an average of 44% cycling stem-like T_{RM} produce an average amount of ~130,000 reinvigorated circulatory memory T cells of which ~80,000 were mildly cytotoxic and ~50,000 had the capacity to regain lung T_{RM} status. After both vaccinations, the proliferative potential of the mLN stem-like T_{RM} were appreciable, as one cycling cell produced between 50-200 progeny.

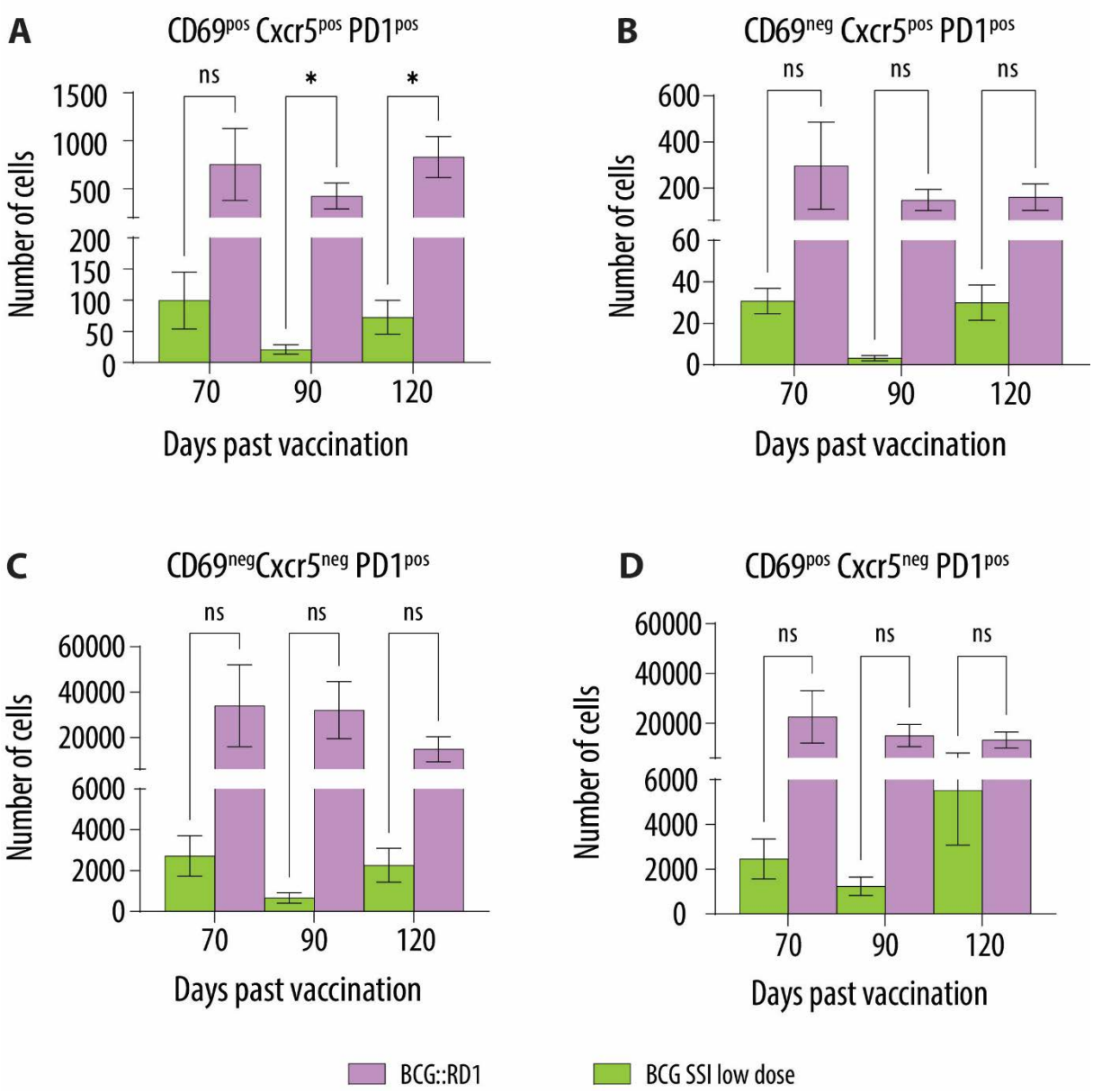

Figure 20. **Stem-like CD8⁺ T_{RM} counts in mLN after mucosal BCG vaccinations.**

A-D) Flow cytometry quantification of mLN stem-like CD8⁺ T_{RM} and progeny phenotypes from 70-120 dpv. Pooled data of mLN CD8⁺ T_{RM} from two independent experiments where n=4-10. *$P < 0.05$; ns: not significant by unpaired Student's *t* test.

Taken together, our experiments demonstrated that development of CD8⁺ T_{RM} following mucosal BCG vaccination was primarily virulence and, to a lesser extent, dose related. In agreement with many other

published pulmonary T_{RM} models, $CD8^+$ T_{RM} were shown to wane in the lungs following all the vaccinations. Our study demonstrated, for the first time, that mucosal BCG vaccination induced cells with ex-lung T_{RM} phenotypes to persist in the mLN for at least 4 months. This is significant in that many of these $CD8^+$ T_{RM} subpopulations are thought to retain the ability to migrate back into the lung forming an effective regional, rather than local, immune memory. Our discovery of persistent cells in the mLN with stem-like T_{RM} phenotypes may have notable implications for future therapeutic interventions for latent TB.

3.4 Discussion

Firstly, our decision not to use intravascular labeling to discriminate between $CD8^+$ T cells in the lung circulation as opposed to those in the lung parenchyma was because across our vaccinations, we observed vascular leakage (extensive in many animals) where exudation of the antibodies into the tissues would have compromised interpretation of the staining. Moreover, previous studies have shown that $CD69^+$ and $CD103^+$ T cells were found only in lung non-lymphoid parenchyma and were protected from intravascular labelling (Anderson et al., 2014; Anderson et al., 2012).

Counts of $CD103^+CD69^+CD49a^+$ T_{RM} in the lungs after BCG SSI high and low dose vaccinations demonstrated a peak at 21 dpv and a gradual waning to 120 dpv; after the BCG::RD1 vaccination, however, the numbers of these cells peaked at 28 dpv and were largely maintained across the four-month period of investigation. In the PR8 mouse influenza model, $CD103^+CD69^+CD49a^+$ are said to undergo homeostatic proliferation as well as seed replacement airway $CD8^+$ T_{RM} (Takamura, 2018). Although homeostatic proliferation may have been a mechanism behind the persistence of $CD103^+CD69^+CD49a^+$ T_{RM} cells across the BCG::RD1 timeline, their proliferation must have been regulated by an injury-intrinsic mechanism that did not function in the BCG SSI high and low dose vaccinations. Of note, it remains unknown whether highly migratory interstitial $CD103^-CD69^+CD49a^+$ T_{RM} differentiate into $CD103^+CD69^+CD49a^+$ T_{RM} should they reach the airway epithelium and upregulate CD103 (Eriksson et al., 2022); this could also explain the persistence of $CD103^+CD69^+CD49a^+$ T_{RM} seen across the timeline after the BCG::RD1 vaccinations as this vaccinations induced high persistent numbers of interstitial $CD103^-CD69^+CD49a^+$ T_{RM} across the timeline.

Recall that during the expansion phase of the T cell response to PR8 mouse influenza infection, CD69 is upregulated in the mLN by recently activated T cells and precedes their migration into the lungs (Eriksson et al., 2022). Takamura *et al.* have stated that inflammation-mediated recruitment, cognate antigen and arrival of $CD8^+$ T cells into the lungs *earlier* than the peak of tissue damage is essential for the establishment of $CD8^+$ T_{RM} cells; moreover, they stated that the T_{RM} RAMD is populated with T_{RM}

precursors *by the peak* of $CD8^+$ T cell responses and the RAMD is no longer available for $CD8^+CD69^+$ T_{RM} precursors recruited later (Takamura et al., 2016). The presence of precursor $CD8^+CD69^+$ T_{RM} was evident in all our vaccinations at the early expansion phase from 7-28 dpv; however, it remains unknown whether the continued numbers of $CD103^-CD69^+CD49a^-$ T_{RM} precursors seen in the BCG::RD1 vaccinated lungs continued to develop into $CD103^+CD69^+CD49a^+$ T_{RM} throughout the timeline.

In the BCG SSI high dose and BCG::RD1 vaccinations, early T_{RM} effectors counts at 14 dpv were higher than counts of $CD103^+CD69^+CD49a^+$ T_{RM}, possibly indicative of their role to combat interstitial pneumonia. Like $CD103^+CD69^+CD49a^+$ T_{RM}, interstitial $CD103^-CD69^+CD49a^+$ T_{RM} numbers were also maintained across the BCG::RD1 post-vaccination timeline to day 120 which may allude to the notion that ongoing inflammation of alveolar septa requires their ongoing function, and therefore persistence, of this subset of interstitial effector $CD8^+$ T_{RM} after the virulent vaccination.

At 21 dpv after the SSI high dose vaccination, numbers of $CD103^+CD69^+CD49a^-$ airway epithelial effector T_{RM} were higher than those seen in the BCG::RD1 vaccination, possibly indicative of dose delivery to the proximal areas of airways thus leading to the T_{RM} phenotype described by Hayward *et al*. (Hayward et al., 2020); indeed, this subset of T_{RM} was not abundant at any time of the BCG SSI low dose vaccination. Finally, despite relatively abundant $CD103^+CD69^+CD49a^+$ T_{RM} numbers across the BCG::RD1 timeline, $CD103^+CD69^+CD49a^-$ airway epithelial effectors waned appreciably, suggesting they were not replaced by $CD103^+CD69^+CD49a^+$ T_{RM} as reported by Wein *et al*. (Wein et al., 2019).

That $CD103^+CD69^+CD49a^+$ archetypal T_{RM} were seen in the mLN early after vaccination may have been linked to their dislodgement from the lungs due to the extreme tissue damage (Carbone, 2023) associated with the high dose or virulence of the mucosal vaccinations as imaged after the BCG SSI high dose and BCG::RD1 vaccinations. This phenomenon may also explain a further peak of these T_{RM} later after the SSI high dose vaccination as this equated with the vaccination's peak of tissue damage and T cell infiltration. Moreover, TGF-β signalling is required for $CD8^+$ T_{RM} maintenance in the lungs and interruption of this signalling is thought to allow $CD103^+CD69^+CD49a^+$ T_{RM} to egress to the mLN

(Carbone, 2023). This phenomenon may have accounted for the presence of those mLN T_{RM} cells seen in the SSI low dose vaccination at later stages; that these numbers increased across the timeline may be linked to the fact that these cells are not senescent and are known to proliferate in the mLN (Stolley et al., 2020).

Lung $CD103^{-}CD69^{+}CD49a^{+}$ T_{RM} are thought to preferentially egress to the mLN linked to a lack of TGF-β-mediated maturation (Carbone, 2023). In the mLN they are thought to retain an increased trans-differentiation potential (Christo et al., 2021), an enhanced capacity to repopulate the lungs (Brewitz et al., 2017) and ability to convert back into secondary lung $CD8^{+}$ T_{RM} (Christo et al., 2021; Paik & Farber, 2021). Notably, when mLN $CD103^{+}CD69^{+}CD49a^{+}$ T_{RM} are restimulated with antigen (whether chronic infection or secondary infection), they lose CD103 expression and become mLN $CD103^{-}CD69^{+}CD49a^{+}$ T_{RM} (Stolley et al., 2020). Thus, these ex-lung TRM that we reported deserve further study to unveil their potential to function back in the lung after secondary mycobacterial challenge.

Our animals harboured $CD103^{-}CD69^{+}CD49a^{-}$ T_{RM} of the precursor phenotype at the *latest* stages of the timeline when tissue was largely restituted. $CD8^{+}$ T cells are known to respond to chronic infection by adaptation of a phenotype that restrains pathogen replication yet reduces immunopathology. This adaptation, or T cell exhaustion, has a hallmark of expression of various inhibitory receptors that becomes imprinted in stem-like cells and propagated to their progeny (see section 1.1.6). Once the chronic phase of infection has been established, stem-like exhausted $CD8^{+}$ T cells acquire a resident program in SLO where it is crucial for them to be protected in a specialised niche that allows maintenance of their quiescence, multipotency, and proliferative potential (Im et al., 2020). A signature of these stem-like T_{RM} cells of the lymph node (G. Li et al., 2022) is high expression of CD69 (Im et al., 2020) which antagonises S1P-mediated egress from SLO (Shiow et al., 2006). As we provided an initial report of stem-like $CD8^{+}CD69^{+}CXCR5^{+}PD\text{-}1^{+}$ T_{RM} in the mLN following mucosal vaccinations with BCG and suggest that further study of these cells may reveal their potential to be harnessed for TB vaccination strategies.

CHAPTER 4. RELATIONSHIPS BETWEEN LUNG EPITHELIAL PROGENITOR AND CD8$^+$ T_{RM} CELLS FOLLOWING MUCOSAL BCG VACCINATION

The human understanding is of its own nature prone to suppose the existence of more order and regularity in the world than it finds. And though there be many things which are singular and unmatched, yet it devises for them parallels and conjugates and relatives which do not exist. Hence the fiction that all celestial bodies move in perfect circles.

F. Bacon, *Novum Organum*

4.1 Introduction

We next investigated putative relationships between lung epithelial progenitor cells and lung CD8$^+$ T_{RM} following mucosal BCG vaccination as we hypothesised that distal airway epithelial progenitor cells provide paracrine induction cues for lung CD8$^+$ T_{RM}. The sum of our analyses thus far inferred that induction and maintenance of lung CD8$^+$ T_{RM} was linked to the tissue milieu associated with alveolar damage. As described in influenza mouse models, CD8$^+$ T_{RM} form in areas of severe alveolar destruction, precisely the areas into which airway epithelial progenitor cells home (Takamura, 2017, 2018; Takamura & Kohlmeier, 2019; Takamura et al., 2016; Vaughan et al., 2015). Thus, we first looked at spatial and temporal relationships of Krt8$^+$ TP and CD8$^+$ T_{RM} using imaging. Given that BCG::RD1 vaccine was associated with the most severe tissue damage, we used it to further dissect mechanistic relationships between distal airway progenitor cells and immune memory in the lungs.

4.2 Methods

4.2.1 Animals

Axin2$^{CreERT2:TdT}$:R26R^{EYFP} mice (a gift from Prof Edward Morrisey, University of Pennsylvania), *Sox2^{CreERT2}* (Jackson Laboratories), *Itgβ6* knockout mice (developed by and a gift of Prof Dean Sheppard, University of California San Francisco), *B6.Cg-Gt(ROSA)26Sor$^{tm14(CAG-tdTomato)Hze}$/J* (also known as *Ai14*) mice (a gift of Prof Scott Mueller, University of Melbourne) were all genotyped by Genetic Research Services (University of Queensland), bred and maintained in the animal facilities of the Australian Institute of Tropical Health and Medicine at James Cook University, Australia.

4.2.2 Bacteria

Bacterial culture and enumeration were as described in section 2.2.2.

4.2.3 Mucosal Vaccination

IT mucosal vaccinations were performed as described in section 2.2.3.

4.2.4 Immunofluorescence

Fluorescence of reporter proteins is known to be 'leaky' or quenched by fixation and tissue processing involved with paraffin embedding (Kusser & Randall, 2003; Remington, 2011; Scandella et al., 2020). Therefore, to preserve the endogenous fluorescence of the reporter mice used in the study, several methods for lung inflation, fixation and freezing were tested to optimise the morphology of the lung tissues and cells (**Table 1; Fig. 21**).

Table 1. **Approaches for optimisation of inflation, fixation, and freezing methods of mouse lung sections for downstream imaging and analyses.**

Lung Inflation	Immersion Fixation	Sucrose Dehydration	Freezing Method	Cutting Procedure (Thickness)	Post-fixation	Reference
OCT	None	None	Snap frozen in liquid nitrogen	7 µm	4% PFA 5m	Vaughan et al, 2015
4% PFA	4% PFA 1h 25°	None	Embedded in OCT, frozen in thawing isopentane	7-10 µm	None	Zuo et al, 2014; Vaughan et al, 2015
2% PFA	2% PFA 12h 25°	None	Embedded in OCT, frozen in thawing isopentane	7 µm	None	
1:1 OCT/PBS	None	None	Snap frozen in liquid nitrogen	4-10 µm	None	Quantius et al, 2016
1:1 OCT/1% PFA	1% PFA 1h 25°	None	Embedded in OCT, frozen in thawing isopentane	4-10 µm	4% PFA 20m	Quantius et al, 2016
1:1 OCT/4% PFA	4% PFA 1h 25°	15% sucrose 4° until tissue sunk; transferred to 30% sucrose until tissue sunk	Embedded in OCT, frozen in thawing isopentane	4-10 µm	None	
1% ZBF	1% ZBF 72h 25°		Embedded in OCT, frozen in thawing isopentane	7µm	None	
1% ZBF	1% ZBF 72h 25°	15% sucrose 4° until tissue sunk; transferred to 30% sucrose until tissue sunk	Embedded in OCT, frozen in thawing isopentane	7µm	None	

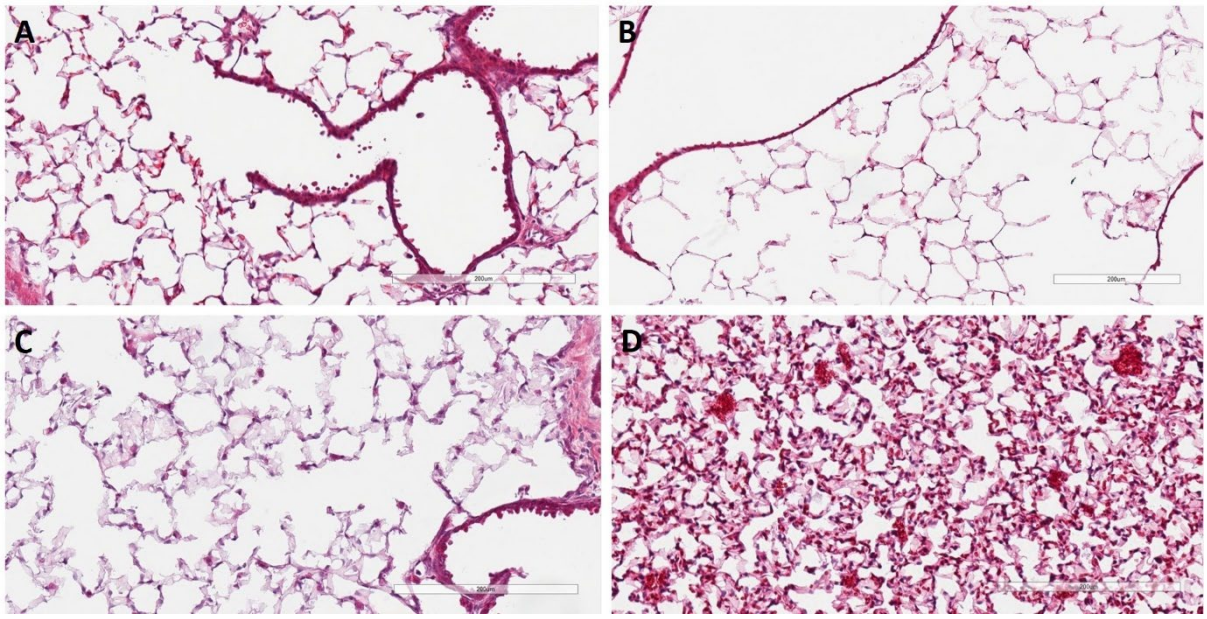

Figure 21. **Frozen sections across numerous methods of lung inflation, fixation and freezing are suboptimal for subsequent immunofluorescent imaging.**

Exemplary micrographs of lung tissue processed using **A)** 4% PFA inflation with 1h 4% PFA immersion, embedded in OCT and frozen in thawing isopentane **B)** OCT/4% PFA inflation with 1h 4% PFA immersion, embedded in OCT and frozen in thawing isopentane **C)** 4% PFA inflation with 1h 4% PFA immersion, sucrose dehydration, embedded in OCT and frozen in thawing isopentane **D)** 1% ZBF inflation with 72h 1% ZBF immersion, sucrose dehydration, embedded in OCT and frozen in thawing isopentane. Note that tissue architecture and cell morphology is lost across all the methods trialled. **A, C, D)** Magnification, 20×; Scale bar 200 µm. **B)** Magnification, 14.6×; Scale bar 200 µm.

Due to the lack of optimal frozen tissue methods (**Fig. 21**), fixation, paraffinisation, sectioning and dewaxing were as described in section 2.2.5. Sectioned tissues were stained using immunofluorescence (IF) methods after washing slides twice with Tris-buffered saline for 5 minutes each; blocking was then performed with 10% normal serum derived from species specific to the secondary antibodies at 25° C for 2 hours. Primary antibodies were incubated overnight at 4° C at optimised dilutions (**Table 2**).

Tissues were washed twice for 5 minutes with TBS and twice for 3 minutes with TBS before incubation with secondary antibodies for 1 hour at 25° C at the optimised dilutions (**Table 2**). Tissue was washed 6 times for 5 minutes with TBS before incubation with Trueview reagent (Vector) prior to cover-slipping with Vectashield Vibrance anti-fade with DAPI mounting media (Vector) and #1.5 coverslips (Leica). Slides were cured for 48 hours in a dark slide box. For double and triple sequential immunostaining, after the first primary and secondary staining was completed and tissue washed, the sequential primary, secondary and tertiary staining was undertaken as above.

4.2.5 Tissue Harvest

Tissue harvest was performed as described in section 2.2.4.

4.2.6 Lung and Mediastinal Lymph Node Dissociation

Lung and mLN dissociations were performed as described in section 3.2.4.

4.2.7 Flow Cytometry and Data Analyses

Flow cytometry and data analyses were performed as described in section 3.2.5. Antibodies and dilutions used are described in Table 2.

4.2.8 Lineage Tracing

For analysis of the lineage fate of the $Sox2^{+}$ cells from airway epithelium and $Axin2^{+}$ cells from the alveolar epithelium, three doses of 0.25 mg/g tamoxifen was administered every second day to *Sox2*^{CreERT2}*/Ai14* mice and every day for 5 days to *Axin2*$^{CreERT2:TdT}$*/EYFP* mice 28 days prior to IT vaccination with BCG SSI (1×10^5 CFU) or BCG::RD1 (1×10^5 CFU). The *Sox2*^{CreERT2}*/Ai14* mice tamoxifen independent recombination was ~1%, while floxed controls were negative for systemic effects.

4.2.9 Microscopy

Images were acquired using an Aperio CS2 Digital Slide Scanner (Leica Biosystems) and analysed using Aperio ImageScope v12.4.3.5008 software (Leica Biosystems). Quantification of $Krt8^{+}$ TP and active TGF-β was undertaken using ImageJ software (ImageJ).

4.2.10 Statistical Analyses

Statistical analysis was performed, and graphs were generated using Prism version 9.5.1 (GraphPad). Two parametric group analyses were carried out using Student's t test, followed by Holm-Šídák multiple comparison tests. $P < 0.05$ was considered significant.

4.3 Results

4.3.1 Spatiotemporal Localisation of Lung Epithelial Progenitors and CD8$^+$ T_{RM}

Reasoning that, should epithelial progenitor and CD8$^+$ T_{RM} be co-dependent, we would see spatial and temporal proximity such as is described in the RAMD of mouse PR8 influenza models, we probed our tissue samples from the three mucosal vaccinations using characteristic markers for CD8$^+$ T_{RM} and progenitor transitional cell marker Krt8, knowing that both distal airway and alveolar progenitors transition through this cell state around the time of T cell contraction and T_{RM} development. We used a 'sandwich' staining method in which serial lung sections were cut at 4 µm and stained for CD8b$^+$, CD103$^+$, or Krt8$^+$. Imaging revealed that across all three vaccinations, there was consistent evidence of a structural localisation between Krt8$^+$ TP and CD8b$^+$ CD103$^+$ cells particularly in areas of severe tissue damage (**Fig. 22**).

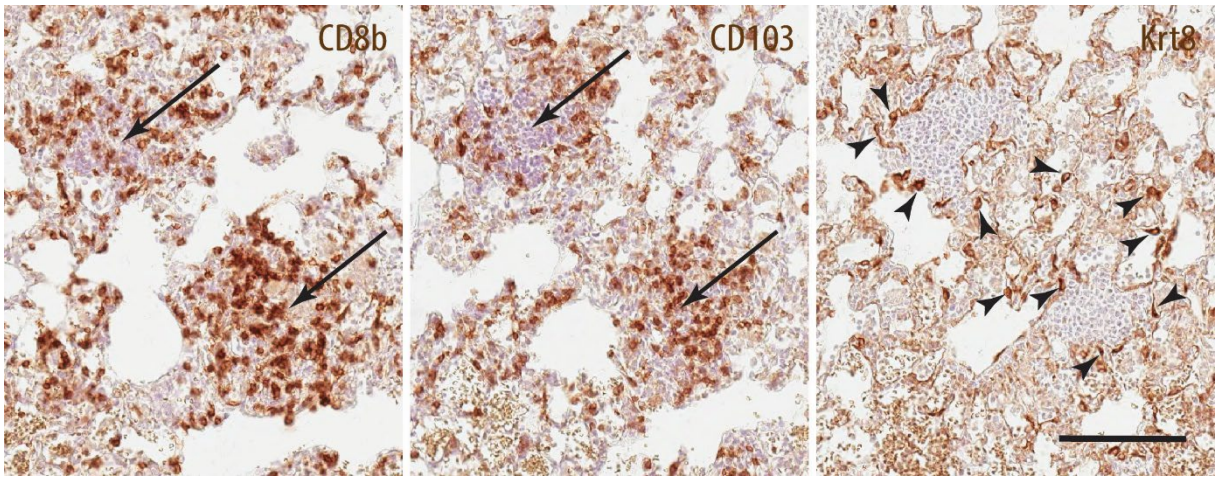

Figure 22. **CD8b$^+$ CD103$^+$ cells invariably adjacent to Krt8$^+$ TP.**

Two areas of severe interstitial damage (arrows) show infiltrating CD8b$^+$CD103$^+$ T_{RM} and Krt8$^+$ TP around the periphery. Results are presented from representative images from 6 mice per group from two independent experiments. Magnification, 20×; Scale bar 100 µm.

4.3.2 Distal Airway Progenitor Cells Provide Paracrine Cues for the Induction of Lung CD8$^+$ T_{RM} Cells Following Mucosal BCG Vaccination

TGF-β is a key regulator of epithelial cell proliferation and differentiation (Lomas et al., 2012; Riemondy et al., 2019) and upregulates the CD8$^+$ T_{RM} transcriptome (Mackay et al., 2013; Nath et al., 2019). A key activator of latent TGF-β in lungs is integrin αVβ6 (Munger et al., 1999) and epithelial progenitors express αVβ6 (Auyeung et al., 2022; Strunz et al., 2020; Takamura, 2017; Topham & Reilly, 2018) which is used by cells for migration across ECM (Brzozowska & Deshmukh, 2022; Hood & Cheresh, 2002; Meecham et al., 2022). Within the lungs, the latent form of TGF-β is stored in the ECM in high concentrations (Munger et al., 1999; Sheppard, 2006) and αVβ6 is known to bind the latent-associated protein (LAP) so that αVβ6-mediated cell traction forces open the LAP to activate TGF-β (Giacomini et al., 2012; Munger et al., 1999; Shi et al., 2011). Active TGF-β generated by αVβ6 is utilised by cells in direct contact with αVβ6 expressing cells (Annes et al., 2004; Henderson & Sheppard, 2013; Munger et al., 1999). We theorised that as airway epithelial progenitor cells migrate into hypoxic alveolar

tissue, they activate interstitial latent TGF-β which then binds TGF-β receptors on adjacent $CD8^+$ T cells to subsequently induce the $CD8^+$ T_{RM} transcriptome (**Fig. 23**).

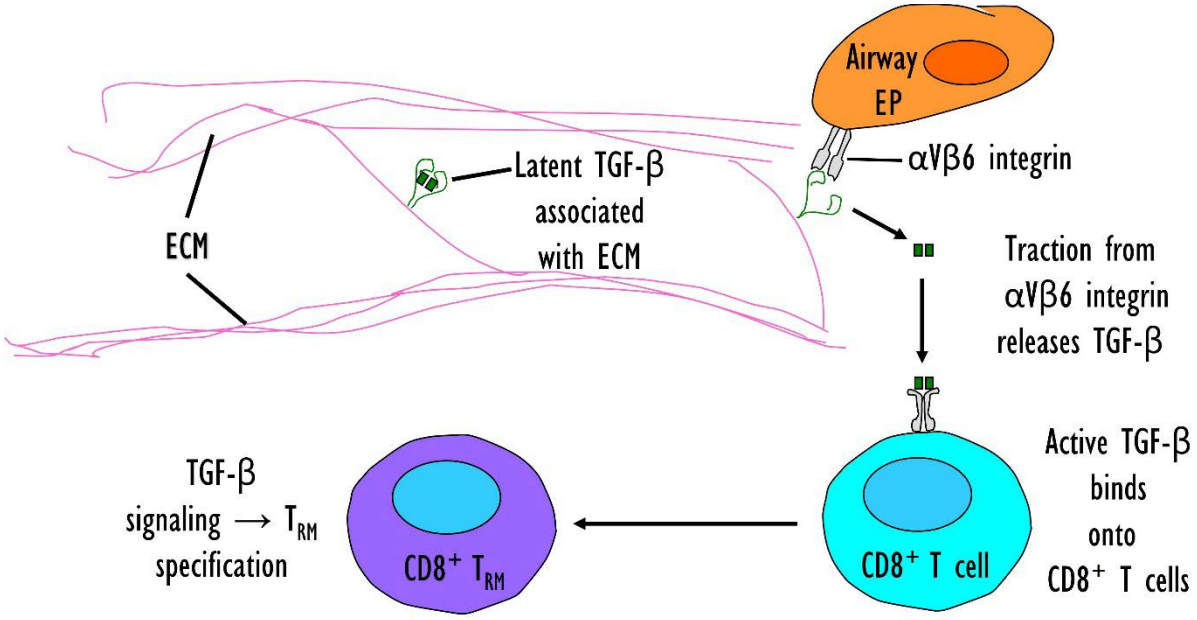

Figure 23. **Model of interaction between airway epithelial cells that express αVβ6 and adjacent $CD8^+$ T cells.**

To first test this hypothesis, we quantified lineage traced $Sox2^+$ airway progenitors at 120 dpv in regenerated alveolar tissue, using *Sox2^{CreERT2}:B6.Cg-Gt(ROSA)26Sor$^{tm14(CAG-tdTomato)Hze}$/J* (aka *Sox2/Ai14*) reporter mice in which progeny of Sox2+ airway progenitors were indelibly tagged with red fluorescent protein (**Fig. 24A**). To ensure there was no tamoxifen persistence, tamoxifen was administered 28 days prior to IT vaccination.

We observed that numbers of lineage traced AEC1 and AEC2 following BCG::RD1 vaccination were 6 and 8-fold higher, respectively, than those observed after BCG SSI low dose (**Fig. 24B**). Therefore, the number of airway epithelial progenitors in the alveolar tissue was significantly higher following mucosal BCG::RD1 vaccination.

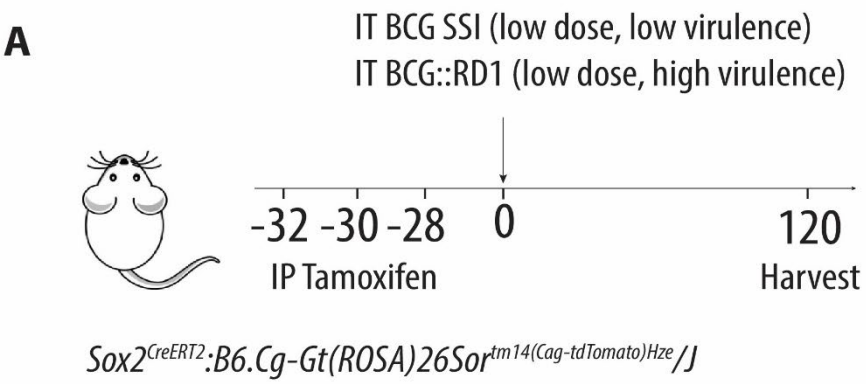

Sox2^{CreERT2}:B6.Cg-Gt(ROSA)26Sor$^{tm14(Cag-tdTomato)Hze}$/J

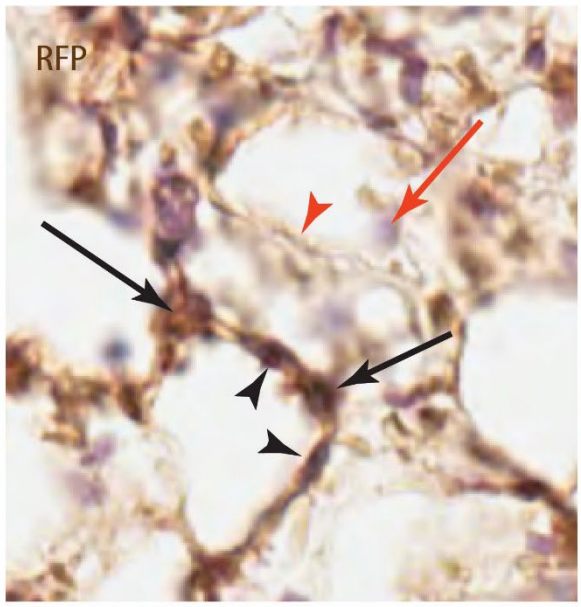

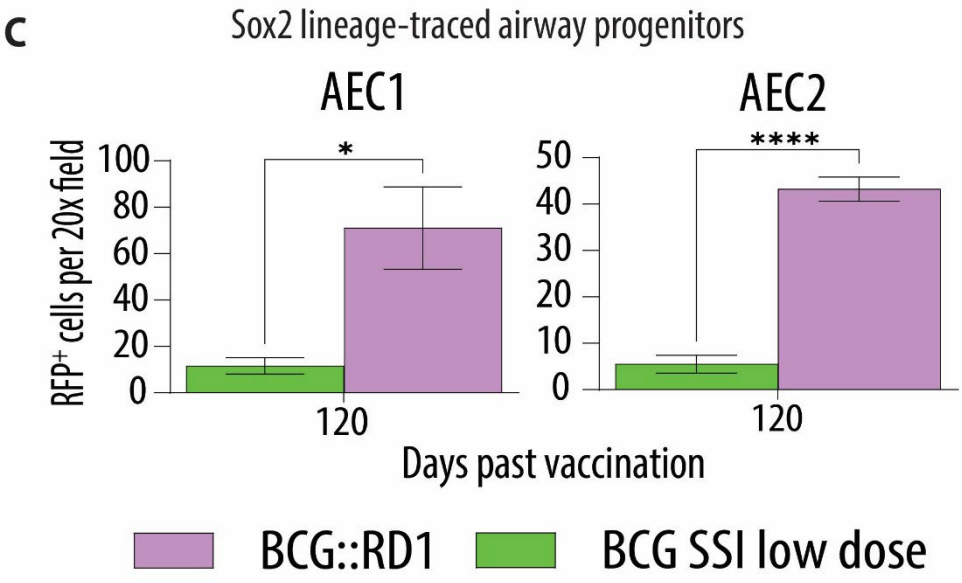

Figure 24. **Lineage-traced distal Sox2 airway epithelial progenitors repopulate mouse alveolar epithelium after virulent mucosal BCG vaccination.**

A) Experimental design to lineage trace Sox2 airway epithelial progenitors following mucosal BCG vaccination. **B)** Sox2 lineage-traced AEC1 (black arrowheads) and AEC2 (black arrows) compared to RFP negative AEC1 (red arrowhead) and AEC2 (red arrow). **C)** Quantification of *Sox2^{CreERT2}:Ai14* lineage-traced progeny in lungs of mice IT vaccinated with the SSI low dose vaccine or BCG::RD1.

We next visualised and quantified extracellular alveolar interstitial tissue active TGF-β from 7-21dpv when airway progenitors were mobilised and $CD8^+$ T_{RM} developed. Results showed that by 7 dpv the BCG::RD1 vaccinated animals had peribronchiolar interstitial active TGF-β expression (data not shown) and by 14 dpv extracellular alveolar interstitial expression was evident (**Fig. 25A, E**). By 21 dpv, extracellular interstitial expression was global, and alveolar areas of severe damage had strong expression (**Fig. 25B, E**).

Animals vaccinated with BCG SSI high dose had sparse peribronchiolar expression of active TGF-β from 14-21 dpv (**Fig. 25E**) with early, strong extracellular airway expression (**Fig. 25C**); in animals vaccinated with the low dose of BCG SSI, scarce alveolar macrophages had cytoplasmic expression of active TGF-β (**Fig. 25D, E**). Therefore, we revealed that after BCG::RD1 vaccination, active TGF-β was significantly more concentrated in alveolar tissues at the time when airway epithelial progenitors were known to restitute severely damaged epithelium.

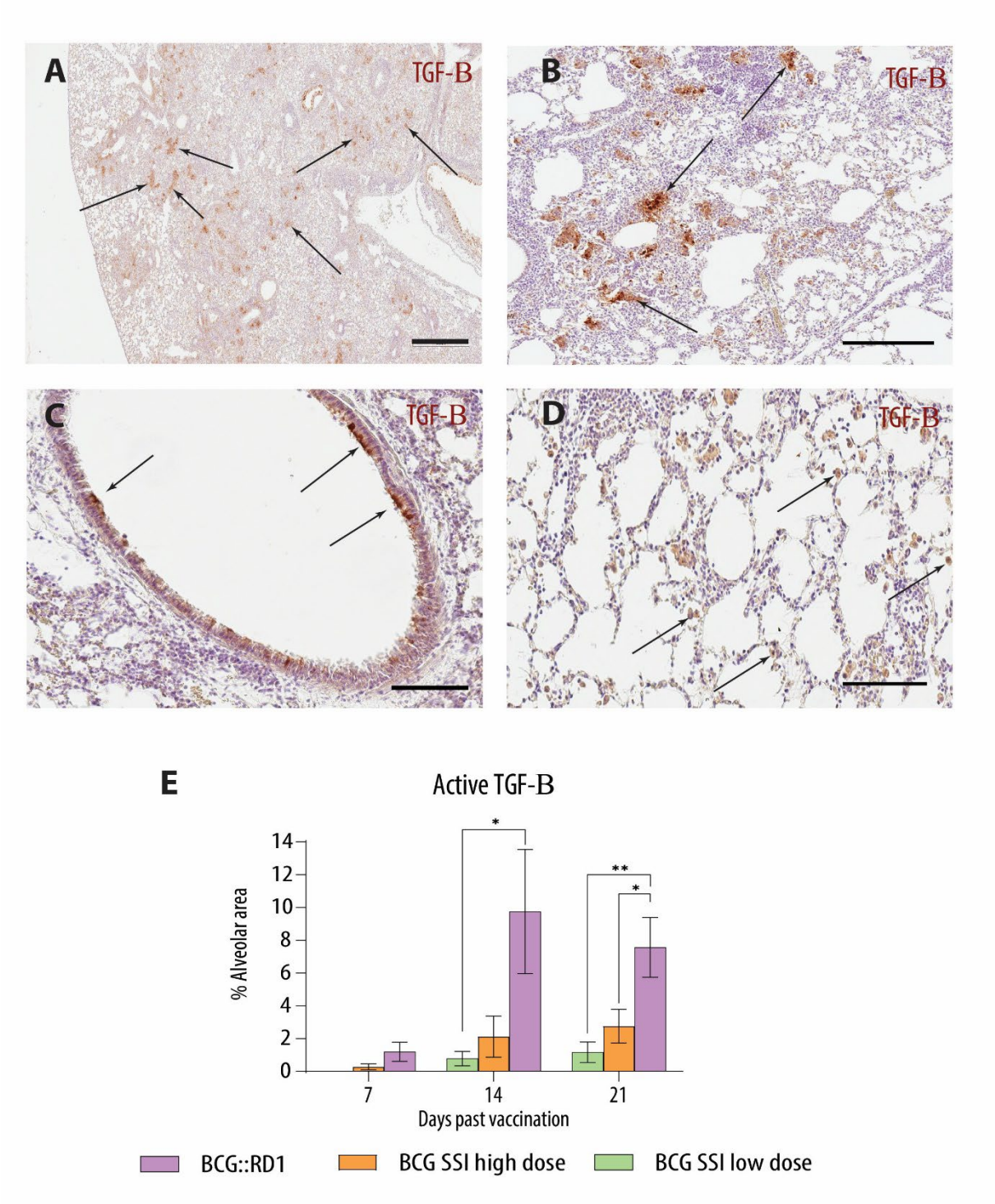

Figure 25. **Quantification of alveolar interstitial tissue active TGF-B following mucosal BCG vaccinations.**

Extracellular alveolar tissue active TGF-β following IT vaccination with BCG::RD1 seen in **A)** distal interstitium (arrows) at 14 days and **B)** areas of severe damage (arrows) at 21 dpv**. C)** Bronchiolar

airway expression (arrows) of active TGF-β at 14 days after IT SSI high dose vaccination. **D)** The cytoplasm of alveolar macrophages (arrows) exhibited active TGF-β at 21 days after IT SSI low dose vaccination. **E)** Quantification of extracellular alveolar interstitial active TGF-β following IT BCG vaccinations. Pooled data from two experiments where n=6. **P* < 0.05; ***P* < 0.01 determined by One-way ANOVA**. A)** Magnification, 4×; Scale bar 600 μm. **B)** Magnification, 11.6×; Scale bar 200 μm. **C)** Magnification, 20×; Scale bar 100 μm. **D)** Magnification 20×; Scale bar 100 μm.

To establish the relative numbers of alveolar epithelial progenitors that restituted the alveolar epithelium after the BCG::RD1 vaccination as compared to the BCG SSI low dose, we sought to lineage trace AEP at 120 dpv, using *Axin2*$^{CreERT2:TdT}$*/EYFP* reporter mice to indelibly tag progeny with enhanced yellow fluorescent protein (**Fig. 26A**). At tissue harvest, however, all animals had an atypical response to the BCG::RD1 across two independent experiments. Numerous lesions of these lungs contained Krt8^{+} TP, AEP and interestingly, Krt5^{+} proximal airway epithelial progenitors as well as copious amounts of active TGF-β. Wounds exemplified lung fibrosis characterised by AEC2 hyperplasia, lack of AEC1 and supraphysiologic levels of TGF-β that likely prevented differentiation of Krt8^{+} TP into AEC1 (Jiang et al., 2020; Strunz et al., 2020) (**Fig. 26B**).

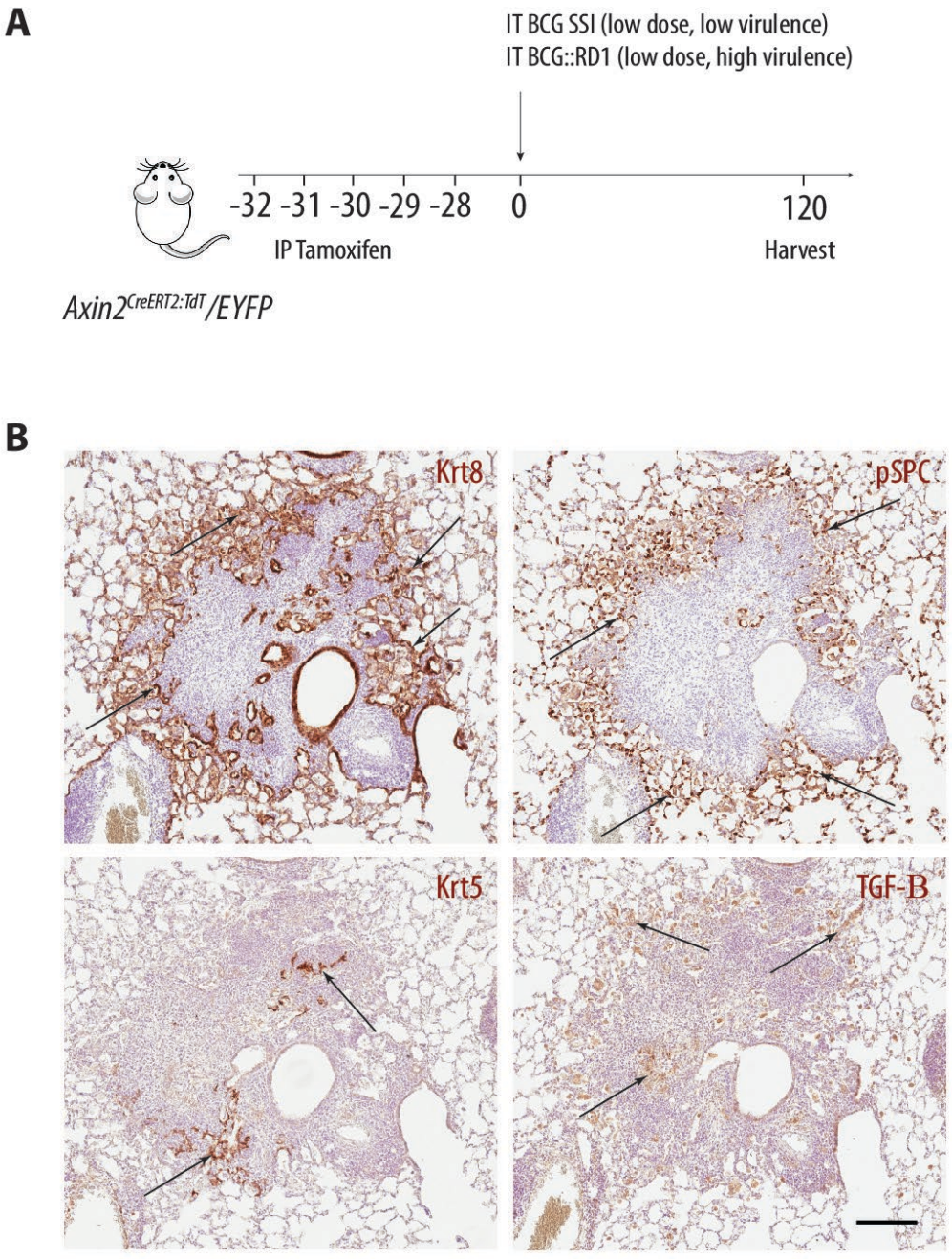

Figure 26. **Lungs of *Axin2$^{CreERT:TdT}$/EYFP* mice develop chronic lesions following mucosal BCG::RD1 vaccination.**

A) Experimental design for lineage tracing of *Axin2$^{CreERT:TdT}$/EYFP* progeny at 120 dpv. **B)** Micrographs show chronic lesions in *Axin2$^{CreERT:TdT}$/EYFP* animals 56 days after mucosal BCG::RD1 vaccination. **B)** Magnification 9.6×; Scale bar 150 µm.

4.3.3 *Itgβ6* knock out mice develop significantly fewer CD8$^+$ T_{RM} following mucosal vaccination with BCG::RD1

To more directly test our hypothesis that epithelial progenitor cell-mediated release of TGF-β regulates the induction of CD8$^+$ T_{RM}, we used knock-out (KO) mice that lacked a functional αVβ6 integrin (Munger & Sheppard, 2011; Peng et al., 2016). *Integrin beta-6 (ItgB6) KO* mice were vaccinated with BCG::RD1 and tissues harvested across 7-35 dpv (**Fig. 27A**). We confirmed levels of lung injury in the *ItgB6 KO* mice were comparable to C57BL/6 wild type mice using histology (data not shown) and quantification of Krt8$^+$ TP numbers (**Fig. 27B**). We then compared tissue active TGF-β, as *ItgB6 KO* airway progenitor cells would not be able to bind the LAP and activate extracellular TGF-β. At 21 dpv, we observed that while C57BL/6 mice had abundant extracellular alveolar interstitial active TGF-β, compared to the *ItgB6 KO* animals which had negligible amounts (**Fig. 27C-E**).

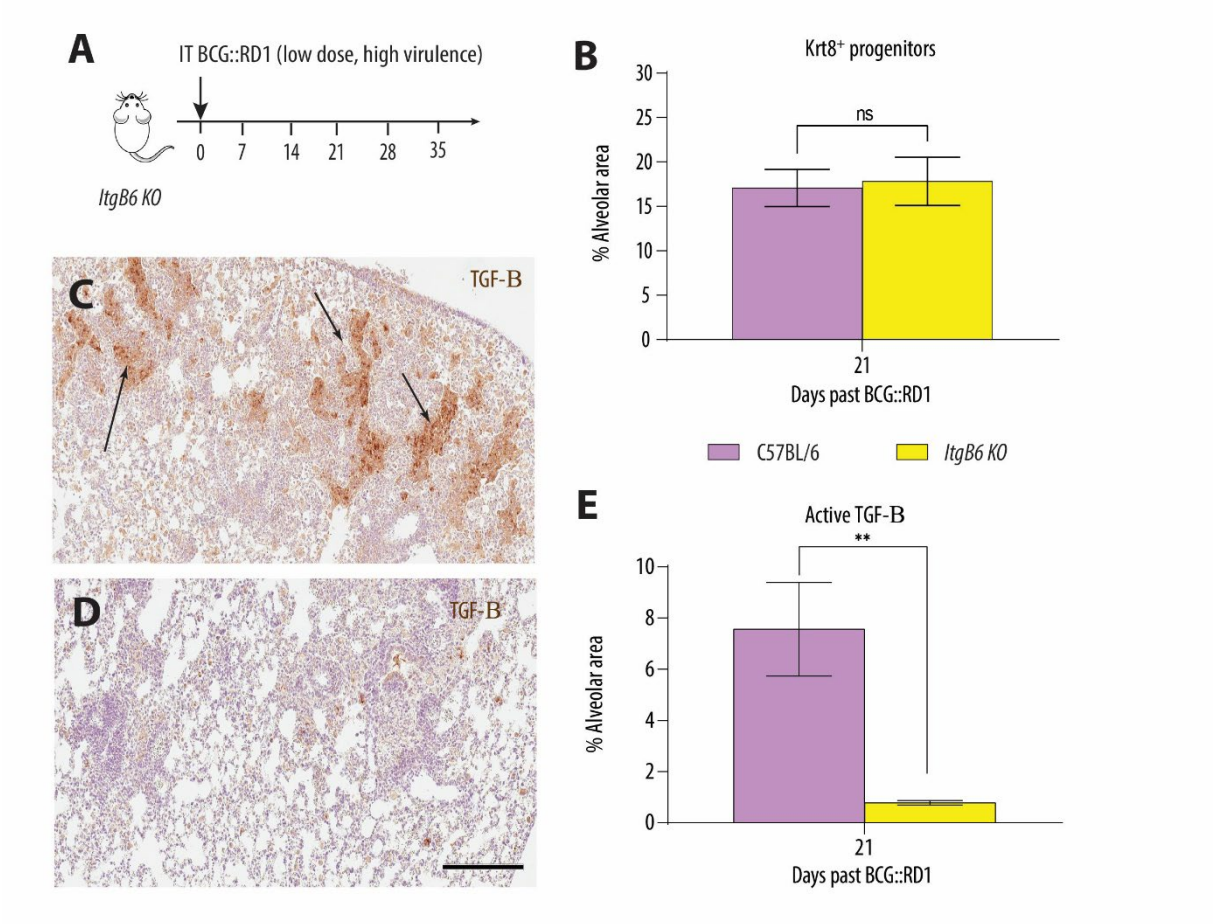

Figure 27. **Airway epithelial progenitors release latent TGF-β in alveolar interstitium.**

A) Experimental design for *Itgβ6 KO* experiments. **B)** Quantification of Krt8$^+$ TP in *Itgβ6 KO* mice. **C, D)** Micrographs of C57BL/6 wild-type and *ItgB6 KO* lungs, respectively, at 21 days after BCG::RD1 vaccination **E)** Corelative quantification of extracellular interstitial expression (**C**-arrows) of extracellular interstitial active TGF-β in alveolar tissue. Pooled data from two independent experiments where n=6-10. *P < 0.05; **P < 0.01; ns: not significant by unpaired Student's t test. **C, D)** Magnification, 10×; Scale bar 200 µm.

We next quantified CD8$^+$ T_{RM} subsets and their proportions in the lungs of the *ItgB6 KO* animals after BCG::RD1 vaccination across 5 weeks and found that while C57BL/6 mice had a 25% increase in CD8$^+$ T_{RM} between 14-21 dpv (**Fig. 28A**), the *IgB6 KO* animals had an increase of 5% (**Fig. 28B**). This smaller increase was despite the fact that the KO mice had more lung CD8$^+$ T cells at 14 dpv and the same

number as WT at 21 dpv (**Fig. 28C**). We also showed that $CD8^+CD103^+$ T_{RM} were specifically significantly decreased in *ItgB6 KO* animals after BCG::RD1 vaccination compared to WT animals (**Fig. 29**), consistent with the role of TGF-β in upregulation of CD103 expression in $CD8^+$ T cells (Casey et al., 2012; Mackay et al., 2013).

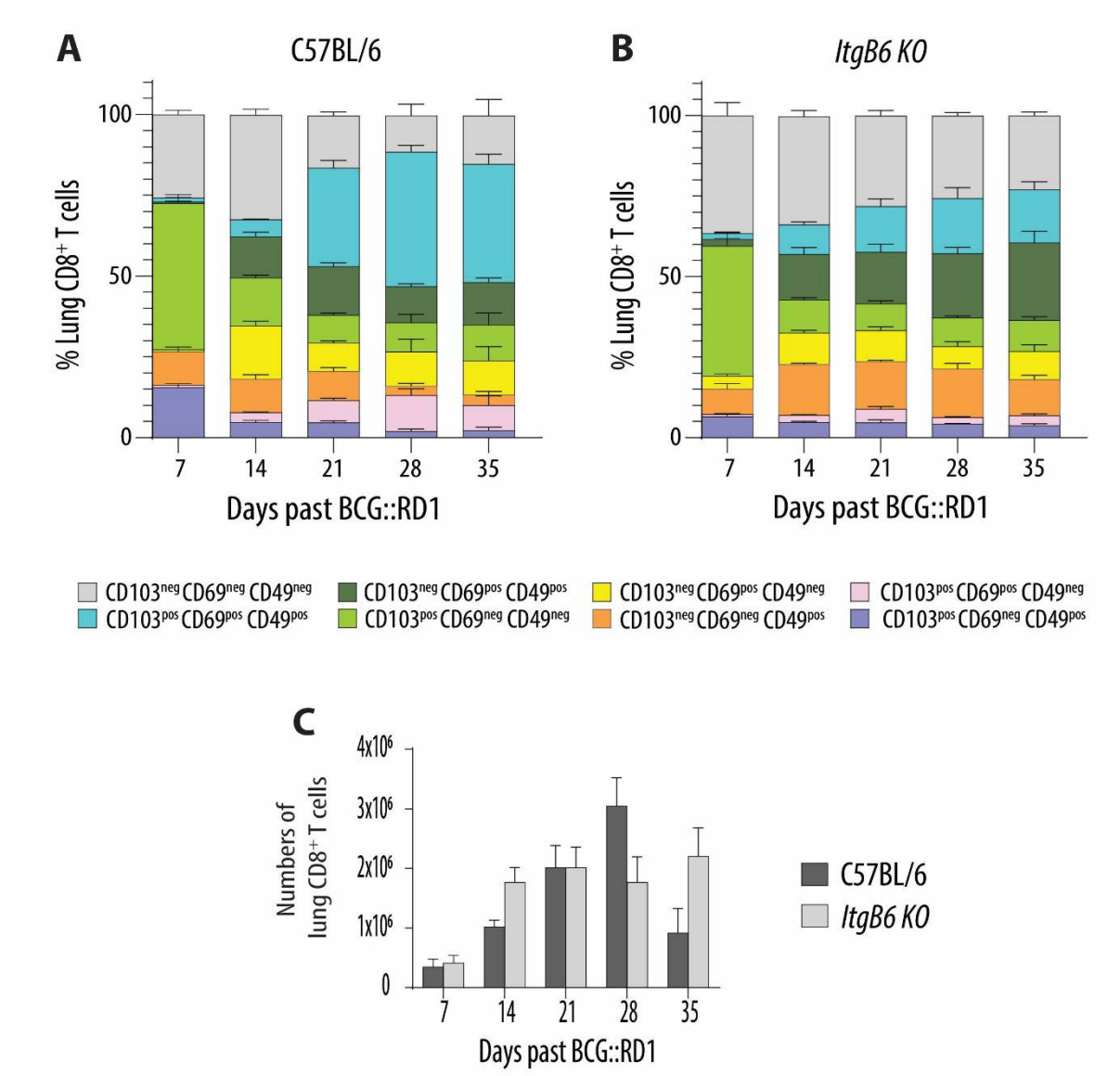

Figure 28. **Comparison of wild type and *ItgB6 KO* lung CD8$^+$ T_{RM} subsets following mucosal BCG::RD1 vaccination.**

Percentages of CD8$^+$ T_{RM} subsets in **A)** *C57BL/6* and **B)** *ItgB6 KO* mice vaccinated with BCG::RD1. **C)** Counts of total CD8$^+$ T cells in lungs of mice IT vaccinated with BCG::RD1.

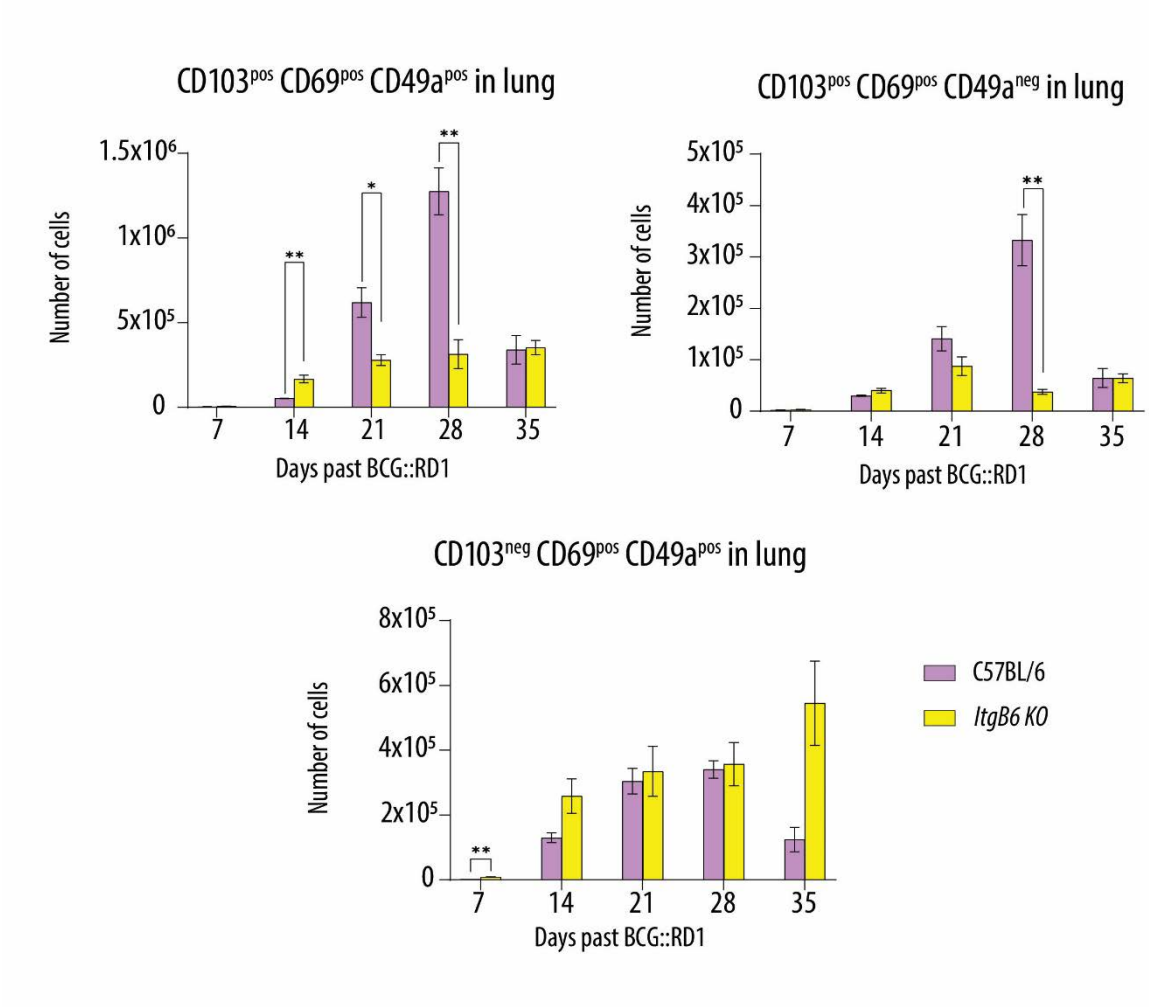

Figure 29. ***ItgB6 KO*** **mice show significantly decreased numbers of lung CD8$^+$CD103$^+$ T_{RM} following mucosal BCG::RD1 vaccination.**

In conclusion, following mucosal BCG vaccination, we demonstrated that wherever Krt8$^+$ TP were, CD8$^+$CD103$^+$ T_{RM} also localised. We found that active TGF-β was robust and widespread throughout the alveolar interstitium following BCG::RD1 vaccination in which significantly higher numbers of distal

airway progenitors were shown. When αVβ6 integrin was knocked out, active TGF-β was absent and $CD8^+CD103^+$ T_{RM} numbers significantly decreased. Taken together, these findings support a model in which lung epithelial progenitor cell-mediated release of TGF-β regulates induction and persistence of lung $CD8^+$ T_{RM} cells following mucosal BCG vaccination.

4.4 Discussion

Early in pulmonary infection, epithelial injury causes secretion of growth factors, chemokines, interleukins, and prostaglandins that coordinate complex processes involving epithelial restitution. In zones of minimal and moderate distal lung tissue damage due to injury, facultative mature epithelial progenitors are capable of local epithelial restitution where they not only modulate immune cell function but also provide paracrine signals into the local milieu. Pathogen clearance usually ensues due to immune responses but can persist in areas where facultative epithelial progenitors are completely lost due to immune effector cell cytolysis (Kumar et al., 2011; Quantius et al., 2016; Vaughan et al., 2015; Zacharias et al., 2018; Zuo et al., 2015). In mice, where loss of distal stem cell proliferation occurs, rare quiescent DASC are activated and migrate into hypoxic areas where they proliferate and organise into pod- or cyst-like structures to 'restore' the epithelial barrier (Kumar et al., 2011; Vaughan et al., 2015). In the PR8 mouse model of influenza, progenitor $Krt5^+$ pods and $CD8^+$ T_{RM} form into a repair associated memory depot where TGF-β and IL-15 are available (Mackay, Wynne-Jones, et al., 2015; Takamura et al., 2016; Yoshizawa et al., 2018) downregulate expression of *KLF2*, upregulate expression of cell surface adhesion molecules CD103 and CD49a (Bankovich et al., 2010; Mackay, Wynne-Jones, et al., 2015) and subsequently tether to 'epithelial' $Krt5^+$ pod cells that express E-cadherin (Vaughan et al., 2015) and reconstituted lamina densa collagen IV (Topham et al., 2019). Although the source of local active TGF-β has not been described in the PR8 influenza mouse model, it has been suggested that $Krt5^+$ DASC activate TGF-β by αV integrins (Topham et al., 2019). Notably, the colocalization of these two cell types does not occur following exposure to non-virulent strains of influenza and it is theorised that this occurs because DASC remain quiescent as facultative local epithelial stem/progenitors accomplish efficient regeneration of lost epithelium (Kanegai et al., 2016)

The responses of AEP, AEC2, LNEP, BASC and DASC to alveolar epithelial cell loss associated with mycobacterial lung injury were unknown at the start of this research; moreover, the literature did not describe colocalisation of $CD8^+$ T_{RM} and epithelial progenitor cells following mycobacterial lung

infection. Knowing the effects that RD1 virulence factors have on AEC2, we initially presumed that vaccination with BCG::RD1 may cause a similar lung injury healing sequalae as reported after PR8 lung infection in mice. Our findings, instead, described sequalae in which $Sox2^+$ distal airway progenitors (we suggest the progeny of LNEP) migrated into alveolar tissues to orchestrate restitution in areas where facultative alveolar epithelial progenitors were lost due to the virulence factors of RD1. Conversely, mucosal lung exposure to doses of non-virulent BCG resulted in efficient regeneration of lost epithelium by local epithelial progenitors.

Each of the IT BCG vaccinations of the C57BL/6 mice resulted in distinct epithelial progenitor and $CD8^+$ T_{RM} interactions. The BCG SSI vaccination of 100,000 CFU led to activation of local $pSPC^+$ facultative alveolar epithelial progenitors which formed foci of progeny across contiguous alveoli. We observed that lack of epithelial cell migration through alveolar ECM resulted in little tissue active TGF-β and subsequently a lesser proportion of $CD8^+$ T_{RM} formed. The BCG SSI vaccination of 500,000 CFU was delivered primarily to the airways and led to activation of $Sox2^+$ distal airway and bronchioalveolar $pSPC^+$ epithelial progenitors that resulted in peri- and luminal bronchiolar active TGF-β with subsequent elevated numbers of airway-specific $CD8^+$ T_{RM}. The virulent BCG::RD1 vaccination of 100,000 CFU led to activation of significant numbers of $Sox2^+$ distal airway epithelial progenitors, significantly more alveolar tissue active TGF-β and correspondently higher proportions of $CD8^+$ $T_{RM.}$ When we vaccinated *Itgβ6 KO* mice (that lacked the integrin necessary for TGF-β activation in lungs) with IT BCG::RD1 at 100,000 CFU we observed significantly less tissue active TGF- β and significantly fewer $CD8^+$ T_{RM} (**Fig. 30**).

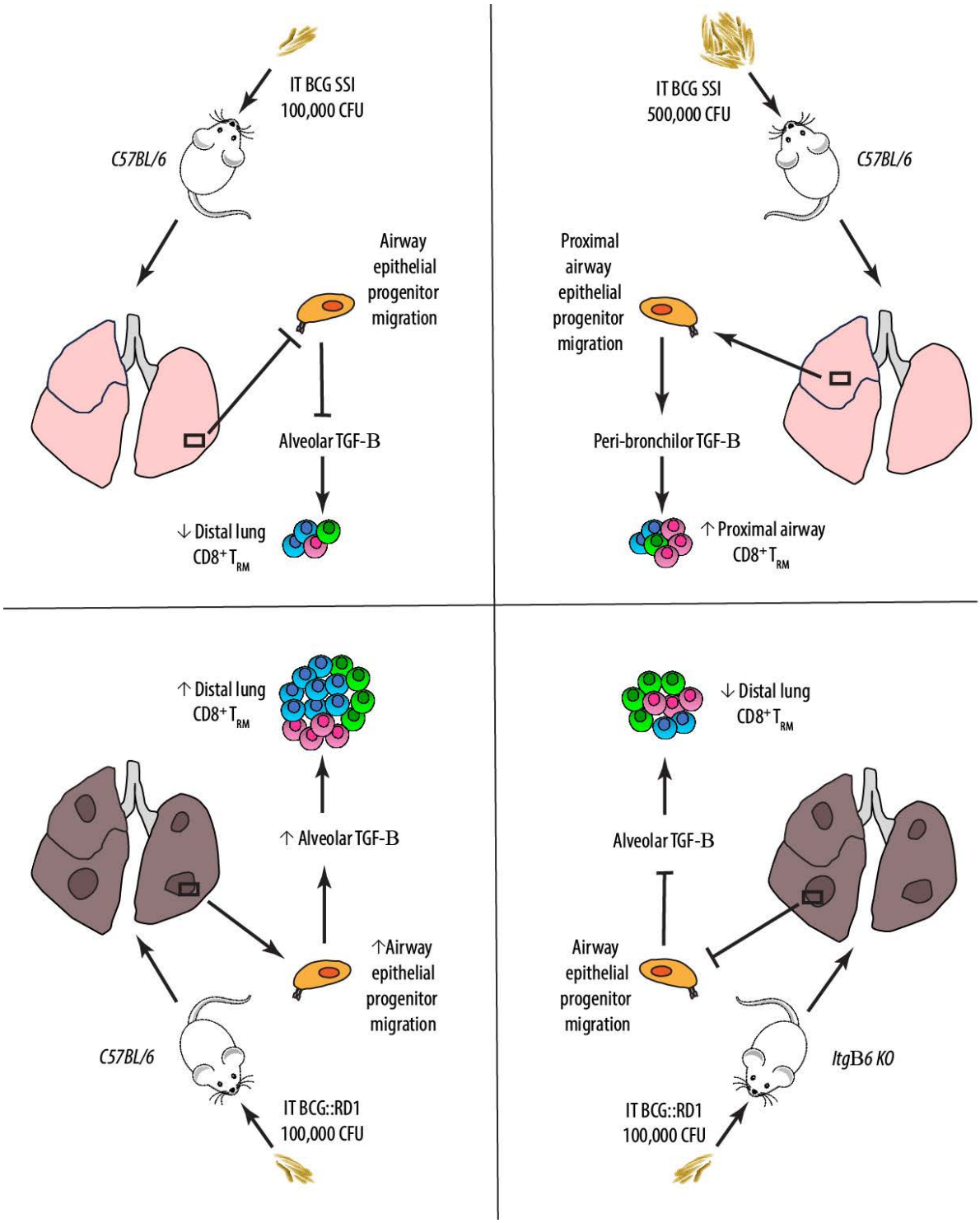

Figure 30. **Model of airway epithelial progenitor responses and subsequent CD8⁺ T_{RM} induction following variant mucosal BCG vaccinations.**

Following mucosal IT vaccination with BCG, immunofluorescent double labelling of CD8b and CD103 or serial IHC staining for CD8b, CD103 and Krt8, did not reveal the formation of peri-bronchiolar RAMD-like structures as described following PR8 infection in mice. Instead, we visualised colocalization of $Krt8^+$ TP, $CD8b^+$ and $CD103^+$ cells throughout the alveolar interstitium, most clustered in areas of moderate to severe injury and some clusters located as far from bronchioles as the visceral pleura. This alludes to the notion that $CD8^+$ T_{RM} patrol other zones of regeneration (other than peri-bronchiolar) in areas of AEP/AEC2 associated re-epithelialisation where inflammatory cytokines such as TGF-β and lamina densa collagen IV are accessible (Sheppard, 2006; West & Mathieu-Costello, 1992).

That peri-bronchiolar RAMD did not form following mucosal exposure to mycobacterium further implies that RAMD formation may be inextricably linked to DASC-mediated factors. The RAMD described in PR8 mouse influenza models (Kumar et al., 2011; Takamura et al., 2016; Vaughan et al., 2015) might form adjacent to bronchioles since both upper and lower airways are severely injured following mucosal exposure to PR8 (Kumar et al., 2011). One theory is that after extensive sloughing of influenza-infected airway epithelium, DASC progeny that are activated to proliferate and differentiate into luminal bronchiolar epithelial cells (Di Gregorio et al., 2016), migrate distally and mistakably inch into the alveoli and "outcompete local stem cell populations" (McQualter, 2019). This may be correct as LNEP are rendered unable to proliferate (Quantius et al., 2016) and AEP/AEC2 are completely destroyed by infection (Kumar et al., 2011; Vaughan et al., 2015; Zacharias et al., 2018; Zuo et al., 2015). Once *in situ*, DASC may use Notch signaling to specify daughter cell fates (hence bronchiolization of alveolar epithelium) and there DASC-secreted Notch ligands may also have a role in development of $CD8^+$ T_{RM} to form the peri-bronchiolar RAMD. Certainly, Notch signaling has been shown obligatory for T_{RM} long-term survival (Hombrink et al., 2016).

Pulmonary biologists describe the formation of $KRT5^+$ $CD8^+$ T_{RM} pods following severe influenza infection as dysplastic (Fernanda de Mello Costa et al., 2020; Planer & Morrisey, 2023). We also

observed Krt5^{+} cells in the centre of dysplastic lung lesions in the *Axin2$^{CreERT:TdT}$/EYFP* mice 56 and 120 days after vaccination with BCG::RD1; the lesions were primarily interstitial and not adjacent to bronchioles. We suggest that DASC were mobilised in these animals due to the severity of lung injury. This notion is supported by human explant and autopsy studies of lung tissue following SARS-CoV-2 infection in which non-resolvable chronic lung disease resulted in the recruitment of Krt5^{+} cells adjacent to fibrotic areas of lung long after clearance of infectious virus (Fang et al., 2020; Jyothula et al., 2022; Wu et al., 2022).

We did not observe the development of fibrosis following any of the three IT vaccinations with BCG, bar in the *Axin2$^{CreERT:TdT}$/EYFP* mice after BCG::RD1 vaccination. At 120 days after IT BCG vaccination, we observed that in the C57BL/6, *Sox2^{CreERT2}/Ai14*, and *Krt5^{CreERT2}* mice, the epithelial progenitors that responded after injury successfully underwent transition from the Sox2^{+} airway and pSPC^{+} alveolar phenotype through the Krt8^{+} TP state and on into differentiation into AEC1 evidenced by overall lung restitution. This implies that the TGF-β signaling necessary for early upregulation of *Krt8* and therefore induction of the Krt8^{+} TP state was appropriate while subsequent inactivation of TGF-β promoted terminal differentiation into AEC1 (Jiang et al., 2020). While out of the scope of this research, in the future the IT BCG vaccinations employed here may be of use to characterise the pathways that induce the Krt8^{+} transitional state and those that abnormally maintain it that are said to cause chronic lung disease and failure (Narasimhan et al., 2023; Yao et al., 2021).

CHAPTER 5. COMPREHENSIVE DISCUSSION

The first man never finished comprehending wisdom, nor will the last succeed in fathoming her.

SIRACH, *THE OLD TESTAMENT*

TB is one of the major causes of death in the world and a new vaccine that induces lung-resident immunity is urgently needed. This is, to our knowledge, the first study to show a mechanistic relationship between lung epithelial progenitor cells and T_{RM} induction/maintenance following mucosal mycobacterial vaccination. Our findings hold several important implications for development of a more effective TB vaccine when broken down into principal criteria that potentially contribute to an effective vaccine.

Firstly, mucosal delivery of BCG is known to induce better systemic and mucosal immune responses compared to parenteral BCG (Aguilo et al., 2017; Perdomo et al., 2016; Sharpe et al., 2016; Uranga et al., 2016). Our findings further support that inhaled BCG not only led to robust induction of lung $CD8^+$ T_{RM} and but also significant populations cells with an ex-lung T_{RM} and stem-like T_{RM} phenotype that persisted for up to 4 months. Our future studies will investigate whether antigen-specific mLN T_{RM} can be harnessed to provide a regional anti-TB arsenal for the lungs. We also demonstrated that a high dose of BCG SSI delivered to the proximal airways induced 4 times the number of airway $CD8^+$ T_{RM} compared to the BCG SSI low dose that affected the distal airways. Thus, if the mucosal route is the way forward for a respiratory TB vaccine, a vaccine that is engineered with both larger particulate matter, delivered to the upper airways (Zareba et al., 2024) and ultrafine particles to the distal airways (He et al., 2023) could have advantages.

As stated previously, a key focus of TB vaccine improvement is BCG modifications that generate persistent $CD8^+$ T cell memory. The BCG::RD1 construct used in our studies has been shown to protect animals from TB challenge following IT administration; however, when bacilli infect AEC2, ESAT-6 causes cell necrosis to allow further spread of bacilli into the interstitium (Krishnan et al., 2010). Our

results confirmed that the RD1 virulence factors had a direct influence on the severity and extended time of AEC losses, inflammation, $CD8^+$ T cell responses and ultimately, tissue regeneration. Importantly, epitopes of a pulmonary mucosal vaccine should be proven not to facilitate BCG adherence and internalisation into AEP. These crucial progenitor cells that function as AEC2 (Zacharias et al., 2018) may be frontline cells for BCG infection and it is known that infection can impede epithelial stem/progenitor cell function, leading to decreased (Parimon et al., 2023), faulty (Toth et al., 2023), or incorrectly timed production of progeny (Yee et al., 2006), and subsequent development of lung disease (Mobius & Thebaud, 2017).

At the time of our experimental design, the standard BCG dose for mouse work was 500,000 CFU since BCG has an unpredictable degree of protection in humans and the World Health Organisation recommends use of high dose vaccination for children (Bretscher, 1992). Mouse studies have shown however, that a higher dose of BCG does not correlate with better protection (Bretscher, 1994; Gruppo & Orme, 2002) and although we administered BCG::RD1 at 100,000 CFU, SSI administered at 3,000 CFU has demonstrated protective efficacy in recent mouse studies (Khatri et al., 2021). Taken together, as BCG::RD1 stimulated a robust local and importantly, regional immune memory, it may be advantageous to continue studies at the 3,000 CFU dose to see whether a lower dose ameliorates severity of lung pathology yet continues to provide protection against *Mtb* challenge. Also, mycobacteria are slow growing and the time to generate immunology data is long; therefore, most studies have been limited to 2-3 months. Future efficacy studies should consider extension to 6 months or a year (Aguilo et al., 2017) before challenge with *Mtb*, as a bi-annual or annual vaccine would be practical for humans.

We demonstrated the importance of the early resolution of inflammation and downregulation of TGF-β as this corresponds to the turning point for lung regeneration (Kim et al., 2018). Clearly, a vaccine that leads to excessive inflammation, while it may induce more $CD8^+ T_{RM}$, is detrimental for the lungs. We learned that excessive AEC losses mobilise airway epithelial progenitors and this was found directly

related to TGF-β activation in bronchiolar epithelium and alveolar interstitium. Although this may have resulted in increased numbers of $CD8^+$ T_{RM}, increased levels or time of activated TGF-β was also shown to harm the lungs. Therefore, an optimal mucosal vaccine should enhance local epithelial progenitor responses and keep TGF-β levels low so as not to tip the balance between $CD8^+$ T_{RM} induction and tissue integrity (Auyeung et al., 2022; Jenkins et al., 2006; Khalil et al., 2001; Kim et al., 2018; Munger et al., 1999; Pittet et al., 2001; Riemondy et al., 2019).

Although there remains optimism in the field that numbers of vaccine induced $CD8^+$ T_{RM} against *Mtb* could be increased and made to persist in the lungs (Ogongo et al., 2019). Here, our results add further evidence that $CD8^+$ T_{RM} have a distinctive *lack* of endurance in the lungs compared to other tissues (Carbone, 2023; Stolley & Masopust, 2017; Takamura, 2017) which is thought to be organ specific (Van Braeckel-Budimir et al., 2018). A future research direction for a new pulmonary mucosal TB vaccine may be to develop one that minimises alveolar harm (and active TGF-β), to generate lung $CD103^-$ $CD69^+CD49a^+$ T_{RM} which are thought to specifically egress to the mLN. Since mLN $CD8^+$ T_{RM} may have the capacity to migrate back to the lungs and orchestrate a timely and efficient innate response (Brewitz et al., 2017; Christo et al., 2021; Paik & Farber, 2021) it could be beneficial if these $CD8^+$ T_{RM} generated from the mucosal vaccination persist in the mLN for six months to a year with the continued capacity to protect the lungs against *Mtb* challenge in the interim.

REFERENCES

Abboud, G., Desai, P., Dastmalchi, F., Stanfield, J., Tahiliani, V., Hutchinson, T. E., & Salek-Ardakani, S. (2016). Tissue-specific programming of memory CD8 T cell subsets impacts protection against lethal respiratory virus infection. *J Exp Med*, *213*(13), 2897-2911. https://doi.org/10.1084/jem.20160167

Adamson, I. Y., & Bowden, D. H. (1974). The type 2 cell as progenitor of alveolar epithelial regeneration. A cytodynamic study in mice after exposure to oxygen. *Lab Invest*, *30*(1), 35-42. https://www.ncbi.nlm.nih.gov/pubmed/4812806

Agudo, J., Park, E. S., Rose, S. A., Alibo, E., Sweeney, R., Dhainaut, M., Kobayashi, K. S., Sachidanandam, R., Baccarini, A., Merad, M., & Brown, B. D. (2018). Quiescent Tissue Stem Cells Evade Immune Surveillance. *Immunity*, *48*(2), 271-285 e275. https://doi.org/10.1016/j.immuni.2018.02.001

Aguilo, N., Gonzalo-Asensio, J., Alvarez-Arguedas, S., Marinova, D., Gomez, A. B., Uranga, S., Spallek, R., Singh, M., Audran, R., Spertini, F., & Martin, C. (2017). Reactogenicity to major tuberculosis antigens absent in BCG is linked to improved protection against Mycobacterium tuberculosis. *Nat Commun*, *8*, 16085. https://doi.org/10.1038/ncomms16085

Alvarado, A. G., & Lathia, J. D. (2016). Taking a Toll on Self-Renewal: TLR-Mediated Innate Immune Signaling in Stem Cells. *Trends Neurosci*, *39*(7), 463-471. https://doi.org/10.1016/j.tins.2016.04.005

Anadon, C. M., Yu, X., Hanggi, K., Biswas, S., Chaurio, R. A., Martin, A., Payne, K. K., Mandal, G., Innamarato, P., Harro, C. M., Mine, J. A., Sprenger, K. B., Cortina, C., Powers, J. J., Costich, T. L., Perez, B. A., Gatenbee, C. D., Prabhakaran, S., Marchion, D.,…Conejo-Garcia, J. R. (2022). Ovarian cancer immunogenicity is governed by a narrow subset of progenitor tissue-resident memory T cells. *Cancer Cell*, *40*(5), 545-557 e513. https://doi.org/10.1016/j.ccell.2022.03.008

Anderson, K. G., Mayer-Barber, K., Sung, H., Beura, L., James, B. R., Taylor, J. J., Qunaj, L., Griffith, T. S., Vezys, V., Barber, D. L., & Masopust, D. (2014). Intravascular staining for discrimination of vascular and tissue leukocytes. *Nat Protoc*, *9*(1), 209-222. https://doi.org/10.1038/nprot.2014.005

Anderson, K. G., Sung, H., Skon, C. N., Lefrancois, L., Deisinger, A., Vezys, V., & Masopust, D. (2012). Cutting edge: intravascular staining redefines lung CD8 T cell responses. *J Immunol*, *189*(6), 2702-2706. https://doi.org/10.4049/jimmunol.1201682

Annes, J. P., Chen, Y., Munger, J. S., & Rifkin, D. B. (2004). Integrin alphaVbeta6-mediated activation of latent TGF-beta requires the latent TGF-beta binding protein-1. *J Cell Biol*, *165*(5), 723-734. https://doi.org/10.1083/jcb.200312172

Ariotti, S., Beltman, J. B., Chodaczek, G., Hoekstra, M. E., van Beek, A. E., Gomez-Eerland, R., Ritsma, L., van Rheenen, J., Maree, A. F., Zal, T., de Boer, R. J., Haanen, J. B., & Schumacher, T. N. (2012). Tissue-resident memory CD8+ T cells continuously patrol skin epithelia to quickly recognize local antigen. *Proc Natl Acad Sci U S A*, *109*(48), 19739-19744. https://doi.org/10.1073/pnas.1208927109

Ariotti, S., Hogenbirk, M. A., Dijkgraaf, F. E., Visser, L. L., Hoekstra, M. E., Song, J. Y., Jacobs, H., Haanen, J. B., & Schumacher, T. N. (2014). T cell memory. Skin-resident memory CD8(+) T cells trigger a state of tissue-wide pathogen alert. *Science*, *346*(6205), 101-105. https://doi.org/10.1126/science.1254803

Atladottir, H. O., Thorsen, P., Ostergaard, L., Schendel, D. E., Lemcke, S., Abdallah, M., & Parner, E. T. (2010). Maternal infection requiring hospitalization during pregnancy and autism spectrum disorders. *J Autism Dev Disord*, *40*(12), 1423-1430. https://doi.org/10.1007/s10803-010-1006-y

Auyeung, V. C., Downey, M. S., Thamsen, M., Wenger, T. A., Backes, B. J., Sheppard, D., & Papa, F. R. (2022). IRE1alpha drives lung epithelial progenitor dysfunction to establish a niche for pulmonary fibrosis. *Am J Physiol Lung Cell Mol Physiol*, *322*(4), L564-L580. https://doi.org/10.1152/ajplung.00408.2021

Baltus, G. A., Kowalski, M. P., Zhai, H., Tutter, A. V., Quinn, D., Wall, D., & Kadam, S. (2009). Acetylation of sox2 induces its nuclear export in embryonic stem cells. *Stem Cells*, *27*(9), 2175-2184. https://doi.org/10.1002/stem.168

Bandaru, A., Devalraju, K. P., Paidipally, P., Dhiman, R., Venkatasubramanian, S., Barnes, P. F., Vankayalapati, R., & Valluri, V. (2014). Phosphorylated STAT3 and PD-1 regulate IL-17 production and IL-23 receptor expression in Mycobacterium tuberculosis infection. *Eur J Immunol*, *44*(7), 2013-2024. https://doi.org/10.1002/eji.201343680

Bank, I., Book, M., & Ware, R. (1994). Functional role of VLA-1 (CD49A) in adhesion, cation-dependent spreading, and activation of cultured human T lymphocytes. *Cell Immunol*, *156*(2), 424-437. https://doi.org/10.1006/cimm.1994.1187

Bankovich, A. J., Shiow, L. R., & Cyster, J. G. (2010). CD69 suppresses sphingosine 1-phosophate receptor-1 (S1P1) function through interaction with membrane helix 4. *J Biol Chem*, *285*(29), 22328-22337. https://doi.org/10.1074/jbc.M110.123299

Barber, D. L., Wherry, E. J., Masopust, D., Zhu, B., Allison, J. P., Sharpe, A. H., Freeman, G. J., & Ahmed, R. (2006). Restoring function in exhausted CD8 T cells during chronic viral infection. *Nature*, *439*(7077), 682-687. https://doi.org/10.1038/nature04444

Barkauskas, C. E., Cronce, M. J., Rackley, C. R., Bowie, E. J., Keene, D. R., Stripp, B. R., Randell, S. H., Noble, P. W., & Hogan, B. L. (2013). Type 2 alveolar cells are stem cells in adult lung. *J Clin Invest*, *123*(7), 3025-3036. https://doi.org/10.1172/JCI68782

Beckstead, J. H. (1994). A simple technique for preservation of fixation-sensitive antigens in paraffin-embedded tissues. *J Histochem Cytochem*, *42*(8), 1127-1134. https://doi.org/10.1177/42.8.8027531

Beers, M. F., & Mulugeta, S. (2005). Surfactant protein C biosynthesis and its emerging role in conformational lung disease. *Annu Rev Physiol*, *67*, 663-696. https://doi.org/10.1146/annurev.physiol.67.040403.101937

Behr, M. A., Wilson, M. A., Gill, W. P., Salamon, H., Schoolnik, G. K., Rane, S., & Small, P. M. (1999). Comparative genomics of BCG vaccines by whole-genome DNA microarray. *Science*, *284*(5419), 1520-1523. https://doi.org/10.1126/science.284.5419.1520

Belkaid, Y., & Hand, T. W. (2014). Role of the microbiota in immunity and inflammation. *Cell*, *157*(1), 121-141. https://doi.org/10.1016/j.cell.2014.03.011

Beltra, J. C., Manne, S., Abdel-Hakeem, M. S., Kurachi, M., Giles, J. R., Chen, Z., Casella, V., Ngiow, S. F., Khan, O., Huang, Y. J., Yan, P., Nzingha, K., Xu, W., Amaravadi, R. K., Xu, X., Karakousis, G. C., Mitchell, T. C., Schuchter, L. M., Huang, A. C., & Wherry, E. J. (2020). Developmental Relationships of Four Exhausted CD8(+) T Cell Subsets Reveals Underlying Transcriptional and Epigenetic Landscape Control Mechanisms. *Immunity*, *52*(5), 825-841 e828. https://doi.org/10.1016/j.immuni.2020.04.014

Bermudez, L. E., & Goodman, J. (1996). Mycobacterium tuberculosis invades and replicates within type II alveolar cells. *Infect Immun*, *64*(4), 1400-1406. https://www.ncbi.nlm.nih.gov/pubmed/8606107

Beura, L. K., Mitchell, J. S., Thompson, E. A., Schenkel, J. M., Mohammed, J., Wijeyesinghe, S., Fonseca, R., Burbach, B. J., Hickman, H. D., Vezys, V., Fife, B. T., & Masopust, D. (2018). Intravital mucosal imaging of CD8(+) resident memory T cells shows tissue-autonomous recall responses that amplify secondary memory. *Nat Immunol*, *19*(2), 173-182. https://doi.org/10.1038/s41590-017-0029-3

Beura, L. K., Wijeyesinghe, S., Thompson, E. A., Macchietto, M. G., Rosato, P. C., Pierson, M. J., Schenkel, J. M., Mitchell, J. S., Vezys, V., Fife, B. T., Shen, S., & Masopust, D. (2018). T Cells in Nonlymphoid Tissues Give Rise to Lymph-Node-Resident Memory T Cells. *Immunity*, *48*(2), 327-338 e325. https://doi.org/10.1016/j.immuni.2018.01.015

Biton, M., Haber, A. L., Rogel, N., Burgin, G., Beyaz, S., Schnell, A., Ashenberg, O., Su, C. W., Smillie, C., Shekhar, K., Chen, Z., Wu, C., Ordovas-Montanes, J., Alvarez, D., Herbst, R. H., Zhang, M., Tirosh, I., Dionne, D., Nguyen, L. T.,…Xavier, R. J. (2018). T Helper Cell Cytokines Modulate Intestinal Stem Cell Renewal and Differentiation. *Cell*, *175*(5), 1307-1320 e1322. https://doi.org/10.1016/j.cell.2018.10.008

Blackwell, T. S., Tager, A. M., Borok, Z., Moore, B. B., Schwartz, D. A., Anstrom, K. J., Bar-Joseph, Z., Bitterman, P., Blackburn, M. R., Bradford, W., Brown, K. K., Chapman, H. A., Collard, H. R., Cosgrove, G. P., Deterding, R., Doyle, R., Flaherty, K. R., Garcia, C. K., Hagood, J. S.,…Eu, J. P. (2014). Future directions in idiopathic pulmonary fibrosis research. An NHLBI workshop report. *Am J Respir Crit Care Med*, *189*(2), 214-222. https://doi.org/10.1164/rccm.201306-1141WS

Borges da Silva, H., Beura, L. K., Wang, H., Hanse, E. A., Gore, R., Scott, M. C., Walsh, D. A., Block, K. E., Fonseca, R., Yan, Y., Hippen, K. L., Blazar, B. R., Masopust, D., Kelekar, A., Vulchanova, L., Hogquist, K. A., & Jameson, S. C. (2018). The purinergic receptor P2RX7 directs metabolic fitness of long-lived memory CD8(+) T cells. *Nature*, *559*(7713), 264-268. https://doi.org/10.1038/s41586-018-0282-0

Bowden, D. H. (1983). Cell turnover in the lung. *Am Rev Respir Dis*, *128*(2 Pt 2), S46-48. https://doi.org/10.1164/arrd.1983.128.2P2.S46

Bretscher, P. A. (1992). A strategy to improve the efficacy of vaccination against tuberculosis and leprosy. *Immunol Today*, *13*(9), 342-345. https://doi.org/10.1016/0167-5699(92)90168-7

Bretscher, P. A. (1994). Prospects for low dose BCG vaccination against tuberculosis. *Immunobiology*, *191*(4-5), 548-554. https://doi.org/10.1016/S0171-2985(11)80461-4

Breuss, J. M., Gallo, J., DeLisser, H. M., Klimanskaya, I. V., Folkesson, H. G., Pittet, J. F., Nishimura, S. L., Aldape, K., Landers, D. V., Carpenter, W., & et al. (1995). Expression of the beta 6 integrin subunit in development, neoplasia and tissue repair suggests a role in epithelial remodeling. *J Cell Sci*, *108 (Pt 6)*, 2241-2251. https://doi.org/10.1242/jcs.108.6.2241

Brewitz, A., Eickhoff, S., Dahling, S., Quast, T., Bedoui, S., Kroczek, R. A., Kurts, C., Garbi, N., Barchet, W., Iannacone, M., Klauschen, F., Kolanus, W., Kaisho, T., Colonna, M., Germain, R. N., & Kastenmuller, W. (2017). CD8(+) T Cells Orchestrate pDC-XCR1(+) Dendritic Cell Spatial and Functional Cooperativity to Optimize Priming. *Immunity*, *46*(2), 205-219. https://doi.org/10.1016/j.immuni.2017.01.003

Bruchfeld, J., Correia-Neves, M., & Kallenius, G. (2015). Tuberculosis and HIV Coinfection. *Cold Spring Harb Perspect Med*, *5*(7), a017871. https://doi.org/10.1101/cshperspect.a017871

Brummelman, J., Mazza, E. M. C., Alvisi, G., Colombo, F. S., Grilli, A., Mikulak, J., Mavilio, D., Alloisio, M., Ferrari, F., Lopci, E., Novellis, P., Veronesi, G., & Lugli, E. (2018). High-dimensional single cell analysis identifies stem-like cytotoxic CD8(+) T cells infiltrating human tumors. *J Exp Med*, *215*(10), 2520-2535. https://doi.org/10.1084/jem.20180684

Brzozowska, E., & Deshmukh, S. (2022). Integrin Alpha v Beta 6 (alphavbeta6) and Its Implications in Cancer Treatment. *Int J Mol Sci*, *23*(20). https://doi.org/10.3390/ijms232012346

Buggert, M., Nguyen, S., Salgado-Montes de Oca, G., Bengsch, B., Darko, S., Ransier, A., Roberts, E. R., Del Alcazar, D., Brody, I. B., Vella, L. A., Beura, L., Wijeyesinghe, S., Herati, R. S., Del Rio Estrada, P. M., Ablanedo-Terrazas, Y., Kuri-Cervantes, L., Sada Japp, A., Manne, S., Vartanian, S.,…Betts, M. R. (2018). Identification and characterization of HIV-specific resident memory CD8(+) T cells in human lymphoid tissue. *Sci Immunol*, *3*(24). https://doi.org/10.1126/sciimmunol.aar4526

Carbone, F. R. (2023). Unique properties of tissue-resident memory T cells in the lungs: implications for COVID-19 and other respiratory diseases. *Nat Rev Immunol*, *23*(5), 329-335. https://doi.org/10.1038/s41577-022-00815-z

Casey, K. A., Fraser, K. A., Schenkel, J. M., Moran, A., Abt, M. C., Beura, L. K., Lucas, P. J., Artis, D., Wherry, E. J., Hogquist, K., Vezys, V., & Masopust, D. (2012). Antigen-independent differentiation and maintenance of effector-like resident memory T cells in tissues. *J Immunol*, *188*(10), 4866-4875. https://doi.org/10.4049/jimmunol.1200402

Castranova, V., Rabovsky, J., Tucker, J. H., & Miles, P. R. (1988). The alveolar type II epithelial cell: a multifunctional pneumocyte. *Toxicol Appl Pharmacol*, *93*(3), 472-483. https://doi.org/10.1016/0041-008x(88)90051-8

Cesta, M. F., Dixon, D., Herbert, R. A., & Staska, L. N. (2024). *National Toxicology Program Nonneoplastic Lesion Atlas (Lung- Inflammation).* https://ntp.niehs.nih.gov/sites/default/files/nnl/respiratory/lung/inflamm/lung-inflammation-508.pdf

Chapman, H. A., Li, X., Alexander, J. P., Brumwell, A., Lorizio, W., Tan, K., Sonnenberg, A., Wei, Y., & Vu, T. H. (2011). Integrin alpha6beta4 identifies an adult distal lung epithelial population with regenerative potential in mice. *J Clin Invest*, *121*(7), 2855-2862. https://doi.org/10.1172/JCI57673

Choi, J., Park, J. E., Tsagkogeorga, G., Yanagita, M., Koo, B. K., Han, N., & Lee, J. H. (2020). Inflammatory Signals Induce AT2 Cell-Derived Damage-Associated Transient Progenitors that Mediate Alveolar Regeneration. *Cell Stem Cell*, *27*(3), 366-382 e367. https://doi.org/10.1016/j.stem.2020.06.020

Christo, S. N., Evrard, M., Park, S. L., Gandolfo, L. C., Burn, T. N., Fonseca, R., Newman, D. M., Alexandre, Y. O., Collins, N., Zamudio, N. M., Souza-Fonseca-Guimaraes, F., Pellicci, D. G., Chisanga, D., Shi, W., Bartholin, L., Belz, G. T., Huntington, N. D., Lucas, A., Lucas, M.,…Mackay, L. K. (2021). Discrete tissue microenvironments instruct diversity in resident memory T cell function and plasticity. *Nat Immunol*, *22*(9), 1140-1151. https://doi.org/10.1038/s41590-021-01004-1

Chua, R. L., Lukassen, S., Trump, S., Hennig, B. P., Wendisch, D., Pott, F., Debnath, O., Thurmann, L., Kurth, F., Volker, M. T., Kazmierski, J., Timmermann, B., Twardziok, S., Schneider, S., Machleidt, F., Muller-Redetzky, H., Maier, M., Krannich, A., Schmidt, S.,…Eils, R. (2020). COVID-19 severity correlates with airway epithelium-immune cell interactions identified by single-cell analysis. *Nat Biotechnol*, *38*(8), 970-979. https://doi.org/10.1038/s41587-020-0602-4

Chuquimia, O. D., Petursdottir, D. H., Rahman, M. J., Hartl, K., Singh, M., & Fernandez, C. (2012). The role of alveolar epithelial cells in initiating and shaping pulmonary immune responses: communication between innate and adaptive immune systems. *PLoS One*, *7*(2), e32125. https://doi.org/10.1371/journal.pone.0032125

Connor, L. M., Harvie, M. C., Rich, F. J., Quinn, K. M., Brinkmann, V., Le Gros, G., & Kirman, J. R. (2010). A key role for lung-resident memory lymphocytes in protective immune responses after BCG vaccination. *Eur J Immunol*, *40*(9), 2482-2492. https://doi.org/10.1002/eji.200940279

Copland, A., Diogo, G. R., Hart, P., Harris, S., Tran, A. C., Paul, M. J., Singh, M., Cutting, S. M., & Reljic, R. (2018). Mucosal Delivery of Fusion Proteins with Bacillus subtilis Spores Enhances Protection against Tuberculosis by Bacillus Calmette-Guerin. *Front Immunol*, *9*, 346. https://doi.org/10.3389/fimmu.2018.00346

Crissman, J. W., Goodman, D. G., Hildebrandt, P. K., Maronpot, R. R., Prater, D. A., Riley, J. H., Seaman, W. J., & Thake, D. C. (2004). Best practices guideline: toxicologic histopathology. *Toxicol Pathol*, *32*(1), 126-131. https://doi.org/10.1080/01926230490268756

Cruz-Guilloty, F., Pipkin, M. E., Djuretic, I. M., Levanon, D., Lotem, J., Lichtenheld, M. G., Groner, Y., & Rao, A. (2009). Runx3 and T-box proteins cooperate to establish the transcriptional program of effector CTLs. *J Exp Med*, *206*(1), 51-59. https://doi.org/10.1084/jem.20081242

Desai, T. J., Brownfield, D. G., & Krasnow, M. A. (2014). Alveolar progenitor and stem cells in lung development, renewal and cancer. *Nature*, *507*(7491), 190-194. https://doi.org/10.1038/nature12930

Di Gregorio, A., Bowling, S., & Rodriguez, T. A. (2016). Cell Competition and Its Role in the Regulation of Cell Fitness from Development to Cancer. *Dev Cell*, *38*(6), 621-634. https://doi.org/10.1016/j.devcel.2016.08.012

Dias, A. A., Raze, D., de Lima, C. S., Marques, M. A., Drobecq, H., Debrie, A. S., Ribeiro-Guimaraes, M. L., Biet, F., & Pessolani, M. C. (2012). Mycobacterial laminin-binding histone-like protein mediates collagen-dependent cytoadherence. *Mem Inst Oswaldo Cruz*, *107 Suppl 1*, 174-182. https://doi.org/10.1590/s0074-02762012000900025

Ely, K. H., Cookenham, T., Roberts, A. D., & Woodland, D. L. (2006). Memory T cell populations in the lung airways are maintained by continual recruitment. *J Immunol*, *176*(1), 537-543. https://doi.org/10.4049/jimmunol.176.1.537

Eriksson, M., Nylen, S., & Gronvik, K. O. (2022). T cell kinetics reveal expansion of distinct lung T cell subsets in acute versus in resolved influenza virus infection. *Front Immunol*, *13*, 949299. https://doi.org/10.3389/fimmu.2022.949299

Evaluation of Tissue Fixation Methods to Inactivate Mycobacterium bovis Under Routine Laboratory Conditions. (2017). *Applied Biosafety*, *22*(4), 152-155. https://doi.org/10.1177/1535676017737315

Evans, M. J., Cabral, L. J., Stephens, R. J., & Freeman, G. (1973). Renewal of alveolar epithelium in the rat following exposure to NO2. *Am J Pathol*, *70*(2), 175-198. https://www.ncbi.nlm.nih.gov/pubmed/4566990

Evans, M. J., Cabral, L. J., Stephens, R. J., & Freeman, G. (1975). Transformation of alveolar type 2 cells to type 1 cells following exposure to NO2. *Exp Mol Pathol*, *22*(1), 142-150. https://doi.org/10.1016/0014-4800(75)90059-3

Evrard, M., Wynne-Jones, E., Peng, C., Kato, Y., Christo, S. N., Fonseca, R., Park, S. L., Burn, T. N., Osman, M., Devi, S., Chun, J., Mueller, S. N., Kannourakis, G., Berzins, S. P., Pellicci, D. G., Heath, W. R., Jameson, S. C., & Mackay, L. K. (2022). Sphingosine 1-phosphate receptor 5 (S1PR5) regulates the peripheral retention of tissue-resident lymphocytes. *J Exp Med*, *219*(1). https://doi.org/10.1084/jem.20210116

Fang, Y., Liu, H., Huang, H., Li, H., Saqi, A., Qiang, L., & Que, J. (2020). Distinct stem/progenitor cells proliferate to regenerate the trachea, intrapulmonary airways and alveoli in COVID-19 patients. *Cell Res*, *30*(8), 705-707. https://doi.org/10.1038/s41422-020-0367-9

Farin, H. F., Jordens, I., Mosa, M. H., Basak, O., Korving, J., Tauriello, D. V., de Punder, K., Angers, S., Peters, P. J., Maurice, M. M., & Clevers, H. (2016). Visualization of a short-range Wnt gradient in the intestinal stem-cell niche. *Nature*, *530*(7590), 340-343. https://doi.org/10.1038/nature16937

Fedchenko, N., & Reifenrath, J. (2014). Different approaches for interpretation and reporting of immunohistochemistry analysis results in the bone tissue - a review. *Diagn Pathol*, *9*, 221. https://doi.org/10.1186/s13000-014-0221-9

Fehrenbach, H. (2001). Alveolar epithelial type II cell: defender of the alveolus revisited. *Respir Res*, *2*(1), 33-46. https://doi.org/10.1186/rr36

Fernanda de Mello Costa, M., Weiner, A. I., & Vaughan, A. E. (2020). Basal-like Progenitor Cells: A Review of Dysplastic Alveolar Regeneration and Remodeling in Lung Repair. *Stem Cell Reports*, *15*(5), 1015-1025. https://doi.org/10.1016/j.stemcr.2020.09.006

Flynn, J. L., Chan, J., Triebold, K. J., Dalton, D. K., Stewart, T. A., & Bloom, B. R. (1993). An essential role for interferon gamma in resistance to Mycobacterium tuberculosis infection. *J Exp Med*, *178*(6), 2249-2254. https://doi.org/10.1084/jem.178.6.2249

Fonseca, R., Beura, L. K., Quarnstrom, C. F., Ghoneim, H. E., Fan, Y., Zebley, C. C., Scott, M. C., Fares-Frederickson, N. J., Wijeyesinghe, S., Thompson, E. A., Borges da Silva, H., Vezys, V., Youngblood, B., & Masopust, D. (2020). Developmental plasticity allows outside-in immune responses by resident memory T cells. *Nat Immunol*, *21*(4), 412-421. https://doi.org/10.1038/s41590-020-0607-7

Fuertes Marraco, S. A., Soneson, C., Cagnon, L., Gannon, P. O., Allard, M., Abed Maillard, S., Montandon, N., Rufer, N., Waldvogel, S., Delorenzi, M., & Speiser, D. E. (2015). Long-lasting stem cell-like memory CD8+ T cells with a naive-like profile upon yellow fever vaccination. *Sci Transl Med*, *7*(282), 282ra248. https://doi.org/10.1126/scitranslmed.aaa3700

Fukushi, M., Ito, T., Oka, T., Kitazawa, T., Miyoshi-Akiyama, T., Kirikae, T., Yamashita, M., & Kudo, K. (2011). Serial histopathological examination of the lungs of mice infected with influenza A virus PR8 strain. *PLoS One*, *6*(6), e21207. https://doi.org/10.1371/journal.pone.0021207

Ganbat, D., Seehase, S., Richter, E., Vollmer, E., Reiling, N., Fellenberg, K., Gaede, K. I., Kugler, C., & Goldmann, T. (2016). Mycobacteria infect different cell types in the human lung and cause species dependent cellular changes in infected cells. *BMC Pulm Med*, *16*, 19. https://doi.org/10.1186/s12890-016-0185-5

Garcia-Perez, B. E., Mondragon-Flores, R., & Luna-Herrera, J. (2003). Internalization of Mycobacterium tuberculosis by macropinocytosis in non-phagocytic cells. *Microb Pathog*, *35*(2), 49-55. https://doi.org/10.1016/s0882-4010(03)00089-5

Gebhardt, T., Wakim, L. M., Eidsmo, L., Reading, P. C., Heath, W. R., & Carbone, F. R. (2009). Memory T cells in nonlymphoid tissue that provide enhanced local immunity during infection with herpes simplex virus. *Nat Immunol*, *10*(5), 524-530. https://doi.org/10.1038/ni.1718

Gebhardt, T., Whitney, P. G., Zaid, A., Mackay, L. K., Brooks, A. G., Heath, W. R., Carbone, F. R., & Mueller, S. N. (2011). Different patterns of peripheral migration by memory CD4+ and CD8+ T cells. *Nature*, *477*(7363), 216-219. https://doi.org/10.1038/nature10339

Gengenbacher, M., Nieuwenhuizen, N. E., & Kaufmann, S. (2017). BCG - old workhorse, new skills. *Curr Opin Immunol*, *47*, 8-16. https://doi.org/10.1016/j.coi.2017.06.007

GeurtsvanKessel, C. H., Willart, M. A., van Rijt, L. S., Muskens, F., Kool, M., Baas, C., Thielemans, K., Bennett, C., Clausen, B. E., Hoogsteden, H. C., Osterhaus, A. D., Rimmelzwaan, G. F., & Lambrecht, B. N. (2008). Clearance of influenza virus from the lung depends on migratory langerin+CD11b- but not plasmacytoid dendritic cells. *J Exp Med*, *205*(7), 1621-1634. https://doi.org/10.1084/jem.20071365

Giacomini, M. M., Travis, M. A., Kudo, M., & Sheppard, D. (2012). Epithelial cells utilize cortical actin/myosin to activate latent TGF-beta through integrin alpha(v)beta(6)-dependent physical force. *Exp Cell Res*, *318*(6), 716-722. https://doi.org/10.1016/j.yexcr.2012.01.020

Giangreco, A., Arwert, E. N., Rosewell, I. R., Snyder, J., Watt, F. M., & Stripp, B. R. (2009). Stem cells are dispensable for lung homeostasis but restore airways after injury. *Proc Natl Acad Sci U S A*, *106*(23), 9286-9291. https://doi.org/10.1073/pnas.0900668106

Grueter, B., Petter, M., Egawa, T., Laule-Kilian, K., Aldrian, C. J., Wuerch, A., Ludwig, Y., Fukuyama, H., Wardemann, H., Waldschuetz, R., Moroy, T., Taniuchi, I., Steimle, V., Littman, D. R., & Ehlers,

M. (2005). Runx3 regulates integrin alpha E/CD103 and CD4 expression during development of CD4-/CD8+ T cells. *J Immunol*, *175*(3), 1694-1705. https://doi.org/10.4049/jimmunol.175.3.1694

Gruppo, V., & Orme, I. M. (2002). Dose of BCG does not influence the efficient generation of protective immunity in mice challenged with Mycobacterium tuberculosis. *Tuberculosis (Edinb)*, *82*(6), 267-273. https://doi.org/10.1054/tube.2002.0340

Guseh, J. S., Bores, S. A., Stanger, B. Z., Zhou, Q., Anderson, W. J., Melton, D. A., & Rajagopal, J. (2009). Notch signaling promotes airway mucous metaplasia and inhibits alveolar development. *Development*, *136*(10), 1751-1759. https://doi.org/10.1242/dev.029249

Haddadi, S., Thanthrige-Don, N., Afkhami, S., Khera, A., Jeyanathan, M., & Xing, Z. (2017). Expression and role of VLA-1 in resident memory CD8 T cell responses to respiratory mucosal viral-vectored immunization against tuberculosis. *Sci Rep*, *7*(1), 9525. https://doi.org/10.1038/s41598-017-09909-4

Haddadi, S., Vaseghi-Shanjani, M., Yao, Y., Afkhami, S., D'Agostino, M. R., Zganiacz, A., Jeyanathan, M., & Xing, Z. (2019). Mucosal-Pull Induction of Lung-Resident Memory CD8 T Cells in Parenteral TB Vaccine-Primed Hosts Requires Cognate Antigens and CD4 T Cells. *Front Immunol*, *10*, 2075. https://doi.org/10.3389/fimmu.2019.02075

Hart, P., Copland, A., Diogo, G. R., Harris, S., Spallek, R., Oehlmann, W., Singh, M., Basile, J., Rottenberg, M., Paul, M. J., & Reljic, R. (2018). Nanoparticle-Fusion Protein Complexes Protect against Mycobacterium tuberculosis Infection. *Mol Ther*, *26*(3), 822-833. https://doi.org/10.1016/j.ymthe.2017.12.016

Hassan, S. S., Akram, M., King, E. C., Dockrell, H. M., & Cliff, J. M. (2015). PD-1, PD-L1 and PD-L2 Gene Expression on T-Cells and Natural Killer Cells Declines in Conjunction with a Reduction in PD-1 Protein during the Intensive Phase of Tuberculosis Treatment. *PLoS One*, *10*(9), e0137646. https://doi.org/10.1371/journal.pone.0137646

Hay, J. G., Danel, C., Chu, C. S., & Crystal, R. G. (1995). Human CC10 gene expression in airway epithelium and subchromosomal locus suggest linkage to airway disease. *Am J Physiol*, *268*(4 Pt 1), L565-575. https://doi.org/10.1152/ajplung.1995.268.4.L565

Hayward, S. L., Scharer, C. D., Cartwright, E. K., Takamura, S., Li, Z. T., Boss, J. M., & Kohlmeier, J. E. (2020). Environmental cues regulate epigenetic reprogramming of airway-resident memory CD8(+) T cells. *Nat Immunol*, *21*(3), 309-320. https://doi.org/10.1038/s41590-019-0584-x

He, R., Hou, S., Liu, C., Zhang, A., Bai, Q., Han, M., Yang, Y., Wei, G., Shen, T., Yang, X., Xu, L., Chen, X., Hao, Y., Wang, P., Zhu, C., Ou, J., Liang, H., Ni, T., Zhang, X.,…Ye, L. (2016). Follicular CXCR5-expressing CD8(+) T cells curtail chronic viral infection. *Nature*, *537*(7620), 412-428. https://doi.org/10.1038/nature19317

He, T., Jin, L., & Li, X. (2023). On the triad of air PM pollution, pathogenic bioaerosols, and lower respiratory infection. *Environ Geochem Health*, *45*(4), 1067-1077. https://doi.org/10.1007/s10653-021-01025-7

Henderson, N. C., & Sheppard, D. (2013). Integrin-mediated regulation of TGFbeta in fibrosis. *Biochim Biophys Acta*, *1832*(7), 891-896. https://doi.org/10.1016/j.bbadis.2012.10.005

Hicks, D. J., Johnson, L., Mitchell, S. M., Gough, J., Cooley, W. A., La Ragione, R. M., Spencer, Y. I., & Wangoo, A. (2006). Evaluation of zinc salt based fixatives for preserving antigenic determinants for immunohistochemical demonstration of murine immune system cell markers. *Biotech Histochem*, *81*(1), 23-30. https://doi.org/10.1080/10520290600725375

Hirai, T., Yang, Y., Zenke, Y., Li, H., Chaudhri, V. K., De La Cruz Diaz, J. S., Zhou, P. Y., Nguyen, B. A., Bartholin, L., Workman, C. J., Griggs, D. W., Vignali, D. A. A., Singh, H., Masopust, D., & Kaplan, D. H. (2021). Competition for Active TGFbeta Cytokine Allows for Selective Retention of Antigen-Specific Tissue- Resident Memory T Cells in the Epidermal Niche. *Immunity*, *54*(1), 84-98 e85. https://doi.org/10.1016/j.immuni.2020.10.022

Hirata, Y., Kakiuchi, M., Robson, S. C., & Fujisaki, J. (2019). CD150(high) CD4 T cells and CD150(high) regulatory T cells regulate hematopoietic stem cell quiescence via CD73. *Haematologica*, *104*(6), 1136-1142. https://doi.org/10.3324/haematol.2018.198283

Hogan, R. J., Cauley, L. S., Ely, K. H., Cookenham, T., Roberts, A. D., Brennan, J. W., Monard, S., & Woodland, D. L. (2002). Long-term maintenance of virus-specific effector memory CD8+ T cells in the lung airways depends on proliferation. *J Immunol*, *169*(9), 4976-4981. https://doi.org/10.4049/jimmunol.169.9.4976

Hogan, R. J., Usherwood, E. J., Zhong, W., Roberts, A. A., Dutton, R. W., Harmsen, A. G., & Woodland, D. L. (2001). Activated antigen-specific CD8+ T cells persist in the lungs following recovery from respiratory virus infections. *J Immunol*, *166*(3), 1813-1822. https://doi.org/10.4049/jimmunol.166.3.1813

Hombrink, P., Helbig, C., Backer, R. A., Piet, B., Oja, A. E., Stark, R., Brasser, G., Jongejan, A., Jonkers, R. E., Nota, B., Basak, O., Clevers, H. C., Moerland, P. D., Amsen, D., & van Lier, R. A. (2016). Programs for the persistence, vigilance and control of human CD8(+) lung-resident memory T cells. *Nat Immunol*, *17*(12), 1467-1478. https://doi.org/10.1038/ni.3589

Hood, J. D., & Cheresh, D. A. (2002). Role of integrins in cell invasion and migration. *Nat Rev Cancer*, *2*(2), 91-100. https://doi.org/10.1038/nrc727

Hsu, T., Hingley-Wilson, S. M., Chen, B., Chen, M., Dai, A. Z., Morin, P. M., Marks, C. B., Padiyar, J., Goulding, C., Gingery, M., Eisenberg, D., Russell, R. G., Derrick, S. C., Collins, F. M., Morris, S. L., King, C. H., & Jacobs, W. R., Jr. (2003). The primary mechanism of attenuation of bacillus Calmette-Guerin is a loss of secreted lytic function required for invasion of lung interstitial tissue. *Proc Natl Acad Sci U S A*, *100*(21), 12420-12425. https://doi.org/10.1073/pnas.1635213100

Hu, B., Huang, S., & Yin, L. (2021). The cytokine storm and COVID-19. *J Med Virol*, *93*(1), 250-256. https://doi.org/10.1002/jmv.26232

Hu, H. H., Chen, D. Q., Wang, Y. N., Feng, Y. L., Cao, G., Vaziri, N. D., & Zhao, Y. Y. (2018). New insights into TGF-beta/Smad signaling in tissue fibrosis. *Chem Biol Interact*, *292*, 76-83. https://doi.org/10.1016/j.cbi.2018.07.008

Hu, Z., Wong, K. W., Zhao, H. M., Wen, H. L., Ji, P., Ma, H., Wu, K., Lu, S. H., Li, F., Li, Z. M., Shu, T., Xu, J. Q., Lowrie, D. B., & Fan, X. Y. (2017). Sendai Virus Mucosal Vaccination Establishes Lung-Resident Memory CD8 T Cell Immunity and Boosts BCG-Primed Protection against TB in Mice. *Mol Ther*, *25*(5), 1222-1233. https://doi.org/10.1016/j.ymthe.2017.02.018

Huang, X., Wu, J., Spong, S., & Sheppard, D. (1998). The integrin alphavbeta6 is critical for keratinocyte migration on both its known ligand, fibronectin, and on vitronectin. *J Cell Sci*, *111 (Pt 15)*, 2189-2195. https://doi.org/10.1242/jcs.111.15.2189

Huster, K. M., Busch, V., Schiemann, M., Linkemann, K., Kerksiek, K. M., Wagner, H., & Busch, D. H. (2004). Selective expression of IL-7 receptor on memory T cells identifies early CD40L-dependent generation of distinct CD8+ memory T cell subsets. *Proc Natl Acad Sci U S A*, *101*(15), 5610-5615. https://doi.org/10.1073/pnas.0308054101

Iborra, S., Martinez-Lopez, M., Khouili, S. C., Enamorado, M., Cueto, F. J., Conde-Garrosa, R., Del Fresno, C., & Sancho, D. (2016). Optimal Generation of Tissue-Resident but Not Circulating Memory T Cells during Viral Infection Requires Crosspriming by DNGR-1(+) Dendritic Cells. *Immunity*, *45*(4), 847-860. https://doi.org/10.1016/j.immuni.2016.08.019

Iijima, N., & Iwasaki, A. (2015). Tissue instruction for migration and retention of TRM cells. *Trends Immunol*, *36*(9), 556-564. https://doi.org/10.1016/j.it.2015.07.002

Iliopoulos, D., Hirsch, H. A., & Struhl, K. (2009). An epigenetic switch involving NF-kappaB, Lin28, Let-7 MicroRNA, and IL6 links inflammation to cell transformation. *Cell*, *139*(4), 693-706. https://doi.org/10.1016/j.cell.2009.10.014

Im, S. J., Hashimoto, M., Gerner, M. Y., Lee, J., Kissick, H. T., Burger, M. C., Shan, Q., Hale, J. S., Lee, J., Nasti, T. H., Sharpe, A. H., Freeman, G. J., Germain, R. N., Nakaya, H. I., Xue, H. H., & Ahmed, R. (2016). Defining CD8+ T cells that provide the proliferative burst after PD-1 therapy. *Nature*, *537*(7620), 417-421. https://doi.org/10.1038/nature19330

Im, S. J., Konieczny, B. T., Hudson, W. H., Masopust, D., & Ahmed, R. (2020). PD-1+ stemlike CD8 T cells are resident in lymphoid tissues during persistent LCMV infection. *Proc Natl Acad Sci U S A*, *117*(8), 4292-4299. https://doi.org/10.1073/pnas.1917298117

Jadhav, R. R., Im, S. J., Hu, B., Hashimoto, M., Li, P., Lin, J. X., Leonard, W. J., Greenleaf, W. J., Ahmed, R., & Goronzy, J. J. (2019). Epigenetic signature of PD-1+ TCF1+ CD8 T cells that act as resource cells during chronic viral infection and respond to PD-1 blockade. *Proc Natl Acad Sci U S A*, *116*(28), 14113-14118. https://doi.org/10.1073/pnas.1903520116

Jayaraman, P., Jacques, M. K., Zhu, C., Steblenko, K. M., Stowell, B. L., Madi, A., Anderson, A. C., Kuchroo, V. K., & Behar, S. M. (2016). TIM3 Mediates T Cell Exhaustion during Mycobacterium tuberculosis Infection. *PLoS Pathog*, *12*(3), e1005490. https://doi.org/10.1371/journal.ppat.1005490

Jenkins, R. G., Su, X., Su, G., Scotton, C. J., Camerer, E., Laurent, G. J., Davis, G. E., Chambers, R. C., Matthay, M. A., & Sheppard, D. (2006). Ligation of protease-activated receptor 1 enhances alpha(v)beta6 integrin-dependent TGF-beta activation and promotes acute lung injury. *J Clin Invest*, *116*(6), 1606-1614. https://doi.org/10.1172/JCI27183

Jiang, P., Gil de Rubio, R., Hrycaj, S. M., Gurczynski, S. J., Riemondy, K. A., Moore, B. B., Omary, M. B., Ridge, K. M., & Zemans, R. L. (2020). Ineffectual Type 2-to-Type 1 Alveolar Epithelial Cell Differentiation in Idiopathic Pulmonary Fibrosis: Persistence of the KRT8(hi) Transitional State. *Am J Respir Crit Care Med*, *201*(11), 1443-1447. https://doi.org/10.1164/rccm.201909-1726LE

Jiang, X., Clark, R. A., Liu, L., Wagers, A. J., Fuhlbrigge, R. C., & Kupper, T. S. (2012). Skin infection generates non-migratory memory CD8+ T(RM) cells providing global skin immunity. *Nature*, *483*(7388), 227-231. https://doi.org/10.1038/nature10851

Johnnidis, J. B., Harris, M. H., Wheeler, R. T., Stehling-Sun, S., Lam, M. H., Kirak, O., Brummelkamp, T. R., Fleming, M. D., & Camargo, F. D. (2008). Regulation of progenitor cell proliferation and granulocyte function by microRNA-223. *Nature*, *451*(7182), 1125-1129. https://doi.org/10.1038/nature06607

Joshi, N. S., Cui, W., Chandele, A., Lee, H. K., Urso, D. R., Hagman, J., Gapin, L., & Kaech, S. M. (2007). Inflammation directs memory precursor and short-lived effector CD8(+) T cell fates via the graded expression of T-bet transcription factor. *Immunity*, *27*(2), 281-295. https://doi.org/10.1016/j.immuni.2007.07.010

Jozwik, A., Habibi, M. S., Paras, A., Zhu, J., Guvenel, A., Dhariwal, J., Almond, M., Wong, E. H. C., Sykes, A., Maybeno, M., Del Rosario, J., Trujillo-Torralbo, M. B., Mallia, P., Sidney, J., Peters, B., Kon, O. M., Sette, A., Johnston, S. L., Openshaw, P. J., & Chiu, C. (2015). RSV-specific airway resident memory CD8+ T cells and differential disease severity after experimental human infection. *Nat Commun*, *6*, 10224. https://doi.org/10.1038/ncomms10224

Jyothula, S. S. K., Peters, A., Liang, Y., Bi, W., Shivshankar, P., Yau, S., Garcha, P. S., Yuan, X., Akkanti, B., Collum, S., Wareing, N., Thandavarayan, R. A., Poli de Frias, F., Rosas, I. O., Zhao, B., Buja, L. M., Eltzschig, H. K., Huang, H. J., & Karmouty-Quintana, H. (2022). Fulminant lung fibrosis in non-resolvable COVID-19 requiring transplantation. *EBioMedicine*, *86*, 104351. https://doi.org/10.1016/j.ebiom.2022.104351

Kaech, S. M., & Cui, W. (2012). Transcriptional control of effector and memory CD8+ T cell differentiation. *Nat Rev Immunol*, *12*(11), 749-761. https://doi.org/10.1038/nri3307

Kaech, S. M., Tan, J. T., Wherry, E. J., Konieczny, B. T., Surh, C. D., & Ahmed, R. (2003). Selective expression of the interleukin 7 receptor identifies effector CD8 T cells that give rise to long-lived memory cells. *Nat Immunol*, *4*(12), 1191-1198. https://doi.org/10.1038/ni1009

Kakaradov, B., Arsenio, J., Widjaja, C. E., He, Z., Aigner, S., Metz, P. J., Yu, B., Wehrens, E. J., Lopez, J., Kim, S. H., Zuniga, E. I., Goldrath, A. W., Chang, J. T., & Yeo, G. W. (2017). Early transcriptional and epigenetic regulation of CD8(+) T cell differentiation revealed by single-cell RNA sequencing. *Nat Immunol*, *18*(4), 422-432. https://doi.org/10.1038/ni.3688

Kalia, V., Sarkar, S., Subramaniam, S., Haining, W. N., Smith, K. A., & Ahmed, R. (2010). Prolonged interleukin-2Ralpha expression on virus-specific CD8+ T cells favors terminal-effector differentiation in vivo. *Immunity*, *32*(1), 91-103. https://doi.org/10.1016/j.immuni.2009.11.010

Kalina, M., Mason, R. J., & Shannon, J. M. (1992). Surfactant protein C is expressed in alveolar type II cells but not in Clara cells of rat lung. *Am J Respir Cell Mol Biol*, *6*(6), 594-600. https://doi.org/10.1165/ajrcmb/6.6.594

Kaminski, N., Allard, J. D., Pittet, J. F., Zuo, F., Griffiths, M. J., Morris, D., Huang, X., Sheppard, D., & Heller, R. A. (2000). Global analysis of gene expression in pulmonary fibrosis reveals distinct programs regulating lung inflammation and fibrosis. *Proc Natl Acad Sci U S A*, *97*(4), 1778-1783. https://doi.org/10.1073/pnas.97.4.1778

Kanegai, C. M., Xi, Y., Donne, M. L., Gotts, J. E., Driver, I. H., Amidzic, G., Lechner, A. J., Jones, K. D., Vaughan, A. E., Chapman, H. A., & Rock, J. R. (2016). Persistent Pathology in Influenza-Infected Mouse Lungs. *Am J Respir Cell Mol Biol*, *55*(4), 613-615. https://doi.org/10.1165/rcmb.2015-0387LE

Kapanci, Y., Weibel, E. R., Kaplan, H. P., & Robinson, F. R. (1969). Pathogenesis and reversibility of the pulmonary lesions of oxygen toxicity in monkeys. II. Ultrastructural and morphometric studies. *Lab Invest*, *20*(1), 101-118. https://www.ncbi.nlm.nih.gov/pubmed/4988417

Kasper, M., & Haroske, G. (1996). Alterations in the alveolar epithelium after injury leading to pulmonary fibrosis. *Histol Histopathol*, *11*(2), 463-483. https://www.ncbi.nlm.nih.gov/pubmed/8861769

Kathiriya, J. J., Brumwell, A. N., Jackson, J. R., Tang, X., & Chapman, H. A. (2020). Distinct Airway Epithelial Stem Cells Hide among Club Cells but Mobilize to Promote Alveolar Regeneration. *Cell Stem Cell*. https://doi.org/10.1016/j.stem.2019.12.014

Kaufmann, S. H. (2013). Tuberculosis vaccines: time to think about the next generation. *Semin Immunol*, *25*(2), 172-181. https://doi.org/10.1016/j.smim.2013.04.006

Kaufmann, S. H., Lange, C., Rao, M., Balaji, K. N., Lotze, M., Schito, M., Zumla, A. I., & Maeurer, M. (2014). Progress in tuberculosis vaccine development and host-directed therapies--a state of the art review. *Lancet Respir Med*, *2*(4), 301-320. https://doi.org/10.1016/s2213-2600(14)70033-5

Khalil, N., Parekh, T. V., O'Connor, R., Antman, N., Kepron, W., Yehaulaeshet, T., Xu, Y. D., & Gold, L. I. (2001). Regulation of the effects of TGF-beta 1 by activation of latent TGF-beta 1 and differential expression of TGF-beta receptors (T beta R-I and T beta R-II) in idiopathic pulmonary fibrosis. *Thorax*, *56*(12), 907-915. https://doi.org/10.1136/thorax.56.12.907

Khatri, B., Keeble, J., Dagg, B., Kaveh, D. A., Hogarth, P. J., & Ho, M. M. (2021). Efficacy and immunogenicity of different BCG doses in BALB/c and CB6F1 mice when challenged with H37Rv or Beijing HN878. *Sci Rep*, *11*(1), 23308. https://doi.org/10.1038/s41598-021-02442-5

Kim, C. F., Jackson, E. L., Woolfenden, A. E., Lawrence, S., Babar, I., Vogel, S., Crowley, D., Bronson, R. T., & Jacks, T. (2005). Identification of bronchioalveolar stem cells in normal lung and lung cancer. *Cell*, *121*(6), 823-835. https://doi.org/10.1016/j.cell.2005.03.032

Kim, K. K., Sheppard, D., & Chapman, H. A. (2018). TGF-beta1 Signaling and Tissue Fibrosis. *Cold Spring Harb Perspect Biol*, *10*(4). https://doi.org/10.1101/cshperspect.a022293

Kim, T. S., & Braciale, T. J. (2009). Respiratory dendritic cell subsets differ in their capacity to support the induction of virus-specific cytotoxic CD8+ T cell responses. *PLoS One*, *4*(1), e4204. https://doi.org/10.1371/journal.pone.0004204

Kim, T. S., Gorski, S. A., Hahn, S., Murphy, K. M., & Braciale, T. J. (2014). Distinct dendritic cell subsets dictate the fate decision between effector and memory CD8(+) T cell differentiation by a CD24-dependent mechanism. *Immunity*, *40*(3), 400-413. https://doi.org/10.1016/j.immuni.2014.02.004

Kinhikar, A. G., Verma, I., Chandra, D., Singh, K. K., Weldingh, K., Andersen, P., Hsu, T., Jacobs, W. R., Jr., & Laal, S. (2010). Potential role for ESAT6 in dissemination of M. tuberculosis via human lung epithelial cells. *Mol Microbiol*, *75*(1), 92-106. https://doi.org/10.1111/j.1365-2958.2009.06959.x

Klopfleisch, R. (2013). Multiparametric and semiquantitative scoring systems for the evaluation of mouse model histopathology--a systematic review. *BMC Vet Res*, *9*, 123. https://doi.org/10.1186/1746-6148-9-123

Kobayashi, Y., Tata, A., Konkimalla, A., Katsura, H., Lee, R. F., Ou, J., Banovich, N. E., Kropski, J. A., & Tata, P. R. (2020). Persistence of a regeneration-associated, transitional alveolar epithelial cell state in pulmonary fibrosis. *Nat Cell Biol*, *22*(8), 934-946. https://doi.org/10.1038/s41556-020-0542-8

Kohlmeier, J. E., Miller, S. C., Smith, J., Lu, B., Gerard, C., Cookenham, T., Roberts, A. D., & Woodland, D. L. (2008). The chemokine receptor CCR5 plays a key role in the early memory CD8+ T cell response to respiratory virus infections. *Immunity*, *29*(1), 101-113. https://doi.org/10.1016/j.immuni.2008.05.011

Krishnan, N., Robertson, B. D., & Thwaites, G. (2010). The mechanisms and consequences of the extra-pulmonary dissemination of Mycobacterium tuberculosis. *Tuberculosis (Edinb)*, *90*(6), 361-366. https://doi.org/10.1016/j.tube.2010.08.005

Kumar, P. A., Hu, Y., Yamamoto, Y., Hoe, N. B., Wei, T. S., Mu, D., Sun, Y., Joo, L. S., Dagher, R., Zielonka, E. M., Wang de, Y., Lim, B., Chow, V. T., Crum, C. P., Xian, W., & McKeon, F. (2011). Distal airway stem cells yield alveoli in vitro and during lung regeneration following H1N1 influenza infection. *Cell*, *147*(3), 525-538. https://doi.org/10.1016/j.cell.2011.10.001

Kuo, C. J., Bell, H., Hsieh, C. L., Ptak, C. P., & Chang, Y. F. (2012). Novel mycobacteria antigen 85 complex binding motif on fibronectin. *J Biol Chem*, *287*(3), 1892-1902. https://doi.org/10.1074/jbc.M111.298687

Kuo, C. J., Ptak, C. P., Hsieh, C. L., Akey, B. L., & Chang, Y. F. (2013). Elastin, a novel extracellular matrix protein adhering to mycobacterial antigen 85 complex. *J Biol Chem*, *288*(6), 3886-3896. https://doi.org/10.1074/jbc.M112.415679

Kusser, K. L., & Randall, T. D. (2003). Simultaneous detection of EGFP and cell surface markers by fluorescence microscopy in lymphoid tissues. *J Histochem Cytochem*, *51*(1), 5-14. https://doi.org/10.1177/002215540305100102

Laidlaw, B. J., Zhang, N., Marshall, H. D., Staron, M. M., Guan, T., Hu, Y., Cauley, L. S., Craft, J., & Kaech, S. M. (2014). CD4+ T cell help guides formation of CD103+ lung-resident memory CD8+ T cells during influenza viral infection. *Immunity*, *41*(4), 633-645. https://doi.org/10.1016/j.immuni.2014.09.007

Lee, L. N., Ronan, E. O., de Lara, C., Franken, K. L., Ottenhoff, T. H., Tchilian, E. Z., & Beverley, P. C. (2011). CXCR6 is a marker for protective antigen-specific cells in the lungs after intranasal immunization against Mycobacterium tuberculosis. *Infect Immun*, *79*(8), 3328-3337. https://doi.org/10.1128/IAI.01133-10

Lee, Y. T., Suarez-Ramirez, J. E., Wu, T., Redman, J. M., Bouchard, K., Hadley, G. A., & Cauley, L. S. (2011). Environmental and antigen receptor-derived signals support sustained surveillance of the lungs by pathogen-specific cytotoxic T lymphocytes. *J Virol*, *85*(9), 4085-4094. https://doi.org/10.1128/JVI.02493-10

Lerner, T. R., Borel, S., & Gutierrez, M. G. (2015). The innate immune response in human tuberculosis. *Cell Microbiol*, *17*(9), 1277-1285. https://doi.org/10.1111/cmi.12480

Li, G., Srinivasan, S., Wang, L., Ma, C., Guo, K., Xiao, W., Liao, W., Mishra, S., Zhang, X., Qiu, Y., Lu, Q., Liu, Y., & Zhang, N. (2022). TGF-beta-dependent lymphoid tissue residency of stem-like T cells limits response to tumor vaccine. *Nat Commun*, *13*(1), 6043. https://doi.org/10.1038/s41467-022-33768-x

Li, M. O., & Flavell, R. A. (2008). TGF-beta: a master of all T cell trades. *Cell*, *134*(3), 392-404. https://doi.org/10.1016/j.cell.2008.07.025

Li, M. O., Sanjabi, S., & Flavell, R. A. (2006). Transforming growth factor-beta controls development, homeostasis, and tolerance of T cells by regulatory T cell-dependent and -independent mechanisms. *Immunity*, *25*(3), 455-471. https://doi.org/10.1016/j.immuni.2006.07.011

Li, Y., Shi, J., Yang, J., Ma, Y., Cheng, L., Zeng, J., Hao, X., Ma, C., Wang, Y., & Liu, X. (2014). A Wnt/beta-catenin negative feedback loop represses TLR-triggered inflammatory responses in alveolar epithelial cells. *Mol Immunol*, *59*(2), 128-135. https://doi.org/10.1016/j.molimm.2014.02.002

Li, Z., Tuong, Z. K., Dean, I., Willis, C., Gaspal, F., Fiancette, R., Idris, S., Kennedy, B., Ferdinand, J. R., Penalver, A., Cabantous, M., Murtuza Baker, S., Fry, J. W., Carlesso, G., Hammond, S. A., Dovedi, S. J., Hepworth, M. R., Clatworthy, M. R., & Withers, D. R. (2022). In vivo labeling reveals continuous trafficking of TCF-1+ T cells between tumor and lymphoid tissue. *J Exp Med*, *219*(6). https://doi.org/10.1084/jem.20210749

Lillehoj, E. P., Kato, K., Lu, W., & Kim, K. C. (2013). Cellular and molecular biology of airway mucins. *Int Rev Cell Mol Biol*, *303*, 139-202. https://doi.org/10.1016/B978-0-12-407697-6.00004-0

Lin, Y., Zhang, M., & Barnes, P. F. (1998). Chemokine production by a human alveolar epithelial cell line in response to Mycobacterium tuberculosis. *Infect Immun*, *66*(3), 1121-1126. https://www.ncbi.nlm.nih.gov/pubmed/9488404

Lindemans, C. A., Calafiore, M., Mertelsmann, A. M., O'Connor, M. H., Dudakov, J. A., Jenq, R. R., Velardi, E., Young, L. F., Smith, O. M., Lawrence, G., Ivanov, J. A., Fu, Y. Y., Takashima, S., Hua, G., Martin, M. L., O'Rourke, K. P., Lo, Y. H., Mokry, M., Romera-Hernandez, M.,…Hanash, A. M. (2015). Interleukin-22 promotes intestinal-stem-cell-mediated epithelial regeneration. *Nature*, *528*(7583), 560-564. https://doi.org/10.1038/nature16460

Liu, K., Wang, D., Yao, C., Qiao, M., Li, Q., Ren, W., Li, S., Gao, M., & Pang, Y. (2022). Increased Tuberculosis Incidence Due to Immunotherapy Based on PD-1 and PD-L1 Blockade: A Systematic Review and Meta-Analysis. *Front Immunol*, *13*, 727220. https://doi.org/10.3389/fimmu.2022.727220

Liu, Q., Liu, K., Cui, G., Huang, X., Yao, S., Guo, W., Qin, Z., Li, Y., Yang, R., Pu, W., Zhang, L., He, L., Zhao, H., Yu, W., Tang, M., Tian, X., Cai, D., Nie, Y., Hu, S.,…Zhou, B. (2019). Lung regeneration by

multipotent stem cells residing at the bronchioalveolar-duct junction. *Nat Genet*, *51*(4), 728-738. https://doi.org/10.1038/s41588-019-0346-6

Liu, Y., Ma, C., & Zhang, N. (2018). Tissue-Specific Control of Tissue-Resident Memory T Cells. *Crit Rev Immunol*, *38*(2), 79-103. https://doi.org/10.1615/CritRevImmunol.2018025653

Lomas, N. J., Watts, K. L., Akram, K. M., Forsyth, N. R., & Spiteri, M. A. (2012). Idiopathic pulmonary fibrosis: immunohistochemical analysis provides fresh insights into lung tissue remodelling with implications for novel prognostic markers. *Int J Clin Exp Pathol*, *5*(1), 58-71. https://www.ncbi.nlm.nih.gov/pubmed/22295148

Lykidis, D., Van Noorden, S., Armstrong, A., Spencer-Dene, B., Li, J., Zhuang, Z., & Stamp, G. W. (2007). Novel zinc-based fixative for high quality DNA, RNA and protein analysis. *Nucleic Acids Res*, *35*(12), e85. https://doi.org/10.1093/nar/gkm433

Ma, C., Li, Y., Zeng, J., Wu, X., Liu, X., & Wang, Y. (2014). Mycobacterium bovis BCG triggered MyD88 induces miR-124 feedback negatively regulates immune response in alveolar epithelial cells. *PLoS One*, *9*(4), e92419. https://doi.org/10.1371/journal.pone.0092419

Ma, H. D., Ma, W. T., Liu, Q. Z., Zhao, Z. B., Liu, M. Z., Tsuneyama, K., Gao, J. M., Ridgway, W. M., Ansari, A. A., Gershwin, M. E., Fei, Y. Y., & Lian, Z. X. (2017). Chemokine receptor CXCR3 deficiency exacerbates murine autoimmune cholangitis by promoting pathogenic CD8(+) T cell activation. *J Autoimmun*, *78*, 19-28. https://doi.org/10.1016/j.jaut.2016.12.012

Mackay, L. K., Braun, A., Macleod, B. L., Collins, N., Tebartz, C., Bedoui, S., Carbone, F. R., & Gebhardt, T. (2015). Cutting edge: CD69 interference with sphingosine-1-phosphate receptor function regulates peripheral T cell retention. *J Immunol*, *194*(5), 2059-2063. https://doi.org/10.4049/jimmunol.1402256

Mackay, L. K., Minnich, M., Kragten, N. A., Liao, Y., Nota, B., Seillet, C., Zaid, A., Man, K., Preston, S., Freestone, D., Braun, A., Wynne-Jones, E., Behr, F. M., Stark, R., Pellicci, D. G., Godfrey, D. I., Belz, G. T., Pellegrini, M., Gebhardt, T.,…van Gisbergen, K. P. (2016). Hobit and Blimp1 instruct a universal transcriptional program of tissue residency in lymphocytes. *Science*, *352*(6284), 459-463. https://doi.org/10.1126/science.aad2035

Mackay, L. K., Rahimpour, A., Ma, J. Z., Collins, N., Stock, A. T., Hafon, M. L., Vega-Ramos, J., Lauzurica, P., Mueller, S. N., Stefanovic, T., Tscharke, D. C., Heath, W. R., Inouye, M., Carbone, F. R., & Gebhardt, T. (2013). The developmental pathway for CD103(+)CD8+ tissue-resident memory T cells of skin. *Nat Immunol*, *14*(12), 1294-1301. https://doi.org/10.1038/ni.2744

Mackay, L. K., Stock, A. T., Ma, J. Z., Jones, C. M., Kent, S. J., Mueller, S. N., Heath, W. R., Carbone, F. R., & Gebhardt, T. (2012). Long-lived epithelial immunity by tissue-resident memory T (TRM) cells in the absence of persisting local antigen presentation. *Proc Natl Acad Sci U S A*, *109*(18), 7037-7042. https://doi.org/10.1073/pnas.1202288109

Mackay, L. K., Wynne-Jones, E., Freestone, D., Pellicci, D. G., Mielke, L. A., Newman, D. M., Braun, A., Masson, F., Kallies, A., Belz, G. T., & Carbone, F. R. (2015). T-box Transcription Factors Combine with the Cytokines TGF-beta and IL-15 to Control Tissue-Resident Memory T Cell Fate. *Immunity*, *43*(6), 1101-1111. https://doi.org/10.1016/j.immuni.2015.11.008

Mangtani, P., Abubakar, I., Ariti, C., Beynon, R., Pimpin, L., Fine, P. E., Rodrigues, L. C., Smith, P. G., Lipman, M., Whiting, P. F., & Sterne, J. A. (2014). Protection by BCG vaccine against tuberculosis: a systematic review of randomized controlled trials. *Clin Infect Dis*, *58*(4), 470-480. https://doi.org/10.1093/cid/cit790

Mangtani, P., Nguipdop-Djomo, P., Keogh, R. H., Trinder, L., Smith, P. G., Fine, P. E., Sterne, J., Abubakar, I., Vynnycky, E., Watson, J., Elliman, D., Lipman, M., & Rodrigues, L. C. (2017). Observational study to estimate the changes in the effectiveness of bacillus Calmette-Guerin (BCG) vaccination with time since vaccination for preventing tuberculosis in the UK. *Health Technol Assess*, *21*(39), 1-54. https://doi.org/10.3310/hta21390

Mason, R. J., & Williams, M. C. (1977). Type II alveolar cell. Defender of the alveolus. *Am Rev Respir Dis*, *115*(6 Pt 2), 81-91. https://doi.org/10.1164/arrd.1977.115.S.81

Masopust, D., & Picker, L. J. (2012). Hidden memories: frontline memory T cells and early pathogen interception. *J Immunol*, *188*(12), 5811-5817. https://doi.org/10.4049/jimmunol.1102695

Masopust, D., Vezys, V., Marzo, A. L., & Lefrancois, L. (2001). Preferential localization of effector memory cells in nonlymphoid tissue. *Science*, *291*(5512), 2413-2417. https://doi.org/10.1126/science.1058867

McDonnell, G., & Russell, A. D. (1999). Antiseptics and disinfectants: activity, action, and resistance. *Clin Microbiol Rev*, *12*(1), 147-179. https://doi.org/10.1128/CMR.12.1.147

McDonough, K. A., & Kress, Y. (1995). Cytotoxicity for lung epithelial cells is a virulence-associated phenotype of Mycobacterium tuberculosis. *Infect Immun*, *63*(12), 4802-4811. https://doi.org/10.1128/iai.63.12.4802-4811.1995

McMaster, S. R., Wilson, J. J., Wang, H., & Kohlmeier, J. E. (2015). Airway-Resident Memory CD8 T Cells Provide Antigen-Specific Protection against Respiratory Virus Challenge through Rapid IFN-gamma Production. *J Immunol*, *195*(1), 203-209. https://doi.org/10.4049/jimmunol.1402975

McQualter, J. L. (2019). Endogenous lung stem cells for lung regeneration. *Expert Opin Biol Ther*, *19*(6), 539-546. https://doi.org/10.1080/14712598.2019.1596256

McQualter, J. L., Yuen, K., Williams, B., & Bertoncello, I. (2010). Evidence of an epithelial stem/progenitor cell hierarchy in the adult mouse lung. *Proc Natl Acad Sci U S A*, *107*(4), 1414-1419. https://doi.org/10.1073/pnas.0909207107

Meecham, A., Cutmore, L. C., Protopapa, P., Rigby, L. G., & Marshall, J. F. (2022). Ligand-bound integrin alphavbeta6 internalisation and trafficking. *Front Cell Dev Biol*, *10*, 920303. https://doi.org/10.3389/fcell.2022.920303

Melms, J. C., Biermann, J., Huang, H., Wang, Y., Nair, A., Tagore, S., Katsyv, I., Rendeiro, A. F., Amin, A. D., Schapiro, D., Frangieh, C. J., Luoma, A. M., Filliol, A., Fang, Y., Ravichandran, H., Clausi, M. G., Alba, G. A., Rogava, M., Chen, S. W.,…Izar, B. (2021). A molecular single-cell lung atlas of lethal COVID-19. *Nature*, *595*(7865), 114-119. https://doi.org/10.1038/s41586-021-03569-1

Mendez-Samperio, P., Alba, L., & Perez, A. (2007). Mycobacterium bovis bacillus Calmette-Guerin (BCG)-induced CXCL8 production is mediated through PKCalpha-dependent activation of the

IKKalphabeta signaling pathway in epithelial cells. *Cell Immunol*, *245*(2), 111-118. https://doi.org/10.1016/j.cellimm.2007.04.005

Mendez-Samperio, P., Miranda, E., & Trejo, A. (2006). Mycobacterium bovis Bacillus Calmette-Guerin (BCG) stimulates human beta-defensin-2 gene transcription in human epithelial cells. *Cell Immunol*, *239*(1), 61-66. https://doi.org/10.1016/j.cellimm.2006.04.001

Mendez-Samperio, P., Miranda, E., & Vazquez, A. (2006). Expression and secretion of CXCL-8 and CXCL-10 from mycobacterium bovis BCG-infected human epithelial cells: role of IL-4. *Mediators Inflamm*, *2006*(1), 67451. https://doi.org/10.1155/MI/2006/67451

Mendez-Samperio, P., Trejo, A., & Perez, A. (2008a). Mycobacterium bovis Bacillus Calmette-Guerin (BCG) stimulates IL-10 production via the PI3K/Akt and p38 MAPK pathways in human lung epithelial cells. *Cell Immunol*, *251*(1), 37-42. https://doi.org/10.1016/j.cellimm.2008.03.002

Mendez-Samperio, P., Trejo, A., & Perez, A. (2008b). Mycobacterium bovis bacillus Calmette-Guerin induces CCL5 secretion via the Toll-like receptor 2-NF-kappaB and -Jun N-terminal kinase signaling pathways. *Clin Vaccine Immunol*, *15*(2), 277-283. https://doi.org/10.1128/CVI.00368-07

Merad, M., & Martin, J. C. (2020). Pathological inflammation in patients with COVID-19: a key role for monocytes and macrophages. *Nat Rev Immunol*, *20*(6), 355-362. https://doi.org/10.1038/s41577-020-0331-4

Messier, B., & Leblond, C. P. (1960). Cell proliferation and migration as revealed by radioautography after injection of thymidine-H3 into male rats and mice. *Am J Anat*, *106*, 247-285. https://doi.org/10.1002/aja.1001060305

Milner, J. J., Toma, C., Yu, B., Zhang, K., Omilusik, K., Phan, A. T., Wang, D., Getzler, A. J., Nguyen, T., Crotty, S., Wang, W., Pipkin, M. E., & Goldrath, A. W. (2017). Runx3 programs CD8(+) T cell residency in non-lymphoid tissues and tumours. *Nature*, *552*(7684), 253-257. https://doi.org/10.1038/nature24993

Mobius, M. A., & Thebaud, B. (2017). Bronchopulmonary Dysplasia: Where Have All the Stem Cells Gone?: Origin and (Potential) Function of Resident Lung Stem Cells. *Chest*, *152*(5), 1043-1052. https://doi.org/10.1016/j.chest.2017.04.173

Mohammed, J., Beura, L. K., Bobr, A., Astry, B., Chicoine, B., Kashem, S. W., Welty, N. E., Igyarto, B. Z., Wijeyesinghe, S., Thompson, E. A., Matte, C., Bartholin, L., Kaplan, A., Sheppard, D., Bridges, A. G., Shlomchik, W. D., Masopust, D., & Kaplan, D. H. (2016). Stromal cells control the epithelial residence of DCs and memory T cells by regulated activation of TGF-beta. *Nat Immunol*, *17*(4), 414-421. https://doi.org/10.1038/ni.3396

Molodtsov, A. K., Khatwani, N., Vella, J. L., Lewis, K. A., Zhao, Y., Han, J., Sullivan, D. E., Searles, T. G., Preiss, N. K., Shabaneh, T. B., Zhang, P., Hawkes, A. R., Malik, B. T., Kolling, F. W. t., Usherwood, E. J., Wong, S. L., Phillips, J. D., Shirai, K., Angeles, C. V.,…Turk, M. J. (2021). Resident memory CD8(+) T cells in regional lymph nodes mediate immunity to metastatic melanoma. *Immunity*, *54*(9), 2117-2132 e2117. https://doi.org/10.1016/j.immuni.2021.08.019

Mori, H., Soonsawad, P., Schuetter, L., Chen, Q., Hubbard, N. E., Cardiff, R. D., & Borowsky, A. D. (2015). Introduction of Zinc-salt Fixation for Effective Detection of Immune Cell-related Markers by

Immunohistochemistry. *Toxicol Pathol*, *43*(6), 883-889. https://doi.org/10.1177/0192623315587593

Mueller, S. N., & Mackay, L. K. (2016). Tissue-resident memory T cells: local specialists in immune defence. *Nat Rev Immunol*, *16*(2), 79-89. https://doi.org/10.1038/nri.2015.3

Mulugeta, S., & Beers, M. F. (2006). Surfactant protein C: its unique properties and emerging immunomodulatory role in the lung. *Microbes Infect*, *8*(8), 2317-2323. https://doi.org/10.1016/j.micinf.2006.04.009

Munger, J. S., Huang, X., Kawakatsu, H., Griffiths, M. J., Dalton, S. L., Wu, J., Pittet, J. F., Kaminski, N., Garat, C., Matthay, M. A., Rifkin, D. B., & Sheppard, D. (1999). The integrin alpha v beta 6 binds and activates latent TGF beta 1: a mechanism for regulating pulmonary inflammation and fibrosis. *Cell*, *96*(3), 319-328. https://doi.org/10.1016/s0092-8674(00)80545-0

Munger, J. S., & Sheppard, D. (2011). Cross talk among TGF-beta signaling pathways, integrins, and the extracellular matrix. *Cold Spring Harb Perspect Biol*, *3*(11), a005017. https://doi.org/10.1101/cshperspect.a005017

Muruganandah, V., Sathkumara, H. D., Pai, S., Rush, C. M., Brosch, R., Waardenberg, A. J., & Kupz, A. (2020). A systematic approach to simultaneously evaluate safety, immunogenicity, and efficacy of novel tuberculosis vaccination strategies. *Sci Adv*, *6*(10), eaaz1767. https://doi.org/10.1126/sciadv.aaz1767

Muzumdar, M. D., Tasic, B., Miyamichi, K., Li, L., & Luo, L. (2007). A global double-fluorescent Cre reporter mouse. *Genesis*, *45*(9), 593-605. https://doi.org/10.1002/dvg.20335

Nabhan, A. N., Brownfield, D. G., Harbury, P. B., Krasnow, M. A., & Desai, T. J. (2018). Single-cell Wnt signaling niches maintain stemness of alveolar type 2 cells. *Science*, *359*(6380), 1118-1123. https://doi.org/10.1126/science.aam6603

Naik, S., Larsen, S. B., Gomez, N. C., Alaverdyan, K., Sendoel, A., Yuan, S., Polak, L., Kulukian, A., Chai, S., & Fuchs, E. (2017). Inflammatory memory sensitizes skin epithelial stem cells to tissue damage. *Nature*, *550*(7677), 475-480. https://doi.org/10.1038/nature24271

Narasimhan, H., Cheon, I. S., Qian, W., Hu, S., Parimon, T., Li, C., Goplen, N., Wu, Y., Wei, X., Son, Y. M., Fink, E., Santos, G., Tang, J., Yao, C., Muehling, L., Canderan, G., Kadl, A., Cannon, A., Young, S.,…Sun, J. (2023). Proximal immune-epithelial progenitor interactions drive chronic tissue sequelae post COVID-19. *Res Sq*. https://doi.org/10.21203/rs.3.rs-3587418/v1

Nath, A. P., Braun, A., Ritchie, S. C., Carbone, F. R., Mackay, L. K., Gebhardt, T., & Inouye, M. (2019). Comparative analysis reveals a role for TGF-beta in shaping the residency-related transcriptional signature in tissue-resident memory CD8+ T cells. *PLoS One*, *14*(2), e0210495. https://doi.org/10.1371/journal.pone.0210495

Ndiaye, B. P., Thienemann, F., Ota, M., Landry, B. S., Camara, M., Dieye, S., Dieye, T. N., Esmail, H., Goliath, R., Huygen, K., January, V., Ndiaye, I., Oni, T., Raine, M., Romano, M., Satti, I., Sutton, S., Thiam, A., Wilkinson, K. A.,…investigators, M. A. t. (2015). Safety, immunogenicity, and efficacy of the candidate tuberculosis vaccine MVA85A in healthy adults infected with HIV-1: a randomised, placebo-controlled, phase 2 trial. *Lancet Respir Med*, *3*(3), 190-200. https://doi.org/10.1016/S2213-2600(15)00037-5

Nie, W., Xue, C., Chen, J., & Xiu, Q. (2013). Secretoglobin 1A member 1 (SCGB1A1) +38A/G polymorphism is associated with asthma risk: a meta-analysis. *Gene*, *528*(2), 304-308. https://doi.org/10.1016/j.gene.2013.06.049

Noguchi, M., Furukawa, K. T., & Morimoto, M. (2020). Pulmonary neuroendocrine cells: physiology, tissue homeostasis and disease. *Dis Model Mech*, *13*(12). https://doi.org/10.1242/dmm.046920

O'Garra, A., Redford, P. S., McNab, F. W., Bloom, C. I., Wilkinson, R. J., & Berry, M. P. (2013). The immune response in tuberculosis. *Annu Rev Immunol*, *31*, 475-527. https://doi.org/10.1146/annurev-immunol-032712-095939

O'Reilly, M. A., Marr, S. H., Yee, M., McGrath-Morrow, S. A., & Lawrence, B. P. (2008). Neonatal hyperoxia enhances the inflammatory response in adult mice infected with influenza A virus. *Am J Respir Crit Care Med*, *177*(10), 1103-1110. https://doi.org/10.1164/rccm.200712-1839OC

Ogongo, P., Porterfield, J. Z., & Leslie, A. (2019). Lung Tissue Resident Memory T-Cells in the Immune Response to Mycobacterium tuberculosis. *Front Immunol*, *10*, 992. https://doi.org/10.3389/fimmu.2019.00992

Ogongo, P., Tezera, L. B., Ardain, A., Nhamoyebonde, S., Ramsuran, D., Singh, A., Ng'oepe, A., Karim, F., Naidoo, T., Khan, K., Dullabh, K. J., Fehlings, M., Lee, B. H., Nardin, A., Lindestam Arlehamn, C. S., Sette, A., Behar, S. M., Steyn, A. J., Madansein, R.,…Leslie, A. (2021). Tissue-resident-like CD4+ T cells secreting IL-17 control Mycobacterium tuberculosis in the human lung. *J Clin Invest*, *131*(10). https://doi.org/10.1172/JCI142014

Ohlstein, B., & Spradling, A. (2007). Multipotent Drosophila intestinal stem cells specify daughter cell fates by differential notch signaling. *Science*, *315*(5814), 988-992. https://doi.org/10.1126/science.1136606

Oliveira, G., Ruggiero, E., Stanghellini, M. T., Cieri, N., D'Agostino, M., Fronza, R., Lulay, C., Dionisio, F., Mastaglio, S., Greco, R., Peccatori, J., Aiuti, A., Ambrosi, A., Biasco, L., Bondanza, A., Lambiase, A., Traversari, C., Vago, L., von Kalle, C.,…Bonini, C. (2015). Tracking genetically engineered lymphocytes long-term reveals the dynamics of T cell immunological memory. *Sci Transl Med*, *7*(317), 317ra198. https://doi.org/10.1126/scitranslmed.aac8265

Ordovas-Montanes, J., Dwyer, D. F., Nyquist, S. K., Buchheit, K. M., Vukovic, M., Deb, C., Wadsworth, M. H., 2nd, Hughes, T. K., Kazer, S. W., Yoshimoto, E., Cahill, K. N., Bhattacharyya, N., Katz, H. R., Berger, B., Laidlaw, T. M., Boyce, J. A., Barrett, N. A., & Shalek, A. K. (2018). Allergic inflammatory memory in human respiratory epithelial progenitor cells. *Nature*, *560*(7720), 649-654. https://doi.org/10.1038/s41586-018-0449-8

Ozga, A. J., Chow, M. T., Lopes, M. E., Servis, R. L., Di Pilato, M., Dehio, P., Lian, J., Mempel, T. R., & Luster, A. D. (2022). CXCL10 chemokine regulates heterogeneity of the CD8(+) T cell response and viral set point during chronic infection. *Immunity*, *55*(1), 82-97 e88. https://doi.org/10.1016/j.immuni.2021.11.002

Paik, D. H., & Farber, D. L. (2021). Influenza infection fortifies local lymph nodes to promote lung-resident heterosubtypic immunity. *J Exp Med*, *218*(1). https://doi.org/10.1084/jem.20200218

Paley, M. A., Kroy, D. C., Odorizzi, P. M., Johnnidis, J. B., Dolfi, D. V., Barnett, B. E., Bikoff, E. K., Robertson, E. J., Lauer, G. M., Reiner, S. L., & Wherry, E. J. (2012). Progenitor and terminal subsets of CD8+ T cells cooperate to contain chronic viral infection. *Science*, *338*(6111), 1220-1225. https://doi.org/10.1126/science.1229620

Pan, J., Zhang, X., Xu, J., Chang, Z., Xin, Z., & Wang, G. (2023). Landscape of Exhausted T Cells in Tuberculosis Revealed by Single-Cell Sequencing. *Microbiol Spectr*, *11*(2), e0283922. https://doi.org/10.1128/spectrum.02839-22

Pardo-Saganta, A., Tata, P. R., Law, B. M., Saez, B., Chow, R. D., Prabhu, M., Gridley, T., & Rajagopal, J. (2015). Parent stem cells can serve as niches for their daughter cells. *Nature*, *523*(7562), 597-601. https://doi.org/10.1038/nature14553

Parimon, T., Chen, P., Stripp, B. R., Liang, J., Jiang, D., Noble, P. W., Parks, W. C., & Yao, C. (2023). Senescence of alveolar epithelial progenitor cells: a critical driver of lung fibrosis. *Am J Physiol Cell Physiol*, *325*(2), C483-C495. https://doi.org/10.1152/ajpcell.00239.2023

Pauls, K., Schon, M., Kubitza, R. C., Homey, B., Wiesenborn, A., Lehmann, P., Ruzicka, T., Parker, C. M., & Schon, M. P. (2001). Role of integrin alphaE(CD103)beta7 for tissue-specific epidermal localization of CD8+ T lymphocytes. *J Invest Dermatol*, *117*(3), 569-575. https://doi.org/10.1046/j.0022-202x.2001.01481.x

Peng, Z. W., Ikenaga, N., Liu, S. B., Sverdlov, D. Y., Vaid, K. A., Dixit, R., Weinreb, P. H., Violette, S., Sheppard, D., Schuppan, D., & Popov, Y. (2016). Integrin alphavbeta6 critically regulates hepatic progenitor cell function and promotes ductular reaction, fibrosis, and tumorigenesis. *Hepatology*, *63*(1), 217-232. https://doi.org/10.1002/hep.28274

Perdomo, C., Zedler, U., Kuhl, A. A., Lozza, L., Saikali, P., Sander, L. E., Vogelzang, A., Kaufmann, S. H., & Kupz, A. (2016). Mucosal BCG Vaccination Induces Protective Lung-Resident Memory T Cell Populations against Tuberculosis. *MBio*, *7*(6). https://doi.org/10.1128/mBio.01686-16

Pittet, J. F., Griffiths, M. J., Geiser, T., Kaminski, N., Dalton, S. L., Huang, X., Brown, L. A., Gotwals, P. J., Koteliansky, V. E., Matthay, M. A., & Sheppard, D. (2001). TGF-beta is a critical mediator of acute lung injury. *J Clin Invest*, *107*(12), 1537-1544. https://doi.org/10.1172/JCI11963

Planer, J. D., & Morrisey, E. E. (2023). After the Storm: Regeneration, Repair, and Reestablishment of Homeostasis Between the Alveolar Epithelium and Innate Immune System Following Viral Lung Injury. *Annu Rev Pathol*, *18*, 337-359. https://doi.org/10.1146/annurev-pathmechdis-031621-024344

Puchelle, E., Zahm, J. M., Tournier, J. M., & Coraux, C. (2006). Airway epithelial repair, regeneration, and remodeling after injury in chronic obstructive pulmonary disease. *Proc Am Thorac Soc*, *3*(8), 726-733. https://doi.org/10.1513/pats.200605-126SF

Puthawala, K., Hadjiangelis, N., Jacoby, S. C., Bayongan, E., Zhao, Z., Yang, Z., Devitt, M. L., Horan, G. S., Weinreb, P. H., Lukashev, M. E., Violette, S. M., Grant, K. S., Colarossi, C., Formenti, S. C., & Munger, J. S. (2008). Inhibition of integrin alpha(v)beta6, an activator of latent transforming growth factor-beta, prevents radiation-induced lung fibrosis. *Am J Respir Crit Care Med*, *177*(1), 82-90. https://doi.org/10.1164/rccm.200706-806OC

Pym, A. S., Brodin, P., Brosch, R., Huerre, M., & Cole, S. T. (2002). Loss of RD1 contributed to the attenuation of the live tuberculosis vaccines Mycobacterium bovis BCG and Mycobacterium microti. *Mol Microbiol*, *46*(3), 709-717. https://doi.org/10.1046/j.1365-2958.2002.03237.x

Pym, A. S., Brodin, P., Majlessi, L., Brosch, R., Demangel, C., Williams, A., Griffiths, K. E., Marchal, G., Leclerc, C., & Cole, S. T. (2003). Recombinant BCG exporting ESAT-6 confers enhanced protection against tuberculosis. *Nat Med*, *9*(5), 533-539. https://doi.org/10.1038/nm859

Quantius, J., Schmoldt, C., Vazquez-Armendariz, A. I., Becker, C., El Agha, E., Wilhelm, J., Morty, R. E., Vadasz, I., Mayer, K., Gattenloehner, S., Fink, L., Matrosovich, M., Li, X., Seeger, W., Lohmeyer, J., Bellusci, S., & Herold, S. (2016). Influenza Virus Infects Epithelial Stem/Progenitor Cells of the Distal Lung: Impact on Fgfr2b-Driven Epithelial Repair. *PLoS Pathog*, *12*(6), e1005544. https://doi.org/10.1371/journal.ppat.1005544

Rawlins, E. L., Okubo, T., Xue, Y., Brass, D. M., Auten, R. L., Hasegawa, H., Wang, F., & Hogan, B. L. (2009). The role of Scgb1a1+ Clara cells in the long-term maintenance and repair of lung airway, but not alveolar, epithelium. *Cell Stem Cell*, *4*(6), 525-534. https://doi.org/10.1016/j.stem.2009.04.002

Ray, S., Chiba, N., Yao, C., Guan, X., McConnell, A. M., Brockway, B., Que, L., McQualter, J. L., & Stripp, B. R. (2016). Rare SOX2(+) Airway Progenitor Cells Generate KRT5(+) Cells that Repopulate Damaged Alveolar Parenchyma following Influenza Virus Infection. *Stem Cell Reports*, *7*(5), 817-825. https://doi.org/10.1016/j.stemcr.2016.09.010

Ray, S. J., Franki, S. N., Pierce, R. H., Dimitrova, S., Koteliansky, V., Sprague, A. G., Doherty, P. C., de Fougerolles, A. R., & Topham, D. J. (2004). The collagen binding alpha1beta1 integrin VLA-1 regulates CD8 T cell-mediated immune protection against heterologous influenza infection. *Immunity*, *20*(2), 167-179. https://doi.org/10.1016/s1074-7613(04)00021-4

Reid, L., Meyrick, B., Antony, V. B., Chang, L. Y., Crapo, J. D., & Reynolds, H. Y. (2005). The mysterious pulmonary brush cell: a cell in search of a function. *Am J Respir Crit Care Med*, *172*(1), 136-139. https://doi.org/10.1164/rccm.200502-203WS

Reilly, E. C., Lambert Emo, K., Buckley, P. M., Reilly, N. S., Smith, I., Chaves, F. A., Yang, H., Oakes, P. W., & Topham, D. J. (2020). T(RM) integrins CD103 and CD49a differentially support adherence and motility after resolution of influenza virus infection. *Proc Natl Acad Sci U S A*, *117*(22), 12306-12314. https://doi.org/10.1073/pnas.1915681117

Reinhardt, R. L., Khoruts, A., Merica, R., Zell, T., & Jenkins, M. K. (2001). Visualizing the generation of memory CD4 T cells in the whole body. *Nature*, *410*(6824), 101-105. https://doi.org/10.1038/35065111

Reis, B. S., Rogoz, A., Costa-Pinto, F. A., Taniuchi, I., & Mucida, D. (2013). Mutual expression of the transcription factors Runx3 and ThPOK regulates intestinal CD4(+) T cell immunity. *Nat Immunol*, *14*(3), 271-280. https://doi.org/10.1038/ni.2518

Remington, S. J. (2011). Green fluorescent protein: a perspective. *Protein Sci*, *20*(9), 1509-1519. https://doi.org/10.1002/pro.684

Rieder, F., Brenmoehl, J., Leeb, S., Scholmerich, J., & Rogler, G. (2007). Wound healing and fibrosis in intestinal disease. *Gut*, *56*(1), 130-139. https://doi.org/10.1136/gut.2006.090456

Riemondy, K. A., Jansing, N. L., Jiang, P., Redente, E. F., Gillen, A. E., Fu, R., Miller, A. J., Spence, J. R., Gerber, A. N., Hesselberth, J. R., & Zemans, R. L. (2019). Single cell RNA sequencing identifies TGFbeta as a key regenerative cue following LPS-induced lung injury. *JCI Insight*, *5*(8). https://doi.org/10.1172/jci.insight.123637

Roberts, A. D., & Woodland, D. L. (2004). Cutting edge: effector memory CD8+ T cells play a prominent role in recall responses to secondary viral infection in the lung. *J Immunol*, *172*(11), 6533-6537. https://doi.org/10.4049/jimmunol.172.11.6533

Robertson, I. B., Horiguchi, M., Zilberberg, L., Dabovic, B., Hadjiolova, K., & Rifkin, D. B. (2015). Latent TGF-beta-binding proteins. *Matrix Biol*, *47*, 44-53. https://doi.org/10.1016/j.matbio.2015.05.005

Rock, J. R., Barkauskas, C. E., Cronce, M. J., Xue, Y., Harris, J. R., Liang, J., Noble, P. W., & Hogan, B. L. (2011). Multiple stromal populations contribute to pulmonary fibrosis without evidence for epithelial to mesenchymal transition. *Proc Natl Acad Sci U S A*, *108*(52), E1475-1483. https://doi.org/10.1073/pnas.1117988108

Rock, J. R., Onaitis, M. W., Rawlins, E. L., Lu, Y., Clark, C. P., Xue, Y., Randell, S. H., & Hogan, B. L. (2009). Basal cells as stem cells of the mouse trachea and human airway epithelium. *Proc Natl Acad Sci U S A*, *106*(31), 12771-12775. https://doi.org/10.1073/pnas.0906850106

Rosen, H. (2005). Chemical approaches to the lysophospholipid receptors. *Prostaglandins Other Lipid Mediat*, *77*(1-4), 179-184. https://doi.org/10.1016/j.prostaglandins.2004.09.011

Russell, A. D., Hammond, S. A., & Morgan, J. R. (1986). Bacterial resistance to antiseptics and disinfectants. *J Hosp Infect*, *7*(3), 213-225. https://doi.org/10.1016/0195-6701(86)90071-x

Ruysseveldt, E., Martens, K., & Steelant, B. (2021). Airway Basal Cells, Protectors of Epithelial Walls in Health and Respiratory Diseases. *Front Allergy*, *2*, 787128. https://doi.org/10.3389/falgy.2021.787128

Sakai, S., Kauffman, K. D., Schenkel, J. M., McBerry, C. C., Mayer-Barber, K. D., Masopust, D., & Barber, D. L. (2014). Cutting edge: control of Mycobacterium tuberculosis infection by a subset of lung parenchyma-homing CD4 T cells. *J Immunol*, *192*(7), 2965-2969. https://doi.org/10.4049/jimmunol.1400019

Sallusto, F., Geginat, J., & Lanzavecchia, A. (2004). Central memory and effector memory T cell subsets: function, generation, and maintenance. *Annu Rev Immunol*, *22*, 745-763. https://doi.org/10.1146/annurev.immunol.22.012703.104702

Sallusto, F., Lenig, D., Forster, R., Lipp, M., & Lanzavecchia, A. (1999). Two subsets of memory T lymphocytes with distinct homing potentials and effector functions. *Nature*, *401*(6754), 708-712. https://doi.org/10.1038/44385

Salwig, I., Spitznagel, B., Vazquez-Armendariz, A. I., Khalooghi, K., Guenther, S., Herold, S., Szibor, M., & Braun, T. (2019). Bronchioalveolar stem cells are a main source for regeneration of distal lung epithelia in vivo. *EMBO J*, *38*(12). https://doi.org/10.15252/embj.2019102099

Sarkar, S., Kalia, V., Haining, W. N., Konieczny, B. T., Subramaniam, S., & Ahmed, R. (2008). Functional and genomic profiling of effector CD8 T cell subsets with distinct memory fates. *J Exp Med*, *205*(3), 625-640. https://doi.org/10.1084/jem.20071641

Sathkumara, H. D., Muruganandah, V., Cooper, M. M., Field, M. A., Alim, M. A., Brosch, R., Ketheesan, N., Govan, B., Rush, C. M., Henning, L., & Kupz, A. (2020). Mucosal delivery of ESX-1-expressing BCG strains provides superior immunity against tuberculosis in murine type 2 diabetes. *Proc Natl Acad Sci U S A*, *117*(34), 20848-20859. https://doi.org/10.1073/pnas.2003235117

Scandella, V., Paolicelli, R. C., & Knobloch, M. (2020). A novel protocol to detect green fluorescent protein in unfixed, snap-frozen tissue. *Sci Rep*, *10*(1), 14642. https://doi.org/10.1038/s41598-020-71493-x

Schenkel, J. M., Fraser, K. A., Beura, L. K., Pauken, K. E., Vezys, V., & Masopust, D. (2014). T cell memory. Resident memory CD8 T cells trigger protective innate and adaptive immune responses. *Science*, *346*(6205), 98-101. https://doi.org/10.1126/science.1254536

Schenkel, J. M., Fraser, K. A., & Masopust, D. (2014). Cutting edge: resident memory CD8 T cells occupy frontline niches in secondary lymphoid organs. *J Immunol*, *192*(7), 2961-2964. https://doi.org/10.4049/jimmunol.1400003

Schenkel, J. M., Fraser, K. A., Vezys, V., & Masopust, D. (2013). Sensing and alarm function of resident memory CD8(+) T cells. *Nat Immunol*, *14*(5), 509-513. https://doi.org/10.1038/ni.2568

Shan, Q., Zeng, Z., Xing, S., Li, F., Hartwig, S. M., Gullicksrud, J. A., Kurup, S. P., Van Braeckel-Budimir, N., Su, Y., Martin, M. D., Varga, S. M., Taniuchi, I., Harty, J. T., Peng, W., Badovinac, V. P., & Xue, H. H. (2017). The transcription factor Runx3 guards cytotoxic CD8(+) effector T cells against deviation towards follicular helper T cell lineage. *Nat Immunol*, *18*(8), 931-939. https://doi.org/10.1038/ni.3773

Sharma, M., Sharma, S., Roy, S., Varma, S., & Bose, M. (2007). Pulmonary epithelial cells are a source of interferon-gamma in response to Mycobacterium tuberculosis infection. *Immunol Cell Biol*, *85*(3), 229-237. https://doi.org/10.1038/sj.icb.7100037

Sharma, P., & Allison, J. P. (2015). The future of immune checkpoint therapy. *Science*, *348*(6230), 56-61. https://doi.org/10.1126/science.aaa8172

Sharpe, S., White, A., Sarfas, C., Sibley, L., Gleeson, F., McIntyre, A., Basaraba, R., Clark, S., Hall, G., Rayner, E., Williams, A., Marsh, P. D., & Dennis, M. (2016). Alternative BCG delivery strategies improve protection against Mycobacterium tuberculosis in non-human primates: Protection associated with mycobacterial antigen-specific CD4 effector memory T-cell populations. *Tuberculosis (Edinb)*, *101*, 174-190. https://doi.org/10.1016/j.tube.2016.09.004

Sheedy, F. J., Palsson-McDermott, E., Hennessy, E. J., Martin, C., O'Leary, J. J., Ruan, Q., Johnson, D. S., Chen, Y., & O'Neill, L. A. (2010). Negative regulation of TLR4 via targeting of the proinflammatory tumor suppressor PDCD4 by the microRNA miR-21. *Nat Immunol*, *11*(2), 141-147. https://doi.org/10.1038/ni.1828

Sheppard, D. (2006). Transforming growth factor beta: a central modulator of pulmonary and airway inflammation and fibrosis. *Proc Am Thorac Soc*, *3*(5), 413-417. https://doi.org/10.1513/pats.200601-008AW

Sheridan, B. S., Pham, Q. M., Lee, Y. T., Cauley, L. S., Puddington, L., & Lefrancois, L. (2014). Oral infection drives a distinct population of intestinal resident memory CD8(+) T cells with enhanced protective function. *Immunity*, *40*(5), 747-757. https://doi.org/10.1016/j.immuni.2014.03.007

Shi, M., Zhu, J., Wang, R., Chen, X., Mi, L., Walz, T., & Springer, T. A. (2011). Latent TGF-beta structure and activation. *Nature*, *474*(7351), 343-349. https://doi.org/10.1038/nature10152

Shin, H., & Iwasaki, A. (2012). Skin T(RM) mediates distributed border patrol. *Cell Res*, *22*(9), 1325-1327. https://doi.org/10.1038/cr.2012.75

Shiow, L. R., Rosen, D. B., Brdickova, N., Xu, Y., An, J., Lanier, L. L., Cyster, J. G., & Matloubian, M. (2006). CD69 acts downstream of interferon-alpha/beta to inhibit S1P1 and lymphocyte egress from lymphoid organs. *Nature*, *440*(7083), 540-544. https://doi.org/10.1038/nature04606

Skon, C. N., Lee, J. Y., Anderson, K. G., Masopust, D., Hogquist, K. A., & Jameson, S. C. (2013). Transcriptional downregulation of S1pr1 is required for the establishment of resident memory CD8+ T cells. *Nat Immunol*, *14*(12), 1285-1293. https://doi.org/10.1038/ni.2745

Slutter, B., Van Braeckel-Budimir, N., Abboud, G., Varga, S. M., Salek-Ardakani, S., & Harty, J. T. (2017). Dynamics of influenza-induced lung-resident memory T cells underlie waning heterosubtypic immunity. *Sci Immunol*, *2*(7). https://doi.org/10.1126/sciimmunol.aag2031

Snyder, M. E., Finlayson, M. O., Connors, T. J., Dogra, P., Senda, T., Bush, E., Carpenter, D., Marboe, C., Benvenuto, L., Shah, L., Robbins, H., Hook, J. L., Sykes, M., D'Ovidio, F., Bacchetta, M., Sonett, J. R., Lederer, D. J., Arcasoy, S., Sims, P. A., & Farber, D. L. (2019). Generation and persistence of human tissue-resident memory T cells in lung transplantation. *Sci Immunol*, *4*(33). https://doi.org/10.1126/sciimmunol.aav5581

Steinert, E. M., Schenkel, J. M., Fraser, K. A., Beura, L. K., Manlove, L. S., Igyarto, B. Z., Southern, P. J., & Masopust, D. (2015). Quantifying Memory CD8 T Cells Reveals Regionalization of Immunosurveillance. *Cell*, *161*(4), 737-749. https://doi.org/10.1016/j.cell.2015.03.031

Stolley, J. M., Johnston, T. S., Soerens, A. G., Beura, L. K., Rosato, P. C., Joag, V., Wijeyesinghe, S. P., Langlois, R. A., Osum, K. C., Mitchell, J. S., & Masopust, D. (2020). Retrograde migration supplies resident memory T cells to lung-draining LN after influenza infection. *J Exp Med*, *217*(8). https://doi.org/10.1084/jem.20192197

Stolley, J. M., & Masopust, D. (2017). Tissue-resident memory T cells live off the fat of the land. *Cell Res*, *27*(7), 847-848. https://doi.org/10.1038/cr.2017.49

Stripp, B. R., & Reynolds, S. D. (2008). Maintenance and repair of the bronchiolar epithelium. *Proc Am Thorac Soc*, *5*(3), 328-333. https://doi.org/10.1513/pats.200711-167DR

Strunz, M., Simon, L. M., Ansari, M., Kathiriya, J. J., Angelidis, I., Mayr, C. H., Tsidiridis, G., Lange, M., Mattner, L. F., Yee, M., Ogar, P., Sengupta, A., Kukhtevich, I., Schneider, R., Zhao, Z., Voss, C., Stoeger, T., Neumann, J. H. L., Hilgendorff, A.,…Schiller, H. B. (2020). Alveolar regeneration through a Krt8+ transitional stem cell state that persists in human lung fibrosis. *Nat Commun*, *11*(1), 3559. https://doi.org/10.1038/s41467-020-17358-3

Swamy, M., Abeler-Dorner, L., Chettle, J., Mahlakoiv, T., Goubau, D., Chakravarty, P., Ramsay, G., Reis e Sousa, C., Staeheli, P., Blacklaws, B. A., Heeney, J. L., & Hayday, A. C. (2015). Intestinal intraepithelial lymphocyte activation promotes innate antiviral resistance. *Nat Commun*, *6*, 7090. https://doi.org/10.1038/ncomms8090

Takamura, S. (2017). Persistence in Temporary Lung Niches: A Survival Strategy of Lung-Resident Memory CD8(+) T Cells. *Viral Immunol*, *30*(6), 438-450. https://doi.org/10.1089/vim.2017.0016

Takamura, S. (2018). Niches for the Long-Term Maintenance of Tissue-Resident Memory T Cells. *Front Immunol*, *9*, 1214. https://doi.org/10.3389/fimmu.2018.01214

Takamura, S., Kato, S., Motozono, C., Shimaoka, T., Ueha, S., Matsuo, K., Miyauchi, K., Masumoto, T., Katsushima, A., Nakayama, T., Tomura, M., Matsushima, K., Kubo, M., & Miyazawa, M. (2019). Interstitial-resident memory CD8(+) T cells sustain frontline epithelial memory in the lung. *J Exp Med*. https://doi.org/10.1084/jem.20190557

Takamura, S., & Kohlmeier, J. E. (2019). Establishment and Maintenance of Conventional and Circulation-Driven Lung-Resident Memory CD8(+) T Cells Following Respiratory Virus Infections. *Front Immunol*, *10*, 733. https://doi.org/10.3389/fimmu.2019.00733

Takamura, S., Yagi, H., Hakata, Y., Motozono, C., McMaster, S. R., Masumoto, T., Fujisawa, M., Chikaishi, T., Komeda, J., Itoh, J., Umemura, M., Kyusai, A., Tomura, M., Nakayama, T., Woodland, D. L., Kohlmeier, J. E., & Miyazawa, M. (2016). Specific niches for lung-resident memory CD8+ T cells at the site of tissue regeneration enable CD69-independent maintenance. *J Exp Med*, *213*(13), 3057-3073. https://doi.org/10.1084/jem.20160938

Tam, A., Wadsworth, S., Dorscheid, D., Man, S. F., & Sin, D. D. (2011). The airway epithelium: more than just a structural barrier. *Ther Adv Respir Dis*, *5*(4), 255-273. https://doi.org/10.1177/1753465810396539

Tameris, M., McShane, H., McClain, J. B., Landry, B., Lockhart, S., Luabeya, A. K., Geldenhuys, H., Shea, J., Hussey, G., van der Merwe, L., de Kock, M., Scriba, T., Walker, R., Hanekom, W., Hatherill, M., & Mahomed, H. (2013). Lessons learnt from the first efficacy trial of a new infant tuberculosis vaccine since BCG. *Tuberculosis (Edinb)*, *93*(2), 143-149. https://doi.org/10.1016/j.tube.2013.01.003

Tameris, M. D., Hatherill, M., Landry, B. S., Scriba, T. J., Snowden, M. A., Lockhart, S., Shea, J. E., McClain, J. B., Hussey, G. D., Hanekom, W. A., Mahomed, H., McShane, H., & Team, M. A. T. S. (2013). Safety and efficacy of MVA85A, a new tuberculosis vaccine, in infants previously vaccinated with BCG: a randomised, placebo-controlled phase 2b trial. *Lancet*, *381*(9871), 1021-1028. https://doi.org/10.1016/S0140-6736(13)60177-4

Teijaro, J. R., Turner, D., Pham, Q., Wherry, E. J., Lefrancois, L., & Farber, D. L. (2011). Cutting edge: Tissue-retentive lung memory CD4 T cells mediate optimal protection to respiratory virus infection. *J Immunol*, *187*(11), 5510-5514. https://doi.org/10.4049/jimmunol.1102243

Thacker, T. C. (2017). Evaluation of Tissue Fixation Methods to Inactivate Mycobacterium bovis Under Routine Laboratory Conditions. *Applied Biosafety*, *22*(4), 4.

Thamsen, M., Ghosh, R., Auyeung, V. C., Brumwell, A., Chapman, H. A., Backes, B. J., Perara, G., Maly, D. J., Sheppard, D., & Papa, F. R. (2019). Small molecule inhibition of IRE1alpha kinase/RNase has anti-fibrotic effects in the lung. *PLoS One*, *14*(1), e0209824. https://doi.org/10.1371/journal.pone.0209824

Tili, E., Michaille, J. J., Cimino, A., Costinean, S., Dumitru, C. D., Adair, B., Fabbri, M., Alder, H., Liu, C. G., Calin, G. A., & Croce, C. M. (2007). Modulation of miR-155 and miR-125b levels following lipopolysaccharide/TNF-alpha stimulation and their possible roles in regulating the response to endotoxin shock. *J Immunol*, *179*(8), 5082-5089. https://doi.org/10.4049/jimmunol.179.8.5082

Tompkins, D. H., Besnard, V., Lange, A. W., Wert, S. E., Keiser, A. R., Smith, A. N., Lang, R., & Whitsett, J. A. (2009). Sox2 is required for maintenance and differentiation of bronchiolar Clara, ciliated, and goblet cells. *PLoS One*, *4*(12), e8248. https://doi.org/10.1371/journal.pone.0008248

Topham, D. J., & Reilly, E. C. (2018). Tissue-Resident Memory CD8(+) T Cells: From Phenotype to Function. *Front Immunol*, *9*, 515. https://doi.org/10.3389/fimmu.2018.00515

Topham, D. J., Reilly, E. C., Emo, K. L., & Sportiello, M. (2019). Formation and Maintenance of Tissue Resident Memory CD8+ T Cells after Viral Infection. *Pathogens*, *8*(4). https://doi.org/10.3390/pathogens8040196

Toth, A., Kannan, P., Snowball, J., Kofron, M., Wayman, J. A., Bridges, J. P., Miraldi, E. R., Swarr, D., & Zacharias, W. J. (2023). Alveolar epithelial progenitor cells require Nkx2-1 to maintain progenitor-specific epigenomic state during lung homeostasis and regeneration. *Nat Commun*, *14*(1), 8452. https://doi.org/10.1038/s41467-023-44184-0

Treutlein, B., Brownfield, D. G., Wu, A. R., Neff, N. F., Mantalas, G. L., Espinoza, F. H., Desai, T. J., Krasnow, M. A., & Quake, S. R. (2014). Reconstructing lineage hierarchies of the distal lung epithelium using single-cell RNA-seq. *Nature*, *509*(7500), 371-375. https://doi.org/10.1038/nature13173

Uhal, B. D. (1997). Cell cycle kinetics in the alveolar epithelium. *Am J Physiol*, *272*(6 Pt 1), L1031-1045. https://doi.org/10.1152/ajplung.1997.272.6.L1031

Uranga, S., Marinova, D., Martin, C., & Aguilo, N. (2016). Protective Efficacy and Pulmonary Immune Response Following Subcutaneous and Intranasal BCG Administration in Mice. *J Vis Exp*(115). https://doi.org/10.3791/54440

Utzschneider, D. T., Charmoy, M., Chennupati, V., Pousse, L., Ferreira, D. P., Calderon-Copete, S., Danilo, M., Alfei, F., Hofmann, M., Wieland, D., Pradervand, S., Thimme, R., Zehn, D., & Held, W. (2016). T Cell Factor 1-Expressing Memory-like CD8(+) T Cells Sustain the Immune Response to Chronic Viral Infections. *Immunity*, *45*(2), 415-427. https://doi.org/10.1016/j.immuni.2016.07.021

Van Braeckel-Budimir, N., Varga, S. M., Badovinac, V. P., & Harty, J. T. (2018). Repeated Antigen Exposure Extends the Durability of Influenza-Specific Lung-Resident Memory CD8(+) T Cells and Heterosubtypic Immunity. *Cell Rep*, *24*(13), 3374-3382 e3373. https://doi.org/10.1016/j.celrep.2018.08.073

Vaughan, A. E., Brumwell, A. N., Xi, Y., Gotts, J. E., Brownfield, D. G., Treutlein, B., Tan, K., Tan, V., Liu, F. C., Looney, M. R., Matthay, M. A., Rock, J. R., & Chapman, H. A. (2015). Lineage-negative progenitors mobilize to regenerate lung epithelium after major injury. *Nature*, *517*(7536), 621-625. https://doi.org/10.1038/nature14112

Vaughan, A. E., & Chapman, H. A. (2013). Regenerative activity of the lung after epithelial injury. *Biochim Biophys Acta*, *1832*(7), 922-930. https://doi.org/10.1016/j.bbadis.2012.11.020

Verbist, K. C., Cole, C. J., Field, M. B., & Klonowski, K. D. (2011). A role for IL-15 in the migration of effector CD8 T cells to the lung airways following influenza infection. *J Immunol*, *186*(1), 174-182. https://doi.org/10.4049/jimmunol.1002613

von Moltke, J., Ji, M., Liang, H. E., & Locksley, R. M. (2016). Tuft-cell-derived IL-25 regulates an intestinal ILC2-epithelial response circuit. *Nature*, *529*(7585), 221-225. https://doi.org/10.1038/nature16161

Wakim, L. M., Smith, J., Caminschi, I., Lahoud, M. H., & Villadangos, J. A. (2015). Antibody-targeted vaccination to lung dendritic cells generates tissue-resident memory CD8 T cells that are highly protective against influenza virus infection. *Mucosal Immunol*, *8*(5), 1060-1071. https://doi.org/10.1038/mi.2014.133

Wakim, L. M., Woodward-Davis, A., Liu, R., Hu, Y., Villadangos, J., Smyth, G., & Bevan, M. J. (2012). The molecular signature of tissue resident memory CD8 T cells isolated from the brain. *J Immunol*, *189*(7), 3462-3471. https://doi.org/10.4049/jimmunol.1201305

Walsh, D. A., Borges da Silva, H., Beura, L. K., Peng, C., Hamilton, S. E., Masopust, D., & Jameson, S. C. (2019). The Functional Requirement for CD69 in Establishment of Resident Memory CD8(+) T Cells Varies with Tissue Location. *J Immunol*, *203*(4), 946-955. https://doi.org/10.4049/jimmunol.1900052

Wein, A. N., McMaster, S. R., Takamura, S., Dunbar, P. R., Cartwright, E. K., Hayward, S. L., McManus, D. T., Shimaoka, T., Ueha, S., Tsukui, T., Masumoto, T., Kurachi, M., Matsushima, K., & Kohlmeier, J. E. (2019). CXCR6 regulates localization of tissue-resident memory CD8 T cells to the airways. *J Exp Med*. https://doi.org/10.1084/jem.20181308

West, J. B., & Mathieu-Costello, O. (1992). Strength of the pulmonary blood-gas barrier. *Respir Physiol*, *88*(1-2), 141-148. https://doi.org/10.1016/0034-5687(92)90035-u

Wester, K., Asplund, A., Backvall, H., Micke, P., Derveniece, A., Hartmane, I., Malmstrom, P. U., & Ponten, F. (2003). Zinc-based fixative improves preservation of genomic DNA and proteins in histoprocessing of human tissues. *Lab Invest*, *83*(6), 889-899. https://doi.org/10.1097/01.lab.0000074892.53211.a5

Whitsett, J. A., & Weaver, T. E. (2015). Alveolar development and disease. *Am J Respir Cell Mol Biol*, *53*(1), 1-7. https://doi.org/10.1165/rcmb.2015-0128PS

Wijeyesinghe, S., Beura, L. K., Pierson, M. J., Stolley, J. M., Adam, O. A., Ruscher, R., Steinert, E. M., Rosato, P. C., Vezys, V., & Masopust, D. (2021). Expansible residence decentralizes immune homeostasis. *Nature*, *592*(7854), 457-462. https://doi.org/10.1038/s41586-021-03351-3

Wong, K. W. (2017). The Role of ESX-1 in Mycobacterium tuberculosis Pathogenesis. *Microbiol Spectr*, *5*(3). https://doi.org/10.1128/microbiolspec.TBTB2-0001-2015

World Health Organisation. (2023). *Global tuberculosis report 2023*. https://www.who.int/teams/global-tuberculosis-programme/tb-reports/global-tuberculosis-report-2023

Wu, K., Zhang, Y., Austin, S. R., Declue, H. Y., Byers, D. E., Crouch, E. C., & Holtzman, M. J. (2022). Lung remodeling regions in long-term Covid-19 feature basal epithelial cell reprogramming. *medRxiv*. https://doi.org/10.1101/2022.09.17.22280043

Wu, Q., Kang, S., Huang, J., Wan, S., Yang, B., & Wu, C. (2021). Antigen-Specific Tissue-Resident Memory T Cells in the Respiratory System Were Generated following Intranasal Vaccination of Mice with BCG. *J Immunol Res*, *2021*, 6660379. https://doi.org/10.1155/2021/6660379

Wu, T., Hu, Y., Lee, Y. T., Bouchard, K. R., Benechet, A., Khanna, K., & Cauley, L. S. (2014). Lung-resident memory CD8 T cells (TRM) are indispensable for optimal cross-protection against pulmonary virus infection. *J Leukoc Biol*, *95*(2), 215-224. https://doi.org/10.1189/jlb.0313180

Wu, T., Ji, Y., Moseman, E. A., Xu, H. C., Manglani, M., Kirby, M., Anderson, S. M., Handon, R., Kenyon, E., Elkahloun, A., Wu, W., Lang, P. A., Gattinoni, L., McGavern, D. B., & Schwartzberg, P. L. (2016). The TCF1-Bcl6 axis counteracts type I interferon to repress exhaustion and maintain T cell stemness. *Sci Immunol*, *1*(6). https://doi.org/10.1126/sciimmunol.aai8593

Xi, Y., Kim, T., Brumwell, A. N., Driver, I. H., Wei, Y., Tan, V., Jackson, J. R., Xu, J., Lee, D. K., Gotts, J. E., Matthay, M. A., Shannon, J. M., Chapman, H. A., & Vaughan, A. E. (2017). Local lung hypoxia determines epithelial fate decisions during alveolar regeneration. *Nat Cell Biol*, *19*(8), 904-914. https://doi.org/10.1038/ncb3580

Xu, H., Zhou, R., & Chen, Z. (2023). Tissue-Resident Memory T Cell: Ontogenetic Cellular Mechanism and Clinical Translation. *Clin Exp Immunol*, *214*(3), 249-259. https://doi.org/10.1093/cei/uxad090

Xu, Y., Mizuno, T., Sridharan, A., Du, Y., Guo, M., Tang, J., Wikenheiser-Brokamp, K. A., Perl, A. T., Funari, V. A., Gokey, J. J., Stripp, B. R., & Whitsett, J. A. (2016). Single-cell RNA sequencing identifies diverse roles of epithelial cells in idiopathic pulmonary fibrosis. *JCI Insight*, *1*(20), e90558. https://doi.org/10.1172/jci.insight.90558

Yao, C., Guan, X., Carraro, G., Parimon, T., Liu, X., Huang, G., Mulay, A., Soukiasian, H. J., David, G., Weigt, S. S., Belperio, J. A., Chen, P., Jiang, D., Noble, P. W., & Stripp, B. R. (2021). Senescence of Alveolar Type 2 Cells Drives Progressive Pulmonary Fibrosis. *Am J Respir Crit Care Med*, *203*(6), 707-717. https://doi.org/10.1164/rccm.202004-1274OC

Yee, M., Vitiello, P. F., Roper, J. M., Staversky, R. J., Wright, T. W., McGrath-Morrow, S. A., Maniscalco, W. M., Finkelstein, J. N., & O'Reilly, M. A. (2006). Type II epithelial cells are critical target for hyperoxia-mediated impairment of postnatal lung development. *Am J Physiol Lung Cell Mol Physiol*, *291*(5), L1101-1111. https://doi.org/10.1152/ajplung.00126.2006

Yoshisue, H., Puddicombe, S. M., Wilson, S. J., Haitchi, H. M., Powell, R. M., Wilson, D. I., Pandit, A., Berger, A. E., Davies, D. E., Holgate, S. T., & Holloway, J. W. (2004). Characterization of ciliated bronchial epithelium 1, a ciliated cell-associated gene induced during mucociliary

differentiation. *Am J Respir Cell Mol Biol*, *31*(5), 491-500. https://doi.org/10.1165/rcmb.2004-0050OC

Yoshizawa, A., Bi, K., Keskin, D. B., Zhang, G., Reinhold, B., & Reinherz, E. L. (2018). TCR-pMHC encounter differentially regulates transcriptomes of tissue-resident CD8 T cells. *Eur J Immunol*, *48*(1), 128-150. https://doi.org/10.1002/eji.201747174

Yuzefpolskiy, Y., Baumann, F. M., Kalia, V., & Sarkar, S. (2015). Early CD8 T-cell memory precursors and terminal effectors exhibit equipotent in vivo degranulation. *Cell Mol Immunol*, *12*(4), 400-408. https://doi.org/10.1038/cmi.2014.48

Zacharias, W. J., Frank, D. B., Zepp, J. A., Morley, M. P., Alkhaleel, F. A., Kong, J., Zhou, S., Cantu, E., & Morrisey, E. E. (2018). Regeneration of the lung alveolus by an evolutionarily conserved epithelial progenitor. *Nature*, *555*(7695), 251-255. https://doi.org/10.1038/nature25786

Zahm, J. M., Chevillard, M., & Puchelle, E. (1991). Wound repair of human surface respiratory epithelium. *Am J Respir Cell Mol Biol*, *5*(3), 242-248. https://doi.org/10.1165/ajrcmb/5.3.242

Zahm, J. M., Kaplan, H., Herard, A. L., Doriot, F., Pierrot, D., Somelette, P., & Puchelle, E. (1997). Cell migration and proliferation during the in vitro wound repair of the respiratory epithelium. *Cell Motil Cytoskeleton*, *37*(1), 33-43. https://doi.org/10.1002/(SICI)1097-0169(1997)37:1<33::AID-CM4>3.0.CO;2-I

Zahm, J. M., Pierrot, D., Chevillard, M., & Puchelle, E. (1992). Dynamics of cell movement during the wound repair of human surface respiratory epithelium. *Biorheology*, *29*(5-6), 459-465. https://doi.org/10.3233/bir-1992-295-606

Zaid, A., Hor, J. L., Christo, S. N., Groom, J. R., Heath, W. R., Mackay, L. K., & Mueller, S. N. (2017). Chemokine Receptor-Dependent Control of Skin Tissue-Resident Memory T Cell Formation. *J Immunol*, *199*(7), 2451-2459. https://doi.org/10.4049/jimmunol.1700571

Zammit, D. J., Turner, D. L., Klonowski, K. D., Lefrancois, L., & Cauley, L. S. (2006). Residual antigen presentation after influenza virus infection affects CD8 T cell activation and migration. *Immunity*, *24*(4), 439-449. https://doi.org/10.1016/j.immuni.2006.01.015

Zareba, L., Piszczatowska, K., Dzaman, K., Soroczynska, K., Motamedi, P., Szczepanski, M. J., & Ludwig, N. (2024). The Relationship between Fine Particle Matter (PM2.5) Exposure and Upper Respiratory Tract Diseases. *J Pers Med*, *14*(1). https://doi.org/10.3390/jpm14010098

Zhang, N., & Bevan, M. J. (2013). Transforming growth factor-beta signaling controls the formation and maintenance of gut-resident memory T cells by regulating migration and retention. *Immunity*, *39*(4), 687-696. https://doi.org/10.1016/j.immuni.2013.08.019

Zhang, Y., Joe, G., Hexner, E., Zhu, J., & Emerson, S. G. (2005). Host-reactive CD8+ memory stem cells in graft-versus-host disease. *Nat Med*, *11*(12), 1299-1305. https://doi.org/10.1038/nm1326

Zhao, Z., Zhao, Y., Zhou, Y., Wang, X., Zhang, T., & Zuo, W. (2020). Single-cell analysis identified lung progenitor cells in COVID-19 patients. *Cell Prolif*, *53*(12), e12931. https://doi.org/10.1111/cpr.12931

Zheng, D., Limmon, G. V., Yin, L., Leung, N. H., Yu, H., Chow, V. T., & Chen, J. (2012). Regeneration of alveolar type I and II cells from Scgb1a1-expressing cells following severe pulmonary damage induced by bleomycin and influenza. *PLoS One*, *7*(10), e48451. https://doi.org/10.1371/journal.pone.0048451

Zheng, D., Limmon, G. V., Yin, L., Leung, N. H., Yu, H., Chow, V. T., & Chen, J. (2013). A cellular pathway involved in Clara cell to alveolar type II cell differentiation after severe lung injury. *PLoS One*, *8*(8), e71028. https://doi.org/10.1371/journal.pone.0071028

Zimmermann, N., Saiga, H., Houthuys, E., Moura-Alves, P., Koehler, A., Bandermann, S., Dorhoi, A., & Kaufmann, S. H. (2016). Syndecans promote mycobacterial internalization by lung epithelial cells. *Cell Microbiol*, *18*(12), 1846-1856. https://doi.org/10.1111/cmi.12627

Zuo, W., Zhang, T., Wu, D. Z., Guan, S. P., Liew, A. A., Yamamoto, Y., Wang, X., Lim, S. J., Vincent, M., Lessard, M., Crum, C. P., Xian, W., & McKeon, F. (2015). p63(+)Krt5(+) distal airway stem cells are essential for lung regeneration. *Nature*, *517*(7536), 616-620. https://doi.org/10.1038/nature13903

Table 2. **List of antibodies used for IHC, IF and flow cytometry.**

Primary Antibody	**Species raised**	**Manufacturer/ Concentration**	**Working dilution**	**Secondary Antibody**	**Species raised**	**Manufacturer/ Concentration**	**Working dilution**
T1α 8.1.1-s	Hamster serum	DSHB 15ug/ml	2ug/ml	Biot-Hamster IgG ab6782	Rabbit	abcam 1.5mg/ml	1:1000 w/2% NRS
Pro-SPC ab90716	Rabbit IgG	abcam 0.7mg/ml	1:1000	HRP-Rabbit IgG ab97057	Goat	abcam 0.5mg/ml	1:50
Krt5 Poly9059	Chicken IgY	BioLegend 0.5 mg/mL	1:200	Biot-Chicken IgY Ab6876	Goat	abcam 2.0mg/ml	1:800
Sox2 EPR3131	Rabbit IgG	abcam 0.214mg/ml	1:200	Biot-Rabbit IgG ab6720	Goat	abcam 2.0mg/ml	1:1000
Krt8 EP1628Y	Rabbit IgG	abcam 0.033mg/ml	1:1000	HRP-Rabbit IgG ab97057	Goat	abcam 0.5mg/ml	1:50
CD3e EPR22667-12	Rabbit IgG	abcam 0.673mg/ml	1:100	HRP-Rabbit IgG ab97057	Goat	abcam 0.5mg/ml	1:50
CD8b EPR22331-54	Rabbit IgG	abcam 0.63mg/ml	1:500	HRP-Rabbit IgG ab97057	Goat	abcam 0.5mg/ml	1:50
CD103 EPR22590-27	Rabbit IgG	abcam 0.516mg/ml	1:200	HRP-Rabbit IgG ab97057	Goat	abcam 0.5mg/ml	1:50
TGF-beta 1/1.2 AF-101-NA	Chicken IgY	R&D Systems 0.2mg/ml	1:100	Biot-Chicken IgY Ab6876	Goat	abcam 2.0mg/ml	1:800
RFP 600-401-379	Rabbit IgG	Rockland 1.06mg/ml	1:1000	HRP-Rabbit IgG ab97057	Goat	abcam 0.5mg/ml	1:100
GFP	Goat IgG	Aves Labs 10mg/ml	1:500	HRP-Goat IgG A15999	Donkey	Thermo Fisher 1 mg/ml	1:500
CD8b EPR22331-54	Rabbit IgG	abcam 0.63mg/ml	1:500	AF647-Rabbit IgG AB_2536183	Donkey	Invitrogen 2 mg/ml	1:1000
CD103 EPR22590-27	Rabbit IgG	abcam 0.516mg/ml	1:200	AF488-Rabbit IgG AB_2536183	Goat	Invitrogen 2 mg/ml	1:1000
Krt8 EP1628Y	Rabbit IgG	abcam 0.033mg/ml	1:1000				
TGF-beta 1/1.2 AF-101-NA	Chicken IgY	R&D Systems 0.2mg/ml	1:100				

CD49a/BV421 Ha31/8	Rat IgG	BD Biosciences 0.2mg/ml	1:200				
CD8a/FITC 53-6.7	Rat IgG	BD Biosciences 0.5mg/ml	1:200				
CD69/PE H1.2F3	Rat IgG	BD Biosciences 0.2mg/ml	1:100				
CD103/AF647 2E7	Rat IgG	BD Biosciences 0.2mg/ml	1:200				
CD16/32 2.4G2	Rat IgG	BD Biosciences 0.5mg/ml	1:500				
CD185/BV421 2G8	Rat IgG	BD Biosciences 0.2mg/ml	1:50				
CD279/APC Lγ-51		BD Biosciences 0.2mg/ml	1:200				